

Doctoral Thesis 2011

Spectroscopic analytical methodologies for the study of Cultural Heritage materials

Àfrica Pitarch i Martí



Institut de Ciències de la Terra Jaume Almera.
Consell Superior d'Investigacions Científiques



Universitat Autònoma de Barcelona.
Departament de Geologia

UAB



**Spectroscopic analytical methodologies for the
study of Cultural Heritage materials**

Àfrica PITARCH MARTÍ



Autonomous University of Barcelona
Faculty of Sciences
Geology Department



Spanish National Research Council
Institute of Earth Sciences Jaume Almera
Laboratory of X-ray Analytical Applications

Spectroscopic analytical methodologies for the study of Cultural Heritage materials

PhD Dissertation presented by

Àfrica Pitarch Martí

In candidacy for the degree of Doctor in Geology at the Autonomous University of
Barcelona

Bellaterra, November 2011

Ignasi Queralt Mitjans, Investigador Científic de l'Institut de Ciències de la Terra Jaume Almera (ICTJA – CSIC), **Aureli Álvarez Pérez**, Professor Emèrit del Departament de Geologia de la Universitat Autònoma de Barcelona (UAB) i **Lluís Casas Duocastella**, Professor Lector del Departament de Geologia de la Universitat Autònoma de Barcelona (UAB).

CERTIFIQUEM:

Que els estudis recollits en la present memòria sota el títol “**Spectroscopic analytical methodologies for the study of Cultural Heritage materials**”, han estat realitzats sota la nostra direcció per Àfrica Pitarch Martí, llicenciada en Geologia, per optar al grau de Doctora en Geologia.

I perquè així consti, signem la present certificació.

Bellaterra, 2 de novembre de 2011

Dr. Ignasi Queralt Mitjans

Dr. Aureli Álvarez Pérez

Dr. Lluís Casas Duocastella

The development of this thesis has been done within the framework of the PhD program in Geology of the Autonomous University of Barcelona (RD 778/1998).

Àfrica Pitarch gratefully acknowledges a PhD research grant from the Spanish Ministry of Education (reference FPU AP2006-4591) as well as the research mobility grants within the framework of the Spanish-Programme for International stay grants (2009-2010, 2010-2011). Part of the experimental work of this thesis was performed in collaboration with:

- Departamento de Física, Linha Experimental do Centro de Física Atómica, Universidade de Lisboa (Lisbon, Portugal).
- IBea Research Group (Ikerkuntza eta Berrikuntza Analitikoa), Department of Analytical Chemistry, University of the Basque Country (Bilbao, Spain).

LIST OF PAPERS PUBLISHED IN ISI / SCI JOURNALS RESULTING FROM THIS RESEARCH

PITARCH A., QUERALT I. (2010) *Energy dispersive X-ray fluorescence analysis of ancient coins: The case of Greek silver drachmae from the Emporion site in Spain.* Nuclear Instruments and Methods in Physics Research B, 268, 1682-1685.

PITARCH A., QUERALT I., ÁLVAREZ-PÉREZ A. (2011) *Analysis of Catalanian silver coins from the Spanish War of Independence period (1808-1814) by Energy Dispersive X-ray Fluorescence.* Nuclear Instruments and Methods in Physics Research B, 269, 308-312.

PITARCH A., RAMÓN A., ÁLVAREZ-PÉREZ A., QUERALT I. (2011) *Characterization of "oil on copper" paintings by energy dispersive x-ray fluorescence spectrometry.* Analytical and Bioanalytical Chemistry. doi: 10.1007/s00216-011-5368-6.

PITARCH A., ÁLVAREZ-PÉREZ A., CASTRO K., MADARIAGA J.M., QUERALT I. (2011) *Raman analysis assessed by Fourier Transformed Infrared and X-Ray Fluorescence spectroscopies: a multianalytical approach of ancient chromolithographs from the nineteenth century.* Journal of Raman Spectroscopy. doi: 10.1002/jrs.3055.

PITARCH A., RAMÓN A., ÁLVAREZ-PÉREZ A., CASTRO K., MADARIAGA J.M., QUERALT I. (2011) *Multispectroscopic characterization of "oil on copper" painting. (Submitted to Current Analytical Chemistry).*

A la familia

Summary	1
Resum	5
Resumen	7
Introduction	13
I. 1. Analysis and Cultural Heritage	15
I. 2. Physicochemical methods of analysis	15
I. 3. Application of electromagnetic radiation to determine the chemical composition of Cultural Heritage materials.	17
I. 3. 1. Infrared	18
I. 3. 2. Visible light	20
I. 3. 3. X-rays	21
I. 3. 4. High resolution imaging – Electron microscopy	23
I. 4. Outline of the thesis	25
I. 5. Methodology	27
I. 6. References	33
Chapter 1: Studies of metallic artefacts	41
1. 1. Introduction	
1. 2. Energy dispersive X-ray fluorescence analyses of ancient silver <i>drachmae</i> from Catalonia	45
1. 2. 1. Historical context	45
1. 2. 2. Research aims	46
1. 2. 3. Materials and Methods	47
1. 2. 3. 1. <i>Samples</i>	47
1. 2. 3. 2. <i>X-ray fluorescence equipment</i>	48
1. 2. 3. 3. <i>Experimental conditions</i>	48
1. 2. 3. 4. <i>Limits of detection</i>	51
1. 2. 4. Results and Discussion	52
1. 2. 4. 1. <i>Quantitative analysis of silver drachmae from the Emporion mint (fifth to first century BC)</i>	52
1. 2. 4. 2. <i>Quantitative analysis of silver drachmae from the Rhode mint (third century BC)</i>	56

1. 2. 4. 3. <i>Quantitative analysis of Iberian silver drachmae (third century BC)</i>	58
1. 2. 5. Conclusions	60
1. 3. Energy dispersive X-ray fluorescence analyses of ancient silver coins from the Spanish War of Independence period (1808 – 1814)	61
1. 3. 1. Historical context	61
1. 3. 2. Research aims	62
1. 3. 3. Materials and Methods	62
1. 3. 3. 1. <i>Sampling</i>	62
1. 3. 3. 2. <i>Experimental</i>	64
1. 3. 4. Results and Discussion	64
1. 3. 4. 1. <i>Coins from Barcelona, Catalonia, Lleida and Tarragona workshops</i>	64
1. 3. 4. 2. <i>Compositional anomalies and forgeries</i>	68
1. 3. 5. Conclusions	70
1. 4. References	71
Chapter 2: Studies of paintings	79
2. 1. Introduction	81
2. 2. Historical context	81
2. 3. Characterization of “oil on copper” paintings by energy dispersive X-ray fluorescence spectrometry	82
2. 3. 1. Research aims	83
2. 3. 2. Materials and Methods	83
2. 3. 2. 1. <i>Artworks</i>	83
2. 3. 2. 2. <i>Equipments</i>	84
2. 3. 2. 3. <i>Standards for EDXRF calibration</i>	84
2. 3. 2. 4. <i>EDXRF quantitative method</i>	85
2. 3. 2. 5. <i>Statistical data treatment</i>	88
2. 3. 3. Results and Discussion	88
2. 3. 3. 1. <i>Elemental and crystalline phase analyses of the supporting materials and preparation layer</i>	88
2. 3. 3. 2. <i>Pigment mass distribution estimation on a Renaissance painting</i>	91
2. 3. 3. 3. <i>Pigment mass distribution estimation on a Contemporary painting</i>	94

2. 3. 4. Conclusions	98
2. 4. Multi-spectroscopic characterization of “oil on copper” painting	99
2. 4. 1. Research aims	99
2. 4. 2. Materials and Methods	100
2. 4. 2. 1. <i>Artwork</i>	100
2. 4. 2. 2. <i>Instruments</i>	100
2. 4. 3. Results and Discussion	102
2. 4. 3. 1. <i>Overall chemistry of the “oil on copper” painting</i>	102
2. 4. 3. 2. <i>Pigments</i>	103
2. 4. 3. 3. <i>Binder</i>	111
2. 4. 3. 4. <i>Preparation layer</i>	112
2. 4. 3. 5. <i>Supporting material</i>	113
2. 4. 4. Conclusions	113
2. 5. References	114
Chapter 3: Studies of ancient documents	121
3. 1. Introduction	123
3. 2. Characterization of ancient chromolithographs	124
3. 2. 1. Historical context	125
3. 2. 2. Research aims	125
3. 2. 3. Materials and Methods	126
3. 2. 3. 1. <i>Specimen</i>	126
3. 2. 3. 2. <i>Analytical techniques</i>	128
3. 2. 4. Results and Discussion	129
3. 2. 4. 1. <i>Paper support</i>	130
3. 2. 4. 2. <i>Inks</i>	132
3. 2. 5. Conclusions	141
3. 3. References	142
Chapter 4: Studies of ancient wall-paintings	149
4. 1. Introduction	151
4. 2. Characterization of decorated stuccoes from the Roman city of Iesso (current Guissona, La Segarra, central Catalonia, NE of Spain).	152
4. 2. 1. Historical context	152
4. 2. 2. Research aims	153
4. 2. 3. Materials and methods	153

CONTENTS

4. 2. 3. 1. <i>Specimen</i>	153
4. 2. 3. 2. <i>Analytical methods</i>	154
4. 2. 4. Results and discussion	155
4. 2. 4. 1. <i>Analysis of pictorial surfaces: characterization of mineral pigments.</i>	155
4. 2. 4. 2. <i>Supporting material</i>	162
4. 2. 5. Conclusions	166
4. 3. References	167
Concluding remarks	173
Agraïments (acknowledgements)	179
Appendix	183
A. 1. Figure captions	185
A. 2. Tables	194
A. 3. Equations	195

In the last few decades, the analytical methods coming from the experimental sciences area had a leading application in the study of Cultural Heritage materials. The increasing use of scientific instrumentation and the data supported from its application open new perspectives for the work of historians and other researchers. Consequently, the employed techniques have contributed to the growth of knowledge of many historical subjects. The use of these techniques is crucial to determine distinguishable features for many topics of Cultural Heritage studies (such as the chronology, the material's intrinsic composition and its provenance or the technology used for the manufacturing). Furthermore, through the study of the material's composition, interpretations of other sort of questions (such as economical and social features) might be done, or even more we could establish the most appropriate restoration and conservation protocols.

Because of the technological advances from the last 15 years, there are 4 important factors that allowed new improvements in the analytical instrumentation: (a) the development of more sensitive detectors, (b) the miniaturization of radiation sources (such as X-ray tubes, laser or infrared) which allowed the fabrication of portable equipments able to do "in situ" analyses, (c) the adequacy of the optical systems (collimators, lenses, beam guides such as monocapillary or polycapillary devices) which permitted analysing reduced areas (from micrometric to nanometric range) and performing mappings of the sample's surface, and (d) the implementation of new software for the spectral analysis, automatic and faster than the old versions. This allows having a wide range of effective analytical tools, which permit obtaining results without altering the object under analysis (a fact of enormous importance in the case of high value materials such as noble metals and / or archaeological materials).

The research presented in this thesis is focused on the application and improvement of analytical existing procedures and the development of new methodologies that can be employed for the study of Cultural Heritage materials. The starting up and modelization of the analytical response was fulfilled by the analysis of different type of ancient materials, starting with materials of relatively simply composition such as metallic alloys, and going through the analysis of materials with more complexes matrices, such as mineral pigments, ancient documents and inks).

In this sense, the first analytical experience was carried out on metallic artefacts. The study involved the characterization of ancient coins from diverse chronology by means of non-destructive energy dispersive X-ray fluorescence (EDXRF). The results of the

analysis allowed determining the elemental composition of the coins and answer some of the questions presented by the historians (such as establish the compositional differences and analogies between the emissions of different workshops, determine the compositional evolution of the alloys throughout the time, and identify possible counterfeits. Moreover the optimization of the experimental parameters and quantification limits (LOQ) were carefully determined for this kind of matrices.

In a second stage, a multi-spectroscopic study of two “oil on copper” paintings from different chronology (seventeenth and nineteenth centuries respectively) was carried out. The results allowed establishing, on one hand, the pigment mass distribution along the painting surfaces by using a semi-quantitative EDXRF method developed specifically for such kind of artworks. On the other hand, identifying the compounds employed to elaborate the paintings (pigments and binders amongst others) by using XRD, RS and FTIR spectroscopies. The obtained spectral data permitted to corroborate that both artworks were conceived in different periods.

In a third stage, a full analytical approach of chromolithographs from the nineteenth century was done by using EDXRF, XRD, RS and FTIR instrumentation. The study was carried out in order to characterize the supporting material and identify the employed inks for colouring the lithographs. Apart of the historical explanations, results of the analysis highlighted the necessity of having a multi-analytical approximation for the proper characterization of such kind of materials.

Finally, a complete archaeometric study of ancient wall-paintings (decorated stuccoes from the 2nd century AC) was accomplished by employing EDXRF, XRD, FTIR, PLM and SEM-EDS. The results of the analytical campaign allowed not only obtaining information related to the nature of the employed pigments and their possible provenance but also characterizing the supporting materials (including their mineralogical and textural description), and determining whether they follow or not the procedures explained in the classical textual sources.

This thesis gives a brief overview of the different analytical methods based on the interaction between the electromagnetic radiation with matter in order to chemically characterize Cultural Heritage materials in a non-destructive way. The obtained results are of considerable interest for the conservation of these materials, as they are usually fragile and have a high potential of alterability.

EDXRF complies with the desired features for the analysis of such kind of materials since it is non-destructive (an essential condition when we work with these sort of materials), it is a multi-elemental technique, it is versatile and the cost per analysis is very low. We can confirm, then, that the EDXRF analysis could be a very useful tool to study ancient materials with diverse matrix:

- For the study of alloys in ancient coins, the EDXRF analysis permits the identification and quantification of the composition of these materials, their classification and the identification of possible counterfeits without applying any sample preparation.
- For the study of oil paintings over metal supports, the semi-quantitative EDXRF analysis allows estimating the pigment mass distribution of the different elements in the painting surface, and elucidating technological features related with the elaboration of such kind of artworks.
- For the archaeometric study of ancient works of art with more complex matrixes (such as mineral pigments and inks) the EDXRF analysis could be used as a screening phase in order to determine the elemental composition of the employed pigments and its surface distribution. Nevertheless, as it is an elemental technique, the use of complementary techniques is necessary. In this sense, XRD allows obtaining information related with the crystalline phases existing in a pigment; RS permits identifying a wide range of organic and inorganic pigments in reduced areas of analysis, while FTIR is indispensable for the characterization of organic compounds such as binders. Finally, by using microscopy techniques such as PLM and SEM-EDS we can obtain detailed information concerning mineralogy, texture and the stratigraphic sequence of the crossed sections precisely prepared.

En les darreres dècades, els mètodes analítics procedents de l'àmbit de les ciències experimentals han tingut una aplicació cabdal a l'estudi de materials del Patrimoni Cultural, ja siguin peces artístiques i/o materials arqueològics. Gràcies a aquests estudis, s'està donant un nou enfocament a les tasques d'historiadors i arqueòlegs. En conseqüència, les tècniques analítiques emprades han contribuït de diverses maneres en l'ampliació dels coneixements en l'àmbit científic i històric. Així, una vegada aplicats els arguments històrics i arqueològics a l'estudi de determinats objectes del Patrimoni Cultural, l'ús de tècniques procedents d'altres disciplines és fonamental per a determinar-ne diferents característiques (ja sigui la cronologia, la composició, la procedència o la tecnologia de producció). A més, a través de l'estudi de la composició d'un material, poden portar-se a terme interpretacions d'un altre tipus (com ara factors econòmics o situacions socials) i fins i tot permet establir, si convé, els protocols de restauració i conservació més adequats.

Gràcies a l'avenç tecnològic dels últims 15 anys, existeixen quatre factors importants que han permès la manufactura d'instrumentació analítica capaç de realitzar anàlisis completament no-destructives: (a) el desenvolupament de detectors de radiació electromagnètica més sensibles, (b) la miniaturització de les fonts de radiació (com ara tubs de raigs X, làsers, infrarojos) que possibilita la fabricació d'equips portàtils i col·locar la instrumentació "in situ", (c) l'adequació de sistemes òptics (co-llimadors, lents, conducció de feix de tipus monocapil·lar o policapil·lar,) que permet analitzar àrees de dimensions reduïdes (des d'una desena de micres fins a rangs nanomètrics) o analitzar variacions areals ("mappings" i "micromappings") de les mostres objecte d'estudi, i (d) el desenvolupament de nous softwares implementats en els equips, per a l'anàlisi espectral de manera ràpida i automatitzada. Aquests avenços han permès disposar d'eines analítiques eficaces, amb la obtenció de resultats sense alterar l'objecte a analitzar, fet que adquireix una transcendència notable en el cas de materials d'un alt valor com poden ser metalls nobles i/o materials arqueològics.

Els estudis que es presenten en aquesta tesi doctoral se centren en l'aplicació i millora de metodologies analítiques existents, relativament senzilles, i el desenvolupament de nous procediments que poden utilitzar-se per a l'estudi de materials del Patrimoni Cultural. La posada en pràctica i la modelització de la resposta analítica de les tècniques utilitzades en aquest treball s'ha dut a terme mitjançant l'anàlisi de materials antics de diferent tipus, començant amb materials de composició relativament senzilla com ara aliatges metàl·lics, i passant gradualment a l'estudi de materials amb matrius més complexes tals com pigments minerals, papers i tintes.

En aquest sentit, en primer lloc es va fer un estudi exhaustiu de monedes antigues de diversa cronologia, mitjançant l'ús de la fluorescència de raigs X per dispersió d'energies (EDXRF). Els resultats de les anàlisis van permetre determinar no només la composició química elemental de les monedes i donar resposta a algunes de les qüestions plantejades pels historiadors (com per exemple, establir quines són les diferències composicionals entre les emissions monetàries de diversos centres productors, definir l'evolució de la composició de les emissions al llarg del temps i inclús identificar possibles falsificacions), sinó que també van permetre optimitzar al màxim les condicions experimentals de les anàlisis i fixar els límits de quantificació per a aquest tipus de matrius.

En segon lloc, es va dur a terme un estudi multi-espectroscòpic de pintures a l'oli sobre suports metàl·lics (coure i llautó) de diversa cronologia (una del segle XVII i l'altra de finals del segle XVIII). Els resultats de les anàlisis van ésser útils, per una banda, per establir la distribució elemental en superfície a partir d'un mètode quantitatiu d'anàlisi EDXRF desenvolupat específicament per aquest tipus d'obres d'art i, per l'altra, identificar els compostos utilitzats en l'elaboració de les pintures (pigments i aglutinants) a partir de la utilització de difracció de raigs X (XRD) i espectroscòpies Raman (RS) i infraroja per transformada de Fourier (FTIR). Les dades obtingudes van permetre corroborar, entre d'altres qüestions, que l'execució d'aquestes obres es va dur a terme en dues èpoques ben diferenciades.

En tercer lloc, es va realitzar un ampli estudi analític (tot emprant EDXRF, RS i FTIR) de cromolitografies del segle XIX, amb l'objectiu de caracteritzar el material de suport i identificar-ne les tintes utilitzades per a la seva coloració. A més de les conclusions històriques, els resultats de les anàlisis posaven de manifest la necessitat de dur a terme una aproximació multi-analítica per a una completa caracterització dels materials estudiats.

Finalment, en quart lloc es va dur a terme un estudi arqueomètric (emprant EDXRF, XRD, FTIR, microscòpia òptica de polarització (PLM) i microscòpia electrònica de centelleig (SEM-EDS)) de pintura mural d'època clàssica (en concret es varen analitzar fragments d'estucs decorats del segle II dC). Els resultats de les anàlisis van permetre obtenir informació relativa a la naturalesa dels pigments utilitzats i la seva possible procedència per una banda, i per l'altra caracteritzar els materials de suport, descriure la qualitat dels estucs i determinar si seguien els models descrits pels autors clàssics.

La present tesis doctoral mostra una visió general dels diversos mètodes analítics basats en la interacció de la radiació electromagnètica amb la matèria per tal de dur a terme la caracterització de materials del Patrimoni Cultural. Els resultats obtinguts són de notable interès per a la conservació d'aquests materials, aspecte rellevant donada la seva fragilitat i elevat potencial d'alterabilitat.

La EDXRF compleix amb els requisits necessaris per a l'anàlisi de materials d'aquesta índole, incloent el seu caràcter no-destructiu (condició imprescindible quan treballem amb materials d'aquestes característiques), la seva capacitat multi-elemental, la seva versatilitat i el baix cost per anàlisi. Podem confirmar que l'anàlisi per mitjà d'EDXRF pot aplicar-se amb èxit a l'estudi de materials antics amb matrius de diversos tipus:

- En el cas d'aliatges metàl·lics en monedes antigues, l'anàlisi EDXRF permet d'una forma molt eficaç i ràpida la identificació i quantificació de la composició química d'aquests materials, la seva classificació en funció de la composició i la identificació de possibles falsificacions sense necessitat d'una preparació prèvia de la mostra.
- En referència a pintures sobre suports metàl·lics, l'anàlisi semi-quantitatiu per EDXRF permet estimar la concentració areal d'elements en superfície i determinar-ne la tecnologia de producció.
- Per a l'estudi arqueomètric d'objectes antics compostos per matrius més complexes (com ara pigments i tintes) l'anàlisi EDXRF pot utilitzar-se com a fase prèvia a la caracterització d'aquests materials en ordre a determinar-ne la seva composició elemental així com la distribució d'aquests en superfície; no obstant, al tractar-se d'una tècnica elemental, per a una correcta caracterització dels materials que componen una obra, es fa necessari l'ús d'altres tècniques complementàries. En aquest sentit, la XRD és útil a l'hora d'obtenir informació relativa a les fases cristal·lines presents en un pigment, especialment en el cas dels pigments coneguts com *brown earth pigments*. La RS permet identificar una gran varietat de pigments (tant orgànics com inorgànics). A més, la versatilitat dels equips de RS permet analitzar àrees de dimensions molt reduïdes, difícils d'analitzar amb un difractòmetre convencional per exemple. L'ús de l'espectroscòpia FTIR es fa indispensable per a la caracterització de compostos inorgànics com ara els aglutinants (ja sigui en obres pictòriques o en papers pintats). Finalment, amb l'ús de tècniques de microscòpia com ara PLM i SEM-EDS, és possible obtenir informació relativa a la mineralogia, la textura i la seqüència estratigràfica de les seccions.

En los últimos años, los métodos analíticos procedentes del ámbito de las ciencias experimentales han tenido una aplicación puntera en el estudio de materiales del Patrimonio Cultural. Gracias a estos estudios, se está dando un nuevo enfoque a las tareas de historiadores y arqueólogos. En consecuencia, las técnicas analíticas utilizadas han contribuido de distintas formas en la ampliación de los conocimientos en el ámbito científico e histórico-arqueológico. El uso de estas técnicas es fundamental para determinar distintas cuestiones en referencia a un determinado objeto del Patrimonio Cultural (ya sea su cronología, su composición, su procedencia o la tecnología de producción). Además, a través del estudio de la composición de un material pueden llevarse a cabo interpretaciones de otra índole (tales como factores económicos o situaciones sociales) e incluso permite establecer, si conviene, los protocolos de restauración y conservación más adecuados.

Debido al avance tecnológico de los últimos 15 años, existen cuatro importantes factores que han permitido la manufactura de instrumentación analítica por medios absolutamente no-destructivos: (a) el desarrollo de detectores de radiación electromagnética mas sensibles, (b) la miniaturización de fuentes de radiación (rayos X, láser, infrarrojos) que posibilita la fabricación de equipos portátiles y colocar equipos "in situ", (c) la adecuación de sistemas ópticos (colimadores, lentes, conducción del haz de tipo monocapilar o policapilar) que permite analizar áreas de dimensiones reducidas (desde décimas de micras hasta rangos nanométricos) o analizar variaciones areales ("mappings" y "micromapping") de las muestras objeto de estudio, y (d) el desarrollo de nuevos softwares, implementado en los instrumentos, para el análisis espectral de forma rápida y automatizada. Todo ello permite disponer de herramientas analíticas eficaces, con obtención de resultados sin alterar en lo más mínimo el objeto a analizar, hecho que adquiere una notable trascendencia en el caso de materiales de alto valor, como los metales nobles y/o materiales arqueológicos.

Los estudios que se presentan en esta tesis doctoral se centran en la aplicación y mejora de metodologías analíticas existentes, relativamente sencillas, y el desarrollo de nuevos procedimientos que pueden ser utilizados para el estudio de materiales del Patrimonio Cultural. La puesta a punto y la modelización de la respuesta analítica de las técnicas utilizadas se han llevado a cabo mediante el análisis de materiales antiguos de distinta índole, empezando con materiales de composición sencilla, tales como metales, pasando paulatinamente al estudio de materiales con matrices más complejas (pigmentos minerales, papeles y tintas).

De este modo, en primer lugar se hizo un estudio exhaustivo de monedas antiguas de diversa cronología mediante el uso de la fluorescencia de rayos X por dispersión de energías (EDXRF). Los resultados de los análisis permitieron determinar no solo la composición química elemental de las monedas y dar respuesta a algunos de los problemas planteados por los historiadores (por ejemplo establecer cuales son las diferencias composicionales entre la emisiones monetarias de diferentes centros productores, definir la evolución de la composición de las emisiones a lo largo del tiempo e incluso identificar posibles falsificaciones) sino que también permitieron optimizar al máximo las condiciones experimentales de los análisis y fijar los límites de cuantificación para este tipo de matrices.

En segundo lugar se llevó a cabo un estudio multi-espectroscópico de pintura al óleo sobre cobre de dos ejemplares de distinta cronología (uno del siglo XVII y otro de finales del siglo XVIII). Los resultados de los análisis han sido útiles, por un lado, para establecer la distribución elemental en superficie a partir de un método cuantitativo de análisis EDXRF desarrollado especialmente para este tipo de obras y, por el otro, identificar los compuestos empleados en la elaboración de las pinturas (pigmentos y aglutinantes entre otros) a partir de la utilización de XRD y espectroscopías Raman y FTIR. Los datos obtenidos permiten corroborar la realización de estas dos obras en dos épocas diferenciadas.

En tercer lugar se realizó un amplio estudio analítico (utilizando un EDXRF, XRD, SEM-EDS, espectroscopías Raman y FTIR) de papeles del siglo XIX, con el fin de caracterizar el soporte e identificar las tintas empleadas. Además de las conclusiones históricas, los resultados de los análisis ponen de manifiesto la necesidad de un estudio multi-analítico para una completa caracterización de los materiales estudiados.

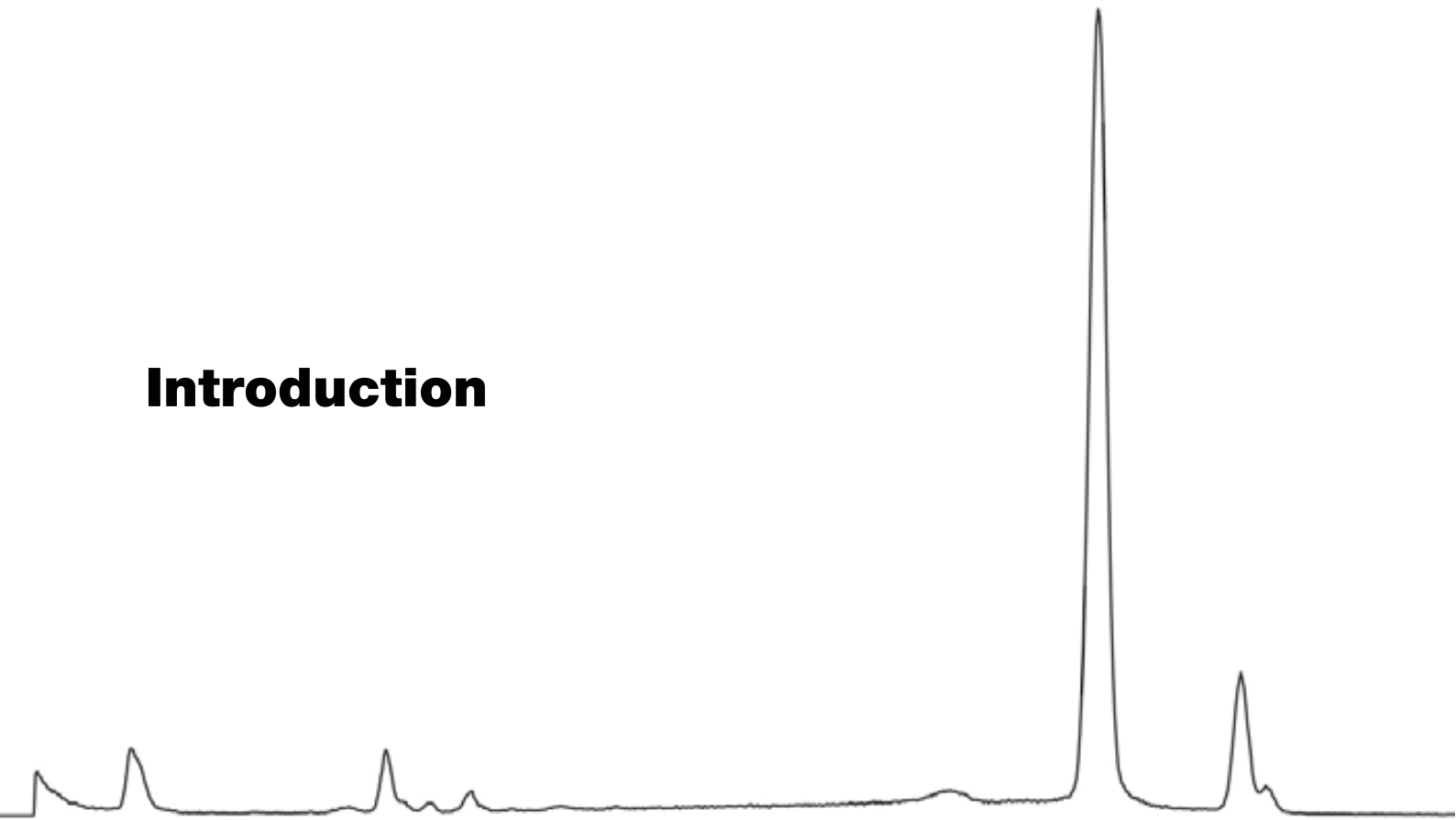
Por último, en cuarto lugar se llevó a cabo estudio arqueométrico completo (empleando EDXRF, XRD, FTIR, microscopía óptica de polarización (PLM) y microscopía óptica de barrido (SEM-EDS)) de pintura mural de época clásica (en concreto se analizaron fragmentos de estucos decorados del siglo II dC). Los resultados de los análisis permitieron obtener información relativa, por un lado, a la naturaleza de los pigmentos utilizados y su posible procedencia y, por otro lado, caracterizar los materiales de soporte, describir la calidad de los estucos y determinar si siguen los modelos descritos por los autores clásicos.

La presente tesis doctoral muestra una visión general de los diferentes métodos analíticos basados en la interacción de la radiación electromagnética con la materia para llevar a cabo la caracterización de materiales del Patrimonio Cultural. Los resultados obtenidos son de notable interés para la conservación de dichos materiales, aspecto relevante dada su fragilidad y elevado potencial de alterabilidad.

La EDXRF cumple con los requisitos necesarios para el análisis de materiales de esta índole, incluyendo su carácter no-destrutivo (condición imprescindible cuando trabajamos con materiales de este tipo), su capacidad multi-elemental, su versatilidad y su bajo coste. Podemos confirmar que el análisis EDXRF puede aplicarse con éxito en el estudio de materiales antiguos con matrices de distinta índole:

- En el caso de aleaciones metálicas en monedas antiguas, de una forma muy eficaz y rápida el análisis EDXRF permite la identificación y cuantificación de la composición química de dichos materiales, su clasificación en función de la composición elemental y la identificación de posibles falsificaciones sin necesidad de una preparación previa de las muestras a analizar.
- En lo que se refiere a pinturas sobre soporte metálico, el análisis semi-cuantitativo por EDXRF permite estimar la concentración areal de elementos en superficie y determinar la tecnología de producción de dichas obras.
- Para el estudio arqueométrico de objetos antiguos compuestos por matrices más complejas (tales como pigmentos y tintas) el análisis EDXRF puede emplearse como fase previa a la caracterización de dichos materiales con el fin de determinar la composición elemental de los pigmentos así como su distribución en superficie; sin embargo, al tratarse de una técnica elemental, se hace necesario el uso de otras técnicas complementarias para una correcta caracterización de los materiales que componen una obra. En este sentido, la XRD es útil a la hora de obtener información referente a las fases cristalinas presentes en un pigmento. La RS, por otro lado, permite identificar una gran variedad de pigmentos, tanto orgánicos como inorgánicos. Además, la versatilidad de los equipos de RS permite analizar zonas de dimensiones muy reducidas, difíciles de analizar con un difractor convencional. El uso de la técnica de FTIR se hace indispensable para la caracterización de compuestos orgánicos tales como aglutinantes (ya sea en obras pictóricas como en papeles pintados). Finalmente, con el uso de técnicas de microscopía tales como PLM y SEM-EDS es posible obtener información acerca de la mineralogía, la textura y la secuencia estratigráfica de las secciones previamente preparadas.

Introduction



I. 1. Analysis and Cultural Heritage

In the last few decades, the analytical methods coming from the experimental sciences area have had a leading application in the study of Cultural Heritage materials (not only artworks, but also objects of archaeological interest or buildings of historical value). Thanks to these studies, a new point of view to the work of historians and other scholars is being given, both in the area of cataloguing and inventory of collections in museums as well as in archaeological excavations. The intensive and multi-disciplinary research that has been carried out in the interface between art, archaeology and solid state science for studies concerning artworks and archaeological artefacts has substantially contributed to the growth of knowledge of many historical subjects. (Ciliberto and Spoto, 2000; Moiola and Seccaroni, 2000; Sándor *et al.*, 2002; Linke *et al.*, 2004 (a); Herrera, 2009).

The use of experimental techniques coming from different scientific disciplines is essential to determine distinguishable features for many topics of Cultural Heritage studies, such as:

- The chronology
- The material's intrinsic composition and its provenance
- The craftsmanship and the technology used for the manufacturing
- The historical reality from the period of time in which the artwork was conceived can be reflected by its composition and other measurable features (i.e. economical and social features).

Furthermore, the fact that we could determine alteration products that may affect the integrity of one particular artwork allows selecting the most appropriate restoration protocols and deciding protective measures to accomplish good conservation strategies (Guerra, 1995; Caneva *et al.*, 2000; Ciliberto and Spoto, 2000; Janssens *et al.*, 2000; Linke *et al.*, 2004 (b)).

I. 2. Physicochemical methods of analysis

Nowadays, there is an extensive range of analytical techniques that are of common use in the field of Archaeometry. The adequate analytical methodology used as well as the choosing of instrumental techniques for each specific case are conditioned by 3 factors: (1) the type of information required and the level of precision that you want to

get, (2) the necessity to minimise damage to the object under study, and (3) the response time, especially when the diagnosis is made to take urgent restoration measures (Gallardo *et al.*, 2001).

In accordance to the current regulations for the protection and preservation of Cultural Heritage, which considers its assets as an irreplaceable legacy that must be transmitted in the best conditions for the future generations (Generalitat de Catalunya (1993) *LLEI 9/1993, de 30 de setembre, del patrimoni cultural català* -Catalonia's Legislation concerning the Catalan Cultural Heritage) the use of traditional elemental analysis methods is almost impossible, since they generally require the destruction of the sample or the object to be studied (Al-Kofahi *et al.*, 2000; Mantler and Schreiner, 2000; Cesareo *et al.*, 2007). Moreover, the fact that historical and archaeological objects are generally unique or artistically relevant increasingly promotes the use of non-destructive analytical techniques as well as micro-destructives ones (Caneva *et al.*, 2000). In the last twenty years, the chemical techniques based on the destruction of the material (such as flame atomic emission spectrometry (FAES), atomic absorption spectrometry (AAS), inductively coupled plasma mass spectrometry (ICP-MS) or inductively coupled plasma optical emission spectrometry (ICP-OES) amongst others) have been gradually replaced by techniques based on the interaction of electromagnetic radiation with matter (Guerra, 1998).

The main goal when using a micro-destructive technique is that the object from which we have taken a micro-sample remains aesthetically intact, this is, we should avoid all visible damage. However, we have to take into consideration that the analytical trustworthiness directly depends on several aspects (Ciliberto and Spoto, 2000) to properly answer the following question: *What is actually the minimum amount of sample required (to analyze) in order to obtain representative results?*

The best solution might be the use of non-destructive techniques, which allow obtaining analytical information with no damage to the sample or object under investigation (Mantler and Schreiner, 2000; Röessiger and Nensel, 2003; Janssens and Van Grieken, 2004). The possibility of using these methods is of enormous benefit when sampling is not viable or when micro-samples used for analysis need to be returned at the end of the study (Gigante and Cesareo, 1998; Ciliberto and Spoto, 2000; Janssens and Van Grieken, 2004). Moreover, removing objects from museums is sometimes not feasible due to the rules preventing their transport to the laboratory.

I. 3. Application of electromagnetic radiation to determine the chemical composition of Cultural Heritage materials.

In the field of analysis of Cultural Heritage and related materials, spectroscopic methods based in the interaction of radiation with matter are the most widely employed. The energy (E) of this radiation is directly proportional to its frequency (c / λ) (**Eq. I. 1**) and defines its effects on molecules. Depending on the range of energies we use from different regions of the electromagnetic spectrum (**Table I. 1**) we will be able to investigate different magnitudes of energy level separation in the sample being analyzed (Stuart, 2007).

The energy applied for study is given by:

$$E = \frac{h \times c}{\lambda} \quad (\text{Eq. I. 1})$$

where E is the energy, λ is the wavelength, h is the Planck constant and c is the speed of light in vacuum.

Table I. 1

Energy range and wavelength of electromagnetic radiation.

Energy range (keV)	Wavelength	Name
$< 10^{-7}$	cm to km	Radio waves
$< 10^{-3}$	μm to cm	Microwaves
$< 10^{-3}$	μm to mm	Infrared
0.0017-0.0033	380 to 750 nm	Visible light
0.0033-0.1	10 to 380 nm	Ultraviolet
0.11-100	0.01 to 12 nm	X-rays
10-5000	0.0002 to 0.12 nm	Gamma rays

While high energetic radiations cause electronic transitions (and consequently provide information about the electronic structure of an atom), the use of less energetic radiations promote vibrational and rotational movements (thus, giving information about the bonds in molecules and their structural configuration).

From the whole electromagnetic spectrum, for the characterization of objects of historical value it is possible to select three regions (infrared radiation (0.74 μm -1000 μm), radiation in the visible range (390-770 nm) and X-rays (0.1 and 100 Å)) as they are considered as being of special interest for characterization of works of art

(Mairinger, 2004). Furthermore, the complementary use of highly energetic electrons (employed in electron microscopy) might be helpful to describe diverse features of artworks.

I. 3. 1. Infrared

Infrared are electromagnetic waves with high wavelengths (they are in the region between 0.74 μm and to 1000 μm of the electromagnetic radiation spectrum, **Table I. 1**). In this work we selected two techniques that use infrared as a radiation source (Raman and Fourier transform infrared spectroscopies) since both of them have been widely used to study Cultural Heritage materials. Both techniques provide molecular information of organic and inorganic materials, this is, the information about how the elements are linked. Infrared spectroscopy involves the excitation of vibrations of bonds in molecules by an incident infrared radiation and determines what fraction of this incident radiation is absorbed at a particular energy. Raman spectroscopy, on the other hand, measures what fraction of this incident radiation is scattered by a molecule (Stuart, 2007).

Raman spectroscopy (RS) measures the radiation scattered by a molecule (Stuart, 2007). When the infrared radiation beam of wavenumber ν_0 striking on a molecule does not correspond to that of absorption process, it is scattered. This scattered radiation might has not changed in wavenumber (Rayleigh scattering) or might has increased or decreased in wavelength (Raman scattering, $\nu_0 \pm \nu_M$) (**Fig. I. 1**). In molecular systems, the wavenumbers ν_M are found to lie mainly in the ranges associated with transitions between vibrational, rotational and energy electronic levels (Long, 2004). In order to be Raman active, a molecular vibration or rotation must cause a change in a component of the molecular polarisability. The most commonly employed source of radiation is the near-infrared region of the electromagnetic spectrum.

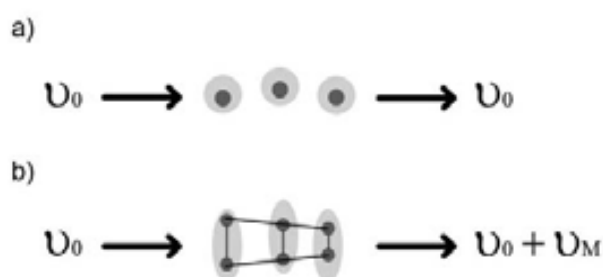


Fig. I. 1 Scattering processes. (a) Rayleigh scattering and (b) Raman scattering.

The analysis of Cultural Heritage and related materials is one of the most auspicious fields of application of Raman spectroscopy since is a quite sensitive technique, reliable, non-destructive and can be used directly on the sample without any kind of sampling procedure (Castro *et al.*, 2005). The development of microscopes and microprobes carried out in the last years has created new opportunities for the non-destructive “in situ” analyses of samples (Castro *et al.*, 2003). The principles of the technique and its application in Art and Art History are widely explained in the book of Edwards and Chalmers (2004).

Infrared (IR) spectroscopy is one of the most important methods for the identification and characterization of chemical functional groups from vibrational spectra (Manso and Carvalho, 2009). An infrared spectrum is commonly obtained by passing infrared radiation through a sample and determining what fraction of the incident radiation is absorbed at a particular energy. The energy at which any peak in an absorption spectrum appears corresponds to the frequency of a vibration of a part of a sample molecule. For a molecule to show infrared absorptions it must possess a specific feature: an electric dipole moment of the molecule must change during the vibration. The first infrared instruments were of the dispersive type. These instruments separated the individual frequencies of energy emitted from the infrared source. This was accomplished by the use of a prism or grating. To overcome the limitations encountered with these instruments (such as slow scanning process), a method for measuring all of the infrared frequencies simultaneously was developed: the so-called Fourier transform infrared (FTIR) spectrometry, which employs an optical device known as interferometer and applies the Fourier transformation mathematical method for the identification of each individual frequency determined by the interferometer (Thermo Nicolet Corporation, 2001).

Despite the fact that FTIR spectroscopy has been extensively used in the study of different materials such as ancient documents (Workman, 2001; Manso and Carvalho 2009), paintings (Franquelo *et al.*, 2008) and old mortars (Genestar *et al.*, 2006), amongst other materials, this technique is of special interest for the identification of organic binding media in artworks (Doménech-Carbó *et al.*, 2001; Castro *et al.*, 2008; Sarmiento *et al.*, 2011). The principles of the technique as well as practical information on the use of IR spectroscopy for the analysis of museum objects are widely explained in the book of Derrick *et al.* (1999).

I. 3. 2. Visible light

Visible light is electromagnetic radiation with wavelengths in the range between 390 nm (violet) and 770 nm (red) (**Table I. 1**) and is made up of waves travelling in all directions of vibration and propagation. In this work we selected one technique that employs visible light as a source of radiation (polarizing light microscopy -PLM).

Light could also be defined as electrically charged particles that, in its displacement have an associated induced magnetic field. When the light beam interacts with the crystalline matter (which in fact is also a set of electric charges in movement (electrons of the atoms) and consequently has its corresponding induced magnetic field) the result is the coupling of these magnetic fields, so that the properties of light are modified by the mineral. These changes depend on the structure and composition of the mineral. PLM employs polarized light (in which waves are travelling in one vibration direction (**Fig. I. 2**)) in order to study the occurred changes and identify the material under analysis as well as to magnify images of small samples; however PLM cannot directly determine the crystal structure or material's chemical composition (Nesse, 1986; Perkins and Henke, 2002).

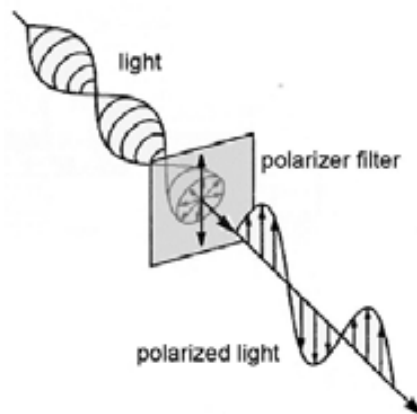


Fig. I. 2 Schematic explanation of the polarization of light
(modified from Perkins and Henke (2002)) .

For the proper observation of the samples, these have to be specially prepared as thin cross sections (30-40 μm thick), so that PLM is considered a micro-destructive technique. Nevertheless, this thin cross section is durable and can be examined as much as needed.

PLM has been a key technique used in the field of Cultural Heritage materials analysis, providing fast and reliable identifications of the structures and mineral components (the obtained results can be helpful to determine provenances and, in the case of manufactured products, the techniques used in its preparation) based on the optical properties of the materials under study (Siddal, 2006).

I. 3. 3. X-rays

X-rays are electromagnetic waves with very low wavelengths (they are in the region between 0.1 and 100 Å of the electromagnetic radiation spectrum, **Table I. 1**). They are typically generated when electrically charged particles lose their energy due to a change on their state of movement (such as braking, change of direction, transition to a lower energy level in the atomic shell or the impact into materials).

Depending on the way in which the X-rays interact with or are emitted by matter, there are different experimental techniques (such as X-ray diffraction –XRD, energy dispersive X-ray fluorescence –EDXRF, proton induced X-ray emission –PIXE, electron micro probe analysis –EPMA, X-ray photoelectron spectroscopy –XPS, Auger electron spectroscopy –AugES, amongst others). Despite the fact that all of them have been widely employed for the characterization of Cultural Heritage materials, in this work only EDXRF and XRD were applied for the compositional and structural analysis of the samples, taking into account the availability of our laboratories and the main features of the samples under investigation.

The XRF is based on the excitation of the atoms of the studied material by an X-ray primary beam (**Fig. I. 3**). This process allows determining the existing in the sample as the energy of the produced secondary X-rays is characteristic of each element. The elements of the sample can be established from the position of maximum intensity (qualitative analysis). If we integrate each elemental profile we may obtain their mass proportions and if we compare them with the spectrum of a standard, we may obtain the quantification of these elements (quantitative analysis). The principles of the technique as well as its advantages and disadvantages are widely explained in the literature (Van Grieken and Markowicz, 1993; Beckhoff *et al.*, 2006).

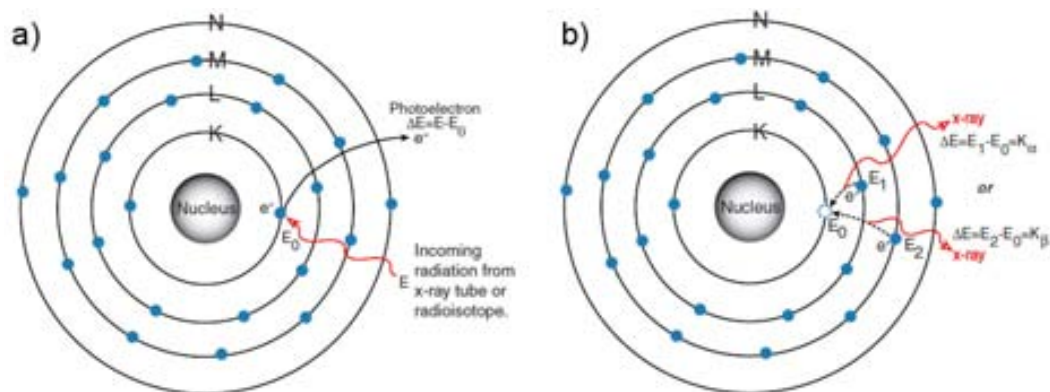


Fig. I. 3 The X-ray fluorescence process: (a) an e^- in the K shell is ejected from the atom by the external primary excitation X-ray beam creating a vacancy; (b) this vacancy is filled by an e^- from the L or M shell. In this process, it emits a characteristic X-ray unique to this element. (Modified from Amptek Inc. (2002))

EDXRF is of special interest in the field of Cultural Heritage for the chemical analysis of inorganic materials and trace elements determination. It is a non-destructive technique, fast and reliable, that allows simultaneous multi-elemental analysis. Moreover, this technique does not require any special sample preparation before the analysis and a large number of measurements can be done without altering the sample under analysis during the process of spectra acquisition (Hall *et al.*, 1973; Pollard and Heron, 1996; Guerra, 1998; Mantler and Schreiner 2000; Moiola and Seccaroni, 2000; Sándor *et al.*, 2000; Vijayan *et al.*, 2004). Recent development of semiconductor detectors and miniaturization of X-ray tubes (Cesareo *et al.*, 1996; Moiola and Seccaroni, 2000) allowed to have portable systems (as small as to facilitate their transport and make “in situ” measurements) able to analyze objects of complex and irregular shapes (none flatted surfaces) with high trueness (Janssens and Van Grieken, 2004).

On the other hand, XRD takes place when an X-ray beam of known wavelength interacts with a crystalline substance. X-rays wavelengths are about equal to the interatomic distances of the components from the crystalline lattice. When the X-rays strike on the sample, they are diffracted to angles that directly depend on these distances (**Fig. I. 4**). Thus, the diffraction signal of a solid compound reflects its crystal structure.

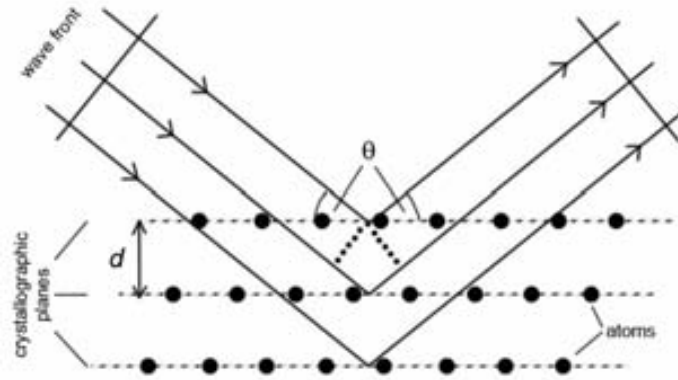


Fig. I. 4 Geometry of Bragg reflection of an X-ray wave front by set of crystallographic planes (modified from Janssens (2004)).

The Bragg's law establishes those directions on which the constructive interference occurs (**Eq. I. 2**):

$$n \lambda = 2 d \sin \theta \quad (\text{Eq. I. 2})$$

where " d " is the distance between the layers of atoms.

The physical approach to the diffraction phenomenon is widely related in the literature (Bermúdez-Polonio, 1981; Rodríguez-Gallego, 1982) and it has been used not only to determine crystal structures but also for some textural analysis (i.e. strength, crystallite size or phase transformation) in materials science research.

X-ray diffraction technique (which is one of the most widely used techniques in the analysis of inorganic materials) was selected to carry out crystalline phase analysis of the studied artworks. Once the diffractograms is properly interpreted, XRD allows identifying the mineral compounds. In some cases the crystalline phases, previously determined by XRD, may be indicative of thermal processes and / or provide information about the manufacturing process of the object itself (Pollard *et al.*, 2007). Recent advances in the field of XRD analysis (Scott, 2004) were significant regarding the implementation of this technique in the field of Cultural Heritage materials analysis.

I. 3. 4. High resolution imaging – Electron microscopy

Scanning electron microscopy (SEM) parallels optical microscopy, but instead of using light and lenses, electrons in a vacuum chamber and electromagnetic fields are used

(Stuart, 2007). The wavelength of an electron is given by the Broglie's equation (**Eq. I. 3**). In a 10 kV SEM, for example, the electron's wavelength is about 0.0123 nm.

$$\lambda = \frac{h}{p} \quad (\text{Eq. I. 3 (Broglie, 1950)})$$

where h is Planck's constant and p the relativistic momentum of the electron.

The magnification produced by the SEM is the relationship between the sizes of the final image with the area of the sample that has been scanned. Thus, for example, if the probe scans an area of about 1 mm² and the image on the screen is 100 mm², this has been amplified 100 times.

The incident beam of energetic electrons scans the surface of a sample and produces number of signals that, appropriately treated, allows obtaining morphological as well as structural and micro-analytical information about the sample under study. The interaction between primary electron beam with the sample causes several types of secondary radiations (**Fig. I. 5**).

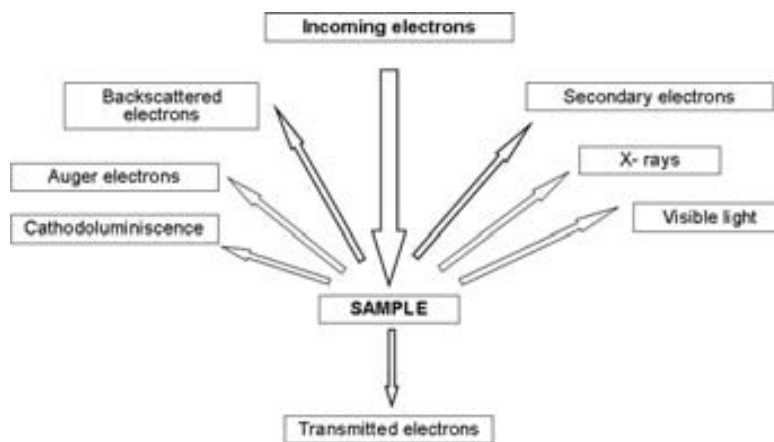


Fig. I. 5 Schematic diagram illustrating various signals emitted when the incident electron beam interacts with the sample.

Of all forms of radiation resulting from the interaction between the incident electron beam and the sample, both secondary and backscattered electrons are the most important ones in electron microscopy. The first ones are electrons with low energies resulting from the emission of the valence electrons of the constituent atoms in the sample. Since the energy of these secondary electrons is very small, only those generated at the top surface of the sample are emitted, so that they provide information

about the surface topography of the sample. The second ones are electrons from the incident beam that have interacted (collided) with the atoms of the sample and have been reflected. The emission intensity of these electrons depends on the average atomic number of atoms in the sample, so heavier atoms produce a larger amount of backscattered electrons. The virtual image given by these electrons reveals differences in chemical composition.

Scanning electron microscopy may also be combined with an energy dispersive system (EDS) in order to carry out elemental analysis (Stuart, 2007). As the electron beam strikes a sample, it also excites the atoms in the sample and produces secondary X-ray emission (the energy of which is characteristic of elements present in the sample).

Amongst the technical studies of works of art, it is difficult to find a publication that does not include SEM analysis. However, conventional high vacuum scanning electron microscopes require a sample be taken and its surface specially prepared to become electrical conductor (usually by carbon or metal coatings), which means that it is considered, at least, a micro-destructive technique. Nevertheless, with the development of environmental scanning electron microscopes (ESEM) at the 80's, the applicability of this technique for the study of such kind of materials has spread out since ESEM is able to image non-conductive samples at a variable range of pressures, temperatures and gas environments (Burnstock and Jones, 2000).

For a more detailed explanation about the theoretical aspects of the technique as well as the application of SEM analysis in Cultural Heritage materials see Goldstein *et al.* (2003) and Adriaens and Dowsett (2004).

I. 4. Outline of the thesis

The research work included in this thesis is focused on the improvement of analytical existing procedures and the development of new methodologies that can be applied to the characterization of Cultural Heritage materials (such as metallic artefacts, paintings, ancient documents -paper support and inks- and decorated stuccoes) in order to reveal some clues to better understand the origin of these objects and how they were produced. The thesis is organised into 4 chapters, which focuses on different material matrices.

Chapter 1 illustrates what should be expected from EDXRF analyses on metallic artefacts by presenting two applications in the numismatic field. Both works focused on the elemental characterization of the coins (mainly determining the type of alloy used for their production), study their compositional evolution throughout the time (whether the alloys changed their composition) and determine the differences and analogies between the emissions, always keeping in mind the historical context of each case. Furthermore, the validity of EDXRF analytical method for the characterization of this type of artwork was evaluated. Chapter 2 aims to report the suitability of EDXRF for the study of paintings on metal supports by presenting two works. The first one deals with the potentiality of a quantitative EDXRF methodology for the estimation of the surface areal distribution of pigments, while the second approach aims to report the effectiveness of EDXRF technique in combination with XRD, Raman and FTIR spectroscopies for the characterization of such kind of artworks. Chapters 3 and 4 assess the capacity of EDXRF for the study of ancient materials with complex matrices (such as chromolithographs and decorated stuccoes) and emphasize the need of having a multi-analytical approach for studying this sort of materials.

The main points reported in the present work can be summarised as follows:

- I. To provide a complete description of the organic and inorganic compounds existing in different artworks.
- II. To evaluate the suitability of EDXRF for the study of different kinds of works of art:
 - i. To demonstrate the effectiveness of EDXRF for the study of ancient coins.
 - ii. To develop a new analytical methodology for the application of EDXRF to study the areal mass distribution of pigments in oil paintings on metallic supports.
 - iii. To assess the adequacy of EDXRF for the study of ancient documents and decorated stuccoes.
- III. To obtain a detailed characterization of the different artworks by combining several experimental laboratory techniques (such as EDXRF, XRD, RS, FTIR, PLM and SEM-EDS).
- IV. To highlight the necessity of having a multi-spectroscopic approach for studying Cultural Heritage materials.

I. 5. Methodology

For the proper characterization of the different artworks studied in this thesis, the combination of techniques of elemental (EDXRF), molecular (XRD, Raman and FTIR) and imaging analysis (PLM and SEM-EDS) has been accomplished by using the following equipments:

Energy dispersive X-ray fluorescence equipments

In this work, two EDXRF equipments were used. The first one is a FISCHERSCOPE® X-RAY XAN® spectrometer (Helmut Fischer GmbH, Germany), equipped with a micro focus tungsten X-ray tube (operating at 10, 30 or 50 kV and at maximum intensity of 1 mA), a Si-Pin detector with 180 eV of resolution at Mn K α energy, several filters to improve peak/background ratio and four X-ray beam collimators (0.2, 0.6, 1 and 2 mm in diameter) (**Fig. I. 6**).



Fig. I. 6 Fisherscope® X-RAY XAN® (Helmut Fischer GmbH, Germany) spectrometer at the Numismatic Cabinet of Catalonia (GNC) facilities in the National Museum of Fine Arts of Catalonia (MNAC) (photography: A. Pitarch).

The second one is a bench top small-spot EDXRF spectrometer (XDV-SD® model, Helmut Fischer GmbH, Germany) designed for coating thickness measurement and materials testing (**Fig. I. 7**). It consists on a microfocus tungsten anode X-ray tube (using a maximum power of 50 W, a maximum voltage of 50 kV and a maximum current of 1 mA) and a Si-Pin semiconductor detector (Peltier cooling at -50°C; with 180 eV FWHM at Mn K α line). The spectrometer is equipped with 5 primary filters (nickel 10 μ m, molybdenum 70 μ m, aluminium 500 μ m and 1000 μ m and titanium 300 μ m) which can be used to reduce spectral background and eliminate the tungsten tube signal, and four collimators (0.1, 0.3, 1 and 3 mm in diameter) which are used to adjust the X-ray focal spot to selected areas. A video camera allows viewing and selecting the irradiated area with up to $\times 45$ magnification and the motorized X-Y-Z stage allows

INTRODUCTION

focusing and searching of the points of interest. The instrument can be used to obtain elemental chemical mappings by programming a grid of points for analysis.

Fig. I. 7 Fisherscope® XDV-SD® (Helmut Fischer GmbH, Germany) spectrometer at the LARX facilities (ICTJA-CSIC) (photography: A. Pitarch).



The EDXRF spectra were processed using the WinFTM® Software Program version 6.20 (Helmut Fischer GmbH + Co. KG, Germany).

X-ray diffraction instrument

The diffractometer used for the study of the artworks was a D8 Advance (Bruker AXS GmbH, Germany) with a Cu K α target tube X-ray source (operating at 40 kV and 40 mA), a primary Göbbel mirror and an energy dispersive SOL-X detector (**Fig. I. 8**). The angular range (2θ) was explored by a goniometer scanning from 4° to 60°, at a step size of 0.05° and a counting time of 3 seconds per step. Evaluation of X-ray diffractograms was performed by using the routines of the Diffrac.Suite™ software package (Bruker AXS GmbH, Germany) and the attached specific powder diffraction file (PDF) database (International Centre for Diffraction Data - ICDD, Pennsylvania, USA).



Fig. I. 8 Diffractometer D8 Advance (Bruker AXS GmbH, Germany) from the Service of X-Ray Diffraction of the ICTJA-CSIC (photography: A. Pitarch).

Raman equipments

Two Raman instruments were used for the characterization of the studied artworks. The first one was an ultramobile innoRam ® Raman spectrometer (B&WTEK_{INC}, Newark, USA) provided with a CleanLaze® technology 785 nm excitation laser and equipped with an Inphotonics RamanProbe™ Fiber Optic Sampling RPS2785-12-5 microprobe (Norwood, USA) (**Fig. I. 9**). Spectral resolution of 2 cm^{-1} . The system was previously calibrated with the 520.5 cm^{-1} silicon line. The equipment is provided with a micrometric manual stage and two microscope lenses ($\times 20$ and $\times 50$ of magnification) in conjunction with a colour TV microcamera which allows searching the area of interest and focusing the laser beam's spot. Data acquisition was done with the software attached to the equipment (B&WTEK 3.26, Newark, USA).



Fig. I. 9 Raman spectrometer innoRam ® (B&WTEK_{INC}, Newark, USA) of the IBea¹ laboratory facilities at Parque Científico y Tecnológico de Bizkaia (photography: A. Pitarch).

The second Raman equipment was a Renishaw InVia Raman spectrometer, joined to a Leica DMLM microscope (**Fig. I. 10**). The spectra were acquired with the Leica $\times 50$ N Plan (0.75 aperture) objective. The spatial resolution for the $\times 50$ objectives is about $2\text{ }\mu\text{m}$. For the focusing and searching of the points of interest, the microscope implements a Prior Scientific motorized stage (XYZ) with a joystick. The system has two lasers: 514 nm (an ion-argon laser which has a nominal power at the source of 50 mW, being the maximum power at the sample 20 mW) and 785 nm (a diode laser).

¹ IBea Research Group (Ikerkuntza eta Berrikuntza Analitikoa, Department of Analytical Chemistry, University of the Basque Country).



Fig. I. 10 Raman spectrometer Renishaw InVia from LASPEA Laboratory from the General Research Services (SGIker) of the University of the Basque Country (photography: K. Castro).

The spectral manipulations and the interpretation of spectra were performed by the Thermo Scientific Omnic software version 7.2 (Thermo Electron Corporation) by comparing the obtained Raman spectra with the spectra of pure standard compounds from several databases (Castro *et al.*, 2005; Downs, 2006).

Infrared instrumentation

Three infrared equipments were used for the characterization of the studied artworks.

The first one was a portable Exoscan FTIR A₂ Technologies (Danbury, Connecticut, USA) spectrometer (**Fig. I. 11**). To obtain a good signal-to-noise ratio, 120 scans were accumulated for each spectrum at a resolution of 4 cm⁻¹, in the spectral range of 650-4000 cm⁻¹. Data acquisition was carried out by using the A₂ Technologies software. The obtained spectra were collected in diffuse reflectance mode (DRIFT) by means of the 4100 Exoscan FTIR Diffuse Reflectance sampling interface.



Fig. I. 11 Exoscan FTIR A₂ Technologies (Danbury, Connecticut, USA) spectrometer of the IBea laboratory facilities at Parque Científico y Tecnológico de Bizkaia (photography: A. Pitarch).

The second infrared equipment was a Thermo Scientific Nicolet iN10 MX Infrared Microscope spectrometer (**Fig. I. 12**) from the Molecular Analysis Laboratory – General Research Services of the University of the Barcelona (SCT-UB). The instrument was provided with a sample holder Spectra-Tech Micro Compression Cell and Diamond Window. To obtain a good signal-to-noise ratio, 64 scans were accumulated for each spectrum at a resolution of 4 cm^{-1} , in the range of $650\text{--}4000\text{ cm}^{-1}$. The obtained spectra were collected in transmittance mode.



Fig. I. 12 Thermo Scientific Nicolet iN10 MX Infrared Microscope spectrometer (source: Thermo Fisher Scientific Inc. (2011)).

The third one was a JASCO 6000 Series FTIR spectrometer (Japan) (**Fig. I. 13**). To obtain a good signal-to-noise ratio, 120 scans were accumulated for each spectrum at a resolution of 4 cm^{-1} , in the range of $400\text{--}4000\text{ cm}^{-1}$ (mid-IR). Data acquisition was carried out by using the Spectra Manager II™ (UK) software. The obtained spectra of specially prepared samples were collected in transmittance mode.



Fig. I. 13 JASCO 6000 Series FTIR (Japan) spectrometer of the IBea laboratory facilities at Parque Científico y Tecnológico de Bizkaia (photography: A. Pitarch).

Interpretation of the spectra was performed by the Thermo Scientific Omnic Software version 7.2 (Thermo Electron Corporation) and the identification of organic and inorganic compounds was based on comparing the recorded FTIR spectra with those of library spectra (Castro *et al.*, 2003).

Polarizing light microscope

Morphological observations of specially prepared thin cross sections (30 μm thick) of the samples were carried out by using a polarized microscope (NIKON Eclipse E400 POL) equipped with 4 objectives ($\times 4$, $\times 10$, $\times 20$ and $\times 40$) and joined to a NIKON COOLPIX5400 microcamera by means of NIKON COOLPIX MDC Lens adaptor (**Fig. I. 14**).



Fig. I. 14 NIKON Eclipse E400 POL microscope of the Ud'EA² laboratory facilities at the Institut Català d'Arqueologia Clàssica, Tarragona (photography: A. Pitarch).

Scanning electron microscope



Observation and characterization of polished cross sections coated with carbon was performed at the Microscopy Services of the UAB³, through a JEOL JSM-6300 scanning electron microscope equipped with energy dispersive X-ray analysis system EDS Link Isis-200. EDS analysis was carried out using 15 mm working distance and an acceleration potential of 20 kV (**Fig. I. 15**).

Fig. I. 15 JEOL JSM-6300 scanning electron microscope
(source: http://www.geol.ucsb.edu/research/labs_equipment.html)

² Ud'EA: "Unitat d'Estudis Arqueomètrics"

³ UAB: Autonomous University of Barcelona

I. 6. References

ADRIAENS A., DOWSETT, M.G. (2004) *Electron microscopy and its role in cultural heritage studies*, in: JANSSENS K., VAN GRIEKEN R. (Eds.) *Non-destructive microanalysis of cultural heritage materials. Vol. XLII*. Wilson and Wilson's, Comprehensive Analytical Chemistry, Elsevier, 73-124.

AL-KOFAHI M.M., AL-TARAWNEH K.F. (2000) *Analysis of Ayyubid and Mamluk Dirhams Using X-Ray Fluorescence Spectrometry*. X-Ray Spectrometry, 29, 39-47.

AMPTEK Inc. (2002) *X-Ray Fluorescence – A Description* [pdf]. Available from: <http://www.amptek.com/pdf/xrf.pdf> (<http://www.amptek.com/appnotes.html> [on-line]) [last accessed 15th September 2011].

BECKHOFF B., KANNGIEBER B., LANGHOFF N., WEDELL R., WOLFF H. (2006) (Eds.) *Handbook of Practical X-Ray Fluorescence Analysis*. Springer, Berlin.

BERMÚDEZ-POLONIO J. (1981) *Métodos de difracción de rayos X: principios y aplicaciones*. Ediciones Pirámide, Madrid.

De BROGLIE L. (1950) *Optique électronique et corpusculaire*. Herman, Paris.

BURNSTOCK A., JONES C. (2000) *Scanning electron microscopy techniques for imaging materials from paintings*, in: CREAGH D.C., BRADLEY D.A. (Eds.) *Radiation in Art and Archaeometry*. Elsevier Science B. V., Amsterdam, 202-231.

CANEVA C., FERRETI M. (2000) *XRF Spectrometers for Non-Destructive Investigations in Art and Archaeology: the Cost of Portability. Proceedings of World Conference on Non-destructive Testing (Roma, Italy, 15-21 October 2000)*.

CASTRO K., PÉREZ M., RODRÍGUEZ-LASO M.D., MADARIAGA J.M. (2003) *Library of FT-Raman spectra of pigments, minerals, pigment media and varnishes, and supplement to existing library of Raman spectra of pigments with visible excitation*. Analytical Chemistry, 75, 214A-221A.

CASTRO K., PÉREZ-ALONSO M., RODRÍGUEZ-LASO M.D., FERNÁNDEZ L.A., MADARIAGA J.M. (2005) *On-line FT-Raman and dispersive Raman spectra database*

of artists' materials (e-VISART database). Analytical and Bioanalytical Chemistry, 382, 248–258.

CASTRO K., SARMIENTO A., MAGUREGUI M., MARTÍNEZ-ARKARAZO I., ETXEBARRIA N., ANGULO M., BARRUTIA M.U., GONZÁLEZ-CEMPELLÍN J.M., MADARIAGA J.M. (2008) *Multianalytical approach to the analysis of English polychromed alabaster sculptures: μ Raman, μ EDXRF and FTIR spectroscopies*. Analytical and Bioanalytical Chemistry, 392, 755-763.

CESAREO R., GIGANTE G. E., CANEGALLO P., CASTELLANOD A., IWANCZYKE J. S., DABROWSKI A. (1996) *Applications of non-cryogenic portable EDXRF systems in archaeometry*. Nuclear Instruments and Methods in Physics Research A: Accelerators, Spectrometers, Detectors and Associated Equipment, 380, 440-445.

CESAREO R., FERRETTI M., GIGANTE G., GUIDA G., MOIOLI P. RIDOLFI S., ROLDÁN GARCIA C. (2007) *The use of European coinage alloy to compare the detection limits of mobile XRF systems. A feasibility study*. X-Ray Spectrometry, 36, 167-172.

CILIBERTO E., SPOTO G. (Eds.) (2000) *Modern Analytical Methods in Art and Archaeology*. Chemical Analysis. A series of monographs on analytical chemistry and its applications. Vol. 155. WILEY-INTERSCIENCE, New York.

DERRICK M.R, STULIK D., LANDRY J.M. (1999) *Infrared Spectroscopy in Conservation Science. Scientific tools for conservation*. The Getty Conservation Institute, Los Angeles.

DOMENECH-CARBÓ M.T., CASAS-CATALÁN M.J., DOMÉNECH-CARBÓ A., MATEO-CASTRO R., GIMENO-ADELANTADO J.V., BOSCH-REIG F. (2001) *Analytical study of canvas painting collection from the Basilica de la Virgen de los Desamparados using SEM/EDX, FT-IR, GC and electrochemical techniques*. Fresenius' Journal of Analytical Chemistry, 369 (7-8), 571-575.

DOWNS R.T. (2006) *The RRUFF Project: an integrated study of the chemistry, crystallography, Raman and infrared spectroscopy of minerals*. Program and Abstracts of the 19th General Meeting of the International Mineralogical Association in Kobe, Japan, O03-13.

EDWARDS H.G.M., CHALMERS J.M. (Eds.) (2004) *Raman Spectroscopy in Archaeology and Art History*. Royal Society of Chemistry - Analytical Spectroscopy Monographs, Great Britain.

FRANQUELO M.L., DURAN A., HERRERA L.K., JIMENEZ DE HARO M.C., PEREZ-RODRIGUEZ J.L. (2008) *Comparison between micro-Raman and micro-FTIR spectroscopy techniques for the characterization of pigments from Southern Spain Cultural Heritage*. Journal of Molecular Structure, 924-926, 404-412.

GALLARDO J.M., GÓMEZ B., BOUZAS A., CUEVAS F.G., VILLEGAS R. (2001) *Determinación de la composición química de piezas metálicas históricas: aplicación a un bronce romano*, in: GÓMEZ-TUBÍO B., RESPALDIZA M.A., PARDO M.L. (Eds.) *Actas del III Congreso Nacional de Arqueometría (Sevilla, Diciembre de 1999)*. Universidad de Sevilla, 497-506.

GENERALITAT DE CATALUNYA (Catalonia's Government) (1993) *LLEI 9/1993, de 30 de setembre, del patrimoni cultural català*. Departament de Cultura i Mitjans de la Comunicació de la Generalitat de Catalunya. DOGC núm. 1807, d'11.10.1993 (in Catalan).

GENESTAR C., PONS C., MÁS A. (2006) *Analytical characterisation of ancient mortars from the archaeological Roman city of Pollentia (Balearic Islands, Spain)*. Analytica Chimica Acta, 557 (1-2), 373-379.

GIGANTE G.E., CESAREO R. (1998) *Non-destructive analysis of ancient metal alloys by in situ EDXRF transportable equipment*. Radiation Physics and Chemistry, 51 (4-6), 689-700.

GOLDSTEIN J.I., NEWBURY D.E., JOY D.C., LYMAN C.E., ECHLIN P., LIFSHIN E., SAWYER L.C., MICHAEL J.R. (2003) *Scanning Electron Microscopy and X-ray Microanalysis, 3rd Ed.* Springer, New York.

GUERRA, M.F. (1995) *Elemental Analysis of Coins and Glasses*. Applied Radiation and Isotopes, 46 (6/7), 583-588.

GUERRA M. F. (1998) *Analysis of archaeological metals. The place of XRF and PIXE in the determination of technology and provenance*. X-Ray Spectrometry, 27 (2), 73-80.

HALL E. T., SCHWEIZER F., TOLLER P. A. (1973) *X-Ray Fluorescence Analysis of Museum Objects: A New Instrument*. *Archaeometry*, 15, 53-78.

HERRERA L.K. (2009) *Physico-Chemical Research of Cultural Heritage Materials Using Microanalytical Methods*. PhD Thesis. Materials Science Institute of Seville (CSIC) / University of Seville.

JANSSENS K. (2004) *X-Ray based methods*, in: JANSSENS K., VAN GRIEKEN R. (Eds.) *Non-destructive microanalysis of cultural heritage materials*. Vol. XLII. Wilson and Wilson's, *Comprehensive Analytical Chemistry*, Elsevier, 129-226.

JANSSENS K., VITTIGLIO G., DERAEDT I., AERTS A., VEKEMANS B., VINCZE L., WEI F., DERYCK I., SCHALM O., ADAMS F., RINDBY A., KNÖCHEL A., SIMIONOVICI A., SNIGIREV A. (2000) *Use of Microscopic XRF for Non-destructive Analysis in Art and Archaeometry*. *X-Ray Spectrometry*, 29, 73-91.

JANSSENS K., VAN GRIEKEN R. (2004) *Introduction an overview*, in: JANSSENS K., VAN GRIEKEN R. (Eds.) *Non-destructive microanalysis of cultural heritage materials*. Vol. XLII. Wilson and Wilson's, *Comprehensive Analytical Chemistry*, Elsevier, 1-10.

LINKE R., SCHREINER M., DEMORTIER G., ALRAM M., WINTER H. (2004) (a) *The provenance of medieval silver coins: analysis with EDXRF, SEM/EDX and PIXE*, in: JANSSENS K., VAN GRIEKEN R. (Eds.) *Non-destructive microanalysis of cultural heritage materials*. Vol. XLII. Wilson and Wilson's, *Comprehensive Analytical Chemistry*, Elsevier, 605-632.

LINKE R., SCHREINER M., DEMORTIER G. (2004) (b) *The application of photon, electron and proton induced X-ray analysis for the identification and characterization of medieval silver coins*. *Nuclear Instruments and Methods in Physics research section B: Beam Interactions with Materials and Atoms*, 226 (1-2), 172-178.

LONG D.A. (2004) *Introduction to Raman Spectroscopy*, in: EDWARDS H.G.M., CHALMERS J.M. (Eds.) *Raman Spectroscopy in Archaeology and Art History*. Royal Society of Chemistry - Analytical Spectroscopy Monographs, Great Britain, 17-40.

MAIRINGER F. (2004) *UV, IR and X-ray imaging*, in: JANSSENS K., VAN GRIEKEN R. (Eds.) *Non-destructive microanalysis of cultural heritage materials. Vol. XLII*. Wilson and Wilson's, Comprehensive Analytical Chemistry, Elsevier, 15-66.

MANTLER M., SCHREINER M. (2000) *X-Ray Fluorescence Spectrometry in Art and Archaeology*. X-Ray Spectrometry, 29, 3-17.

MANSO M., CARVALHO M.L. (2009) *Application of spectroscopic techniques for the study of paper documents: A survey*. Spectrochimica Acta Part B: Atomic Spectroscopy, 64 (6), 482-490.

MOIOLI P., SECCARO C. (2000) *Analysis of Art Objects Using a Portable X-Ray Fluorescence Spectrometer*. X-Ray Spectrometry, 29, 48-52.

NESSE W.D. (1986) *Introduction to Optical Mineralogy*. Oxford University Press.

PERKINS D., HENKE K.R. (2002) *Minerales en Lámina Delgada*. Pearson Educación, Madrid.

POLLARD M., HERON C. (1996) *Archaeological Chemistry*. Royal Society of Chemistry, Cambridge.

POLLARD M., MATT C., STERN B., YOUNG S. (2007) *Analytical Chemistry in Archaeology. Manuals in Archaeology*. Cambridge University Press.

RODRÍGUEZ-GALLEGO M. (1982) *La difracción de los rayos X*. Editorial Alhambra, Madrid, Spain.

RÖESSIGER V., NENSEL B. (2003) *Non Destructive Analysis of Gold Alloys using Energy Dispersive X-ray Fluorescence Analysis*. Gold Bulletin 36/4, 125-137.

SÁNDOR Zs., TÖLGYESI S., GRESITS I., KÁPLÁN-JUHÁSZ M. (2000) *Qualitative and quantitative analysis of medieval silver coins by energy dispersive X-ray fluorescence method*. Journal of Radionanalytical and Nuclear Chemistry, 246 (2), 385-389.

SÁNDOR Zs., TÖLGYESI S., GRESITS I., KASZTOVSZKY Zs. (2002) *Determination of alloying elements in ancient silver coins by X-ray fluorescence*. Journal of Radioanalytical and Nuclear Chemistry, 254 (2), 283-288.

SARMIENTO A., PÉREZ-ALONSO M., OLIVARES M., CASTRO K., MARTÍNEZ-ARKARAZO I., FERNÁNDEZ L.A., MADARIAGA J.M. (2011) *Classification and identification of organic binding media in artworks by means of Fourier transform infrared spectroscopy and principal component analysis*. Analytical and Bioanalytical Chemistry, 399, 3601-3611.

SIDDAL, R. (2006) *Not a day without a line drawn: pigments and painting techniques of Roman Artists*. Infocus Magazine – Proceedings of the Royal Microscopical Society, Issue 2, 19-31.

SCOTT D.A. (2004) *The non-destructive investigation of copper alloy patinas*, in: JANSSENS K., VAN GRIEKEN R. (Eds.) *Non-destructive microanalysis of cultural heritage materials*. VOL. XLII. Wilson and Wilson's, Comprehensive Analytical Chemistry, Elsevier, 465-492.

STUART B.H. (2007) *Analytical Techniques in Materials Conservation*. John Wiley & Sons Ltd, England.

THERMO FISHER SCIENTIFIC Inc (2011) *Nicolet* iN 10 Infrared Microscope* <http://www.thermoscientific.com/ecommservlet/productsdetail?productId=11961666&groupType=PRODUCT&searchType=0&storeId=11152> [on-line resource]. Available from: <http://www.thermoscientific.com> [last accessed: 10th October 2011]

THERMO NICOLET CORPORATION (2001) *Introduction to Fourier Transform Infrared Spectrometry* [pdf]. Available from: <http://mmrc.caltech.edu/FTIR/FTIRintro.pdf> [last accessed: 14th September 2011].

VAN GRIEKEN R., MARKOWICZ A.A. (Eds.) (1993) *Handbook of X-Ray Spectrometry: Methods and Techniques*. Marcel Dekker Inc., New York.

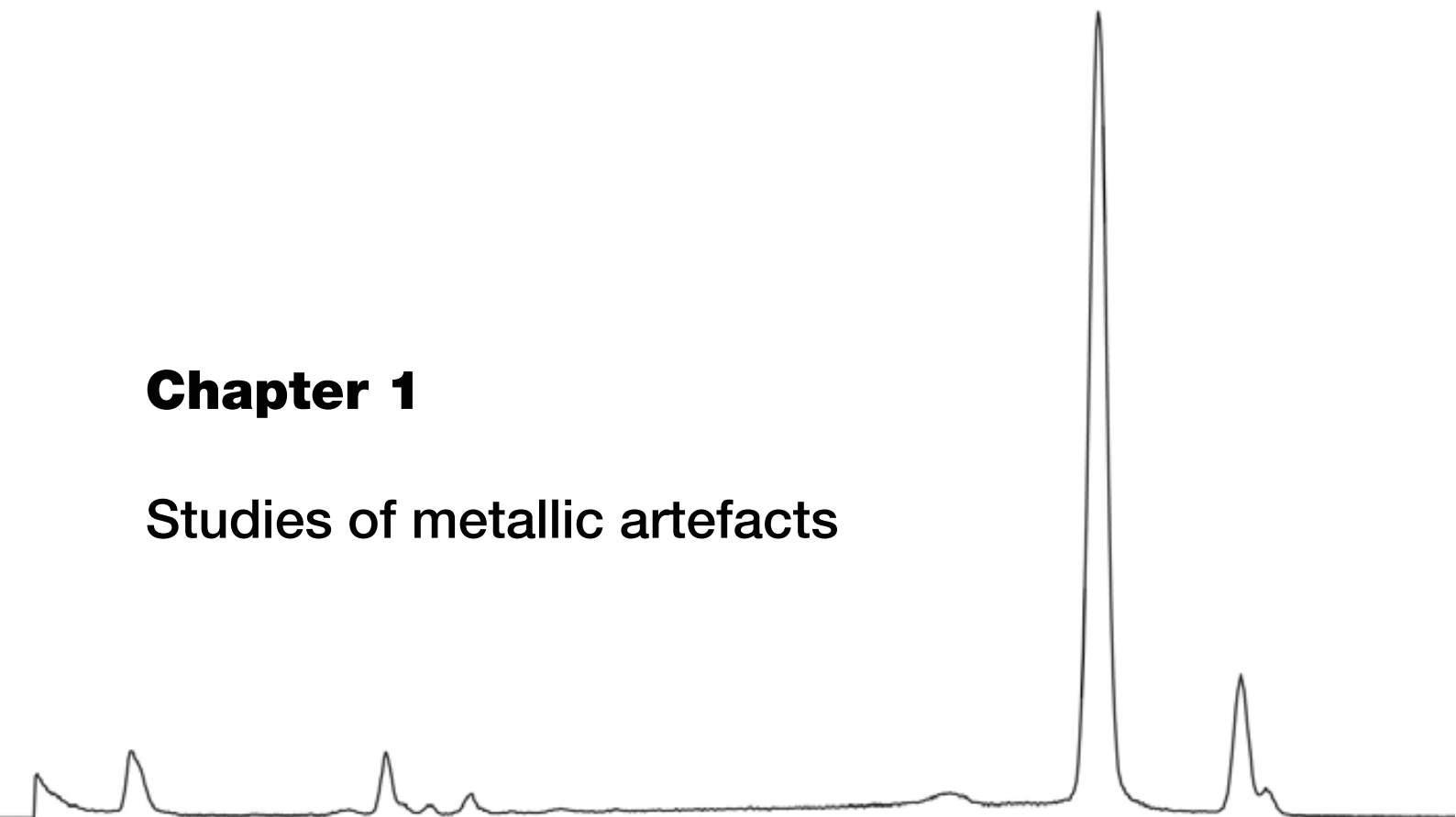
VIJAYAN V., RAUTRAY T.R., BASA D.K. (2004) *EDXRF study of Indian punch-marked silver coins*. Nuclear Instruments and Methods in Physics Research B: Beam Interactions with Materials and Atoms, 225, 353-356.

WORKMAN J.J. (2001) *Infrared and Raman spectroscopy in paper and pulp analysis*. Applied Spectroscopy Reviews, 36 (2-3) 139–169

http://www.geol.ucsb.edu/research/labs_equipment.html [on-line resource]. Available from: <http://www.geol.ucsb.edu> [last accessed: 13th October 2011]

Chapter 1

Studies of metallic artefacts



Part of the contents of this chapter is published in:

PITARCH A., QUERALT I. (2010) *Energy dispersive X-ray fluorescence analysis of ancient coins: The case of greek silver drachmae from the Emporion site in Spain*. Nuclear Instruments and Methods in Physics Research B, 268, 1682-1685.

PITARCH A., QUERALT I., ALVAREZ-PEREZ A. (2011) *Analysis of Catalonian silver coins from the Spanish War of Independence period (1808-1814) by Energy Dispersive X-ray Fluorescence*. Nuclear Instruments and Methods in Physics Research B, 269, 308-312.

1. 1. Introduction

Energy dispersive X-ray fluorescence (EDXRF) has become a powerful tool to obtain qualitative and semi-quantitative information of Cultural Heritage materials since it is a non-destructive, fast and multi-elemental technique which analyses the surface of samples and determines their elemental composition (Guerra, 1998; Ferretti, 2000; Janssens *et al.*, 2000; Moiola and Seccaroni, 2000; Janssens and Van Grieken, 2004; Vijayan *et al.*, 2004; Paternoster *et al.*, 2005; Gianoncelli and Kourousias, 2007; Manso *et al.*, 2008 (a); Manso *et al.*, 2008 (b); Pessanha *et al.*, 2009; de Viguerie *et al.*, 2009; Guilherme *et al.*, 2010).

Amongst archaeological materials, metals are particularly appropriate to be analysed by means of XRF (Gigante and Cesareo, 1998; Guerra, 1998; Mantler and Schreiner, 2000). Both, their high density and their high atomic number (Z) provide a good analytical response and, in the specific case of metal alloys, one could go so far as to detect almost all the major and minor constituents and the trace elements of the alloy.

In this sense, among all metallic archaeological objects, ancient coins¹ have been extensively studied (the works of Gallardo *et al.*, 2001; Sándor *et al.*, 2002; Constatinescu *et al.*, 2003; Lönnqvist, 2003; Dominguez *et al.*, 2004; Constatinescu *et al.*, 2005; Pistofidis *et al.*, 2006; Civici *et al.*, 2007; Montero-Ruiz *et al.*, 2007; Montero-Ruiz *et al.*, 2008; Rodrigues *et al.*, 2010; Moreno-Suárez *et al.*, 2011; Rizzo *et al.*, 2011; Rodrigues *et al.*, 2011 are some examples of the available literature from the last decade reporting the scientific study of coins). This fact is due to the relationship between the chemical composition of the alloys, the economy and technology features of the mintage period and the differences between mint factories (Kallithrakas-Kontos *et al.*, 1996; Vijayan *et al.*, 2004; Queralt *et al.*, 2007). Moreover, minting chronology, typology and metrology of the coins are usually well established by numismatics. Therefore, the possibility to relate the compositional changes of the monetary series to specific historic circumstances turns the elemental analysis of coins into a very useful tool.

As mentioned above, a distinctive feature between modern and ancient coins is that the last ones have an intrinsic value. The value of an ancient coin depends on the

¹ Ancient coins are those in which the face value is the same as the metal content. They were usually struck with a well controlled alloy and their assay value was guaranteed by the authority in charge of the mint (Hackens, 1975; Sejas del Piñal, 1993; Guerra, 1995).

quantity (absolute mass and relative content in the minting alloy) of three considered precious metals: gold, silver and copper. The basis for the use of these three metals is the possibility to obtain coins of pure metal, binary alloys or ternary alloys, whatever the chemical formulation, due to the complete miscibility among them. Other metals used for coinage are introduced to debase the value, increase the coin production in periods of raw metal scarcity and also for counterfeit manufacturing.

In the study of coins, the ones alloyed with precious metals such as gold (Au) and silver (Ag)² are preferred for elemental analysis (Guerra, 1998) against other low-value alloys (usually Cu) used for common coinage, since gold, silver and their alloys do not usually exhibit neither surface enrichments nor corrosion, oxidation or other weathering layers (Carter, 1964; Guerra, 1995; Guerra, 1998; Constantinescu *et al.*, 2005). Even in the case in which there is an alteration on the surface, most of the times restorers cannot apply any cleaning procedure. In this sense, EDXRF can be used directly to characterize coins without sample surface treatment (such as polishing or scrapping off) when the corrosion layer is thin enough (McKerrel and Stevenson, 1972; Denker *et al.*, 2005).

The analysis of the elemental composition of ancient coins by means of EDXRF may be very useful in numismatic studies (Carter, 1993; Sándor *et al.*, 2000, 2002; Linke *et al.*, 2003; Vijayan *et al.*, 2004; Constantinescu *et al.*, 2005) for the following purposes:

1. Originally testing. Determination of elemental composition (always taking into account the historical data) may give clues regarding the authenticity of the coins.
2. Provenance. Determination of minor constituents (contents between 10 and 0.1%) and trace elements (contents below 0.1%) in some cases may provide clues concerning the origin of the metal used.
3. Conservation and restoration. Treatment methods may be selected according compositional criteria.
4. Historical studies. Analysis of major constituents and minting technology can give information about the economical development of a particular period of time. On the other hand, determination of minor constituents and trace

² Silver and gold alloys were usually the starting point and reference for the monetary system. Their alloys directly reflect socio-economical changes (Kallithrakas-Kontos *et al.*, 1996).

elements may indicate the presence of pollutants introduced during manufacture.

This work tries to explain what should be expected from EDXRF analyses by presenting two applications using this technique “in situ” (in this case, inside the museum) to study ancient silver coins.

1. 2. Energy dispersive X-ray fluorescence analyses of ancient silver *drachmae*³ from Catalonia.

One of the most fascinating components of the Numismatic Cabinet of Catalonia (GNC-MNAC) is made up of pieces from the earliest mintings at the Iberian territories. In this sense, pieces from the first Greek mintings in the colonies of *Emporion* and *Rhode* (NE of Catalonia region, Spain) and even coins struck by the Iberians are part of the collection. These coins represent a magnificent testimony to the history of the Iberian Peninsula. The historical importance of this collection motivated to conduct an extensive campaign of EDXRF analyses in order to ascertain the composition of a number of *drachmae* silver coins from different periods and mints⁴.

1. 2. 1. Historical context

At the beginning of the sixth century BC, a small colony known as *Emporion*⁵ (Empúries, North-East of Catalonia region, Spain) was founded by Phocaeen sailors in order to have a trading port in the far west of the Mediterranean and, thus, exchange cereals from Iberia for Greek manufactured products. During this historical period, *Emporion* became one of the first and most important places where silver currency was minted in the Western Mediterranean area and played an important commercial role throughout the following centuries. In this context, the first mintages were small fractional silver coins, archaic in style and technique and very varied in kind. The production volume of these first issues was low (Campo *et al.*, 2006).

Both, the minting technique and the volume of production gradually improved and increased. The workshop tended to establish the iconographies. At the beginning of the

³ *Drachmae*: silver Greek monetary unit (Campo *et al.*, 2006).

⁴ Mint: the place where coins are made (Campo *et al.*, 2006).

⁵ *Emporion*: meaning “market” in Greek (Campo *et al.*, 2006).

third century BC *Emporion* established new commercial relationships with Italy and created a new monetary system, stronger than the previous one. This phase began with the minting of a small issue of *drachmae* weighing on average 4.7 g. At the same time, the Greek colony of *Rhode* (founded at the beginning of the fourth century BC and located on the north coast of the Bay of Roses, nearby *Emporion*) opened a workshop due to the economic development and the urban process that took place in the town. Although the emissions were irregular and brief, they should be very important for the economy of that town (Campo *et al.*, 2006).

Well into the third century BC, coinciding with the Second Punic War (219-202 BC), the city of *Emporion* modified once again its monetary system. Its system of fraction was reformed by minting three new divisors and the design of its *drachmae* was changed. In this period, the city became an important military settlement for the operation of Roman armies in Iberia (Mar and Ruiz de Arbulo, 1993). This long period of wars generated the need for money and, consequently, *Emporion* minted a huge amount of *drachmae*. At the same time, the Iberian community began to mint silver coins that imitated the iconography of the *drachmae* of *Emporion* (Campo, 2002).

After the war was over, not only the production of divisors was ceased but also the manufacturing of *drachmae* strongly deteriorated. By the beginning of the first century BC, the Romans imposed their monetary system so that the production of *drachmae* was ceased (Campo *et al.*, 2006).

1. 2. 2. Research aims

The general objectives connected with the aim of this work were the following ones:

- a) *Emporion* mint. We studied whether the alloys had changed their composition through more than four centuries (from fifth century BC to first century BC), taking into consideration the historical context.
- b) *Rhode* mint. Analyses were focused on the determination of the type of alloy used for the coins (third century BC). The differences and analogies with the contemporary emission from *Emporion* were also studied.
- c) Iberian imitations. Main efforts were concentrated on those imitations from the Second Punic War (219-202 BC) trying to characterize not only the type of alloys used for the coinage but also determine the differences and analogies with the *Emporion* issues from the same period.

1. 2. 3. Materials and Methods

1. 2. 3. 1. Samples

The examined coins belong to the *Emporion* Greek Colony collection of the Numismatic Cabinet of Catalonia (GNC) at the National Museum of Fine Arts of Catalonia (MNAC) and have been dated from the fourth century to first century BC. The elemental characterization by means of EDXRF analysis was carried out to 185 coins from the mint of *Emporion*, 4 *drachmae* from the mint of *Rhode* and 19 Iberian imitation *drachmae*. **Fig. 1. 1** shows some examples of the analysed coins.



Fig. 1.1 Obverse and reverse of some of the coins: (a) *Emporion drachmae* from the 300-260 BC period (MNAC/GNC ref. 20543); (b) *Emporion drachmae* from the 260-218 BC period (MNAC/GNC ref. 20552); (c) *Emporion drachmae* from the 218-200 BC period (MNAC/GNC ref. 33578); (d) *Emporion drachmae* from the second century BC period (MNAC/GNC ref. 20623); (e) *Emporion drachmae* from the first century BC period (MNAC/GNC ref. 20680); (f) *drachmae* from the third century BC period minted in *Rhode* (MNAC/GNC ref. 20491); (g) Iberian *drachmae* from the 218-200 BC period (MNAC/GNC ref. 20633). (Images provided by Dr. M. Campo – GNC/MNAC).

Due to the high value of the *drachmae* and the prevention to transport them to X-ray laboratory, measurements were carried out “in situ”, after bringing the EDXRF instrument to the MNAC museum. The coins were analyzed directly in a non-destructive way and without applying any cleaning treatment.

1. 2. 3. 2. X-ray fluorescence equipment

The elemental composition of coins was obtained by using an EDXRF spectrometer (FISCHERSCOPE® X-RAY XAN, Helmut Fischer GmbH, Germany). Main features of the equipment were described in section I. 5.

1. 2. 3. 3. Experimental conditions

Looking for the best conditions for the systematic analysis of ancient coins we must check and optimize the entire variables that influence on the EDXRF analysis. In this sense, different conditions (filter, voltage, collimator diameter and measuring time) were checked by using a set of silver standards⁶. The members of the series had the same matrix as the coins to be analysed, i.e., they consisted of silver and copper and were of high analytical purity. The composition of the standard samples is given in

Table 1.1.

Table 1. 1
Compositional data of the silver standards

Reference	Ag (g)	Cu (g)	% Ag
M0	?	0	100
M1	5,18	0,518	90,901
M2	5,16	1,032	83,332

In order to reduce the background noise from tungsten tube we used an aluminium primary filter. The use of this filter allowed not only to obtain the higher net peak intensities of the elements present in the sample but also to obtain good statistics counting time (**Fig. 1. 2**).

⁶ This silver standard set was kindly provided by Dr. J. L. Ferrero, member of the “Unitat d’Arqueometria” from the “Institut Universitari de Ciència de Materials” (ICMUV, University of València).

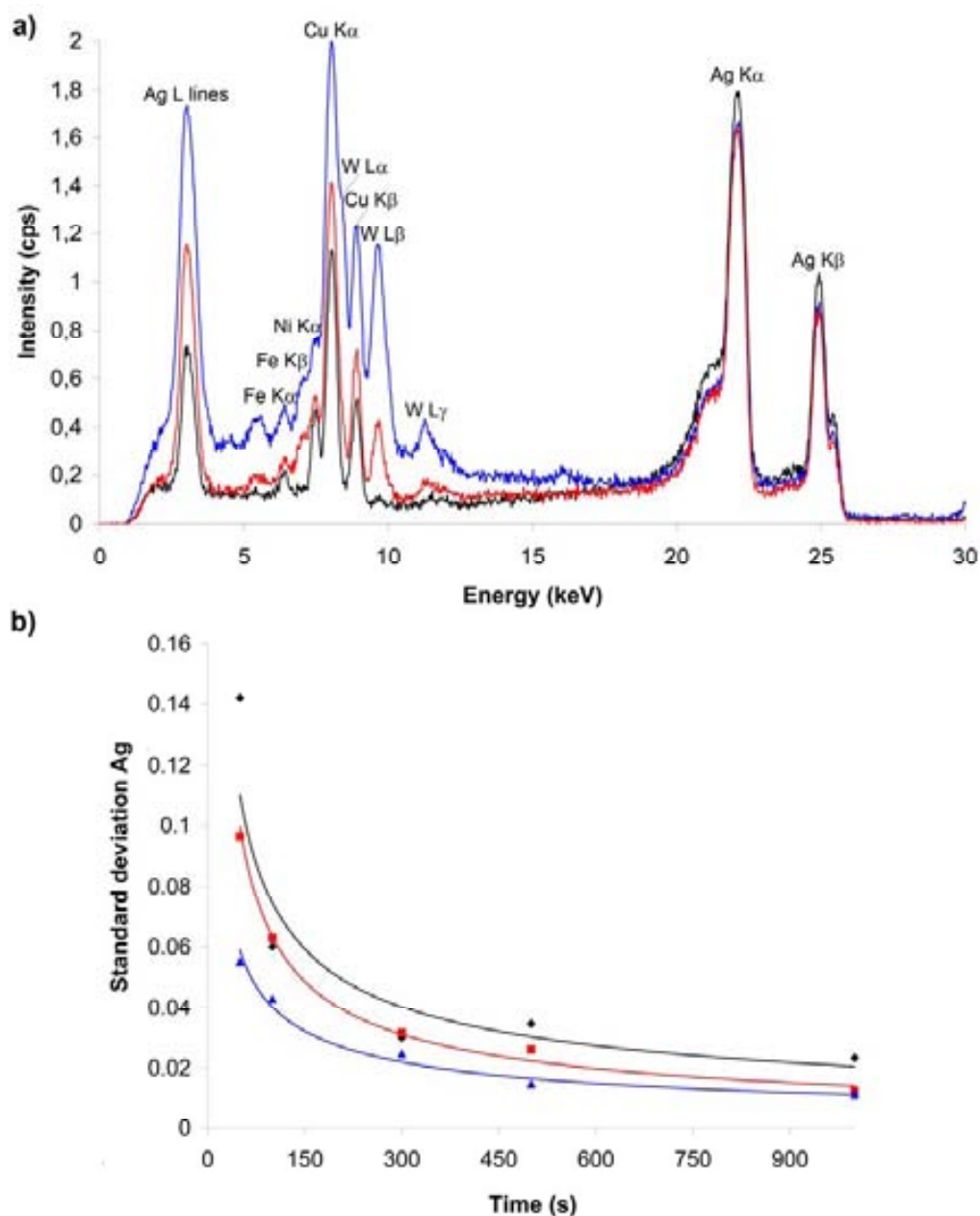


Fig. 1. 2 (a) EDXRF spectra of an Ag/Cu alloy by using several filters (experimental conditions: 50 kV, focal spot 2 mm, 300 s of measuring time), and (b) plot of standard deviation vs. measuring time using different filters (experimental conditions: 20 measurements on each point, 50 kV, focal spot 2 mm). Key: black - measurement made with aluminium filter; red - use of nickel filter; blue - measurements without filter.

Spectra of a silver/copper alloy were recorded using the 0.20, 0.60, 1.00, and 2.00 mm X-ray beam sizes, at 300 s of acquisition time. To properly excite the silver, we use two voltage modes (30 and 50 kV). The overall results are presented in **Fig. 1. 3**. Increases of voltage and collimator diameter imply consequently an increase of the net peak intensity of the silver K α line.

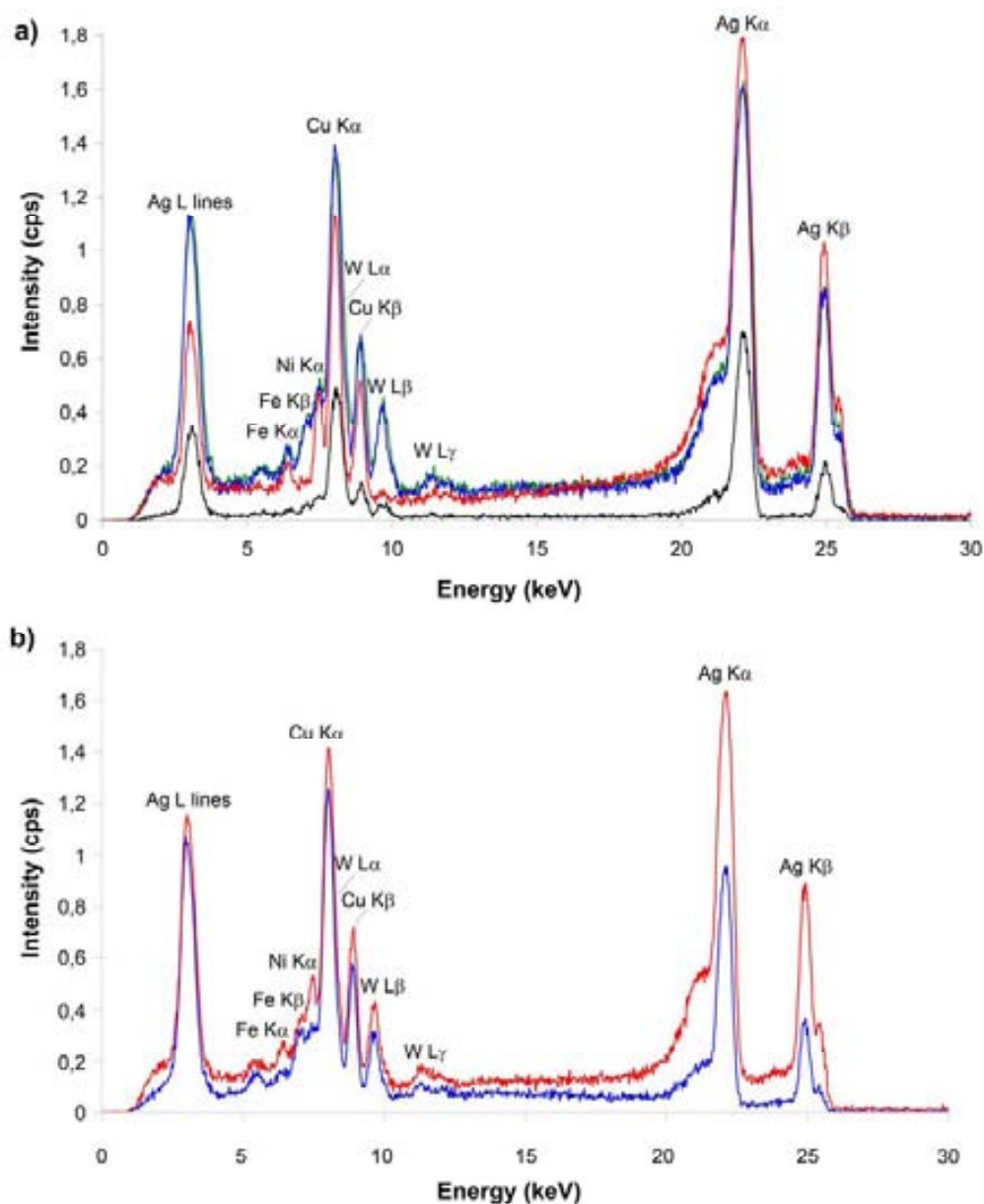


Fig. 1. 3 (a) EDXRF spectra of an Ag/Cu alloy by using several collimators (0.1 mm in black; 0.6 mm in green; 1 mm in blue; 2 mm in red), 50 kV, Ni filter and 300 s. (b) EDXRF spectra of an Ag/Cu alloy by employing two voltage modes (30 kV in blue; 50 kV in red). Experimental conditions: focal spot 2 mm, 300 s of measuring time.

The spectra acquisition time was optimised to obtain the minor relative standard deviation (RSD) of the intensity of the silver K α line by repeated measurements. On the same point, 20 repeated analyses were made at different measuring conditions (50, 100, 300, 500 and 1000 s). In the following plot (**Fig. 1. 4**) the improvement of the RSD for silver is shown. According to the obtained results and taking into account the main features of our samples, we used a measuring time of 100 s, which delivers standard

deviation of ± 0.06 . A more extended time does not imply a substantial reduction in the RSD value.

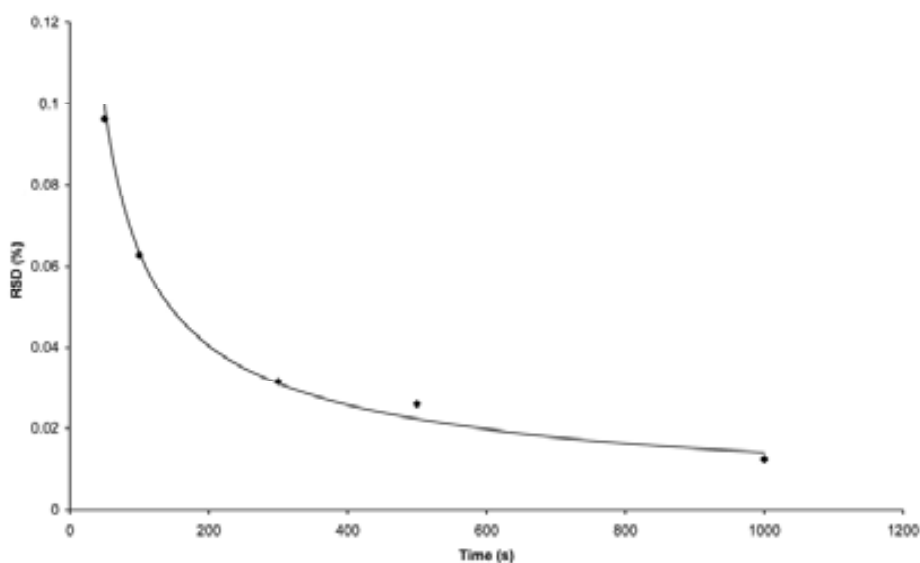


Fig. 1. 4 Relative standard deviation vs. measuring time. Each point represents 20 measurements. Experimental conditions: 50 kV, focal spot 2 mm, Ni filter.

Hence, after these experiences we used a collimator of 2 mm in diameter to adjust the X-ray focal spot in order to irradiate the maximum surface of coin and the analyses were carried out operating at 50 kV power, using a nickel primary filter and a counting time of 100 seconds.

For each coin we obtained a spectrum which was processed and subsequently quantified using the fundamental parameters method, through the software attached to the equipment (WinFTM[®], 6.20Lab L-PDM version, Helmut Fischer GmbH + Co. KG). The fundamental parameters evaluation procedure was calibrated and set up with the analysis of fourteen certified pure metals, from silicon (lightest element) to lead (heaviest element), used as a reference materials to make up the internal software library of elemental sensitivities.

1. 2. 3. 4. Limits of detection

The detection limit is defined as the minimum net intensity of an analyte, expressed in a concentration unit, which can be detected by an instrument in a given analytical context with a 99.5% confidence level (Van Grieken and Markowicz, 1993). Usually, it is expressed as (Eq. 1. 1):

$$DL = 3 \frac{C_i \sqrt{N_b}}{N_p} \quad (\text{Eq. 1. 1}) \text{ (Helsen and Kuczumow, 1993)}$$

where C_i is the concentration of the element i ; N_b is the net peak area of the background and N_p is the net peak area of the analytical line of the element i .

The quantification limit (LOQ) is defined as the concentration at which quantitative results can be reported with a high degree of confidence (Armbruster *et al.*, 1994), which is roughly expressed as (Eq. 1. 2):

$$LOQ = 10 \frac{C_i \sqrt{N_b}}{N_p} \quad (\text{Eq. 1. 2})$$

where C_i is the concentration of the element i ; N_b is the net peak area of the background and N_p is the net peak area of the analytical line of the element i .

In our particular case, the quantification limits were determined from the calculation of the detection limits of the fourteen standards included in the software. Thus, the quantification limits were: 0.1% for Ag, 0.03% for Cu, 0.03% for Zn, 0.2% for Sn, 0.13% for Pb, 0.14% for Au, 0.03% for Ni and finally 0.04% for Fe.

1. 2. 4. Results and Discussion

1. 2. 4. 1. Quantitative analysis of silver *drachmae* from the *Emporion* mint (fifth to first century BC)

The elemental concentration range and other statistical information of the examined coins from different periods are presented in **Table 1. 2**. The results of the analysis were expressed in weight percentage (wt %).

The *drachmae* coins show silver as a main constituent (contributing around of 98% to overall composition) (**Fig. 1. 5**). Apart from silver, the presence of minor constituents (0.1-10%) and trace elements (less than 0.1%) such as copper, tin, lead, gold, platinum, bismuth, iron, chromium, nickel, zinc, manganese and titanium was also recorded.

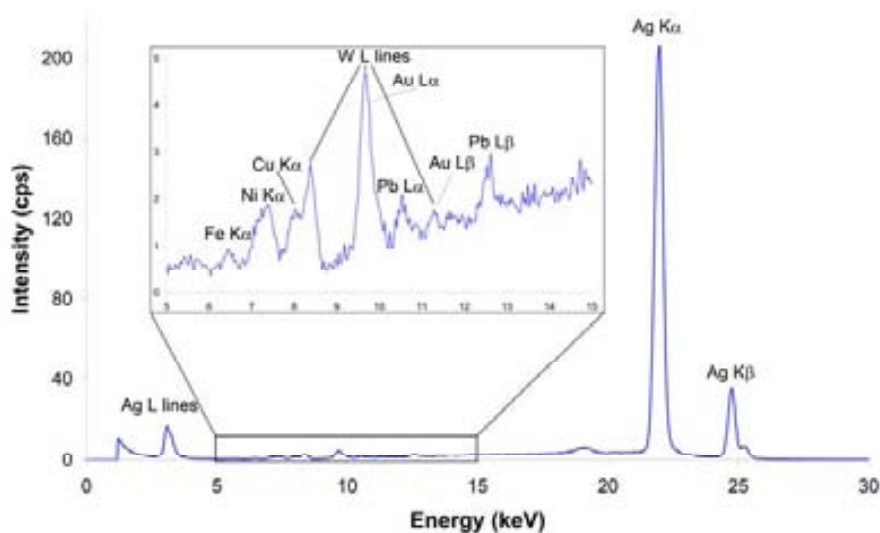


Fig. 1. 5 EDXRF spectrum of a silver drachma (MNAC/GNC ref. 30049).

Table 1. 2

Elemental concentration range of the examined coins from different period measured by EDXRF (wt.%) and 95 % confidence interval of %Ag .

	Weight (g)	Ag	Cu	Sn	Pb	Au	Pt	Bi	Fe	Cr	Ni	Zn	Mn	Ti	Ag/Cu
<i>300-260 B.C.</i>															
n	4	4	4	1	4	3	4	4	4	3	3	3	4	3	4
min	4.5	97.08	0.36	0.04	0.21	0.01	0.02	0.04	0.09	0.02	0.02	0.01	0.01	0.04	59.33
max	4.95	98.81	1.64	0.04	0.69	0.15	0.04	0.12	0.26	0.05	0.05	0.31	0.03	0.07	274.50
mean	4.81	98.29	0.78	0.04	0.4	0.1	0.03	0.07	0.14	0.03	0.04	0.11	0.02	0.06	183.27
St. dev	0.21	0.82	0.6		0.2	0.08	0.01	0.03	0.08	0.01	0.02	0.18	0.01	0.01	106.48
COV	4.35	0.83	76.9		50.94	74.89	38.75	44.83	57.82	44.76	44.86	161.3	36.26	24.98	58.10
Confidence interval 96.99 - 99.59															
<i>260-220 B.C.</i>															
n	18	18	18	8	18	18	14	18	18	15	17	15	16	12	18
min	3.18	95.65	0.24	0.24	0.06	0.05	0	0.01	0.02	0.01	0	0	0	0.01	26.80
max	4.91	99.27	3.58	0.56	0.71	0.6	0.06	0.1	2.7	0.09	0.05	0.09	0.07	0.33	417.57
mean	4.51	97.63	0.87	0.35	0.37	0.17	0.03	0.04	0.54	0.05	0.03	0.03	0.03	0.14	164.12
St. dev	0.46	1.11	0.76	0.11	0.2	0.12	0.02	0.02	0.85	0.03	0.01	0.03	0.02	0.11	93.62
COV	10.26	1.13	87.61	31.69	55.2	69.43	54.18	49.99	157.32	46.26	42.32	106.88	67.99	82.41	57.05
Confidence interval 97.08 - 98.18															
<i>218-200 B.C.</i>															
n	17	18	18	2	18	16	16	18	18	14	14	15	13	8	18
min	4.16	95.32	0.06	0.03	0.05	0.11	0	0	0.02	0.01	0	0	0.01	0	26.00
max	4.86	99.57	3.67	0.09	0.8	0.7	0.06	0.11	1.95	0.08	0.06	0.3	0.1	0.17	1711.20
mean	4.56	98.18	0.71	0.06	0.21	0.38	0.03	0.04	0.32	0.04	0.02	0.04	0.04	0.1	365.37
St. dev	0.19	1.02	0.89	0.04	0.19	0.14	0.02	0.03	0.51	0.02	0.01	0.07	0.03	0.06	410.28
COV	4.25	1.04	124.11	71.91	92.29	36.7	63.49	70.11	157.38	39.09	60.77	168.94	76.31	58.07	112.29
Confidence interval 98.7 - 97.66															
<i>Second century B.C.</i>															
n	81	81	81	20	81	28	60	81	81	72	70	39	68	55	81
min	3.79	90.81	0.02	0.03	0.05	0.02	0	0.01	0.02	0	0	0	0	0	55.41
max	4.36	99.57	1.74	1.62	2.61	0.85	0.18	0.45	2.97	0.33	0.1	0.2	0.31	1.74	4980.00
mean	4.15	98.55	0.23	0.48	0.33	0.18	0.03	0.15	0.33	0.05	0.02	0.02	0.03	0.15	1133.48
St. dev	0.12	1.27	0.3	0.39	0.41	0.21	0.03	0.09	0.53	0.04	0.02	0.04	0.04	0.24	958.75
COV	2.81	1.29	129.7	81.27	121.71	113.75	98.57	57.85	163.16	78.68	78.16	153.13	137.78	154.89	84.59
Confidence interval 98.78 - 98.32															
<i>First century B.C.</i>															
n	11	11	11	2	11	4	9	11	11	9	10	8	9	3	11
min	3.53	92.61	0.06	0.23	0.1	0.07	0	0.01	0	0	0	0.01	0.01	0.08	14.12
max	4.26	99.33	6.56	0.6	0.5	0.15	0.12	0.06	1.37	0.09	0.05	0.08	0.07	0.15	1555.74
mean	4.06	98.05	1.08	0.41	0.26	0.11	0.04	0.03	0.31	0.04	0.02	0.02	0.03	0.12	367.88
St. dev	0.21	1.9	1.84	0.26	0.15	0.03	0.04	0.02	0.4	0.03	0.02	0.03	0.02	0.04	508.46
COV	5.16	1.94	169.34	63.45	56.89	29.6	103.23	59.05	128.16	75.97	82.62	130.19	68.48	31.14	138.21
Confidence interval 99.28 - 96.72															

It is assumed that in ancient times the lead cupellation process was the main technique used to obtain silver (Gale *et al.*, 1980; Gozalbes and Ripollès, 2002; Flament and Marchetti, 2004). Accordingly, the presence of copper and lead is interpreted as an end by-product of the process and low lead concentration is an indicator of a good smelting process (Civici *et al.*, 2007). On the other hand, the presence of iron is generally attributed to external impurities (Constantinescu *et al.*, 2003) and the presence of gold and bismuth has sometimes been reported as raw constituents of the silver ores (Gale *et al.*, 1980; Civici *et al.*, 2007). Minor and trace elements are other common impurities due to the coin manufacturing process (from mining to minting) and, in some cases, could be present from surface contamination (Constantinescu *et al.*, 2003).

Fig. 1. 6 shows the changes on the average silver content according to their minting period. The average silver concentration found for the *drachmae* minted during the 300-260 BC period in *Emporion* is 98.29%, for 260-220 BC period 97.63%, for 218-200 period 98.18%, for second century BC 98.55% and for first century BC 98.05%. Despite changes in the mean value and according to the analytical data, no significant variations were found between the silver concentration in the different minting periods and the alloys of the *drachmae* were found to have a very high fineness. However, it is certain that a slight reduction of the mean silver content during the 260-200 BC period is observed. This fact can be interpreted in the light of the economic decadence suffered by the *Emporion* colony owing to the Carthaginian landing in the Iberian Peninsula and the subsequent Ebro treaty between Rome and Carthage.

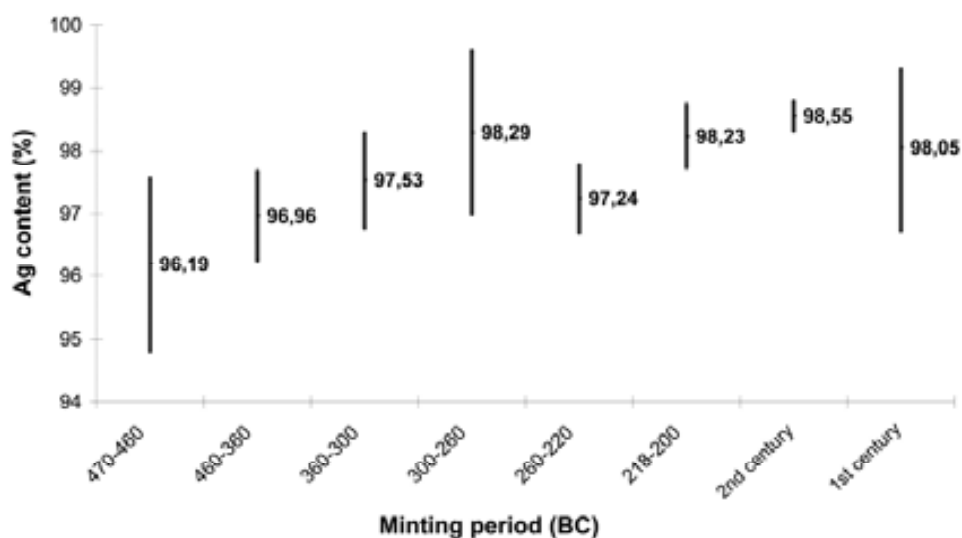


Fig. 1. 6 Ag content vs. the strike⁷ period of the coins.

⁷ To strike: to mint coinage.

The statistical analysis by means of Principal Component Analysis routine (PCA) was carried out with the software package STATISTICA 7[®]. In this particular case, PCA was restricted to minor and trace elements because, according to the data present in **Table 1. 2**, they have a high C.O.V.⁸, while the C.O.V for silver is very low, which means that the statistical silver data treatment is not relevant. By comparing the minor and trace element pattern, the principal components analysis did not allow us to clearly differentiate the *drachmae* according to their strike period. As it is shown in **Fig. 1. 7**, no significant clustering was obtained regarding these constituents of the alloy since an overlap of the samples is observed in the scatter plot.

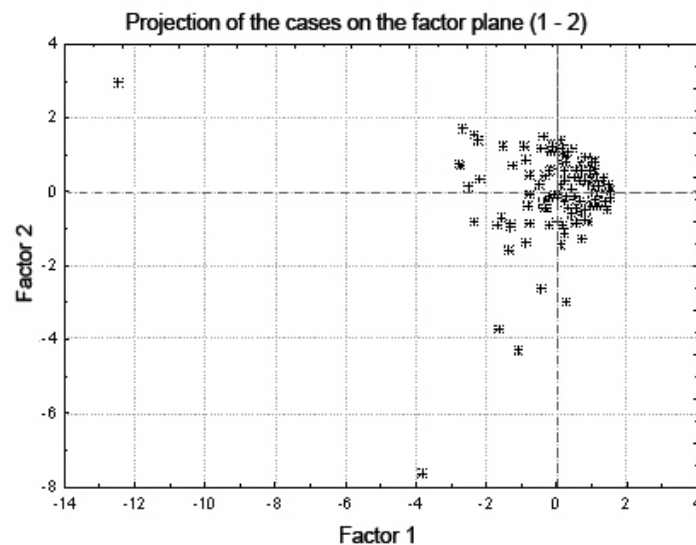


Fig. 1. 7 Scatterplot of factor 1 vs. factor 2.

For the proper interpretation of the whole dataset a confidence bound (CI) with a trustworthiness of 95% was previously calculated (see **Table 1. 2**) according to **Eq. 1.3**.

$$\bar{X} \pm t_{0.975}^{n-1} \frac{S_n}{\sqrt{n}} \quad (\text{Eq. 1. 3})^9$$

where \bar{X} is the mean value of the element; t is the Student's t-distribution; S_n is standard deviation of the element n .

⁸ The coefficient of variation is a simplest index of variability and allows us to identify the more changing variables.

⁹ Note that the *Student t* was used rather than the normal standard, as the number of elements in the sample is very small.

From this table we can clearly observe that the mean silver content show a significant homogeneity along the studied periods. These little changes of the silver content have been previously reported in Greek coins (Sejas del Piñal, 1993; Kallithrakas-Kontos *et al.*, 2000; Constantinescu *et al.*, 2003; Pistofidis *et al.*, 2006; Montero-Ruiz *et al.*, 2008). On the other hand, the maximum range (difference between the end points of the boundary) was studied to know how accurate the technique was (see **Table 1. 2**). According to the data, for the first three centuries (from fourth to second century BC) the variability on the silver content is minimized, being the lowest one at the second century BC.

Focusing our attention to the second century BC, it is worth mentioning that despite the fact that during this century the technique of mintage wasn't consistent (both the reuse of stamps and the decrease of coinage weight were reported (Campo, 2002)) a change of quality is not recorded. On the contrary, if we study the relative proportion between silver and copper (**Table 1. 2**), we can clearly see that almost the fifty percent of the *drachmae* have an Ag/Cu ratio > 1000 (while the other periods have an Ag/Cu ratio < 1000), concluding that there was an increase in the silver content average of the *drachmae* coins during this century. The quantity of silver in the alloy could be connected with either the raw material's source or the improvement of the recovery at the refining process.

1. 2. 4. 2. Quantitative analysis of silver *drachmae* from the *Rhode* mint (third century BC)

In this work, investigations were carried out in order to both characterize the type of alloy used for the coins minted in *Rhode* (third century BC) and figure out the differences and analogies with the emission from the *Emporion* mint.

These coins are of special interest to archaeologists and historians due to their scarcity and rarity. Despite the fact that from the numismatic point of view there are strong differences for both the minting quality and metrology, it seems that the productions made in the *Rhode* mint might have been influenced by the technology used in the *Emporion* workshop.

Although for a correct statistical evaluation the number of available coins minted in *Rhode* was not enough (a representative number of coins are usually required in this kind of studies since untypical values influence the interpretation of the analytical

results) comparison between the compositional data of both emissions might contribute to corroborate this hypothesis.

The elemental concentration range and other statistical information of the examined coins from different periods are presented in **Table 1. 3**. The results of the analysis were expressed in weight percentage (wt %).

Table 1. 3
Elemental concentration of the examined coins from the Rhode workshop measured by EDXRF (wt.%).

Minting period (BC)	Reference	Ag	Cu	Sn	Pb	Au	Pt	Bi	Fe	Cr	Ni	Zn	Mn	Ti
c. 300-260	20.491	98.47	0.54	nd	0.65	0.07	nd	0.1	0.07	0.05	0.04	0.01	0.01	nd
c. 300-260	20.493	93.17	0.52	4.55	0.29	0.26	0.01	0.07	0.7	0.04	0.06	0.12	0.04	0.17
c. 260-200	30.001	98.46	0.21	0.3	0.39	0.1	0.04	0.07	0.12	0.04	0.01	0.02	0.03	0.21
c. 260-200	33.583	97.92	1.15	nd	0.21	0.08	0.01	0.03	0.51	0.04	0.03	0	0	nd

nd, non detected

The coins from *Rhode* show similar compositional patterns to those from *Emporion* (**Fig. 1. 8**). Likewise, the main constituent of the alloy is silver, and copper, tin, lead, gold, platinum, bismuth, iron, chromium, nickel, manganese and titanium represent the trace elements of the alloy.

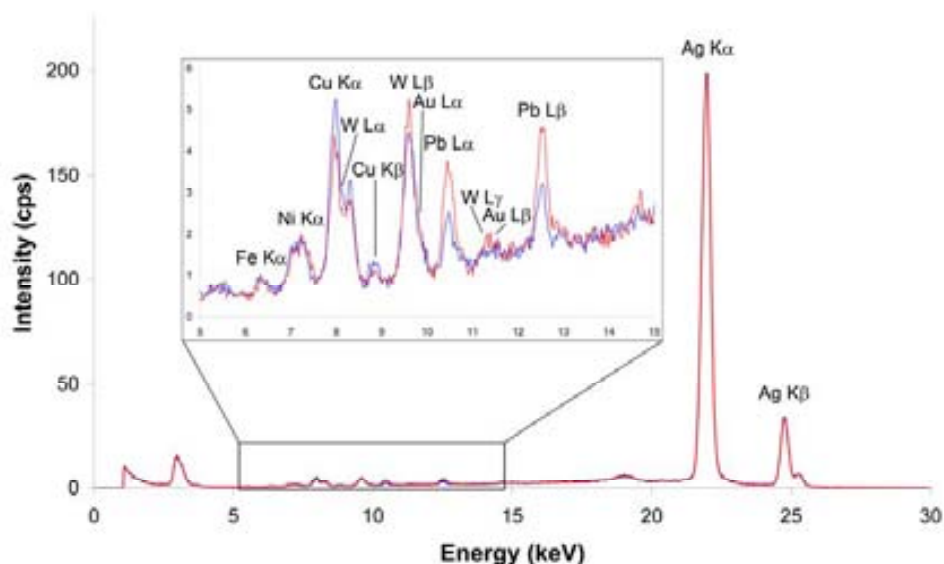


Fig. 1. 8 Comparison between EDXRF spectra of a drachma from *Emporion* (in blue, MNAC/GNC 20543) and from *Rhode* (in red, MNAC/GNC 20491).

For the proper comparison of both emissions, the next criterion was defined: *The group of coins of largest number is taken as the model sample (reference). Assuming that the % Ag follows a normal distribution, the 95 % confidence bound (CI) is calculated from*

the average % Ag in that issue of coins. Thus, it can be assumed with a 95 % CI that a coin from another production centre belongs to that of the model sample if the % Ag is within the defined range for the CI of the model sample.

In our case, we took the *Emporion* mint as a reference (see **Table 1. 2** to consult the confidence bound (CI) with a trustworthiness of 95% calculated for the *Emporion* mint of 300 - 260 and 260 - 200 BC periods). According to the obtained results and following the criterion defined above, we might consider the coins 20491 and 33583 as being analogous to the *drachmae* from the *Emporion* mint while, on the contrary, the coins 20493 and 30001 do not belong to the established intervals.

In order to establish some kind of reference behaviour path we might have had a higher amount of *drachmae* from the *Rhode* mint.

1. 2. 4. 3. Quantitative analysis of Iberian silver *drachmae* (third century BC)

In this research we concentrated our attention on those imitations from the Second Punic War (219-202 BC) trying to characterize both the type of alloys used for the coinage and determine the differences and analogies with the contemporary issues from *Emporion*.

The coins show silver as a main constituent and the presence of minor constituents and trace elements such as copper, tin, lead, gold, platinum, bismuth, iron, chromium, nickel, manganese and titanium as illustrated in **Fig. 1. 9 (a)**. Notice that both spectra are very similar.

Fig. 1. 9 (b) shows the relationship between the silver content and weight of the examined coins. According to the data, although the Iberian imitations have a degree of variability relatively high, the mean silver content on the alloy is clearly alike in both mints.

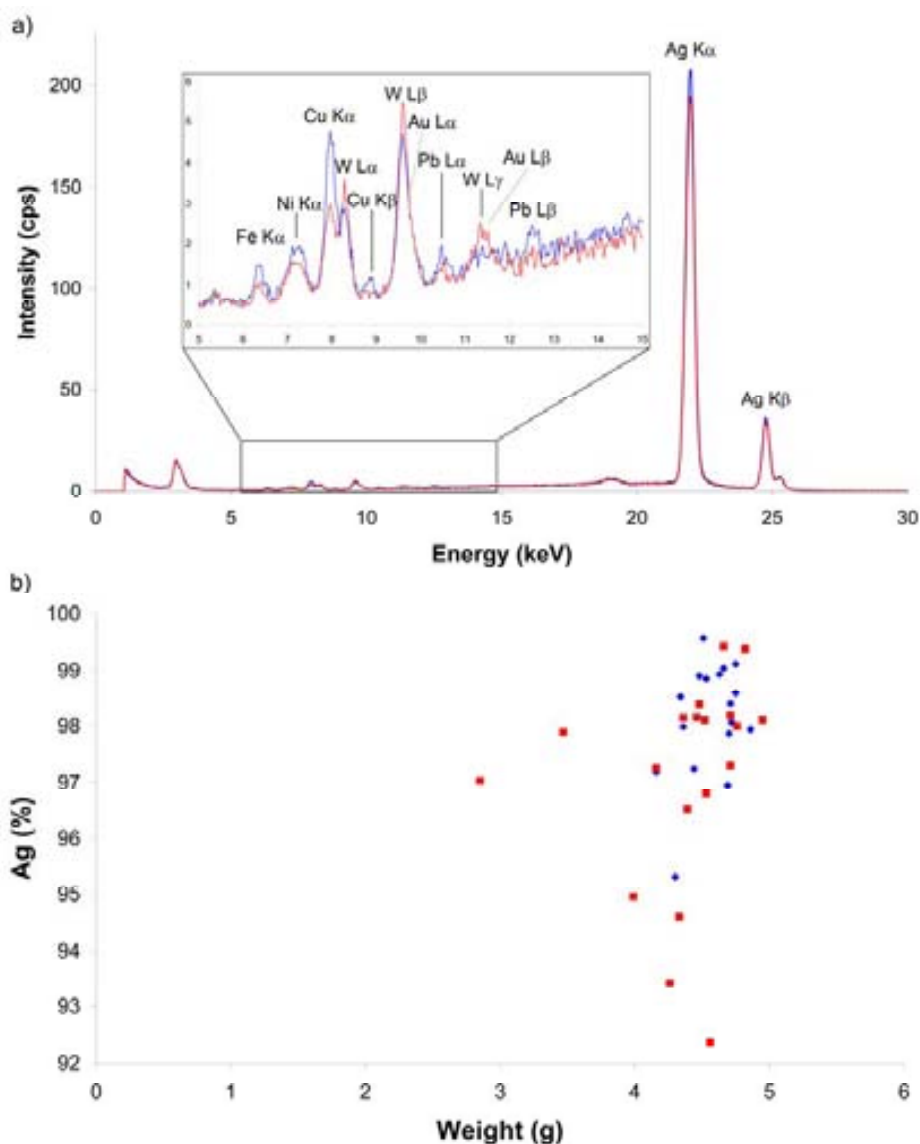


Fig. 1. 9 (a) Comparison between EDXRF spectra of a drachma from *Emporion* (in red, MNAC/GNC 20634) and an Iberian imitation (in blue, MNAC/GNC 109097); (b) plot of the relation between the weight of the coins and the silver content (%) from both emissions (red rhombus represents the *Emporion drachmae*; blue squares represents the Iberian imitations).

The silver content (wt %) and other features of the examined coins from both mints are presented in **Table 1. 4**. For the proper comparison between both emissions, a confidence bound (CI) with a trustworthiness of 95% was calculated for the *Emporion* mint: CI 95% Ag = (97.67, 98.68).

Table 1. 4

Ag content of the Iberian coins			Ag content of the <i>Emporion drachmae</i>		
Reference	Weight (g)	Ag (%)	Reference	Weight (g)	Ag (%)
20639	4,52	98,11	20622	4,71	98,40
20638	4,53	96,80	33554	4,48	98,91
20643	4,76	97,99	30014	4,75	98,59
109099	4,66	99,42	109096	4,44	97,24
33551	4,71	98,18	20570	4,36	97,99
20627	4,33	94,60	FS	4,66	99,04
20649	4,71	97,32	33547	4,3	95,32
20637	4,95	98,11	5056	4,63	98,94
20633	4,56	92,37	20556	4,86	97,94
20644	4,16	97,26	4507	4,53	98,86
20642	4,26	93,41	20566	4,72	98,06
20634	4,82	99,39	109097	4,75	99,12
20650	4,36	98,14	33578	4,34	98,52
20635	4,48	98,39	20652	4,51	99,57
20645	3,47	97,89	20563	-	98,81
20647	4,39	96,52	20630	4,69	96,95
33577	4,46	98,15	20569	4,7	97,86
33582	3,99	94,96	33562	4,16	97,19
20640	2,85	97,04			

As we can clearly observe in **Table 1. 4**, almost the 50% of the examined Iberian imitations might be considered analogous to those of the *Emporion* mint (on the compositional point of view).

1. 2. 5. Conclusions

The analysed Greek silver coins from the *Emporion* mint have found to have a very high fineness (they are composed by almost pure silver, being the average content around 98.32%). In the same way, in most of the *drachmae* the concentration of lead is below 0.5%, indicating a good silver refining process. The results of EDXRF analyses exhibit a great uniformity of the elemental chemistry of its alloys during more than three centuries. No significant variations were found between the silver concentration in the different minting periods, and the principal component analysis of minor and trace elements did not show us a clear difference between those periods. This regularity in the composition of the coins clearly evidence that the Greek craftsmen knew very well the art of making coins.

Dealing with the coins minted in *Rhode*, it is worth mentioning that on the compositional point of view it is difficult differentiate them with its homologous from the *Emporion* mint.

Concerning the Iberian imitations the results of EDXRF analyses exhibit a great uniformity of the elemental chemistry of both Iberian and *Emporion* alloys. Despite the fact that the Iberian community did not have a long tradition of mintage and that the style of the coinage was different (some coins were strongly influenced by indigenous style), on the compositional point of view the coins exhibit strong similarities with the *drachmae* of *Emporion*.

1. 3. Energy dispersive X-ray fluorescence analyses of ancient silver coins from the Spanish War of Independence period (1808-1814).

To mark the two hundred anniversary of the beginning of the Spanish War of Independence (1808-1814), the National Museum of Fine Arts of Catalonia (MNAC) and the Numismatic Cabinet of Catalonia (GNC-MNAC) organized the exhibition “Coinage at War. Catalonia in Napoleonic Europe”, held between June 2008 and May 2009. That period of war generated the need for money in order to fulfil the financial demands. This prompted the interest to carry out for the first time an extensive campaign of EDXRF measurements of some of the coins minted during that period.

1. 3. 1. Historical context

The type of coins we studied in this investigation was minted during the War of Spanish Independence (1808-1814). This occurrence was a contest between France and the allied powers of Spain, the United Kingdom and Portugal for the control of the Iberian Peninsula during the Napoleonic Wars. The war began after the Treaty of Fontainebleau when French armies invaded Portugal and the main Spanish cities were occupied by the Napoleonic troops and Napoleon handed the Spanish crown to his brother Joseph Bonaparte, in 1808.

This period, locally known as “Guerra del Francès”, generated the need for money and consequently five mints were opened around the Catalan territory. Thus coinage played a fundamental part in it from both the political and the economic perspective. The city of Barcelona reopened its mint due to the lack of coinage. In line with these events, on June 18th 1808 the Superior Committee of the Principality was created (a body that coordinated the defence of Catalonia against Napoleon’s armies). This committee allowed some cities in the Principality, the ones not occupied by the French, to mint emergency coinage in the years 1808 and 1809. Thus, Girona, Lleida,

Tarragona and Tortosa minted the so-called “duros” (silver coins equivalent to five “pesetas”, being “peseta” the coinage unit for Spain territory), just to satisfy the financial necessity generated by the war. The simplicity of the manufacture reflects the precarious nature of the available means to fabricate those (Campo *et al.*, 2006).

During that period plundering dynamics were promoted in order to obtain the raw metal to mint coinage, thus, causing huge loss, plunder, thefts and destruction of the cultural and artistic heritage (Bracons, 2003; Bracons, 2008). In this way, silver was obtained from different silvery sources, not only from civil productions (such as tableware, chalices or candelabrum) but also from religious works (such as silver sculptures or liturgical objects). They all were brought to the mint and then melted.

1. 3. 2. Research aims

Taking into consideration the historical context and having in mind that there are marked differences on style and metrology, the general objectives of this work were the characterization of the type of alloy used for the manufacture of the coins and the determination of differences and analogies between the five emissions using EDXRF. Furthermore, a collection of contemporary forgeries was studied.

1. 3. 3. Materials and Methods

1. 3. 3. 1. Sampling

A total of 130 silver coins that circulated during the Spanish War of Independence period were investigated. These coins came from the five different mints existing in Catalonia during this period and can be easily identified by the illustration and images of the coin surface. The elemental analysis by means of EDXRF was carried out on 68 coins from the mint of Barcelona, 19 coins from the mint of Girona, 9 coins from the mint of Lleida, 20 coins from the mint of Tarragona and 14 coins from the mint of Catalonia. In **Fig. 1. 10** are shown some of the analysed coins.



Fig. 1. 10 Obverse and reverse of coins from the Spanish War of Independence: (a) 5 “pesetas” from the mint of Barcelona (MNAC/GNC ref. 0021- 013787); (b) 1 “duro” from the mint of Girona (MNAC/GNC ref. 1242-03293); (c) 5 “pesetas” minted in Lleida (MNAC/GNC ref. 1256-013779); (d) 5 “pesetas” from the mint of Tarragona (MNAC/GNC ref. 1270-040723); (e) 8 “reales” from the mint of Catalonia (MNAC/GNC ref. 1298-037670). (Images provided by Dr. A. Estrada - MNAC/GNC).

Additionally, 7 contemporary forgeries were chemically characterized (in **Fig. 1. 11** some of the coins are illustrated). Three of those supposedly false coins were minted in Lima; other three of them were minted in Guatemala; one of them was minted in Seville.



Fig. 1. 11 Obverse and reverse of forgeries from the Spanish War of Independence: (a) coin from Guatemala (MNAC/GNC ref. 41147); (b) coin minted in Lima (MNAC/GNC ref. 41182); (c) coin from Seville (MNAC/GNC ref. 43222). (Images provided by Dr. A. Estrada - MNAC/GNC).

As the major requirement for this analytical campaign was the ability to perform “in situ” non-destructive measurements (due to the value of the coins and the rules preventing their transport to the X-ray laboratory) the analysis were carried out after bringing the EDXRF equipment to the National Museum of Fine Arts of Catalonia (MNAC). The coins were analyzed directly in a non-destructive way and without applying any cleaning treatment. In order to avoid possible surface heterogeneities, two EDXRF measurements, one for each side of the coin, were performed on the flat bright regions of all the coins. This method of measurements has been previously reported in other works (Al-Kofahi *et al.*, 2000; Constantinescu *et al.*, 2003; Civici *et al.*, 2007).

1. 3. 3. 2. Experimental

The equipment, the measurement conditions and the spectral data treatment (processing and quantification) are described elsewhere (see chapters 1. 2. 3. 2. to 1. 2. 3. 4.). The results were interpreted through typical multivariate statistic methods such as principal component analysis (PCA) with the software package SPSS Statistics 17.0.

1. 3. 4. Results and Discussion

1. 3. 4. 1. Coins from Barcelona, Catalonia, Lleida, Girona and Tarragona workshops

The analyzed coins were found to have a very high fineness. The average concentrations of silver (main constituent of the alloy) and copper in each group of coins are very close to each other and, respectively, are around 93% for silver and around 6% for copper. The copper can be considered as base alloying metal.

Additionally, the presence of minor constituents and trace elements such as zinc, tin, lead, gold, platinum, antimony, nickel and iron were identified. Minor and trace elements impurities can be due to: (a) the raw metal used in coin production, (b) the manufacturing process, and (c) in some coins could be from surface contamination (Constantinescu *et al.*, 2003).

If we focus our attention in the compositional analysis of each mint, **Table 1. 5**, we can clearly see that an approximate average silver content of 95% and about 4.5% for copper is recorded in Barcelona mint. The average silver concentration found for the

coins minted in the Catalonia workshop is 95% and a 4% of copper. Regarding the other mints, Lleida, Girona and Tarragona, although in general they present a high silver content, coins from Girona mint have a lower silver content (the average content is about 91.7%), which implies an increase of the copper proportion (average content about 7.6%). Likewise, the copper content of this mint has the lowest coefficient of variation of all the groups, thus revealing that the level of copper is not by chance but probably an addition to the melting batch.

Table 1.5
Elemental concentration range of examined coins (%wt)

	Ag	Cu	Zn	Sn	Pb	Au	Pt	Sb	Ni	Fe
<i>Barcelona</i>										
<i>n</i>	68	68	68	18	68	68	68	52	68	68
<i>min.</i>	91.40	2.02	0.05	0.02	0.07	0.08	0.02	0.01	0.01	0.00
<i>max.</i>	97.30	8.40	0.30	0.42	0.32	0.43	0.10	0.40	0.13	0.27
<i>mean</i>	94.95	4.45	0.12	0.12	0.18	0.19	0.05	0.17	0.06	0.08
<i>stdev.</i>	1.33	1.42	0.05	0.12	0.05	0.06	0.02	0.11	0.03	0.05
<i>C. O. V.</i>	1.41	31.86	39.01	95.37	30.85	32.43	35.16	65.73	44.57	62.44
<i>Catalonia</i>										
<i>n</i>	13	13	13	5	13	13	13	13	13	13
<i>min.</i>	93.50	2.63	0.02	0.05	0.09	0.02	0.04	0.01	0.01	0.02
<i>max.</i>	96.40	5.75	0.44	0.18	0.30	0.40	0.09	0.41	0.08	0.19
<i>mean</i>	94.94	4.23	0.16	0.09	0.20	0.21	0.06	0.22	0.05	0.07
<i>stdev.</i>	0.91	0.91	0.11	0.05	0.06	0.11	0.01	0.13	0.02	0.05
<i>C. O. V.</i>	0.95	21.48	72.43	57.69	27.40	51.39	19.40	58.00	40.39	76.06
<i>Girona</i>										
<i>n</i>	18	18	18	4	18	18	18	13	18	18
<i>min.</i>	89.30	5.34	0.09	0.02	0.19	0.14	0.02	0.02	0.04	0.02
<i>max.</i>	93.90	9.62	0.26	0.13	0.53	0.41	0.09	0.45	0.14	0.89
<i>mean</i>	91.68	7.55	0.17	0.07	0.30	0.20	0.06	0.13	0.09	0.10
<i>stdev.</i>	1.11	1.22	0.05	0.05	0.08	0.06	0.02	0.12	0.03	0.20
<i>C. O. V.</i>	1.21	16.18	26.90	68.30	27.03	29.60	32.57	89.81	28.29	188.67
<i>Lleida</i>										
<i>n</i>	9	9	9	2	9	9	9	8	9	8
<i>min.</i>	91.50	3.07	0.07	0.04	0.12	0.09	0.01	0.08	0.02	0.03
<i>max.</i>	96.20	7.11	0.24	0.19	0.47	0.66	0.10	0.33	0.12	0.47
<i>mean</i>	94.14	5.06	0.15	0.11	0.25	0.22	0.07	0.14	0.07	0.09
<i>stdev.</i>	1.65	1.49	0.05	0.11	0.10	0.17	0.03	0.08	0.03	0.15
<i>C. O. V.</i>	1.76	29.40	31.65	94.07	38.16	78.92	41.38	57.99	48.84	162.35
<i>Tarragona</i>										
<i>n</i>	17	17	17	3	17	17	17	15	17	17
<i>min.</i>	90.00	3.45	0.15	0.02	0.12	0.01	0.02	0.00	0.05	0.01
<i>max.</i>	95.30	9.26	0.31	0.21	0.43	0.32	0.09	0.21	0.13	0.12
<i>mean</i>	92.10	7.25	0.20	0.10	0.26	0.12	0.06	0.10	0.08	0.06
<i>stdev.</i>	1.49	1.49	0.05	0.10	0.09	0.07	0.02	0.06	0.02	0.03
<i>C. O. V.</i>	1.62	20.53	23.09	99.84	32.80	59.36	32.10	61.30	27.82	47.24

In order to identify clustering concerning the five mint factories, a statistical analysis by means of multivariate statistical methods (PCA) was performed. In this particular case,

the statistical analysis was restricted to minor and trace elements because, according to the data present in **Table 1. 5**, they have a high C.O.V.

The Catalan coins of the five different mints show similar trends in their composition, which clearly evidence the regularity of the manufacturing process, so that by using PCA statistical routine no significant clustering was obtained concerning the minor and trace constituents of the alloy. As shown in **Fig. 1. 12** (a scatter plot of the coins of mints of Barcelona, Catalonia, Lleida, Tarragona and Girona) once the factor analysis is applied, an overlap of the samples is observed, which does not allow us to distinguish the five mints between them. Once again it is demonstrated the sophisticated and controlled technology used by all the different minting factories in Catalonia region.

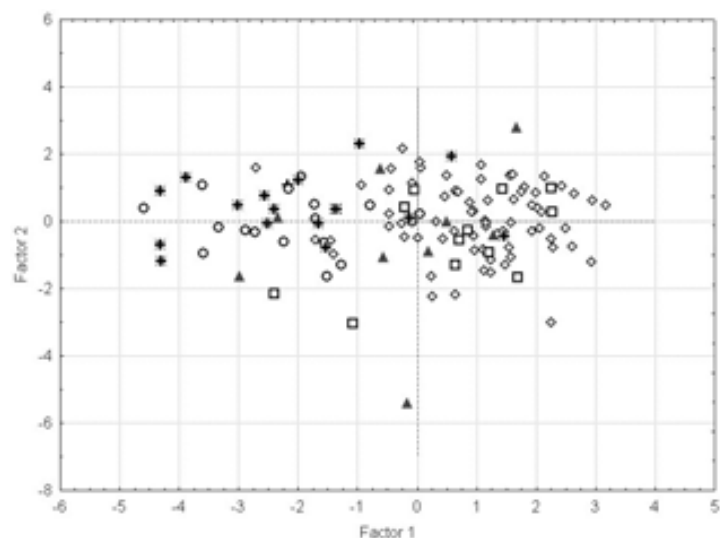


Fig. 1. 12 Scatterplot of factor 1 vs. factor 2 of some of the coins from different mints. 5 “pesetas” from the mint of Barcelona are represented by rhombus; 8 “reales” from the mint of Catalonia are shown by squares; “duros” from the mint of Girona are represented by circles; 5 “pesetas” minted in Lleida are shown by triangles and 5 “pesetas” from the mint of Tarragona are represented by stars.

During this period the craftsmen were able to produce alloys of great precision. According to Estrada-Rius (2008) the determination of the assay value was a constant concern during all the process and was carried out at the same time and twice by the two assayers in the mint. Equally, the metal weight was controlled after every transformation process. This could be an explanation for the lack of significant compositional variations between the alloys in the different mints.

Nevertheless, some little differences are observed regarding the Ag/Cu and Ag/Pb ratios, especially between the Catalonia and Girona mints. Concerning the silver and copper contents of the coins, the results (in **Fig. 1. 13 (a)**) show that all the groups of coins which belong to different mints are made of a similar Ag–Cu alloy. The logical strong negative correlation between silver and copper indicates the binary composition of silver-based coins and the deliberate controlled addition of this last metal in the batch used for the manufacturing of the coins. Copper was added to debase the silver coins and save the more expensive silver or to increase the strength, hardness and wear-resistance of silver (Constantinescu *et al.*, 2003; Al-Saad *et al.*, 2007; Civici *et al.*, 2007). On the other side, if we focus our attention in the silver and lead contents of the coins, **Fig. 1. 13 (b)**, we can clearly see that there is a low degree of correlation between silver and lead. The presence of lead, then, is totally random and it could be explained not only for the metallurgic process of the obtaining of silver but also for manufacturing process of the coins.

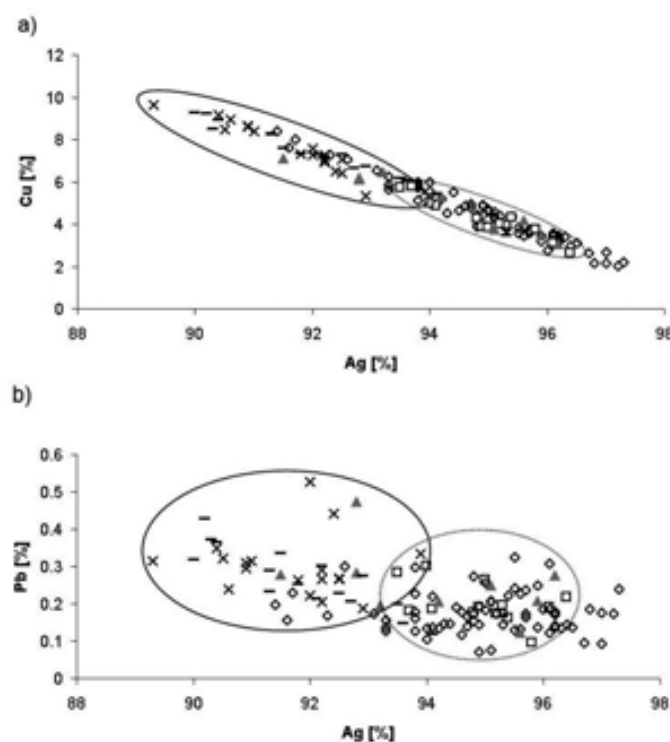


Fig. 1. 13 (a) Silver and copper contents, and (b) silver and lead contents of the coins from different groups. Key: 5 “pesetas” from the mint of Barcelona are represented by rhombus; 8 “reales” from the mint of Catalonia are shown by squares; “duros” from the mint of Girona are represented by crosses; 5 “pesetas” minted in Lleida are shown by triangles and 5 “pesetas” from the mint of Tarragona are represented by hyphens.

1. 3. 4. 2. Compositional anomalies and forgeries

According to the results of the analyses carried out on the 130 coins from different mints, we have found out at least 4 potentially forgeries (one of them belongs to the Girona mint and the other ones to the Tarragona mint).

The coin MNAC/GNC ref. 40707 from the Girona mint (**Table 1. 6**) is a Cu-Zn¹⁰ alloy (65% of copper and 33.6% of zinc). As illustrated in **Fig. 1. 14** we can clearly observe not only that the copper and zinc peaks are very intense but also that silver is almost absent on the false one.

Table 1. 6
Compositional anomalies of the coins from the Girona mint (%wt).

Reference	Ag	Cu	Zn	Sn	Pb	Au	Pt	Sb	Ni	Fe
40707	0.12	65.26	33.61	0.02	0.88	0.07	0.01	nd	nd	0.02

nd, non detected

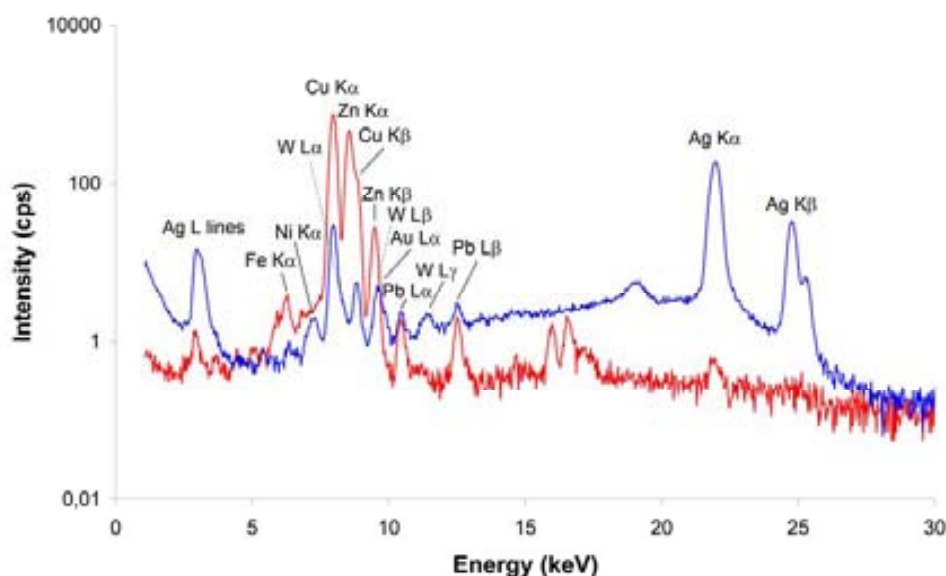


Fig. 1. 14 Comparison between EDXRF spectra of a counterfeit (in red, MNAC/GNC ref. 40707) and a genuine coin from the mint of Girona (in blue, MNAC/GNC ref. 40985).

Dealing with the coins minted in Tarragona (MNAC/GNC ref. 65206, 40721 and 25084) all of the identified counterfeits present silver, copper, zinc and tin^{11, 12} in different

¹⁰ Cu-Zn alloy: brass.

¹¹ Cu-Sn alloy: bronze

¹² Cu-Sn-Ag alloy: silvery bronze

relative amounts (**Table 1. 7**). It is worth mentioning the appearance of lead (around the 6%) as part of the alloy in some of the coins. Typical EDXRF patterns of a counterfeit coin and a real one are shown in **Fig. 1. 15**. Notice that the presence of copper, lead and tin on relative high amounts is recorded, while the silver content is extremely low in comparison to the real coin.

Table 1. 7
Compositional anomalies of the coins from the Tarragona mint (%wt).

Reference	Ag	Cu	Zn	Sn	Pb	Au	Pt	Sb	Ni	Fe
65206	48.18	37.64	1.12	10.94	0.36	0.02	0.07	0.28	0.88	nd
40721	5.97	70.43	0.21	16.31	5.97	0.33	0.19	nd	0.08	0.01
25084	0.18	76.46	0.15	15.15	6.57	0.15	0.19	nd	0.04	nd

nd, non detected

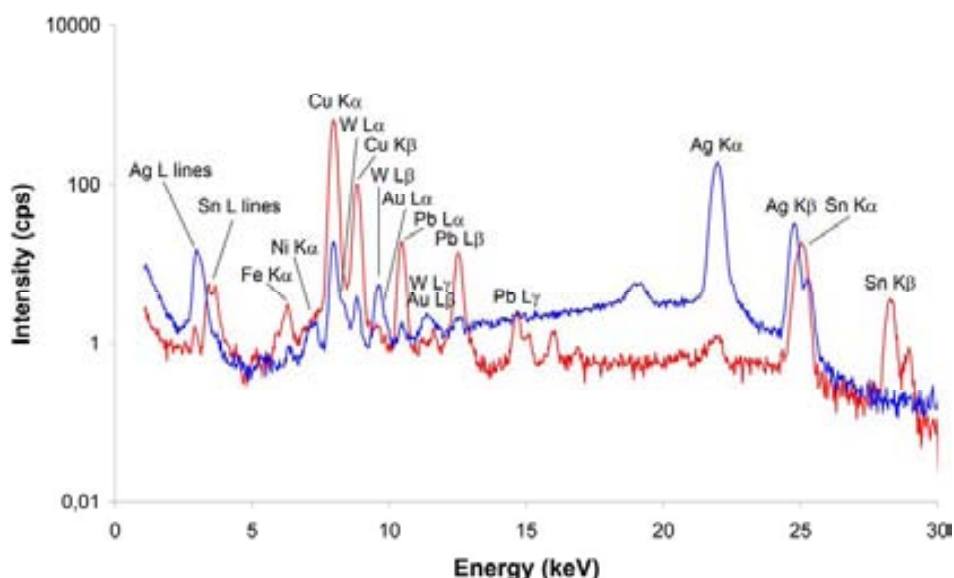


Fig. 1. 15. Comparison between EDXRF of coins struck in Tarragona. The red spectrum represents the counterfeit (MNAC/GNC ref. 25084) while the blue spectrum represents an authentic coin (MNAC/GNC ref. 40715).

Concerning the seven supposedly false coins, although by visual examination (which is the first step of a numismatist's work) was sufficient to identify them, their chemical composition has been determined in order to compare it with the composition of the real ones.

The obtained results revealed the presence of copper, zinc, tin lead and antimony in relative high amount (**Table 1. 8, Fig 1. 16**) and the consequent reduction in the silver content. These elements were deliberately added to debase the silver coins.

Table 1. 8
Elemental concentration of contemporary forgeries (%wt)

Provenance	Reference	Ag	Cu	Zn	Sn	Pb	Au	Pt	Sb	Ni	Fe	Cd	Ga	Ge
Guatemala	41150	3.21	1.68	3.75	81.66	0.86	0.17	0.07	8.24	0.12	nd	0.23	0.07	0.11
Guatemala	41147	1.6	81.89	0.26	15.1	0.33	0.15	0.18	nd	0.07	nd	nd	0.37	0.12
Guatemala	41146	7.62	2.43	4.06	76.93	2.05	0.44	0.25	5.58	0.17	nd	0.51	0.07	0.09
Sevilla	43222	0.16	7.24	0.22	90.3	0.59	0.08	0.01	1.38	0.16	nd	0.05	0.09	0.09
Lima	41183	13.62	66.09	0.42	17.54	0.65	0.56	0.25	nd	0.13	nd	nd	0.47	0.3
Lima	41182	85.68	0.82	0.01	13.35	0.05	nd	0	nd	0.07	0.1	nd	0	0.06
Lima	41180	18.16	0.81	7.1	68.26	0.65	0.59	0.35	2.79	0.26	nd	0.83	0.12	0.12

nd, non detected

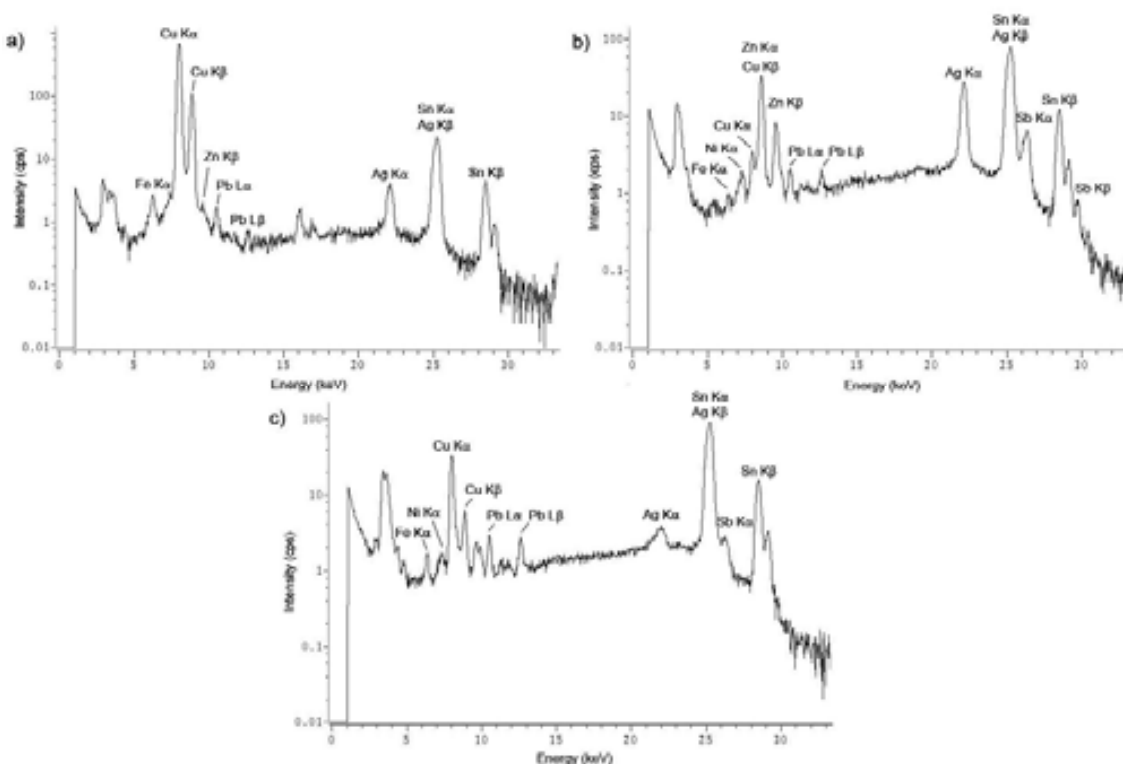


Fig. 1. 16 EDXRF spectra of some of the forgeries: (a) Spectrum of a counterfeit from Guatemala (MNAC/GNC ref. 41147); (b) spectrum of a counterfeit minted in Lima (MNAC/GNC ref. 41180); (c) spectrum of a counterfeit from Seville (MNAC/GNC ref. 43222).

1. 3. 5. Conclusions

This study reveals that the Catalan coins from the Spanish War of Independence period (1808-1814) collection exhibit a great uniformity of the elemental chemistry of alloys from different workshops. Apart of the silver content (major constituent of almost all the studied coins) it was possible to recognize copper as main metal alloying element. Likewise, zinc, tin, lead, gold, platinum, antimony, nickel and iron were found as minor or trace constituents of the alloy. The high silver content indicates the high quality control of the manufacturing process of these Catalan coins. However, the study

has also pointed out the existence of compositional anomalies on some of the coins, highlighting the presence of copper, zinc, tin and antimony in relative high amounts (concentrations above 1%).

During that period of war, the Barcelona mint operated under the commandment of Joseph Bonaparte and Catalonia, Lleida, Girona and Tarragona mints worked under the direction of the Superior Committee of the Principality. According to the EDXRF results we can affirm that, even though these mints were under the control of different authorities, there are no strong compositional differences between the alloys of the five mints. Nevertheless, the average silver content of Girona mint is slightly lower than the other mints, especially than the Catalonia mint. This tendency allows us to differentiate, on the compositional point of view, the coins from both mints.

Dealing with the supposed contemporary counterfeits, the study highlighted that most of the forgeries exhibit a considerably reduction in the silver content and, consequently, an increase in the copper, zinc, tin, lead and antimony contents. These last elements were intentionally added to debase the silver coins and save the more expensive silver. The most common alloys are bronze (Cu-Sn), silvery bronze (Cu-Sn-Ag) and other alloys such as Sn-Sb-Ag, Sn-Cu, Cu-Ag-Sn, Ag-Sn and Sn-Ag. It is worth mentioning, however, that EDXRF analysis was very useful on those cases in which it was practically impossible distinguish an authentic coin from a counterfeit one.

1. 4. References

AL-KOFAHI M.M., AL-TARAWNEH K.F. (2000) *Analysis of Ayyubid and Mamluk Dirhams Using X-Ray Fluorescence Spectrometry*. X-Ray Spectrometry, 29, 39-47.

AL-SAAD Z., BANI HANI M. (2007) *Corrosion behaviour and preservation of Islamic Silver Coins*, in: ARGYROPOULOS V., HEIN A., ABDEL-HARITH M. (Eds.) *Strategies for Saving Our Cultural Heritage: Papers presented at the International Conference on Strategies for Saving Indoor Metallic Collections with a special section on Legal Issues in the Conservation of Cultural Heritage*, Cairo 26-28 February 2007, 177-183.

ARMBRUSTER D.A., TILLMAN M.D., HUBBS L.M. (1994) *Limit of detection (LQD)/ limit of quantitation (LOQ): comparison of the empirical and the statistical methods exemplified with GC-MS assays of abused drugs*. Clinical Chemistry, 40,1233-1238.

BRACONS J. (2003) *Per una història del vandalisme a Catalunya (segles XV-XX)*. Unicum. Revista de l'Escola Superior de Conservació i Restauració de Béns Culturals de Catalunya, 2, 44-51.

BRACONS J. (2008) *L'aprovisionament de les seques i la pèrdua de patrimoni a Catalunya*, in: ESTRADA-RIUS A. et al., *Monedes en lluita: Catalunya a l'Europa napoleònica*. Edited by Museu Nacional d'Art de Catalunya, Barcelona, 85-93

CAMPO M. (2002) *Las emisiones de Emporion y su difusión en el entorno Ibérico*, in: ROMAGNOLI D., STAZIO A. (Eds.) *La monetazione dei Focei in Occidente. Atti Dell'XI Centro Internazionale Di Studi Numismatici (Napoli, 25-27 Ottobre 1996)*. Istituto Italiano Di Numismatica, Roma, 139-166.

CAMPO M., ESTRADA-RIUS A., CLUA M. (2006) *Numismatics guide*. Edited by Museu Nacional d'Art de Catalunya, Barcelona, 20-27, 28-35, 36-43, 166-173.

CARTER G.F. (1993) *Chemical and Discriminant Analyses of Augustan Asses*. *Journal of Archaeological Science*, 20, 101-115.

CIVICI N., GJONGECAJ Sh., STAMATI F., DILO T., AVLIDOU E.P., POLYCHRONIADIS K., SMIT Z. (2007) *Compositional study of IIIrd century BC silver coins from Kreshpan hoard (Albania) using EDXRF spectrometry*. *Nuclear Instruments and Methods in Physics Research B: Beam Interactions with Materials and Atoms*, 258, 414-420.

CONSTANTINESCU B., SASIANU A., BUGOI R. (2003) *Adulterations in first century BC: the case of Greek silver drachmae analyzed by X-ray methods*. *Spectrochimica Acta Part B: Atomic Spectroscopy*, 58, 759-765.

CONSTANTINESCU B., BUGOI R., OBERLÄNDER-TARNOVEANU E., PARVAN K. (2005) *Some considerations on X-ray fluorescence use in museum measurements-The case of medieval silver coins*. *Romanian Reports in Physics*, 57 (4), 1021-1031.

DENKER A., BOHNE W., OPITZ-COUTUREAU J., RAUSCHENBERG J., RÖHRICH J., STRUB E. (2005) *Influence of corrosion layers on quantitative analysis*. *Nuclear Instruments and Methods in Physics Research B: Beam Interactions with Materials and Atoms*, 239, 65-70.

DOMINGUEZ A., ROVIRA S., MONTERO I. (2004) *Aportación a la composición metalográfica de las monedas hispanas. Análisis cuantitativos de monedas de la ceca de Bolskan/Osca*. Acta Numismática, 34, 79-101.

ESTRADA-RIUS A. (2008) *Fabricar moneda en temps de guerra: organització i processos de producció a la seques catalanes (1808-1814)*, in: ESTRADA-RIUS et al., *Monedes en lluita: Catalunya a l'Europa napoleònica*. Edited by Museu Nacional d'Art de Catalunya, Barcelona, 95-105.

FERRETTI M. (2000) *X-ray Fluorescence Applications for the Study and Conservation of Cultural Heritage*, in: CREAGH D.C., BRADLEY D.A. (Eds.) *Radiation in Art and Archeometry*. Elsevier, Amsterdam, 285-296.

FLAMENT C., MARCHETTI P. (2004) *Analysis of ancient silver coins*. Nuclear Instruments and Methods in Physics Research B: Beam Interactions with Materials and Atoms, 226, 179-184.

GALE N.H., GENTNER W., WAGNER G.A. (1980) *Mineralogical and Geographical Silver Sources of Archaic Greek Coinage*, in: METCALF D.M., ODDY W.A. (Eds.) *Metallurgy in Numismatics I*. Royal Numismatic Society, London, 3-49.

GALLARDO J.M., GÓMEZ B., BOUZAS A., CUEVAS F.G., VILLEGAS R. (2001) *Determinación de la composición química de piezas metálicas históricas: aplicación a un bronce romano*, in: GÓMEZ-TUBÍO B., RESPALDIZA M.A., PARDO M.L. (Eds.) *Actas del III Congreso Nacional de Arqueometría (Sevilla, Diciembre de 1999)*. Universidad de Sevilla, Spain, 497-506.

GIANONCELLI A., KOUROUSIAS G. (2007) *Limitations of portable XRF instruments in evaluating depth information: an archaeometric perspective*. Applied Physics A, 89, 857-863.

GIGANTE G.E., CESAREO R. (1998) *Non-destructive analysis of ancient metal alloys by in situ EDXRF transportable equipment*. Radiation Physics and Chemistry, 51 (4-6), 689-700.

GOZALBES M., RIPOLLÈS P.P. (2003) *La fabricación de moneda en la antigüedad*, in: *Actas XI Congreso Nacional de Numismática (Zaragoza, 16-19 de Octubre 2002)*.

Edited by Real Casa de la Moneda and Fábrica Nacional de Moneda y Timbre, Madrid, 11-34.

GUERRA M.F. (1995) *Elemental Analysis of Coins and Glasses*. Applied Radiation and Isotopes, 46 (6/7), 583-588.

GUERRA M.F. (1998) *Analysis of Archaeological Metals. The Place of XRF and PIXE in the Determination of Technology and Provenance*. X-Ray Spectrometry, 27, 73-80.

GUILHERME A., PESSANHA S., CARVALHO M.L., SANTOS J.M.F. dos, COROADO J. (2010) *Micro energy dispersive X-ray fluorescence analysis of polychrome lead-glazed Portuguese faiences*. Spectrochimica Acta Part B: Atomic Spectroscopy, 268 (10), 328-333.

HACKENS T. (1975) *Le rythme de la production monétaire dans l'Antiquité: Actes du colloque de Numismatique antique*. Problèmes et méthodes. Nancy-Louvain, 1971, 189-196.

HELSEN J. A., KUCZUMOW A. (1993) *Wavelength-Dispersive X-ray Fluorescence*, in: VAN GRIEKEN R, MARKOWICZ AA (eds.) *Handbook of X-Ray Spectrometry: Methods and Techniques*. Marcel Dekker Inc., New York, p. 129.

JANSSENS K., VITTIGLIO G., DERAEDT I., AERTS A., VEKEMANS B., VINCZE L., WEI F., DERYCK I., SCHALM O., ADAMS F., RINDBY A., KNÖCHEL A., SIMIONOVICI A., SNIGIREV A. (2000) *Use of Microscopic XRF for Non-destructive Analysis in Art and Archaeometry*. X-Ray Spectrometry, 29, 73-91.

JANSSENS K., VAN GRIEKEN R. (2004) *Preface*, in: JANSSENS K. and VAN GRIEKEN R. (Eds.) *Non-destructive Microanalysis of Cultural Heritage Materials*. Wilson and Wilson's, Comprehensive Analytical Chemistry Vol. XLII, ELSEVIER, 1-10.

KALLITHRAKAS-KONTOS N., KATSANOS A.A., POTIRIADIS C., OECONOMIDOU M., TORATSOGLU J. (1996) *PIXE analysis of ancient Greek copper coins minted in Epirus, Illyria, Macedonia and Thessaly*. Nuclear Instruments and Methods B: Beam Interactions with Materials and Atoms, 109-110, 662-666.

KALLITHRAKAS-KONTOS N., KATSANOS A.A., TOURATSOGLU J. (2000) *Trace element analysis of Alexander the Great's silver tetradrachms minted in Macedonia*. Nuclear Instruments and Methods in Physics Research B: Beam Interactions with Materials and Atoms, 171, 342-349.

LINKE R., SCHREINER M., DEMORTIER G. (2003) *Determination of the provenance of medieval silver coins: potential and limitations of x-ray analysis using photons, electrons or protons*. X-Ray Spectrometry 32 (5), 373-380.

LÖNNQVIST K.K.A. (2003) *A second investigation into the chemical composition of the Roman Provincial (Procuratorial) coinage of Judea, AD 6-66*. Archaeometry, 45 (1), 45-60.

MANSO M., COSTA M., CARVALHO M.L. (2008) (a) *Comparison of elemental content on modern and ancient papers by EDXRF*. Applied Physics A: Materials Science & Processing, 90, 43-48.

MANSO M., COSTA M., CARVALHO M.L. (2008) (b) *X-ray fluorescence spectrometry on paper characterization: A case study on XVIII and XIX century documents*. Spectrochimica Acta Part B: Atomic Spectroscopy, 63, 1320–1323.

MANTLER M., SCHREINER M. (2000) *X-Ray Fluorescence Spectrometry in Art and Archaeology*. X-Ray Spectrometry, 29, 3-17.

MAR R., RUIZ DE ARBULO J. (1993) *Ampurias Romana. Historia, Arquitectura y Arqueología*. Editorial AUSA, Sabadell.

MCKERREL H., STEVENSON R.B.K. (1972) *Some analyses of Anglo-Saxon and associated oriental silver coinage*, in: HALL E. T. and METCALF D. M. (Eds.) *Methods of chemical and metallurgical investigation of ancient coinage*. Royal Numismatics Society, 8, London, 195.

MOIOLI P., SECCARO C. (2000) *Analysis of Art Objects Using a Portable X-Ray Fluorescence Spectrometer*. X-Ray Spectrometry, 29, 48-52.

MONTERO-RUIZ I., CASTANYER P., GENER M., HUNT M., MATA J.M., PONS E., ROVIRA-LLORENS S., ROVIRA-HORTALÁ C., RENZI M., SANTOS-RETOLAZA M.,

SANTOS-ZALDUEGUI J.F. (2007) *Lead and Silver Metallurgy in Emporion (L'Escala, Girona, Spain). 2nd Internacional Conference Archaeometallurgy in Europe (Aquileia, 17-21 June 2007)*. [CD-ROM].

MONTERO-RUIZ I., CASTANYER P., GENER M., HUNT M., MATA J.M., PONS E., ROVIRA-LLLORENS S., ROVIRA-HORTALÀ C., RENZI M. (2008) *Caracterización analítica de la producción metalúrgica protohistórica de plata en Cataluña*. *Revista d'Arqueologia de Ponent*, 18, 292-316.

MORENO-SUÁREZ A.I., GÓMEZ-TUBÍO B., RESPALDIZA M.A., CHAVES F., ORTEGA-FELIU I., ONTALBA-SALAMANCA M.Á., AGERA F.J. (2011) *Combining non-destructive nuclear techniques to study Roman leaded copper coins from Ilipe (II–I centuries B.C.)*. *Nuclear Instruments and Methods in Physics Research Section B: Beam Interactions with Materials and Atoms*, doi:10.1016/j.nimb.2011.04.077.

PATERNOSTER G., RINZIVILLO R., NUNZIATA F., CASTELLUCCI E. M., LOFRUMENTO C., ZOPPI A., FELICI A. C., FRONTEROTTA G., NICOLAIS C., PIACENTINI M., SCIUTI S., VENDITTELLI M. (2005) *Study on the technique of the Roman age mural paintings by micro-XRF with Polycapillary Conic Collimator and micro-Raman analyses*. *Journal of Cultural Heritage*, 6, 21–28.

PESSANHA S., GUILHERME A., CARVALHO M.L. (2009) *Comparison of matrix effects on portable and stationary XRF spectrometers for cultural heritage samples*. *Applied Physics A: Materials Science & Processing*, 97, 497-505.

PISTOFIDIS N., VOURLIAS G., PAVLIDOU E., DILO T., CIVICI N., STAMATI F., GJONGECAJ S., PRIFTI I., BILANI I., STERGIODIS G., POLYCHRONIADIS E.K. (2006) *On the comparative study of three silver coins of the IIIrd century B.C. minted in Korkyra, Dyrrachion and by the Illyrian king Monounios*. *Applied Physics A: Materials Science & Processing*, 83, 637-642.

QUERALT I., ÁLVAREZ A., PITARCH À., TEIXELL, I. (2007) *Compositional characterization of copper-based Roman coins by non-destructive WDXRF*, in: *Technart 2007: Non-destructive and Microanalytical Techniques in Art and Cultural Heritage Research (Lisboa, Portugal, 25-27 April)*. Book of abstracts, 137.

RIZZO F., CIRRONE G.P., CUTTONE G., ESPOSITO A., GARRAFFO S., PAPPALARDO G., PAPPALARDO L., ROMANO F.P., RUSSO S. (2011) *Non-destructive determination of the silver content in Roman coins (nummi), dated to 308–311 A.D., by the combined use of PIXE-alpha, XRF and DPAA techniques*. *Microchemical Journal*, 97 (2), 286-290

RODRIGUES M., SCHREINER M., MÄDER M., MELCHER M., GUERRA M., SALOMON J., RADTKE M., ALRAM M., SCHINDEL N. (2010) *The hoard of Beçin—non-destructive analysis of the silver coins*. *Applied Physics A: Materials Science & Processing*, 99, 351–356.

RODRIGUES M., SCHREINER M., MELCHER M., GUERRA M., SALOMON J., RADTKE M., ALRAM M., SCHINDEL N. (2011) *Characterization of the silver coins of the Hoard of Beçin by X-ray based methods*. *Nuclear Instruments and Methods in Physics Research Section B: Beam Interactions with Materials and Atoms*, doi:10.1016/j.nimb.2011.04.068.

SÁNDOR Zs., TÖLGYESI S., GRESITS I., KÁPLÁN-JUHÁSZ M. (2000) *Qualitative and quantitative analysis of medieval silver coins by energy dispersive X-ray fluorescence method*. *Journal of Radionanalytical and Nuclear Chemistry*, 246 (2), 385-389.

SÁNDOR Zs., TÖLGYESI S., GRESITS I., KASZTOVSZKY Zs. (2002) *Determination of alloying elements in ancient silver coins by X-ray fluorescence*. *Journal of Radioanalytical and Nuclear Chemistry*, 254 (2), 283-288.

SEJAS DEL PIÑAL G. (1993) *Consideraciones sobre la política monetaria Bárquida a partir del análisis de sus monedas de plata*. *Rivista di studi fenici*, Vol. XXI, 1, 111-136. Consiglio nazionale delle ricerche, Roma.

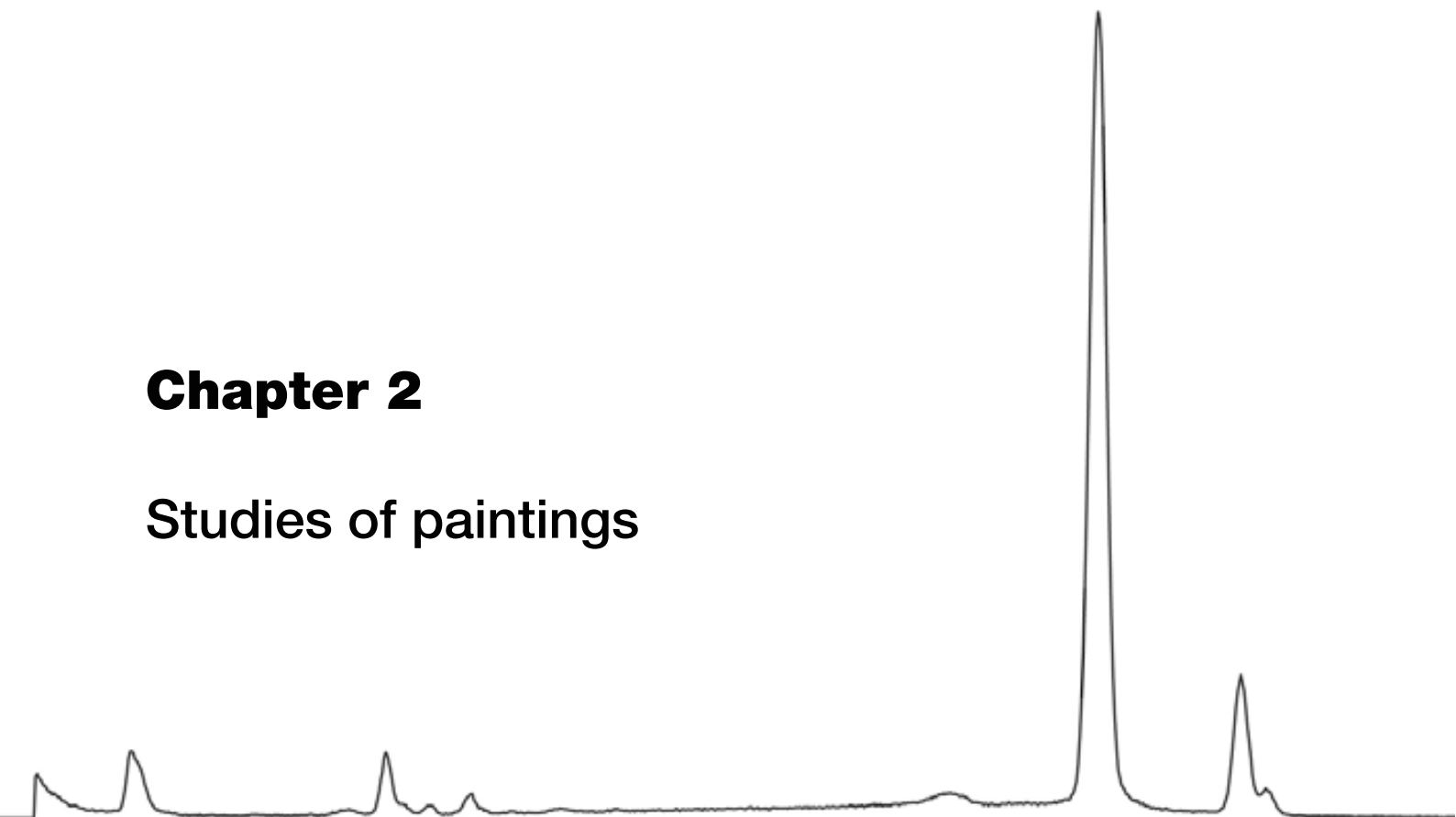
VAN GRIEKEN R.E., MARKOWICZ A.A. (Eds.) (1993) *Handbook of X-ray Spectrometry. Methods and Techniques*. Marcel Dekker Inc., New York.

De VIGUERIE L., SOLE V. A., WALTER P. (2009) *Multilayers quantitative X-ray fluorescence analysis applied to easel paintings*. *Analytical Bioanalytical Chemistry*, 395, 2015–2020.

VIJAYAN V., RAUTRAY T.R., BASA D.K. (2004) *EDXRF study of Indian punch-marked silver coins*. Nuclear Instruments and Methods in Physics Research B: Beam Interactions with Materials and Atoms, 225, 353-356.

Chapter 2

Studies of paintings



Part of the contents of this chapter is published in:

PITARCH A., RAMÓN A., ALVAREZ-PEREZ A., QUERALT I. (2011) *Characterization of "oil on copper" paintings by energy dispersive x-ray fluorescence spectrometry*. Analytical and Bioanalytical Chemistry. doi: 10.1007/s00216-011-5368-6.

PITARCH A., RAMÓN A., ALVAREZ-PEREZ A., CASTRO K., MADARIAGA, J.M., QUERALT I. *Multispectroscopic characterization of "oil on copper" painting*. (Submitted to *Current Analytical Chemistry*).

2. 1. Introduction

It is well known the usefulness of X-ray fluorescence (XRF) technique for the elemental characterization of inorganic pigments. In this sense, several archaeological objects and other artworks of all sizes, forms and materials have been usually characterised by XRF spectrometry, amongst other techniques (Desnica and Schreiner, 2006; Castro *et al.*, 2008 (a); Cesareo *et al.*, 2008; Desnica *et al.*, 2008; Gil *et al.*, 2008; Hradil *et al.*, 2008; Sotiropoulou *et al.*, 2008; Herrera *et al.*, 2009; Scott *et al.*, 2009).

In the particular topic of “oil on copper” paintings analytical studies, however, they have only been discussed in museum catalogues and conservator’s reports (Horovitz, 1986, 2002; Pavolopoulou and Watkinson, 2006) while scarce analytical data have been found in the literature (Bonizzoni *et al.*, 2008 (a)) and none of them carried out a specific scientific investigation in order to obtain a complete characterization of these unique objects in a non-destructive way.

This chapter aims to report the suitability of EDXRF for the study of paintings on metallic supports by presenting two different approaches. The first one deals with the potentiality of a quantitative EDXRF methodology for the estimation of the areal distribution of pigments on such kind of pictorial artworks, whilst the second one aims to report the effectiveness of EDXRF technique in combination with other spectroscopic techniques for the chemical characterization of these “oil on copper” paintings.

Therefore, this study intends to contribute, from the analytical point of view, to the enlargement of the information about this kind of artworks within the national scientific production.

2. 2. Historical context

The practice of painting in oil on a copper support dates back to the mid-sixteenth century. It has its origins in Italy and was widespread in the rest of Europe and South America during the early seventeenth century. Italian artists began to use the thin metal sheets (often old printmaking plates) as a part of broader experimentation with painting on smooth surfaces (Komanecy, 1999). The masterworks usually painted portraiture and landscapes, typically small but incredibly detailed and richly coloured, to decorate objects such as furniture or dresses. The works also depicted devotional and sacred themes, especially in the religious circles of Italian sixteenth century. Objects such as

reliquaries and crucifixes were painted by large workshops of artists working under the supervision of a well known artist (known as *maestro*, “the master”) and were used for religious and ceremonial purposes. These paintings usually show the saints of the holy orders ornamented with golden details that further emphasised its devotional function.

According to the literature (Komanecky *et al.*, 1998, Horovitz, 1999) the painting technique had diverse stages; once the artist obtained his copper plate, it required roughening prior to painting because of the potential problems of adherence between the support and the paint. Then, a priming coat or *imprimatura* (typically a thin layer of white lead and umber in oil) was applied by hand to also help the paint to adhere. Other authors (Veiga, 2010) also suggest that the application of this white layer has mostly an optical function (i.e. brighten the surface). Anyway, the practice of using a ground layer made by white lead remained till the end of the nineteenth century, when lead grounds began to be substituted by zinc white grounds (Carlyle, 2001).

2. 3. Characterization of “oil on copper” paintings by energy dispersive x-ray fluorescence spectrometry.

In the area of Cultural Heritage, energy dispersive X-ray fluorescence (EDXRF) technique has become a powerful tool towards the obtaining of qualitative information about the chemical composition of inorganic pigments (Desnica and Schreiner, 2006; Desnica *et al.*, 2008; Gil *et al.*, 2008; Sotiropoulou *et al.*, 2008; Sawczak *et al.*, 2009; Scott *et al.*, 2009). Moreover, recent studies reported that EDXRF spectrometry in combination with other techniques such as visible reflectance spectrometry (vis-RS) or even alone can be successfully applied, in a wide range of cases, to reconstruct stratigraphy and thickness of paint layers or even in photograph films (Stulik and Khanjian, 2003; Bonizzoni *et al.*, 2007; Bonizzoni *et al.*, 2008 (b); Cesareo *et al.*, 2008; Bertucci *et al.*, 2010; Bonizzoni *et al.*, 2010; Bonizzoni *et al.*, 2011). In the particular topic of quantitative analysis of multilayered paintings by XRF, there had been published few works (Kanggiesser *et al.*, 2005; Dupuis and Menu, 2006; Pappalardo *et al.*, 2008; de Viguerie *et al.*, 2009) but there are no specific research in order to obtain semi-quantitative information of the areal distribution of pigments from XRF spectral data. On this context, such kind of artwork (paintings on metal support) becomes a perfect material to be analysed by means XRF spectrometry, due to the metallic nature of the substrate, which allows applying similar procedures as those reported in the ISO 3497 (International Standards Organization, 2000) for the characterization and measuring of coating thickness by X-ray spectrometric methods.

2. 3. 1. Research aims

The aim of this work is to study the suitability of a quantitative EDXRF method designed specifically for the approximation of pigment mass distribution on “oil on copper” multilayered paintings. As an example of application, we estimated pigment mass distribution of two “oil on copper” paintings.

2. 3. 2. Materials and methods

2. 3. 2. 1. Artworks

Two “oil on copper” paintings from presumable different ages were selected for this study. Both of them belong to the private collection of Artur Ramon Art Gallery (Barcelona, Spain). The first one represents a scene of a Franciscan habit saint holding a wooden cross in his outstretched arms. The accuracy of the stroke and the employed colours (its palette is composed by green, golden, red, skin-coloured and brown in different tonalities) suggest that this is an Italian work made at the second half of the sixteenth century (**Fig. 2. 1 (a)**). The second painting under study represents a river landscape scene. Although the painting is in bad state of conservation (it has micro-cracks in excess, probably due to the poor preparation of the copper plate) the colours are still very vivid (its palette is composed by white, yellow, pink, orange, deep red, brown, green and blue). Such kind of detailed scenes was in vogue during the eighteenth century, especially in the bourgeois Dutch market (**Fig. 2. 1 (b)**).



Fig. 2. 1 Analysed paintings: (a) portrait of Saint Bernardino of Siena (Renaissance period); (b) river landscape scene (Contemporary period) (photography: A. Pitarch).

The major requirement for this analytical study was the ability to perform non-destructive measurements, due to the historical value of both artworks. In a first stage, then, the “oil on copper” paintings were examined using non-destructive EDXRF to qualitatively determine the elemental composition of pigments present in the paintings. In addition, X-ray diffraction (XRD) was also employed not only to reach information on the compositional properties of the painting by crystalline phase analysis but also to characterise the nature of the different layers for the proper development of the EDXRF layer model.

2. 3. 2. 2. Equipments

Elemental analysis of painting surfaces was obtained by using a bench top small-spot EDXRF spectrometer (XDV-SD® model, Helmut Fischer GmbH, Germany). See section **I. 5** to check the instrument’s parameters.

The crystalline phase analyses of the artworks were carried out by using a diffractometer D8 Advance (Bruker AXS GmbH, Germany) instrument. Main features of the equipment were described in section **I. 5**. The samples were mounted on a mobile plate stage to adequately align the system, so that measurements were carried out in a completely non-destructive way, without previously preparing or adapting the sample for the analyses on the conventional sample holders.

2. 3. 2. 3. Standards for EDXRF calibration

After the screening phase analysis carried out on the artworks, nine elements were selected for the preparation of a standard set to calibrate the EDXRF instrument for the analysis of “oil on copper” paintings. Elemental stock solutions (TraceCERT®, Fluka, Sigma Aldrich Chemie, GmbH, Germany; 1000mg/L) of calcium, chromium, manganese, iron, zinc, cadmium, gold, mercury and lead were used for this purpose, following similar procedures than those reported by Fittschen and Havrilla (2010) but at different scale. An aliquot of 1 µL of each solution was transferred onto a copper support by using a micro-syringe (7000 Series Modified Microliter™, Hamilton, USA) and left to dry at room temperature before EDXRF analysis. We obtained some small dried residues, each one containing 1 µg of the different considered elements (**Fig. 2. 2**). These dried residues have an approximate diameter of around 600 microns. The estimated mass deposition of each standard is about 127 µg cm⁻², which is close to the same order of magnitude of our samples.

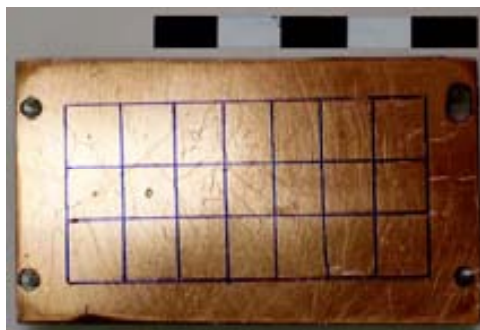


Fig. 2. 2 Standard set of copper support with dried drops of different elements at the surface.

2. 3. 2. 4. EDXRF quantitative method

An analytical application code for analysis of “oil on copper” multilayered paintings was developed by using the WinFTM® Software Program version 6.20 (Helmut Fischer GmbH + Co. KG, Germany). This software program uses the fundamentals described in Roessiger and Kaiser (1998) and Roessiger and Nensel (2006) for the evaluation of the measured spectrum, and allows designing different layered models (single, double, multilayers) taking into account the main features of the layers and substrates. The WinFTM software uses experimental spectra of pure elements and different background matrix matching for the best fit between experimental data and theoretical ones. This process is done by iteration, and the minimum value for a least-squares calculation is considered to be the best fit. Amongst the possibilities and variables needed to define a method for the measuring layer, the program allows introducing the following spectral data: (a) spectra of material’s base of standards (a copper support in this case); (b) spectra of the standards used for the calibration (monoelemental solutions) and (c) spectra of the material’s base of the samples to be analysed (**Fig. 2. 3**). This last point was fulfilled by the analysis of the backside of the “oil and copper” paintings.

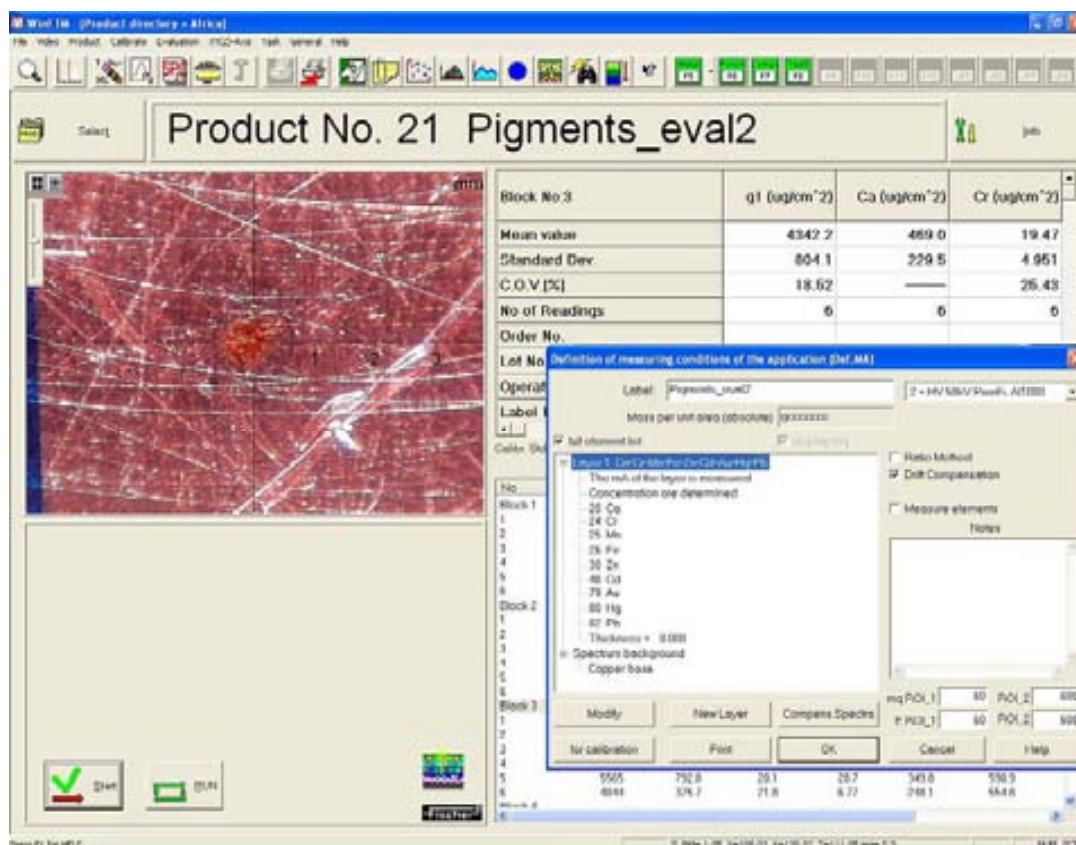


Fig 2. 3 Display of the WinFTM software menu with image of the standard set.

Looking for the best conditions for analysis of the previously prepared standard set, different conditions (filter, collimator, voltage and current) were checked. We used an aluminium filter of 1000 µm in thickness (in order to reduce the background noise from tungsten tube at the region of interest in the spectrum) and the collimator of 1 mm in diameter (in order to adjust the X-ray focal spot for the irradiation of the whole dried droplet surface of calibration dataset). The spectra acquisition time was optimised to ensure that counting statistics was good enough to guarantee the quality of analytical results. We choose 50 kV and 1000 µA as voltage excitation and anode current, respectively, taking into consideration the counting rates. To obtain the minor relative standard deviation (RSD), repeated measurements were carried out (on the same point and using the same analytical conditions, 6 analyses at different measuring times: 50, 100, 300, 500, 1000 s) choosing the Mn K α line for the experience. A measuring time of 300 s delivers an RSD near 1% whilst a more extended time does not imply a significant reduction (improvement) in the RSD value (**Fig. 2. 4**). Then, we select this counting time as the best for spectra obtaining at our instrumental design.

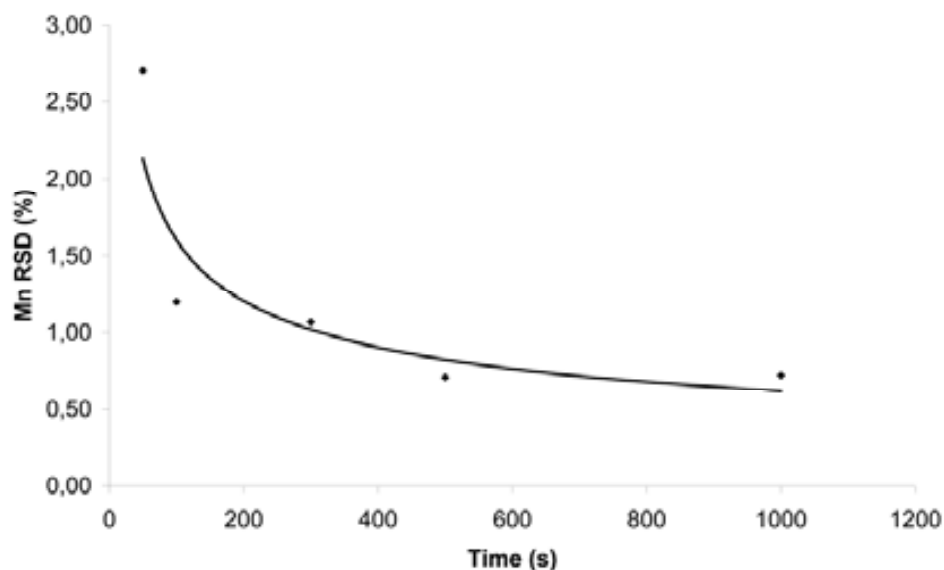


Fig. 2. 4 Plot of RSD vs. measuring time for Mn K α line intensity. Experimental conditions: 6 measurements on each point, Al 1000 μ m filter, 50 kV, 1000 μ A, focal spot 1 mm.

The detection limit (DL) obtained by EDXRF was calculated according to the equation **Eq. 1. 1** (see section 1. 2. 3. 4)

The results for the standard set are presented in **Table 2. 1**.

Table 2. 1

Estimated areal detection limits ($\mu\text{g}\cdot\text{cm}^{-2}$)

Ca	Cr	Mn	Fe	Zn	Cd	Au	Hg	Pb
14.4	2.6	3.1	2.7	5.9	7.7	5.3	6.9	4.2

Once the methodology for routine analysis of “oil on copper” multilayered paintings was tuned up, and taking into consideration the particular features of both artworks, measurements were carried out by using a voltage excitation of 50 kV, an anode current of 1000 μ A, an aluminium filter of 1000 μ m in thickness, a spectrum measuring time of 300 s and a focal spot of 1 mm in diameter. Chemical mappings were also carried out in order to observe the distribution of elements along selected areas of the paintings. For the mapping, a grid of 20 x 20 points was defined in which the spot distance was about 600 μ m. Measuring conditions were the same ones as the defined for punctual analyses with exception of the counting time, which was reduced to 60 s per each point due to the large number of measurements to be done. In some cases, we analysed some artwork details smaller than 1 mm by using the 0.3-mm collimator

mask then determining the elemental concentration by the areal ratio of both focal spots (1 and 0.3 mm).

2. 3. 2. 5. Statistical data treatment

As it has been recently pointed out (Rosi *et al.*, 2009; 2010) the data resulting from non-invasive analytical techniques combined with statistical analysis can be extremely useful to characterise the elements (pigments, dyes, glazes, ...) used by artist to perform an artwork. In addition to cluster analysis, so far used for classification of materials in archaeology, the application of other multivariate statistical treatment, such as Scatter Matrix Plot (Guilherme *et al.*, 2010) or Principal Component Analysis (PCA) has been recently applied (Sawczak *et al.*, 2009).

Once we quantified the elements from both artworks, we tried to identify clustering concerning the different colouration by using PCA. The main objective of PCA is to simplify the study of complex data systems by identifying a relative small number of components that can be used to represent relationships amongst groups of many interrelated discrete variables, in this case the features of both studied artworks. Statistical analysis was performed with the software package STATISTICA 7.0.

2. 3. 3. Results and discussion

2. 3. 3. 1. Elemental and crystalline phase analyses of the supporting materials and preparation layer.

Analysis of the supporting material was made by obtaining an EDXRF spectrum from the backside of each plate, in which we can only distinguish the signal from copper and minor titanium, iron and lead impurities at trace level, thus inferring the use of pure copper plate as a supporting material of the Franciscan saint painting (**Fig. 2. 5 (a)**). The river landscape painting exhibit copper and zinc as a major elements, joined by titanium, iron and lead impurities at trace level, thus deducting the use of zinc-bearing brass plate as a supporting material (**Fig. 2. 5 (b)**). XRD spectral data of the painting sides supported these results, revealing the presence of the characteristic peaks of a copper based alloy (**Fig. 2. 6 (a)**, see peaks labelled as #) and brass (**Fig. 2. 6 (b)**, see peaks labelled as β).

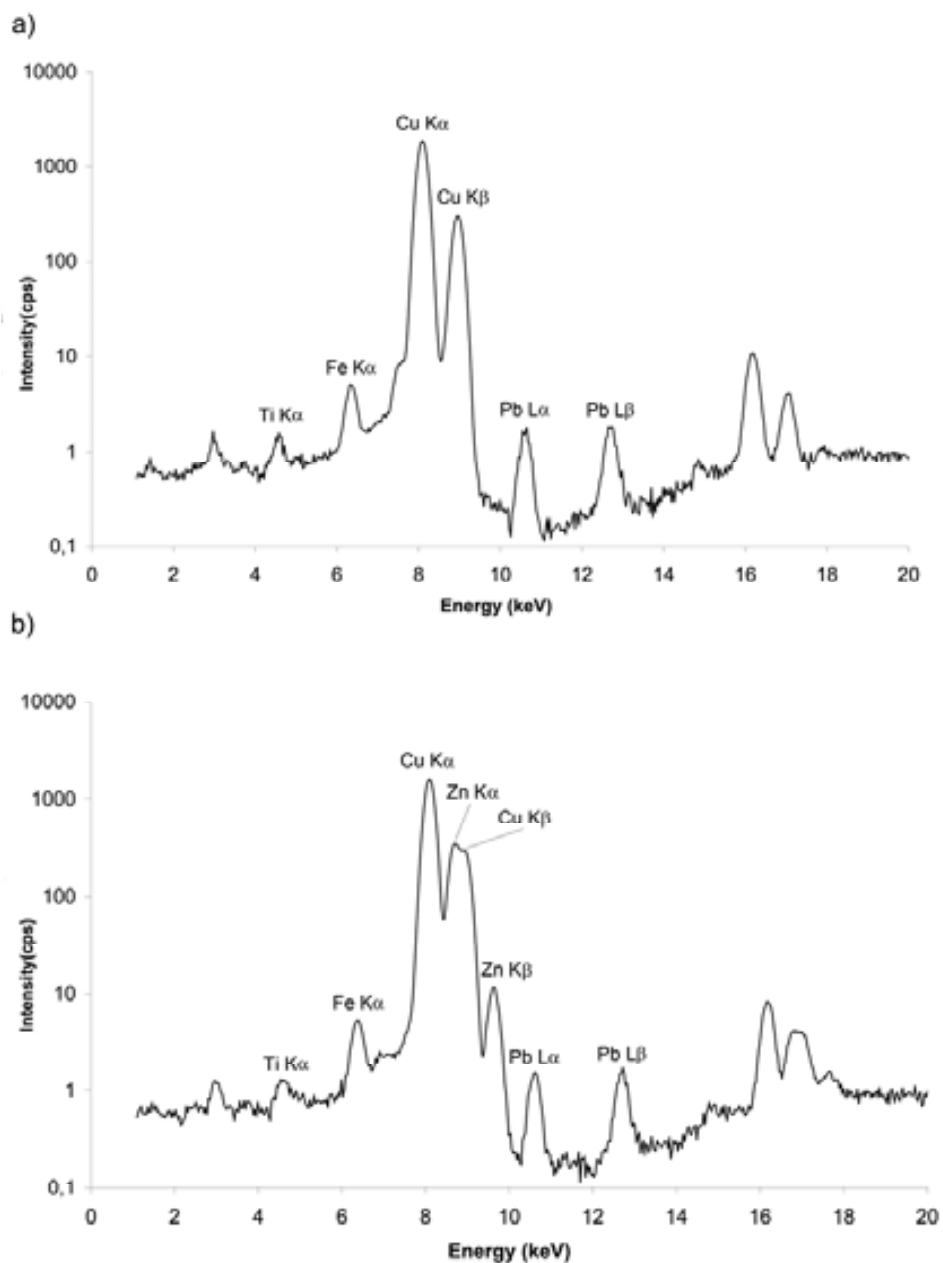


Fig. 2. 5 EDXRF spectra (300 s of life measuring time) from: (a) the backside of the Renaissance painting, and (b) the backside of the Contemporary artwork.

The omnipresence of lead all over the painting showed the important role of some lead compound in painting work, so that it was investigated by XRD. As it was previously mentioned, the painting technique on such kind of supports was usually based on laying down one white lead thin layer to promote enough roughness to help oil paint adhere (Komanecy *et al.*, 1998). XRD experimental data confirmed the presence of hydrocerussite (**Fig. 2. 6 (a)**, see peaks labelled as *) which is a lead carbonate hydroxide mineral with the composition $(\text{Pb}(\text{CO}_3)_2 \cdot \text{Pb}(\text{OH})_2)$, and cerussite (PbCO_3) (**Fig. 2. 6 (b)**, see peaks labelled as &). These terms should properly refer to the

natural mineral forms, so further on we will refer to the pigment as lead white. Although the artificial form was synthesised since ancient times, the fact that we only identified lead white in the preparation layer would confirm that both artworks were surely done before the nineteenth century.

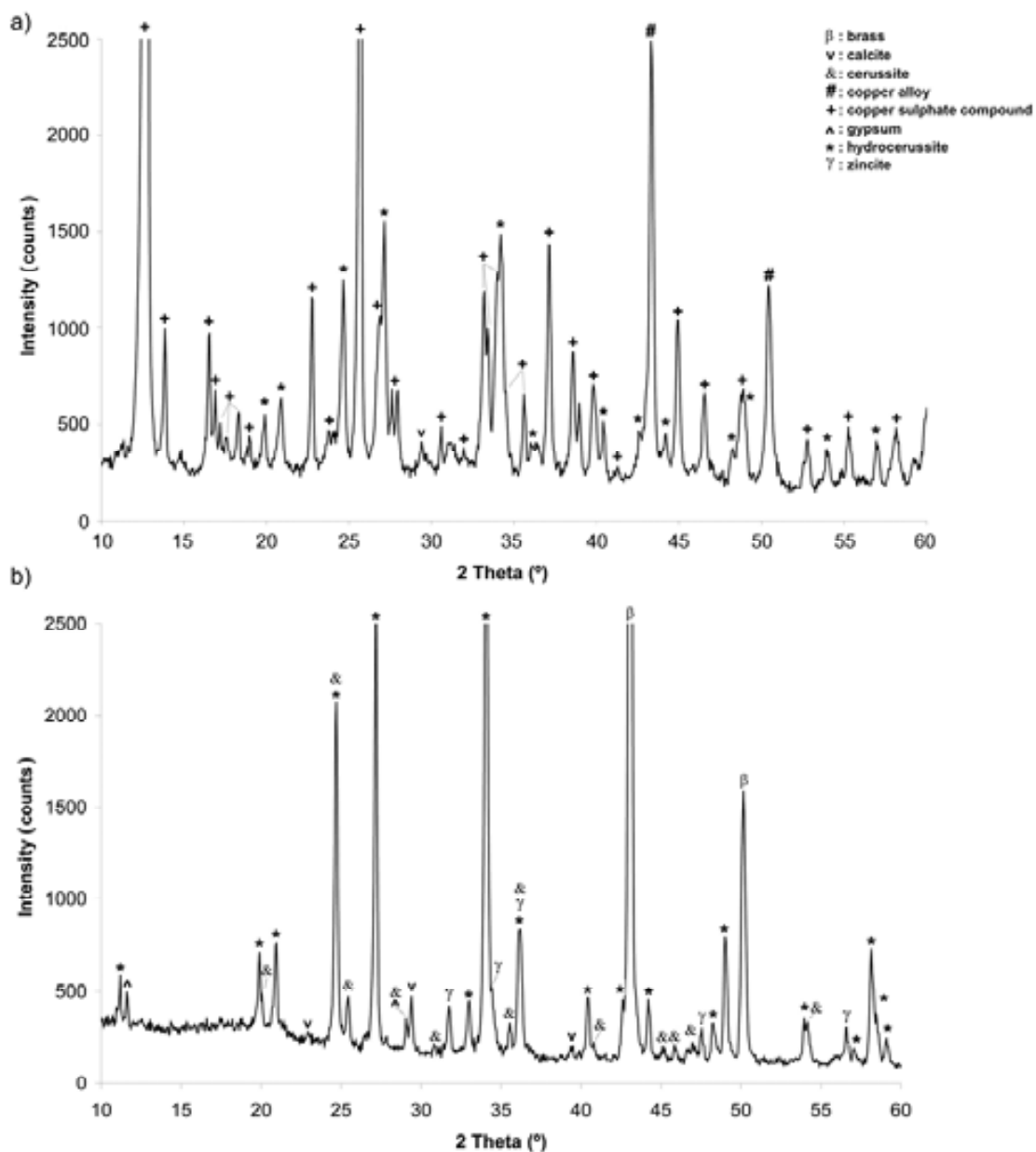


Fig. 2. 6 (a) Diffractogram of the Renaissance painting and (b) diffractogram of the Contemporary artwork Key: #: copper alloy; *: hydrocerussite; +: copper sulphate compound; v: calcite; β: brass (Cu-Zn alloy); &: cerussite; ^: gypsum; γ: zincite.

2. 3. 3. 2. Pigment mass distribution estimation on a Renaissance painting

The main results relating to the elemental chemistry of the Renaissance painting are summarised in **Table 2. 2**. As revealed by the spectral data obtained by EDXRF analyses we can distinguish the presence of calcium, manganese, iron, copper, gold, mercury and lead.

Table 2. 2

Elemental concentration values ($\mu\text{g cm}^{-2}$) from different areas of the "oil on copper" portrait. The included uncertainties are the statistical deviation of the mean values.

	Ca	Mn	Fe	Au	Hg	Pb
<i>skin coloured</i>						
min	tr	tr	tr	nd	30	5814
max	175	tr	39	-	157	7539
mean	53 ± 1	-	19 ± 1	-	93 ± 2	6646 ± 80
<i>red</i>						
min	62	tr	60	nd	229	1093
max	180	6	110	-	572	1816
mean	100 ± 3	3 ± 1	78 ± 2	-	320 ± 4	1474 ± 18
<i>orangey brown cross</i>						
min	51	tr	358	nd	0	1835
max	173	14	643	-	65	3193
mean	101 ± 3	9 ± 1	447 ± 5	-	36 ± 1	2456 ± 30
<i>green</i>						
min	tr	tr	55	nd	nd	827
max	79	5	112	-	-	1043
mean	32 ± 1	3 ± 1	75 ± 2	-	-	959 ± 12
<i>dark brown clothes</i>						
min	120	13	353	nd	tr	829
max	163	38	711	-	33	1598
mean	139 ± 3	25 ± 1	546 ± 7	-	18 ± 1	1111 ± 13
<i>light brown clothes</i>						
min	104	6	92	nd	tr	2001
max	182	11	111	-	15	2638
mean	148 ± 3	9 ± 1	101 ± 3	-	3 ± 1	2306 ± 28
<i>crown</i>						
min	29	tr	62	463	12	935
max	55	3	76	585	31	1023
mean	41 ± 1	-	69 ± 2	549 ± 7	20 ± 1	974 ± 12

nd: non detected

tr: traces

Copper signal is present in all the spectra, and it can appear as a result of the emission of copper from support and by its potential presence in the pigments of green colouration. However, as we cannot clearly differentiate by EDXRF experimental data the origin of the copper signal in the spectra, the estimated areal concentration cannot be distinguished. Nevertheless, the contribution from the support is clearly ascertained from the attenuation of Cu K α line intensity in the carnations, due to the strong lead-bearing pigment absorption. Despite the fact that the contribution of copper-based pigments cannot be distinguished by EDXRF analysis, XRD experimental data confirmed the presence of basic copper sulphates (**Fig. 2. 6 (a)**, see peaks labelled as +). The first mention of the use of these pigments dates back to the seventeenth century (Gilbert *et al.*, 2003).

The relationship between colouration and chemical data can be deduced from the elemental surface distribution reported in **Fig. 2. 7**. Calcium is concentrated around the Saint's face and the wooden cross. Intense brownish colours exhibit the highest contents of iron ($711 \mu\text{g}\cdot\text{cm}^{-2}$) and major presence of manganese ($38 \mu\text{g}\cdot\text{cm}^{-2}$). Lead is widely distributed all over the piece, although the amount of lead is several times higher in the carnations ($7539 \mu\text{g}\cdot\text{cm}^{-2}$) indicating their additional use for the base pigment at these parts. Reddish parts of the picture (lips, eyebrows and carnations) exhibit the presence of mercury being the highest one in the saint's lips ($572 \mu\text{g}\cdot\text{cm}^{-2}$). Gold is restricted to golden crown ($585 \mu\text{g}\cdot\text{cm}^{-2}$).

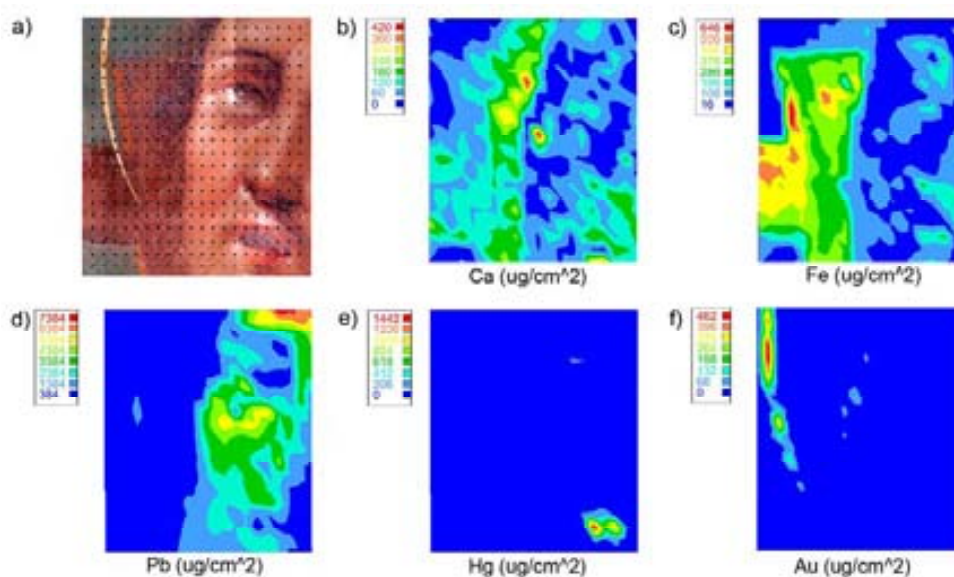


Fig. 2. 7 a) Detailed image of the studied area showing the gridding of the X-ray map (grid of 20x20 points). Elemental surface distribution in $\mu\text{g cm}^{-2}$ of: b) Ca; c) Fe; d) Pb; e) Hg and f) Au. The measurement time per point was fixed to 60 s.

For the proper interpretation of the whole dataset, a PCA routine was carried out. Gold was not taken into account since it is only characteristic of the golden crown. By comparing the compositional pattern (the selected variables were Ca, Mn, Fe, Hg and Pb) the principal component analyses allowed us to differentiate colours according to their elemental content. The extraction of two factors implies the 68% of the explained variance. Factor 1, explaining the 47% of the total variance, has positive high loads for manganese and iron while factor 2, which explains the 21% of the total variance, has a strong negative load for mercury. As shown in **Fig. 2. 8**, which illustrates the position of different cases respect to the two main factors, 3 main groups can be observed. The first group (**Fig. 2. 8 (a)**) is composed by red tonalities (lips and skin-coloured carnations) probably due to the use of mercury-based pigments; brownish shades (light and dark brown from clothes and orangey brown from the cross) compound the second group (**Fig. 2. 8 (b)**) probably due to the use of similar raw materials. In this particular case, the wide dissemination of dark-brown colouration can be attributed to the variable content of manganese and iron. The third group is composed by green and golden colours (**Fig. 2. 8 (c)**). Despite of being pigments with different origin, its grouping may be due to the common presence of copper in its composition.

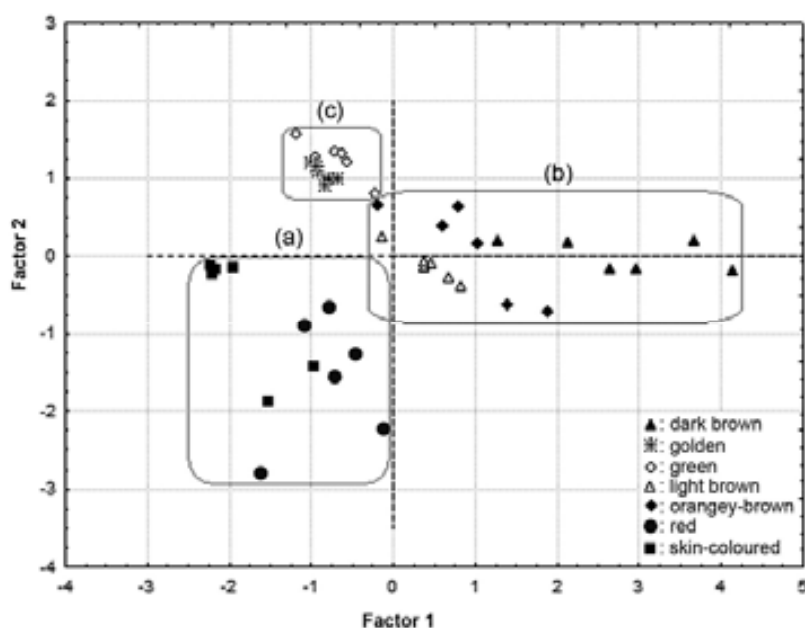


Fig. 2. 8 Scatter plot of factor 1 vs. factor 2 of the analysed areas from the Renaissance painting. (a) cluster composed by red tonalities (red colour is represented by black circles and skin colour is shown by black squares); (b) cluster composed by brownish shades (dark brown is represented by black triangles; orangey-brown is shown by black rhombus; light brown is represented by triangles); (c) cluster composed by golden (represented by stars) and green colour (shown by circles).

2. 3. 3. 3. Pigment mass distribution estimation on a Contemporary painting

The main results relating to the elemental chemistry of the Contemporary painting are summarised in **Table 2. 3**. As revealed by the spectral data obtained by EDXRF analyses we can observe the presence of Ca, Mn, Cr, Fe, Cu, Zn, Cd and Pb.

Zinc signal is present in all the spectra, and it can appear as a result of the emission of zinc-bearing brass from support and also by its potential presence in the pigments. As it has happened with copper in the Renaissance portrait, we cannot clearly differentiate by EDXRF analysis whether the potential contribution of the zinc signal in the spectra is related to the pictorial layer, the preparation layer, the supporting base or from the three of them; however, by using XRD analysis, the presence of zincite (ZnO) was identified in some areas (**Fig. 2. 9**), which suggests that this compound was in fact used as a pigment rather than as a preparation layer. The presence of this compound revealed the use of modern pigments such as zinc white, which is not typical in paintings before the middle of the nineteenth century¹.

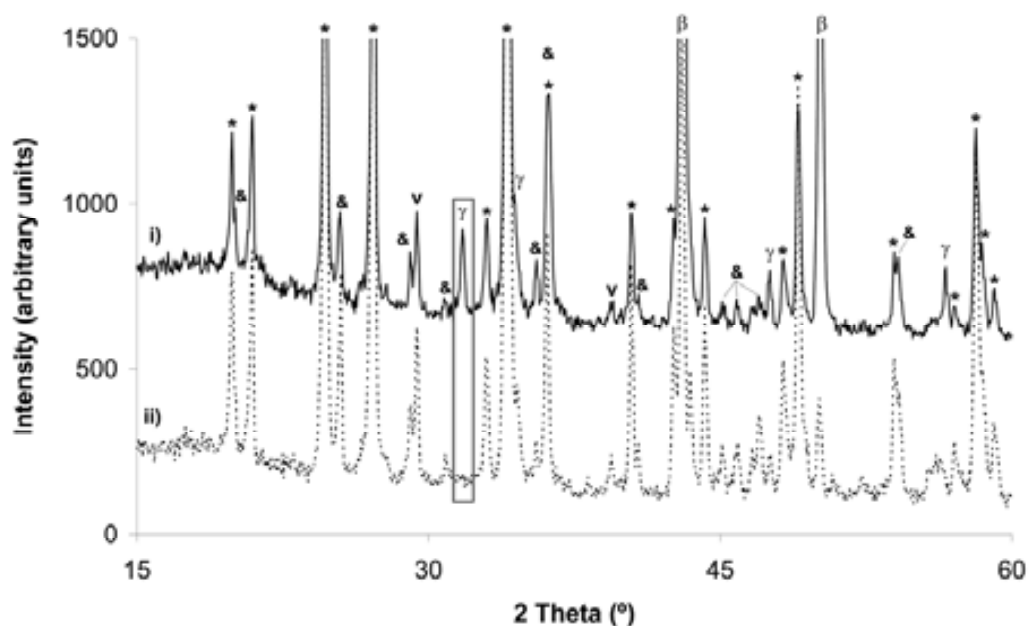


Fig. 2. 9 Diffractograms of the Contemporary artwork obtained in different areas: i) blue water; ii) blue sky. Key: *: hydrocerussite; v: calcite; β: brass (Cu-Zn alloy); γ: zincite. The main peak of zincite is highlighted.

¹ Although zinc white was first synthesised in small quantities as an artificial pigment in 1780, due to its price it was not widely used as a pigment prior to 1835 (Hahn *et al.*, 2004)

Table 2. 3

Elemental concentration values ($\mu\text{g cm}^{-2}$) from different areas of the "oil on copper" River Landscape. The included uncertainties are the statistical deviation of the mean values.

	Ca	Cr	Mn	Fe	Cd	Pb
<i>Orange man</i>						
min	282	15	7	215	555	2290
max	793	28	29	350	704	3782
mean	469 ± 6	20 ± 1	14 ± 1	282 ± 4	610 ± 7	2948 ± 35
<i>Orange Boatman</i>						
min	180	24	tr	55	341	1917
max	474	32	9	95	475	2901
mean	339 ± 4	27 ± 1	4 ± 1	79 ± 2	407 ± 5	2338 ± 28
<i>Pink House</i>						
min	341	8	tr	46	248	1748
max	415	15	4	67	305	2526
mean	378 ± 5	10 ± 1		55 ± 2	273 ± 4	2122 ± 26
<i>Dark Brown Bridge</i>						
min	71	9	tr	84	0	571
max	155	13	10	189	27	754
mean	94 ± 2	11 ± 1	6 ± 1	121 ± 2	9 ± 1	646 ± 8
<i>Green flag</i>						
min	184	7	4	251	tr	1101
max	421	18	11	445	51	2835
mean	287 ± 3	14 ± 1	8 ± 1	342 ± 4	23 ± 1	1654 ± 20
<i>Blue Water</i>						
min	341	45	nd	tr	11	2015
max	900	180	-	21	74	4461
mean	627 ± 7	87 ± 1	-	11 ± 1	35 ± 1	3147 ± 38
<i>Blue Sky</i>						
min	545	52	tr	tr	20	3220
max	872	88	4	22	74	4456
mean	740 ± 9	72 ± 2	-	11 ± 1	53 ± 1	3949 ± 47
<i>Yellow Sky</i>						
min	192	118	tr	3	tr	1523
max	372	157	10	21	21	1941
mean	306 ± 4	139 ± 2	5 ± 1	13 ± 1	13 ± 1	1749 ± 21
<i>White Sky</i>						
min	1055	tr	tr	tr	42	6909
max	2258	17	14	33	78	14416
mean	1944 ± 23	3 ± 1	5 ± 1	11 ± 1	61 ± 2	12146 ± 146

nd: non detected

tr: traces

The relationship between colouration and chemical data can be deduced from the elemental surface distribution illustrated in **Fig. 2. 10**. Calcium and lead are distributed all over the piece. Highest contents are found on the white shades but also in other colours, suggesting that they were probably used as a pigmenting supports. (Ca: $2258 \mu\text{g}\cdot\text{cm}^{-2}$, Pb: $14416 \mu\text{g}\cdot\text{cm}^{-2}$). Cadmium is restricted to pinkish and orangey colours ($704 \mu\text{g}\cdot\text{cm}^{-2}$ and $305 \mu\text{g}\cdot\text{cm}^{-2}$ respectively). The highest contents of iron are recorded in the green flag, although the brownish parts of the picture also show iron in relevant amount ($445 \mu\text{g}\cdot\text{cm}^{-2}$ and $189 \mu\text{g}\cdot\text{cm}^{-2}$ respectively). The presence of manganese is restricted to warm colours (pink, orange and brown) and its content is often at trace level. Chromium is mainly distributed in both the bluish and yellowish shades of the sky and the water (the highest contents being $1567 \mu\text{g}\cdot\text{cm}^{-2}$ for the sky and $180 \mu\text{g}\cdot\text{cm}^{-2}$ for water).

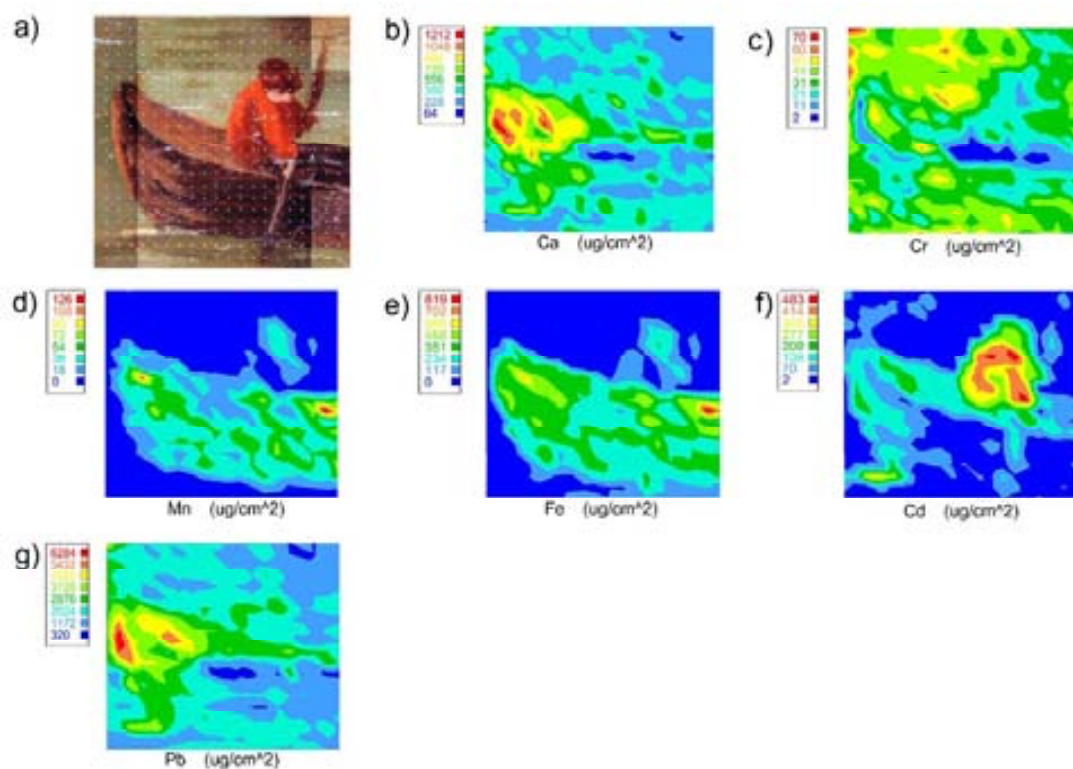


Fig. 2.10 (a) Detailed image of the studied area from the Contemporary painting illustrating the gridding of the X-ray map. Elemental surface distribution in $\mu\text{g cm}^{-2}$ of: b) Ca; c) Cr; d) Fe; e) Cd and f) Pb.

Statistical routine was also performed to the obtained semi-quantitative data from this artwork. The first two factors found for the river landscape “oil on copper” painting explain the 71% of the variability of the system. Factor 1, which explains the 38.86% of

the total variance, has high positive load for calcium and negative load is for iron. Factor 2, explaining the 32.26% of the total variance, has high positive loads for lead while a high negative load of this factor for chromium. In **Fig. 2. 11**, which represents the position of the different cases respect to the two main factors, we broadly distinguish 3 main clusters. The evident separation between them, highlights the compositional differences of the employed pigments. Clusters corresponding to warm tonalities and the green colour are found approximately in the same region of the scatter plot and constitute the first cluster (**Fig. 2. 11 (a)**) probably due to the common presence of iron in their composition. The second one is constituted by bluish and yellow tonalities from both the sky and the water (**Fig. 2. 11 (b)**). These colourations are grouped due to the use of similar compounds based on chromium. The third cluster is composed by white colour (**Fig. 2. 11 (c)**) and its clear separation is accompanied by the higher presence of lead.

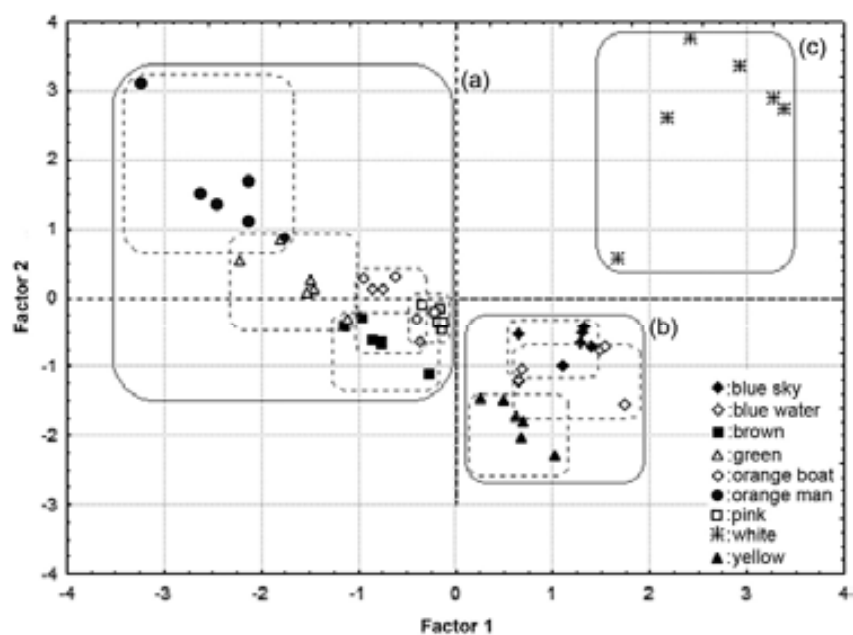


Fig. 2. 11. Scatter plot of Factor 1 vs. Factor 2 of the analysed areas from the Contemporary painting. (a) first cluster (orange colour from the man is represented by black circles; orange colour from the boatman is shown by circles, brown colour is shown by black squares, green is shown by triangles and pink colour is shown by squares); (b) second cluster (yellow is represented by black triangles, blue from the sky is shown by black rhombus and the blue from the water is represented by rhombus); (c) third cluster (white is represented by stars).

2. 3. 4. Conclusions

Two “oil on copper” paintings, from presumable different ages, were investigated and characterised by X-ray spectroscopy (X-ray diffraction and energy dispersive X-ray fluorescence) revealing differences not only in the support but also in the elemental chemistry of pigments.

In both cases, results of the analyses suggest that there are at least two superimposed layers (apart of the supporting media made of copper or brass): a priming coat mainly composed by lead white and a pictorial layer of different composition (depending on the area of analysis). The areal mass distribution of the different elements identified in the painting pigments (Ca, Cr, Mn, Fe, Zn, Cd, Hg and Pb) were determined by elemental mapping of some parts of the artworks.

The first painting, attributed to the Renaissance period, is characterised by a copper plate support, a white lead pictorial base ($\text{Pb}(\text{CO}_3)_2 \cdot \text{Pb}(\text{OH})_2$) and the presence of Ca, Mn, Fe, Cu, Au, Hg and Pb. The second one, presumably from the second half of the eighteenth century and made over a brass support, is characterised by a white lead pictorial base ($\text{Pb}(\text{CO}_3)_2 \cdot \text{Pb}(\text{OH})_2$ and PbCO_3) and the presence of Ca, Cr, Mn, Fe, Cu, Zn, Cd and Pb. The presence of white lead as a preparation layer suggest that both artworks where conceived before the nineteenth century since it was on that period when the use of white lead was progressively abandoned due to its high toxicity (Carlyle, 2001).

The compositional features, revealed by the combined use of XRD and EDXRF, not only suggest that the second painting is more recent than the attributed to Renaissance period but also confirm that the second one (the river landscape “oil on copper” painting) was in fact carried out at the end of the nineteenth century since the joint presence of zinc, chromium and cadmium was determined. According to the literature (Eastaugh *et al.*, 2004) zinc white was commercially available at the end of the eighteenth century, and chromium pigments were introduced into the market at the nineteenth century. Dealing with the presence of cadmium, although some authors (Hahn *et al.*, 2006) suggest that its presence may indicate the use of cadmium-red (which was commercially available from 1910), the use of other cadmium compounds such as cadmium orange, first introduced in 1862 (Eastaugh *et al.*, 2004), cannot be discarded.

A simple and rapid method based on non-invasive direct analysis of solid sample was developed for the determination of pigment mass distribution of “oil on copper” multilayered paintings by using the WinFTM® Software Program version 6.20 (Helmut Fischer GmbH, Germany). The method is calibrated by using the dried residues of small droplets of pure elemental solutions, thus obtaining the sensitivity library for estimations of the areal absolute mass distribution. The program allows the possibility to compensate spectral differences from different metallic supports used to create these paintings, by introducing the whole spectrum of standard’s support, and the spectrum of the pictorial support. By treating the obtained results with the proper statistical routines (such as Principal Component Analysis) it is possible to find out some differences between colours according to their elemental content.

2. 4. Multi-spectroscopic characterization of “oil on copper” painting

The performed study allowed quite a thorough knowledge of the materials used in both paintings. The work pointed out that the combined use of XRD and EDXRF is highly effective for the compositional characterization of such kind of supports. Results of the analyses revealed differences not only in the support but also in the elemental chemistry of pigments and allowed estimating the chronology of both artworks. However, since EDXRF is capable of determining the elements but not the compounds to which they belong and due to the space limitations that presents the sample holder in the XRD equipment, the use of other techniques is mandatory to better characterise the samples under investigation. In that respect, the complete study of a small plate of “oil on copper” painting was carried out by using the combination of EDXRF, XRD, Raman spectroscopy (RS) and Fourier-transformed infrared (FTIR) analysis techniques.

2. 4. 1. Research aims

The main objective of this experimental work was to report a complete multi-spectroscopic characterization of an “oil on copper” painting presumably from the second half of the sixteenth century to study the materials used for its elaboration (pigments and binders) and determine the technology production process in such kind of pictorial artworks.

2. 4. 2. Materials and Methods

We choose four non-invasive techniques to avoid sample micro-extraction or other damaging sampling procedure. The first analytical step was the examination of the artwork by the use of EDXRF for both, identify the pigments through the detection of their chemical elements and determine their distribution along the surface. After this screening phase, XRD was employed to obtain information about the crystalline phases existing in the painting. Lately, RS was used to obtain the necessary molecular information to properly characterise the studied artwork. Finally, FTIR was used for the determination of the binder.

2. 4. 2. 1. Artwork

The “oil on copper” painting under study represents a Franciscan habit saint holding a wooden cross (see section **2. 3. 2. 1.**, **Fig. 2. 1 (a)**). It presents the Niobe’s look, very popular in the representation of saints of the time.

It is very difficult to make a precise attribution of the artwork, but the used colours and the accuracy of the stroke suggest that is an Italian work presumably made in the second half of the sixteenth century. According to the owner’s criteria, we can even specify that it is a work in affiliation with other examples of the same time and style leading to the north of Italy, between Tuscany and Lombardy.

2. 4. 2. 2. Instruments

The screening phase analysis was again obtained by using the EDXRF spectrometer (XDV-SD® model). Main features of the equipment were described in section **I. 5**. Once the artwork was placed inside the XRF chamber, the analyses were carried out operating the X-ray generator with a potential of 50 kV and an anode current of 1 mA, an aluminium filter 1000 µm in thickness, a collimator of 0.3 mm and 300 s of effective counting time. In the specific case of the golden pigment, the crown was analysed at different anode current values (1000, 750, 500, 250 and 125 µA).

For the crystalline phase analysis we used a Bruker D-8 Advance X-ray diffractometer (see section I. 5. to check the instrument's parameters). Due to its size, the whole artwork was placed inside the diffractometer by using a special sample support designed to maintain the alignment of the X-ray beam. (Fig. 2. 12).



Fig. 2. 12 Diffractometer Bruker D8 Advance (photography: A. Pitarch).

Two Raman instruments were used for the characterization of the individual pigments of the artwork. The first one was an ultramobile innoRam® Raman spectrometer (B&WTEK_{INC.}, Newark, USA) (see section I. 5 for a more detailed explanation of the main features of the equipment). In order to avoid thermal decomposition of the sample, the laser power at the sample was always lower than 10 mW. Spectra were acquired in the spectral range 100–2200 cm^{-1} , accumulating several scans for each spectrum to improve the signal-to-noise ratio. We always considered three or more points of the same shade in order to reach reliable results.

The second Raman equipment, used in those cases in which the fluorescence phenomena made it not possible to record a Raman spectrum with the laser of 785 nm, was the Renishaw InVia Raman spectrometer joined to a Leica DMLM microscope (see section I. 5 to check the instrument's parameters). For each spectrum at least 10 seconds were employed and 10 scans were accumulated with the 1% of the maximum power of the laser in the spectral window from 100 cm^{-1} (cut off) to 2500 cm^{-1} . This is the spectral window in which almost all signals of organic and inorganic compounds of interest can be found.

The FTIR spectrum of the binder was collected by using the portable Exoscan FTIR A₂ Technologies (Danbury, Connecticut, USA) spectrometer (see section I. 5).

2. 4. 3. Results and discussion

2. 4. 3. 1. Overall chemistry of the “oil on copper” painting

The main results relating to the elemental chemistry of the artwork are summarised in **Table 2. 4**. The relationship between colouration and chemical data can be deduced from the elemental chemistry reported in this table. As revealed by the spectral data obtained by EDXRF analyses, we can distinguish the presence of calcium, manganese, iron, copper, gold, mercury and lead.

Table 2. 4

Elemental chemistry of different coloured zones of the artwork. Reported values are the averaged intensity (counts per second) of the characteristic X-ray emission lines.

Colour	Mn Ka	Fe Ka	Cu Ka	Pb La	Au La	Hg La
Green	-	0.75 ± 0.12	84.33 ± 11.25	8.11 ± 0.41	-	-
Pale brown	-	0.92 ± 0.08	76.67 ± 13.62	17.38 ± 4.95	-	-
Orangey-brown	0.16 ± 0.04	3.49 ± 0.52	95.20 ± 1.88	8.70 ± 1.87	-	-
Dark-brown	0.55 ± 0.15	3.32 ± 0.73	86.71 ± 26.48	6.09 ± 4.82	-	-
Golden	-	0.74 ± 0.03	87.11 ± 3.36	7.5 ± 0.05	3.48 ± 0.29	-
Red	-	0.95 ± 0.23	77.57 ± 2.07	13.70 ± 0.75	-	1.97 ± 1.63
Skin-coloured	-	0.19 ± 0.02	16.33 ± 5.78	41.45 ± 3.02	-	0.31 ± 0.03

We observe that gold is restricted to golden crown whilst the rest of elements are irregularly distributed along the picture. The use of vermilion is out of doubt by the presence of mercury in different parts of the piece (lips, eyebrows and carnations). Intense brownish colours show the highest contents of iron and minor presence of manganese. Lead is widely distributed all over the piece, suggesting the use of a lead pigment for the preparation layer underneath. However the intensity of lead lines is several times higher in the skin coloured parts of the artwork, indicating their additional use for the base pigment at these parts. As happened with lead, the copper signal is present in all the EDXRF spectra. However, as reported in section **2. 2. 4. 2**, we cannot clearly distinguish by EDXRF whether the origin of copper signal in the spectra is related to the pictorial layer, the supporting base or from both parts. Nonetheless, the contribution from the support is assured from the attenuation of Cu K α line intensity in the skin coloured parts, due to the strong lead-bearing pigment absorption, whilst the potential contribution from pigments cannot be distinguished by EDXRF analysis.

2. 4. 3. 2. Pigments

Table 2. 5 gives an overview of the identified pigments, as well as the analytical techniques that allowed their identification.

Table 2. 5
Identification of pigments found in the "oil on copper" painting.

Color	Area of analysis	Colouring material	Formula	Analytical techniques				Raman bands (cm^{-1}) and relative intensities ^a
				XRF*	XRD	innoRam ® Raman spectrometer (785 nm laser)	Renishaw InVia Raman spectrometer (514 nm laser)	
Green	Background	Brochantite	$\text{CuSO}_4 \cdot 3\text{Cu}(\text{OH})_2$ (basic copper (II) sulfate)	Cu	ok	ok	ok	144 m, 161 m, 173 w, 201 m, 246 w, 321 w, 389 m, 425 w, 451 w, 484 m, 508 w, 598 w, 611 w, 623 w, 731 vw, 871 vw, 908 vw, 973 vs, 1076 vw, 1126 vw(br) (Gilbert et al., 2003)
		Posnjakite	$\text{CuSO}_4 \cdot 3\text{Cu}(\text{OH})_2 \cdot \text{H}_2\text{O}$ (copper (II) sulfate hydrate)	Cu	ok	ok	-	160 vw, 179 w, 235 vw, 337 vw, 419 m(sh), 445 s, 505 m, 611 w(br) 827 vw, 974 vs, 1057 vw, 1076 vw, 115 vw(br), 1154 vw (Gilbert et al., 2003)
Pale brown	Clothes	Red lead	Pb_3O_4 (lead (II, IV) oxide)	Pb	-	**	ok	54 w, 65 w, 86 vw, 122 vs, 152 w, 225 vw, 313 vw, 391 w, 549 s (Burgio and Clark, 2001)
		Carbon black	C (amorphous carbon)	-	-	**	ok	1325 vs(br), 1580 vs(br) (Bell et al., 1997)
		Calcite	CaCO_3 (calcium (II) carbonate)	Ca	-	**	ok	157 vw, 282 vw, 1088 vs (Bell et al., 1997)
		Yellow ochre	Goethite + silica + clay	Fe	-	**	ok	240 w(sh), 246 w, 300 m, 387 s, 416 m, 482 w, 551 w, 1008 s (Bell et al., 1997)
Dark brown	Clothes	Goethite	$\text{FeO} \cdot \text{OH}$ (iron oxyhydroxide)	Fe, Mn	ok	**	**	
		Pyrolusite	MnO_2 (manganese (IV) oxide)	Fe, Mn	ok	**	**	319 w, 377 w, 486 w, 538 s, 665 s, 750 w (Julien et al., 2004)
		Rhodochrosite	MnCO_3 (manganese (II) carbonate)	Fe, Mn	ok	**	**	285, 720, 1085, 1299 w, 1748 w (Coleyshay and Griffith, 1994)
		Szomolnokite	$\text{FeSO}_4 \cdot \text{H}_2\text{O}$ (iron (II) sulfate hydrate)	Fe, Mn	ok	**	**	
Golden	Crown	Gold and copper	Cu-Au based alloy	Au	ok	-	-	
Red	Lips	Vermilion/Cinnabar	HgS (mercury (II) sulfide)	Hg	ok	ok	-	42 vs, 253 vs, 284 w, 343 m (Burgio and Clark, 2001)
	Eyes	Vermilion/Cinnabar	HgS (mercury (II) sulfide)	Hg	ok	ok	-	43 vs, 253 vs, 284 w, 343 m (Burgio and Clark, 2001)
Skin coloured	Arms	White lead/Hydrocerussite	$\text{Pb}(\text{CO}_3)_2 \cdot \text{Pb}(\text{OH})_2$ (basic lead (II) carbonate)	Pb	-	ok	ok	665 vw, 687 vw, 829 vw, 1050 vs (Bell et al., 1997)
		Vermilion/Cinnabar	HgS (mercury (II) sulfide)	Hg	-	ok	ok	43 vs, 253 vs, 284 w, 343 m (Burgio and Clark, 2001)
White	Preparation layer	White lead/Hydrocerussite	$\text{Pb}(\text{CO}_3)_2 \cdot \text{Pb}(\text{OH})_2$ (basic lead (II) carbonate)	Pb	ok	ok	-	665 vw, 687 vw, 829 vw, 1050 vs (Bell et al., 1997)

^a Relative intensities. s: strong; m: medium; w: weak; v: very; sh: shoulder; br: broad
* The element indicates which key-element may indicate the presence of this pigment.
** The fluorescence phenomena made it not possible to record a Raman spectrum.

Green

The green colour appears as a background colour along the piece. EDXRF analysis carried out on this colour revealed the presence of copper. However, as we already pointed out, we cannot ascertain which the origin of copper is by using EDXRF technique, thus, the green colour was also analysed by means of XRD and RS. XRD experimental data confirmed the presence of brochantite (a basic copper sulphate, $\text{Cu}_4(\text{SO}_4)(\text{OH})_6$) together with another copper sulphate hydrate compound (**Fig. 2. 13**), posnjakite $\text{Cu}_4(\text{SO}_4)(\text{OH})_6 \cdot \text{H}_2\text{O}$, as it will be described below.

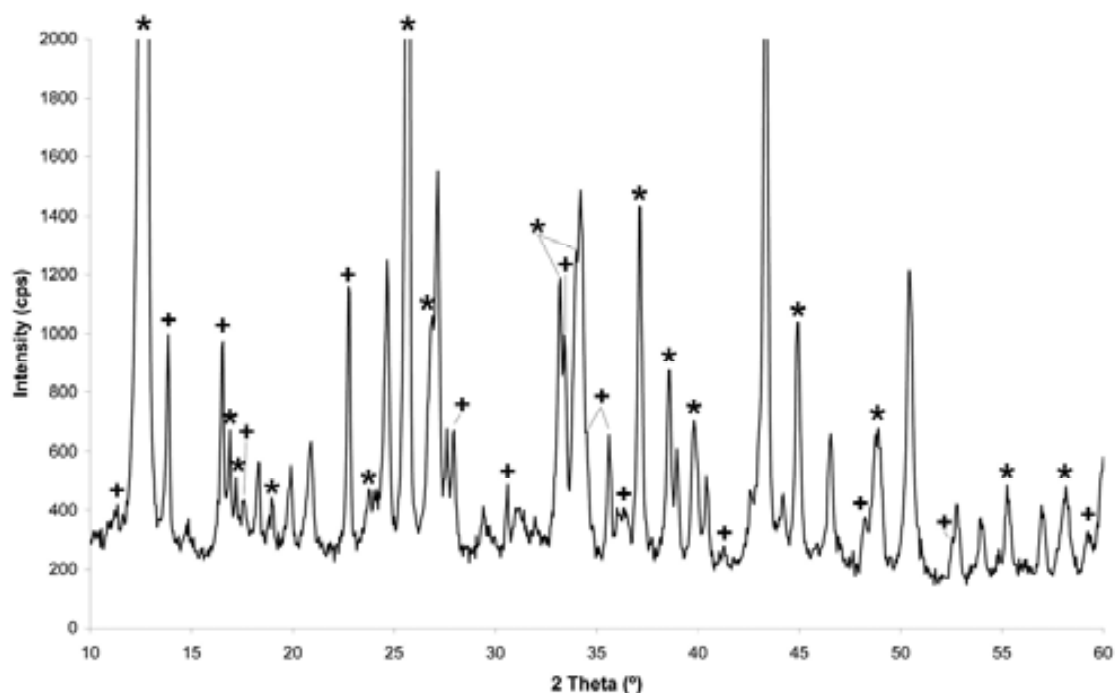


Fig. 2. 13 Diffractogram of the green colour. Key: +: brochantite; *: copper sulphate hydrate compound.

As it has already been reported in the literature (Gilbert *et al.*, 2003; Castro *et al.*, 2007), basic copper sulphates are extremely difficult to differentiate between them not only because they are chemically close one to each other, but also because they are unstable compounds and might be found together on the same artwork. Furthermore, we cannot surely know whether it was analysed the original compound or a derived degradation product (Gilbert *et al.*, 2003; Castro *et al.*, 2008 (b)).

RS is a powerful technique for the identification of green copper pigments of very similar nature, because they can be easily identified by comparing the lower frequency bands pattern (Gilbert *et al.*, 2003). Although in this particular study Raman analyses

carried out with the 785 nm laser were frustrated by fluorescence, probably caused by the presence of some kind of varnish, the alternative use of a short wavelength laser (514 nm) allowed us to obtain a weak Raman signal on some areas, along with the fluorescence signal.

After baseline correction, Raman spectrum of the green colour (**Fig. 2. 14**) reveals strong bands at 447, 611 and 973 cm^{-1} together with other weak bands at 481, 418, 396 and 318 cm^{-1} . These bands would be consistent with the presence of brochantite. However, the relative intensity of the band located at 447 cm^{-1} did not correspond with the expected intensity of brochantite. According to Gilbert *et al.* (2003), the mineral posnjakite has a very similar Raman spectra but with a medium to strong band at 445 cm^{-1} . The rest of the bands would overlap with those of brochantite. Thus, we could assume that green colour is a mixture of brochantite and posnjakite, as expected according to XRD results. The presence of these pigments is not unusual since the first recipe describing the preparation procedure dates back to the seventeenth century (Gilbert *et al.*, 2003).

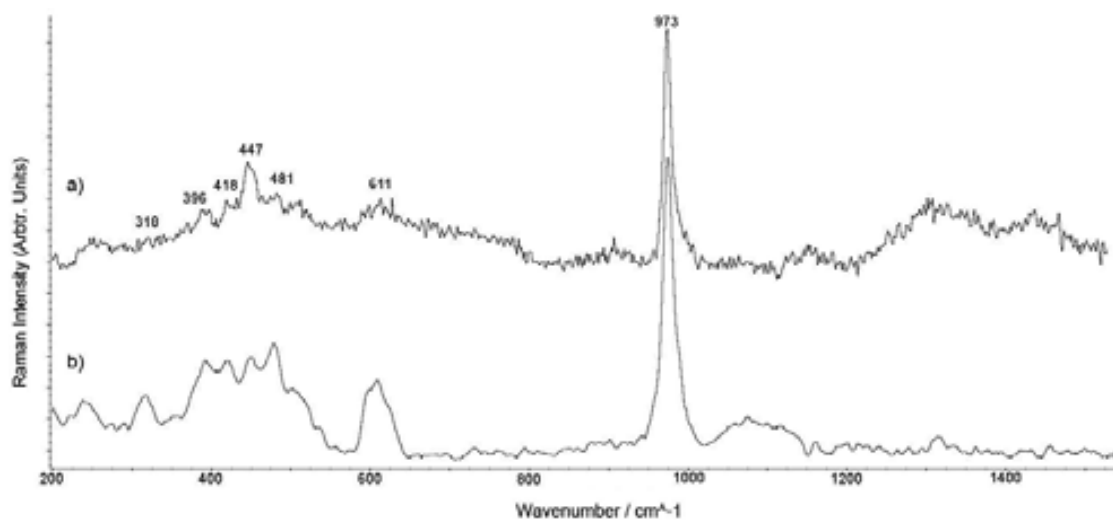


Figure 2. 14 (a) Raman spectrum from green colour parts of the painting (obtained by using the Renishaw InVia Raman spectrometer with the laser of 514 nm; after baseline correction). The reference brochantite spectrum (b) is displayed for comparison in the inset.

Brown

Three shades of brown colour were analysed on the painting: pale brown, dark brown (both from the clothes) and orangey-brown (from the cross). The EDXRF results showed amongst other elements the presence of manganese and iron in different

relative amounts depending on the tonality, which might suggest the use of different brown-earth pigments.

According to the Raman analyses (**Fig. 2. 15**), the pale brown shade (**Fig. 2. 15 (a)**) is an admixture of at least two pigments: carbon black (C, broad bands centred at 1300 and 1600 cm^{-1}) and red lead (Pb_3O_4 , bands at 226, 311, 391 and 548 cm^{-1}). Additionally, Raman spectrum showed four more bands at 164 (w), 480 (s), 1041 (w) and 1094 (w) cm^{-1} ; unfortunately we were not able to do a clear attribution.

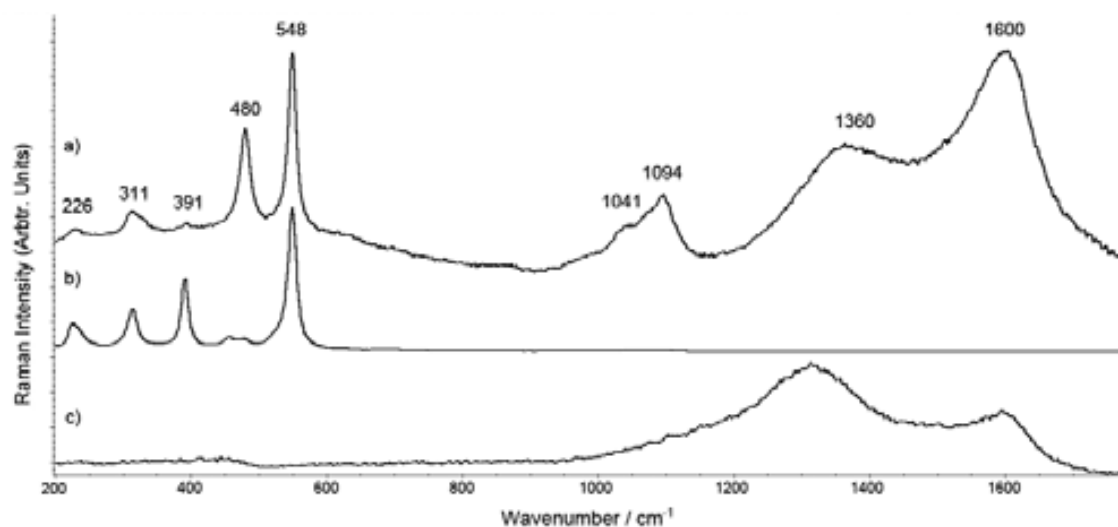


Fig. 2. 15 (a) Raman spectrum of the pale brown colour (obtained by using the Renishaw InVia Raman spectrometer with the laser of 514 nm). The reference red lead (b) and carbon black (c) spectra are displayed for comparison in the inset.

Dealing with the dark brown colour, it was not possible to identify by RS (even when using the 514 nm laser) due to the intense fluorescence. However, by using XRD (**Fig. 2. 16**) we successfully determined the presence of iron compounds (goethite $-\text{FeO}\cdot\text{OH}$ and szomolnokite $-\text{FeSO}_4\cdot\text{H}_2\text{O}$) and manganese compounds (pyrolusite $-\text{MnO}_2$ and rhodocrosite $-\text{MnCO}_3$).

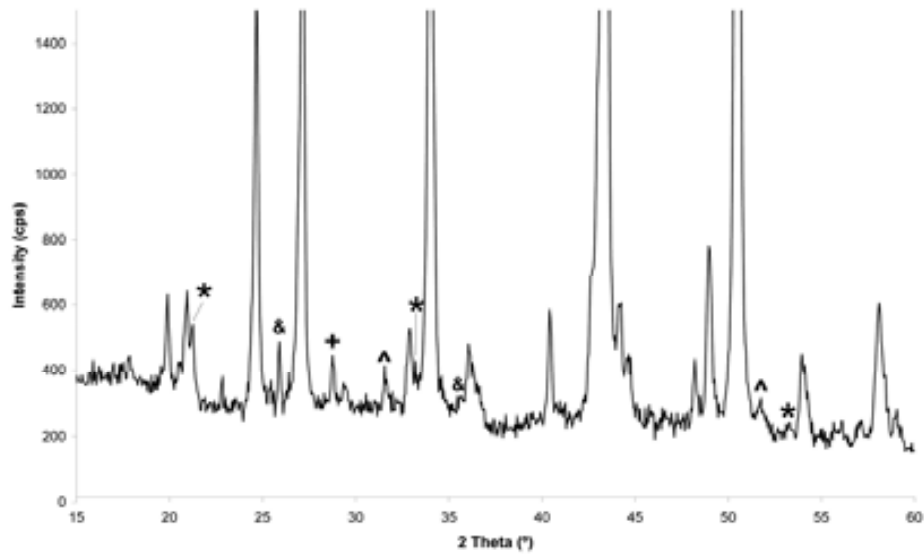


Fig. 2. 16 Diffractogram of the dark brown colour. Key: *: goethite; ^: rhodocrosite; +: pyrolusite; &: szomolnokite.

Regarding the orangey-brown colour it was not possible to identify its composition neither by RS nor by XRD. As it was mentioned before, the presence of manganese and iron determined by EDXRF (**Fig. 2. 17**) may indicate the use of brown-earth pigments.

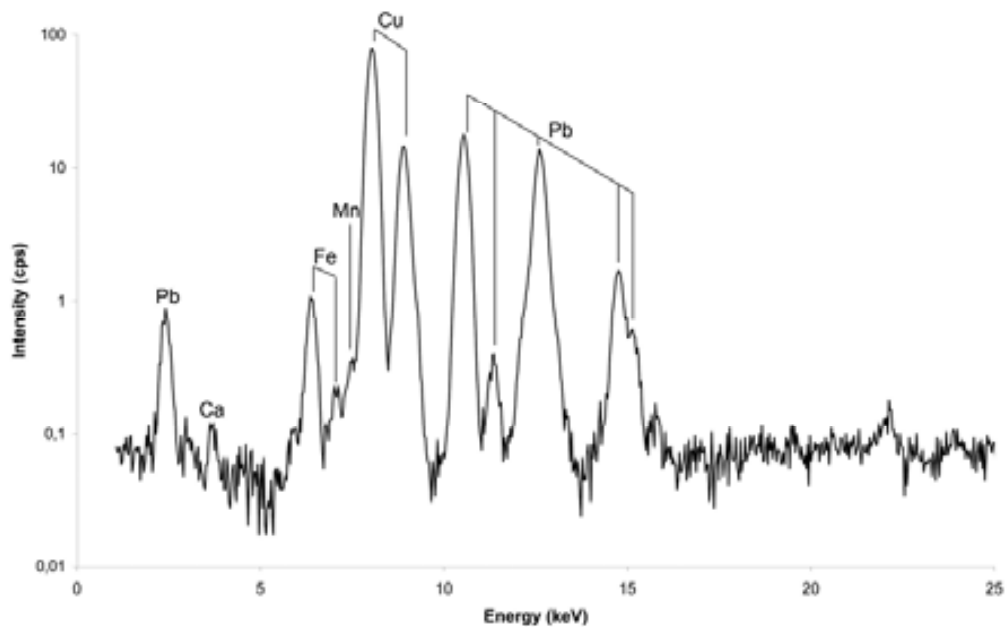


Figure 2. 17 EDXRF spectrum from the orangey-brown shade.

Golden

Gold, amongst other metals and alloys, was usually employed on Renaissance paintings to embellish some details of the representations such as haloes. Like many metals, gold is not possible to determine by means of RS since it does not give a first order Raman spectrum (Burgio *et al.*, 2008). In this case, EDXRF and XRD gave us the necessary information to chemically characterise the golden crown; in **Fig. 2. 18 (a)** and **2. 18 (b)**, peaks corresponding to copper and gold are clearly identified.

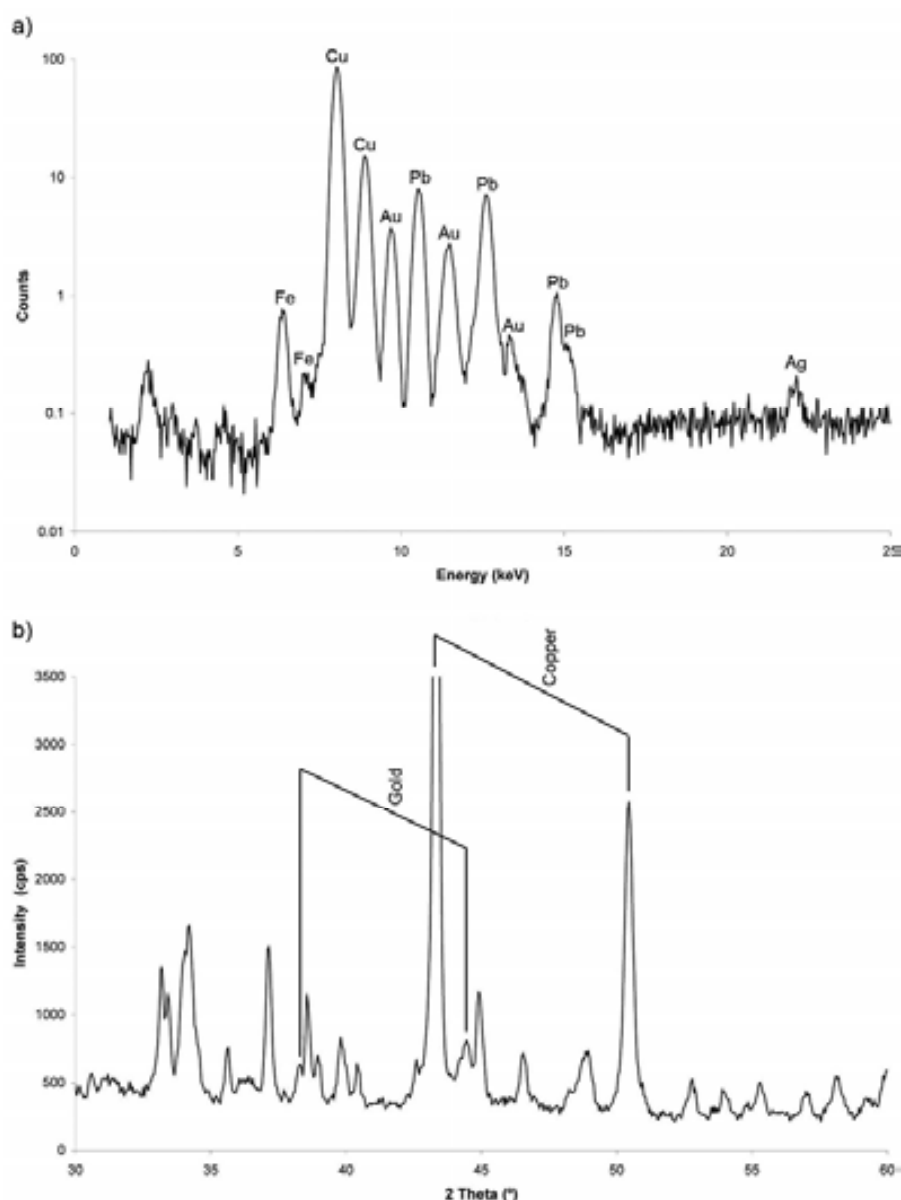


Figure 2. 18 Results of the analysis carried out in the golden crown: (a) EDXRF spectrum, and (b) XRD diffractogram.

As it has been mentioned before, the copper signal can appear not only as a result of the emission from the copper support or by its presence in green pigments, but also by its potential presence on the golden areas. When studying the Cu/Au peak ratio at different anode current values in the EDXRF analyses we observed that the ratios did not change substantially (**Table 2. 6**). Thus, one might assume that the golden pigment used for the elaboration of the crown is composed by a Cu-Au alloy.

Table 2. 6
Cu / Au peak ratios for different anode current values

Anode current (μA)	Cu K α / Au L α
125	20.9
250	23.7
500	23.0
750	23.3
1000	22.5

Red

Two red shades were identified on the artwork: a bright red (lips) and an orangey red (eyelids). The EDXRF spectrum on the bright red of the saint's lips is displayed in **Fig. 2. 19**. The high amount of mercury (Hg) might imply the use of cinnabar or vermilion (HgS).

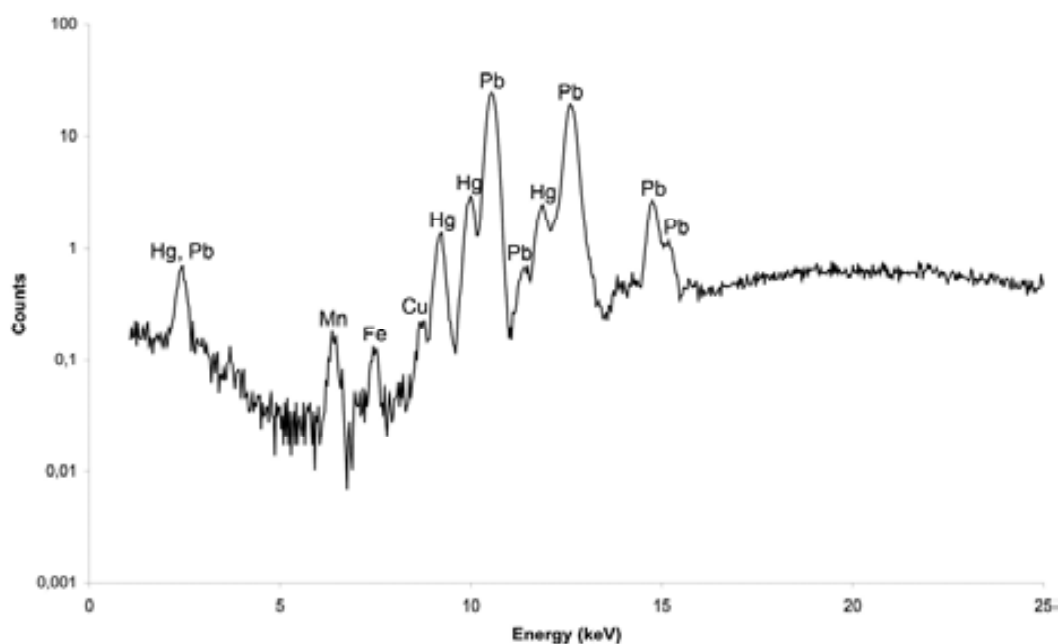


Figure 2. 19 EDXRF spectrum of the red lips.

In fact, in the Raman spectra measured on these areas (**Fig. 2. 20**), three Raman active modes can be observed (254, 284, 343 cm^{-1}) being the first one the most intense vibrational mode of HgS.

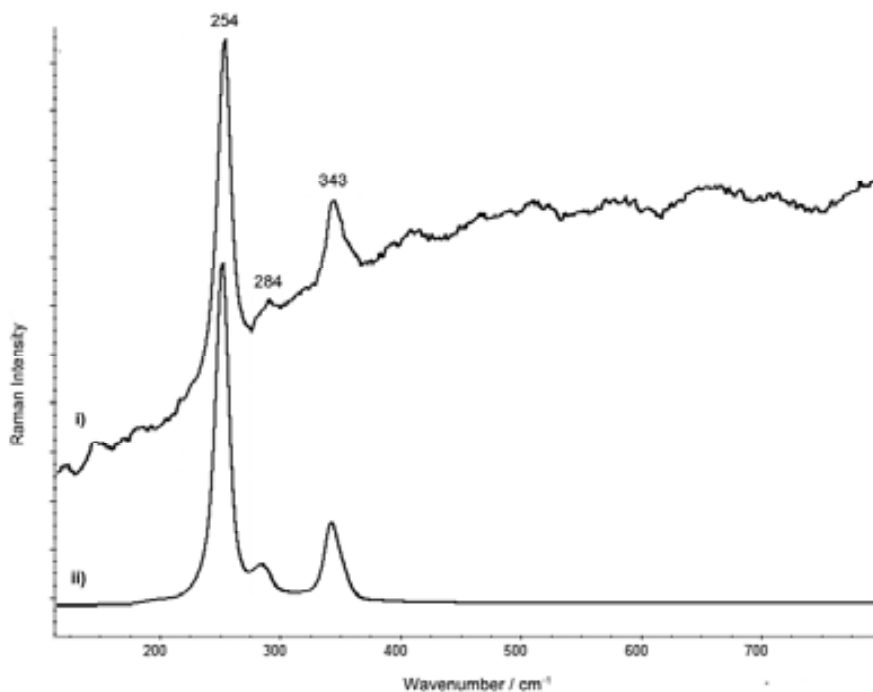


Figure 2. 20 Raman spectra of the eyelid (i) and vermilion reference material (ii). Spectrum obtained by using the innoRam® Raman spectrometer with the laser of 785 nm.

From the results obtained by using EDXRF and RS we conclude that the red pigment used in this oil on copper painting is cinnabar or vermilion. They cannot be distinguished neither by EDXRF nor by RS. Both of them are mercury sulphides, but the first one is of natural origin while the second one is a synthetic production of the mineral (Eastaugh *et al.*, 2004). They were both well known in the seventeenth century, as the natural mineral form was used since the antiquity and the manufactured form was produced in Europe since the eighth century AD (Eastaugh *et al.*, 2004).

Skin-coloured areas

The skin-coloured areas analysed by EDXRF (**Fig. 2. 21 (a)**) revealed the presence of lead and a small amount of mercury. These results were supported by RS (**Fig. 2. 21 (b)**), which confirmed the hypothesis of using an admixture of two pigments: the intense band at 254 cm^{-1} is due to the presence of vermilion (HgS) while the bands at 1049 (s) and 408 (w) cm^{-1} are characteristic of white lead ($\text{Pb}(\text{CO}_3)_2 \cdot \text{Pb}(\text{OH})_2$).

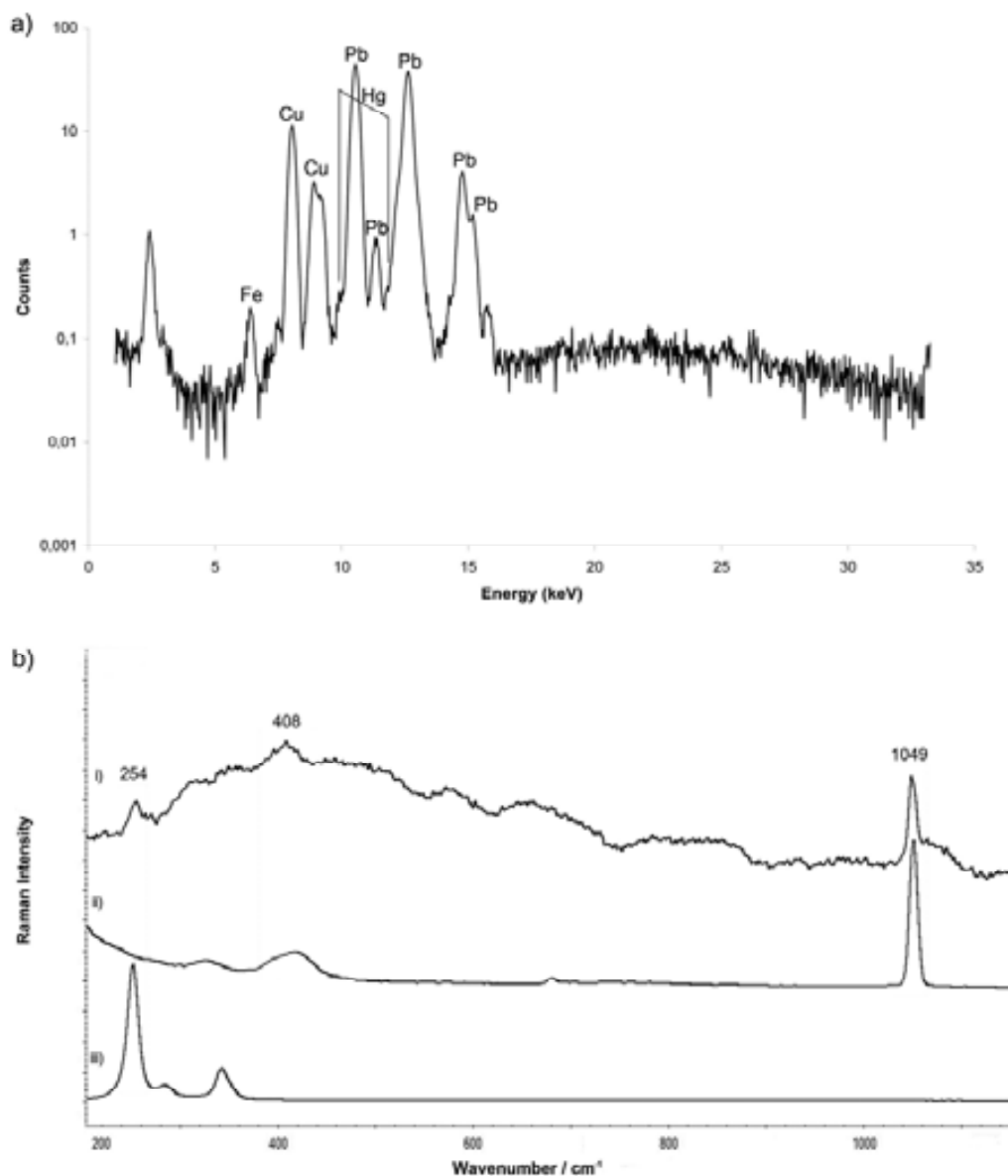


Figure 2. 21 Skin-coloured shades. (a) EDXRF spectrum and (b) Raman spectra of (i) skin-coloured area (obtained by using the innoRam ® Raman spectrometer with the laser of 785 nm; after baseline correction), (ii) hydrocerussite and (iii) vermilion.

2. 4. 3. 3. Binder

According to the literature (Horovitz, 1999) the paint for the preparatory and paint layers consisted, most of the times, of pigments ground in linseed oil. The use of FTIR spectroscopy was absolutely necessary for the characterization of the binder due to the strong fluorescence that frustrated the interpretation of Raman spectra almost all the time. The DRIFT spectrum (see **Fig. 2. 22**) showed intense bands due to the presence of oil, probably linseed oil. The bands due to C-H vibrational modes at 2930, 2848 and

1464 cm^{-1} are coincident with those of linseed oil. Finally, the presence of a band at 1734 cm^{-1} due to C=O bond gave us the definitive clue. Despite the notable noise present in the spectra in the region between 1700-1500 cm^{-1} due to the presence of moisture, it can be seen that the band of the C=O bond is not symmetric. This fact could be due to the presence of another compound with C=O bonds different to linseed oil. In fact, some resins used in natural varnishes (such as shellac, dammar or sandarac) present characteristic C=O feature around 1720 cm^{-1} . In the collected spectra there was a shoulder in that position. However, according to Sarmiento *et al.* (2011), during the curing and ageing process of oils, the C=O band become wider and asymmetric. Nevertheless, in the collected DRIFT spectrum there is a weak to medium feature at 780 cm^{-1} that could be consistent with the presence of a resin (varnish) (Derrick *et al.*, 1999). In some of the spectra, the presence of lead white was evident due to the features at 3540, 1048 and 690 cm^{-1} . The bands around 1450 cm^{-1} of lead white seemed to be overlapped by those of the binder.

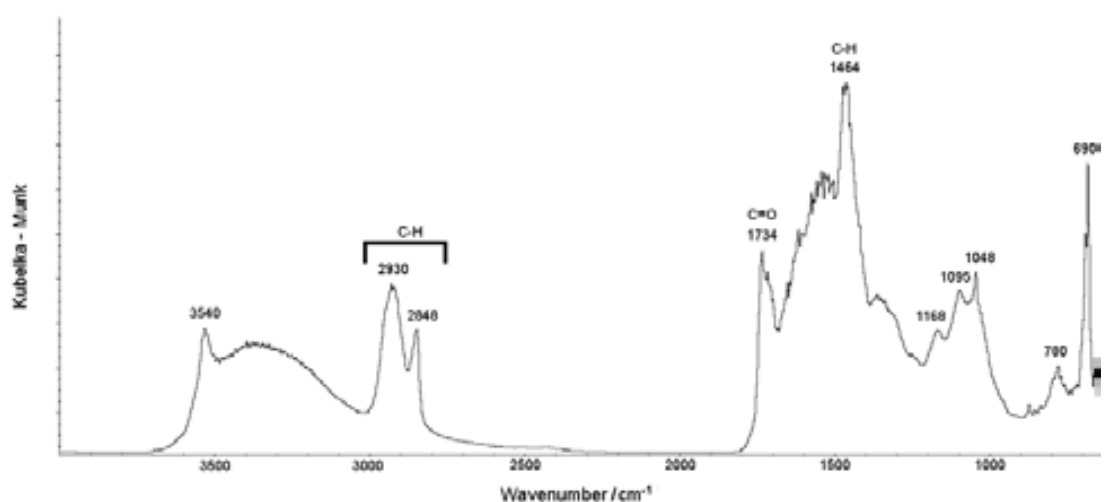


Figure 2. 22 DRIFT spectrum of the surface of the sample (after Kubelka-Munk data treatment). Vibrations due to the presence of oil, resin and lead white can be seen.

2. 4. 3. 4. Preparation layer

As explained in the previous case of study (see 2. 3. 3. 1, 2. 3. 3. 2) the preparation layer showed the ubiquitous presence of lead in the EDXRF analysis. According to the XRD spectral data, the presence of lead white (hydrocerussite) was confirmed. Moreover, Raman analysis (not shown) corroborated this finding, revealing the presence of the characteristic band of lead white at 1050 cm^{-1} (due to the symmetric

stretching vibration mode of carbonate anion in lead white). This result would confirm that the artwork was done before nineteenth century.

2. 4. 3. 5. Supporting material

The analysis of the supporting material, made by EDXRF analysis of the backside of the plate (see section 2. 3. 3. 1.) showed the signal from copper and minor iron impurities at trace level were present, thus, deducing the use of pure copper plate as a supporting material and discarding other copper based alloys used in antiquity such as zinc-bearing brass or leaded copper alloys.

2. 4. 4. Conclusions

A full multi-analytical approach was carried out in order to study an “oil on copper” painting presumably from second half of the sixteenth century. The use of energy dispersive X-ray fluorescence (EDXRF) technique in combination with X-ray diffraction (XRD), Raman spectroscopy (RS) and Fourier-transformed infrared spectroscopy (FTIR) techniques has proven to be very effective in the characterization of such kind of artwork, since they are completely non-destructive, which is a requisite to study valuable pieces, and provide valuable and complete information for the proper identification of all the compounds. EDXRF was very useful to determine both the elemental chemistry of pigments (mainly composed by calcium, manganese, iron, copper, gold, mercury and lead) and their distribution along the painting surface. By using XRD and RS we obtained information about almost all pigments present in the painting, while FTIR was useful to obtain information about the binding medium. Comparing with RS, by using XRD the results obtained from the study of the brown earths pigments present in the sample were much more successful while RS presented some difficulties in the acquisition of the signals from these colours. However, the versatility of the Raman instrumentation used in this work allowed analysing very small areas, such as red eyelids and lips, which XRD could not analyse due to spatial resolution limitations of the conventional XRD equipment employed in this work.

Apart from the copper support, we could identify two different superimposed layers: a) a preparation layer mainly composed by lead white (hydrocerussite) and b) the pictorial layer of variable composition (brochantite, posnjakite, red lead, carbon black, brown earth pigments such as goethite, szomolnokite, pyrolusite or rhodocrosite, a copper-gold alloy, vermilion and lead white). The compositional features of the green

colouration revealed by the combined use of XRD and RS, suggest that the artwork was in fact conceived in the seventeenth century rather than in the second half of the sixteenth century, as the presence of brochantite and posnjakite was determined. In accordance with the literature (Gilbert *et al.*, 2003) these compounds began to be used at the seventeenth century. The use of white lead as a priming layer was a common practice on the “oil on copper” painting technique.

2. 5. References

BELL I.M., CLARK R.J.H., GIBBS P.J. (1997) *Raman spectroscopic library of natural and synthetic pigments (pre ~ 1850 AD)*. Spectrochimica Acta Part A: Molecular and Biomolecular Spectroscopy, 53 (2), 159-2179.

BERTUCCI M., BONIZZONI L., LUDWIG N., MILAZZO M. (2010) *A new model for x-ray fluorescence autoabsorption analysis of pigment layers*. X-Ray Spectrometry, 39, 135 -141.

BONIZZONI L., GALLI A., POLDI G., MILAZZO M. (2007) *In situ non-invasive EDXRF analysis to reconstruct stratigraphy and thickness of Renaissance pictorial multilayers*. X-Ray Spectrometry, 36, 55–61.

BONIZZONI L., GALLI A., POLDI G. (2008) (a) *In situ EDXRF analyses on Renaissance plaquettes and indoor bronzes patina problems and provenance clues*. X-Ray Spectrometry, 37, 388-394.

BONIZZONI L., CAGLIO S., GALLI A., POLDI G. (2008) (b) *A non invasive method to detect stratigraphy, thicknesses and pigment concentration of pictorial multilayers based on EDXRF and vis-RS: in situ application*. Applied Physics A: Materials Science & Processing, 92, 203 -210.

BONIZZONI L., CAGLIO S., GALLI A., POLDI G. (2010) *Comparison of three portable EDXRF spectrometers for pigment characterization*. X-Ray Spectrometry, 39, 233 -242.

BONIZZONI L., COLOMBO C., FERRATI S., GARGANO M., GRECO M., LUDWIG N., REALINI M. (2011) *A critical analysis of the application of EDXRF spectrometry on complex stratigraphies*. X-Ray Spectrometry, doi: 10.1002/xrs.1320.

BURGIO L., CLARK R.J.H. (2001) *Library of FT-Raman spectra of pigments, minerals, pigment media and varnishes, and supplement to existing library of Raman spectra of pigments with visible excitation*. Spectrochimica Acta Part A: Molecular and Biomolecular Spectroscopy, 57, 1491-1521.

BURGIO L., CLARK R.J.H., MURALHA V.S.F., STANLEY T.J. (2008) *Pigment analysis by Raman microscopy of the non-figurative illumination in 16th- to 18th-century Islamic manuscripts*. Journal of Raman Spectroscopy, 39, 1482-1493.

CARLYLE L. (2001) *The Artist's assistant: oil painting instruction manuals and handbooks in Britain 1800-1900: with reference to selected eighteenth-century sources*. Archetype Publications, London

CASTRO K., PÉREZ-ALONSO M., RODRÍGUEZ-LASO M.A., ETXEBARRIA N., MADARIAGA J.M. (2007) *Non-invasive and non-destructive micro-XRF and micro-Raman analysis of a decorative wallpaper from the beginning of the 19th century*. Analytical and Bioanalytical Chemistry, 387, 847-860.

CASTRO K., PESSANHA S., PROIETTI N., PRINCI E., CAPITANI D., CARVALHO M.L., MADARIAGA J.M. (2008) (a) *Noninvasive and nondestructive NMR, Raman and XRF analysis of a Blaeu coloured map from the seventeenth century*. Analytical and Bioanalytical Chemistry, 391, 433-441.

CASTRO K., SARMIENTO A., MARTÍNEZ-ARKARAZO I., MADARIAGA J.M., FERNÁNDEZ L.A. (2008) (b) *Green copper pigments biodegradation in cultural heritage: From malachite to moolooite, thermodynamic modeling, X-ray fluorescence and raman evidence*. Analytical Chemistry, 80 (11), 4103-4110.

CESAREO L., BRUNETI A., RIDOLFI S. (2008) *Pigment layers and precious metal sheets by energy-dispersive x-ray fluorescence analysis*. X-Ray Spectrometry, 37, 309-316.

COLEYSBOW E.E., GRIFFITH W.P. (1994) *Fourier-transform raman spectroscopy of minerals*. Spectrochimica Acta Part A: Molecular Spectroscopy, 50 (11), 1909-1918.

DERRICK M.R., STULIK D., LANDRY J.M. (1999) *Infrared spectroscopy in Conservation Science*. Edited by The Getty Conservation Institute, Los Angeles, USA.

DESNICA V., SCHREINER M. (2006) *A LabVIEW-controlled portable x-ray fluorescence spectrometer for the analysis of art objects*. *X-Ray Spectrometry*, 35, 280-286.

DESNICA V., SKARIC K., JEMBRIH-SIMBUERGER D., FAZINIC S., JAKSIC M., MUDRONJA D., PAVLICIC M., PERANIC I., SCHREINER M. (2008) *Portable XRF as a valuable device for preliminary in situ pigment investigation of wooden inventory in the Trski Vrh Church in Croatia*. *Applied Physics A: Materials Science & Processing*, 92, 19-23.

DUPUIS G., MENU M. (2006) *Quantitative characterisation of pigment mixtures used in art by fibre-optics diffuse-reflectance spectroscopy*. *Applied Physics A: Materials Science & Processing*, 83, 469-474.

EASTAUGH N., WALSH V., CHAPLIN T., SIDDAL R. (2004) *Pigment Compendium, a dictionary of historical pigments*. Elsevier Butterworth - Henemann, Oxford.

FITTSCHEN U.E.A., HAVRILLA G.J. (2010) *Picoliter Droplet Deposition Using a Prototype Picoliter Pipette: Control Parameters and Application in Micro X-ray Fluorescence*. *Analytical Chemistry*, 82, 297-306.

GIL M., CARVALHO M.L., SERUYA A., RIBEIRO I., QUERALT I., CANDEIAS A.E., MIRAJO J. (2008) *Limewashing paintings in Alentejo urban heritage: pigment characterization and differentiation by WDXRF and XRD*. *Applied Physics A: Materials Science & Processing*, 90, 49-54.

GILBERT B., DENOËL S., WEBER G., ALLART D. (2003) *Analysis of green copper pigments in illuminated manuscripts by micro-Raman spectroscopy*. *Analyst* 128, 1213-1217.

GUILLERME A., PESSANHA S., CARVALHO M. L., DOS SANTOS J. M. F., COROADO J. (2010) *Micro energy dispersive X-ray fluorescente análisis of plichrome lead-glazed Portuguese faiences*. *Spectrochim Acta Part B: Atomic Spectroscopy*, 65 (4), 328-333.

HAHN O., OLTROGGE D., BEVERS H. (2004) *Coloured prints of the 16th century: non-destructive analyses on coloured engravings from Albrecht Dürer and contemporary artists*. *Archaeometry*, 46 (2), 273-282.

HAHN O., REICHE I., STEGE H. (2006) *Application in Arts and Archaeology*, in: BECKHOFF B., KANNGIEBER B., LANGHOFF N., WEDELL R., WOLFF H. (Eds.) *Handbook of Practical X-Ray Fluorescence Analysis*. Springer, Berlin, p. 690.

HERRERA L.K., MONTALBANI S., CHIAVARI G., COTTE M., SOLÉ V.A., BUENO J., DURAN A., JUSTO A., PÉREZ-RODRÍGUEZ J.L. (2009) *Advanced combined application of μ X-ray diffraction/ μ X-ray fluorescence with conventional techniques for the identification of pictorial materials from Baroque Andalusia paintings*. *Talanta*, 80 (1), 71-83.

HOROVITZ I. (1986) *Paintings on copper supports: techniques, deterioration and conservation*. *The Conservator*, 10, 44-48.

HOROVITZ I. (1999) *The Materials and Techniques of European Paintings on Copper Supports*, in: KOMANECKY M.K. (1999) *Copper as Canvas: Two Centuries of Masterpiece Painting on Copper, 1575-1775*. Phoenix Art Museum, Oxford University Press, USA, 63-92.

HOROVITZ I. (2002) *Techniques and conservation of paintings on copper*. *The Picture Restorer*, 22.

HRADIL D., HRADILOVA J., BEZDICKA P., SVARCOVÁ S. (2008) *Provenance study of Gothic paintings from North-East Slovakia by handheld x-ray fluorescence, microscopy and x-ray microdiffraction*. *X-Ray Spectrometry*, 37, 376-382.

INTERNATIONAL STANDARDS ORGANIZATION (2000) ISO 3497 norm "Metallic coatings - measurement of coating thickness - X-ray spectrometric methods, Geneva, Switzerland, p. 24

JULIEN C.M., MASSOT M., POINSIGNON C. (2004) *Lattice vibrations of manganese oxides: Part I. Periodic structures*. *Spectrochimica Acta Part A: Molecular and Biomolecular Spectroscopy*, 60, 689-700.

KANNGIESSER B., MALZER W., FUENTES-RODRIGUEZ A., REICHE I. (2005) *Three-dimensional micro-XRF investigations of paint layers with a tabletop setup*. Spectrochimica Acta Part B: Atomic Spectroscopy, 60, 41 -47.

KOMANECKY M.K., HOROVITZ I., EASTAUGH N. (1998) *Antwerp artists and the practice of painting on copper*, in: ROY A. and SMITH P. (Eds.) *Painting Techniques History, Materials and studio Practice. Contributions to the Dublin Congress (7-11 September 1998, Dublin)*. The International Institute for Conservation of Historic and Artistic Works, London, 136-139.

KOMANECKY M.K. (1999) *Introduction*, in: KOMANECKY M.K. (1999) *Copper as Canvas: Two Centuries of Masterpiece Painting on Copper, 1575-1775*. Phoenix Art Museum, Oxford University Press, USA, 3-7.

PAPPALARDO L., PAPPALARDO G., AMORINI F., BRANCIFORTI M.G., ROMANO F.P., SANOIT J., RIZZO F., SCAFIRI E., TAORMINA A., ROTONDO G. (2008) *The complementary use of PIXE-a and XRD non-destructive portable systems for the quantitative analysis of painted surfaces*. X-Ray Spectrometry, 37, 370 -375.

PAVLOPOULOU L.C., WATKINSON D. (2006) *The degradation of oil painted copper surfaces*. Reviews in Conservation 7:55-65.

ROESSIGER V., KAISER K.H. (1998) *WinFTM: eine neue Software für die Schichtdickenmessung nach dem Röntgenfluoreszenz-Verfahren*, Jahrbuch Oberflächentechnik, Metall Verlag, Heidelberg, p. S313.

ROESSIGER V., NENSEL B. (2006) *Analysis of Layers*, in: BECKHOFF B., KANNIGIEBER B., LANGHOFF N., WEDELL R. (Eds.) *Handbook of Practical X-ray Fluorescence Analysis*. Springer-Verlag, Berlin, 554-600.

ROSI F., BURNSTOCK A., VAN DEN BERG K.J., MILIANI C., BRUNETTI B.G., SGAMELLOTTI A. (2009) *A non-invasive XRF study supported by multivariate statistical analysis and reflectance FTIR to assess the composition of modern painting materials*. Spectrochim Acta Part A: Molecular and Biomolecular Spectroscopy, 71 (5), 1655-1662.

ROSI F., MILIANI C., CLEMENTI C., KAHRIM K., PRESCIUTTI F., VAGNINI M., MANUALI V., DAVERI A., CARTECHINI L., BRUNETTI B.G., SGAMELLOTTI A. (2010) *An integrated spectroscopic approach for the non-invasive study of modern art materials and techniques*. Applied Physics A: Materials Science & Processing, 100 (3), 613-624.

SARMIENTO A., PÉREZ-ALONSO M., OLIVARES M., CASTRO K., MARTÍNEZ-ARKARAZO I., FERNÁNDEZ L.A., MADARIAGA J.M. (2011) *Classification and identification of organic binding media in artworks by means of Fourier transform infrared spectroscopy and principal component analysis*. Analytical and Bioanalytical Chemistry, 399, 3601-3611.

SAWCZAK M., KAMINSKA A., RABCZUK G., FERRETTI M., JENDRZEJEWSKI R., SLIWINSKI G. (2009) *Complementary use of the Raman and XRF techniques for non-destructive analysis of historical paint layers*. Applied Surface Science, 255, 5542 - 5545.

SCOTT D.A., WARMLANDER S., MAZUREK J., QUIRKE S. (2009) *Examination of some pigments, grounds and media from Egyptian cartonnage fragments in the Petrie Museum, University College London*. Journal of Archeological Science, 36, 923 -932.

SOTIROPOULOU S., SISTER DANIILIA, MILLAN C., ROSI F., CARTECHINI L., PAPANIKOLA-BAKIRTZIS D. (2008) *Microanalytical investigation of degradation issues in Byzantine wall paintings*. Applied Physics A: Materials Science & Processing, 92, 143 -150.

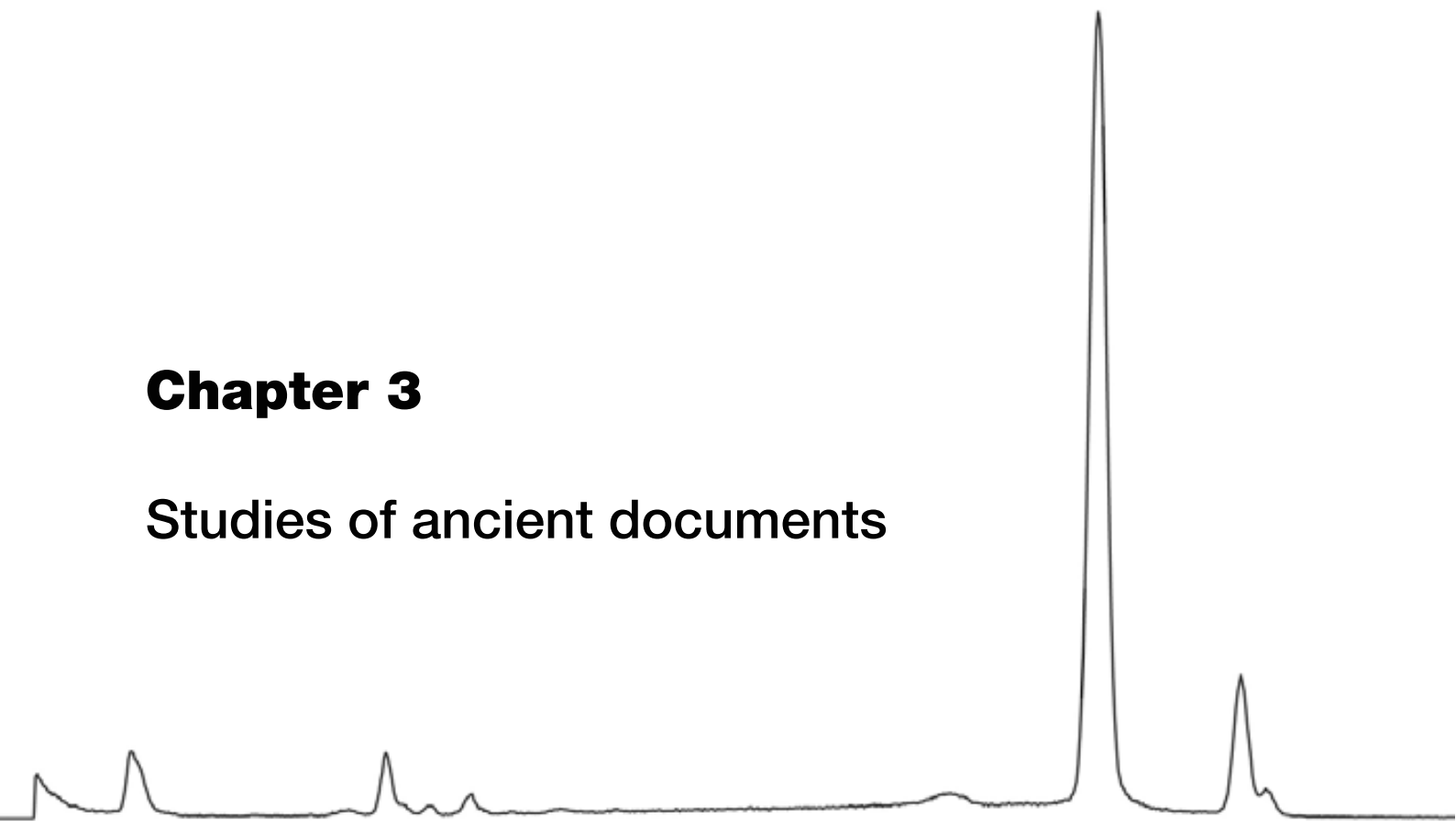
STULIK D.C., KHANJIAN H.P. (2003) *Insight into early photographic processes: quantitative XRF approach*, in: TOWNSEND J.H., EREMIN K., ADRIAENS A. (Eds.) *Conservation Science 2002: papers from the conference held in Edinburgh, Scotland 22-24 may 2002*. Archetype Publications, London, 188-194.

VEIGA A.R. (2010) *Oil painting on tinsplate by Francisco José Resende: Techniques, materials and degradation of three nineteenth century paintings*. Paru dans CeROArt, hors-série.

de VIGUERIE L., SOLE V. A., WALTER P. (2009) *Multilayers quantitative X-ray fluorescence analysis applied to easel paintings*. *Analytical and Bioanalytical Chemistry* 395, 2015 -2020.

Chapter 3

Studies of ancient documents



Part of the contents of this chapter is published in:

PITARCH A., ALVAREZ-PEREZ A., CASTRO K., MADARIAGA J.M., QUERALT I. (2011)
*Raman analysis assessed by Fourier Transformed Infrared and X-Ray Fluorescence
spectroscopies: a multianalytical approach of ancient chromolithographs from the nineteenth
century.* Journal of Raman Spectroscopy. doi: 10.1002/jrs.3055.

3. 1. Introduction

The material characterization of ancient works on paper can provide valuable data relating to many aspects. On one hand, identification and quantification of the raw materials employed in the manufacturing process of the paper support may provide a first indication of its origin, chronology and technology for its elaboration. On the other hand, pigment identification may be useful to determine the period of time in which the works on paper were performed. Furthermore, material characterization on works on paper can supply information helpful to develop conservation strategies. Good examples of the importance of these studies are the increasing number of references available in the literature from the last years. The most recent studies covered the analysis of different kinds of paper support such as books (Frausto-Reyes *et al.*, 2009; Ganzerla *et al.*, 2009; Doncea *et al.*, 2010), folding screens (Pessanha *et al.*, 2010); illuminated manuscripts (Duran *et al.*, 2009), wallpapers (Pessanha *et al.*, 2009; Colomban, 2011), polychrome prints (Striová *et al.*, 2009), maps (Castro *et al.*, 2008 (a)), pastels (Caggiani and Colomban, 2011), articles concerning several conservation strategies (Manso *et al.*, 2009; Castro *et al.*, 2011) and there even is an article reporting the “state of the art” on the use of spectroscopic techniques in the field of conservation and characterization concerning ancient documents (Manso and Carvalho, 2009).

Amongst all the available analytical techniques, Raman spectroscopy (RS) has become a powerful tool in the study of works on paper not only because its non-invasiveness, but also because its increasing ability during last decades to access the low wave-number regions ($<500\text{ cm}^{-1}$), which is decisive for the identification of many inorganic pigments (Edwards and Chalmers, 2005). Furthermore, this technique can indeed be used as a fingerprint since most pigments produce clear Raman spectra, as well as allowing for the identification of chemical compounds (Striová *et al.*, 2009). However, despite all the advantages in the qualitative identification of inorganic pigments in works on paper, Raman analysis can be thwarted by the natural fluorescence of organic and inorganic materials usually present in artworks (such as binders and varnishes) or by atomic fluorescence inherent in some materials (Smith and Clark, 2004). The use of extremely long or extremely short wavelength lasers and the application of spectral manipulations such as subtracted-shifted Raman analysis (Bell *et al.*, 2000) are some of the numerous tools that have been developed to avoid fluorescence. Sometimes, the use of other complementary techniques is advisable, such as Fourier transform infrared (FTIR) spectroscopy, which provides the necessary

information on those organic materials whose Raman signals might be shielded by the fluorescence emission. Another source of difficulties with using RS may arise when analysing metallic paints (which are sometimes applied in different shades, ranging from silver to gold or a more reddish copper-colour). Like many metals, gold does not provide a Raman spectrum, thus it is virtually undetectable by this technique (Burgio *et al.*, 2008). Once again, the use of complementary techniques (such as X-ray fluorescence, XRF) is compulsory for the proper characterization of the object under analysis. In this sense, several papers in literature have highlighted the necessity of a multianalytical approach for the complete study of pigments used in ancient paperwork (Castro *et al.*, 2008 (b); Pessanha *et al.*, 2009; Striová *et al.*, 2009).

3. 2. Characterization of ancient chromolithographs.

The literature reporting on specific examination of historical polychrome prints is not numerous (Wiedemann, 2001; Marcolli and Wiedemann, 2001; Ferrero *et al.*, 2004; Hahn *et al.*, 2004; Castro *et al.*, 2005; Centeno *et al.*, 2006; Vandenabeele *et al.*, 2008; Striová *et al.*, 2009). In the work of Wiedemann (2001) the authenticity of Chinese and Japanese woodcuts and European lithographs was investigated by differential scanning calorimetry (DSC) and RS. The paper type and the employed colours were identified. Marcolli and Wiedemann (2001) also used these techniques to distinguish between the original paper used by the artists and possible forgeries. Their study included Asian woodprints from China and Japan, and lithographs of European artists. Ferrero *et al.* (2004) published a study on several coloured and one polychrome engraving by means of XRF analysis; however, the determination of inorganic compounds was done by identifying certain elements (which is rather than risky, since this technique is capable of determining the elements but not the compounds to which they belong). Hahn *et al.* (2004) undertook a survey of painted printed graphics from the sixteenth century using micro-XRF and visible spectrophotometry, techniques that do not allow for the differentiation between some pigments. Castro *et al.* (2005) chose micro-Raman spectroscopy for the identification of the pigments present in four nineteenth-century hand-coloured lithographs. According to the obtained results, several doubts about the date of the lithographs appeared due to the presence of compounds first synthesized at the twentieth century. Centeno *et al.* (2006) used RS for the systematic study on the colorants and other additives present in posters manufactured during the period between 1890 and 1920. The results reflected that lithographers were actively experimenting to achieve new hues. Vandenabeele *et al.* (2008) applied RS for the analysis of nineteenth century porcelain cards (produced by

a lithographic procedure and painted by hand). Although they gained information on the manufacturing process and the pigments that were used for their production, the necessity of a more extended study was claimed since it was not possible to identify by RS the metallic pigments, nor the binding medium and the paper fillers. Finally, the work by Striová *et al.* (2009) focused on the analysis of five polychrome prints from the eighteenth century by using XRF, micro-FTIR and micro-Raman spectroscopies. The combination of techniques allowed identifying all the compounds used for the elaboration of the engravings.

3. 2. 1. Historical context

The paper manufacturing process remained unchanged for many centuries until, in the eighteenth century -coinciding with the Industrial Revolution, it suffered from many transformations (new production processes with different raw materials such as esparto rags, cotton rags and ground wood paper were patented) (Ganzerla *et al.*, 2009). At the same time, the pigment industry suffered from many innovations and several mineral pigments were synthesised (Gettens and Stout, 1966; Castro *et al.*, 2005). The technical developments in colour illustration that took place during that period of time have led us several collections of fully coloured lithographs of plants and animals amongst others.

Lithography process was invented by Aloïs Senefelder in Germany in 1796 and is based on the chemical repellence of oil and water (Senefelder, 1911). For the elaboration of a lithograph, the stone was dampened with water and the printing ink was then applied with a roller. This ink adhered only to the greased image but was repelled by the wet parts of the stone. The image could then be taken away from the inked drawing on a sheet of damp paper. By using several stones (a technique known as "Lithotint process", developed in 1840) the appearance of a wash drawing made by brush could be obtained and ornate designs of dozens of bright colour impressions could be obtained.

3. 2. 2. Research aims

The aim of this work is to try to fill the lack of literature on coloured lithographs as well as to highlight the necessity of a multi-analytical approach in the study of ancient works on paper. As an example, a full chemical characterization of chromolithographs from the nineteenth century is presented.

3. 2. 3. Materials and Methods

3. 2. 3. 1. Specimen

The object under analysis, which belongs to a private collection¹, is the book entitled *Les Orchideés. Histoire Iconographique. Organographie – Classification - Géographie – Collections - Commerce – Emplot - Culture avec une revue descriptive des espèces cultivées en Europe*, written by Paul Émile de Puydt and edited by J. Rothschild in Paris in 1880.

This high-quality book was elaborated with considerable accuracy (it has a green gilt-lettered label) and contains both engravings printed in black ink and chromolithographs characterized with ornate designs of orchards. Its 50 plates contain subtle gradations in tone and complex overprinting. Once the lithographs were coloured, they were finished by hand, heightening them with varnish.

Although the paper support seems to be in bad state of conservation (according to Laguardia *et al.* (2005) paper made with wood pulp becomes yellow and rapidly loses its original flexibility) the chromolithographs remain in a good state.

For the present study a set of thirteen representative lithographs from the book were selected, considering the whole palette of colours used for its elaboration (**Fig. 3. 1**).

¹ A. Pitarch would like to thank the owner, R. Puig, for lending her private collection of books to proceed with this study.

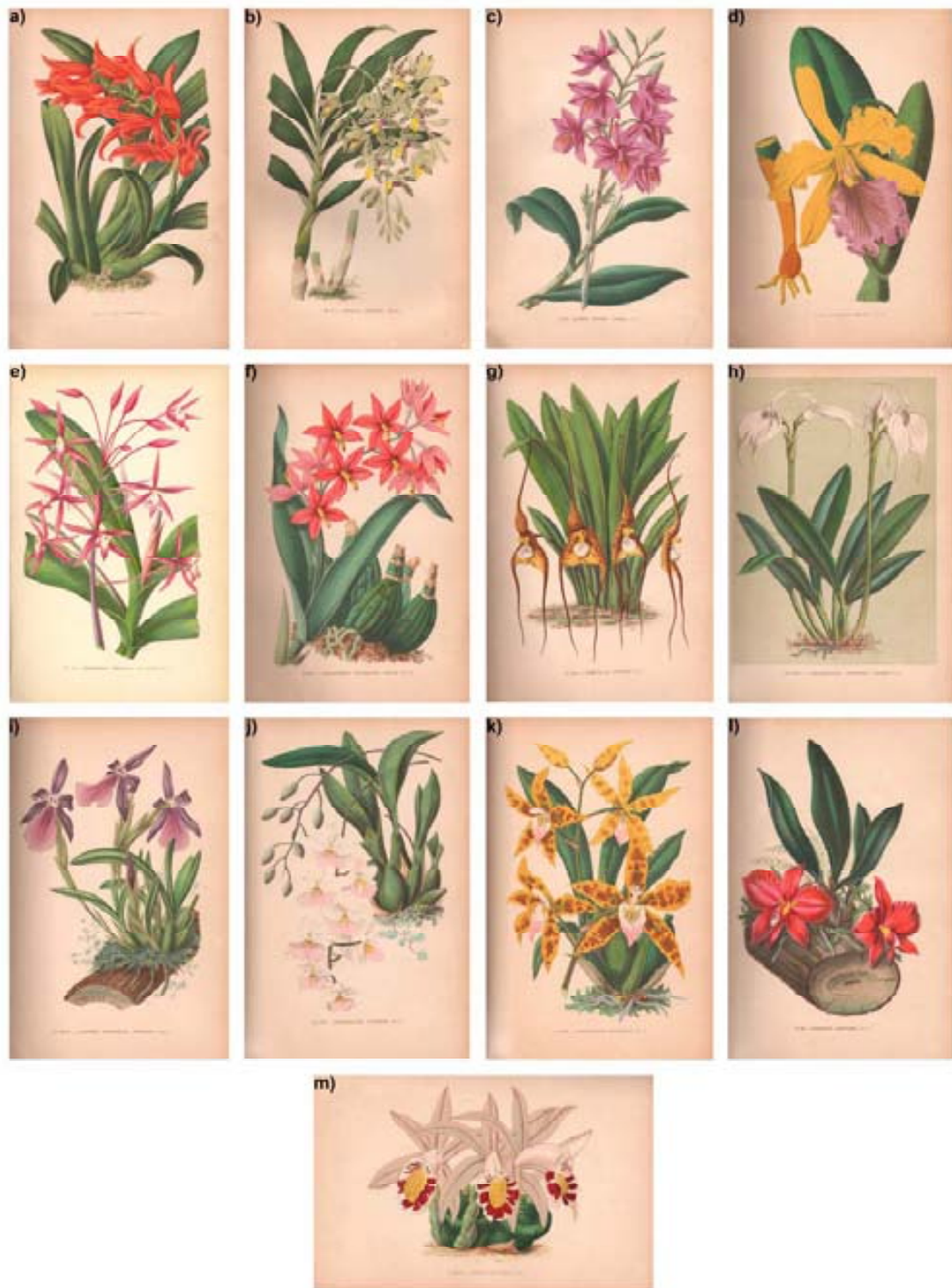


Fig. 3. 1 Selected chromolithographs from the book *Les Orchideés. Histoire Iconographique. Organographie – Classification - Géographie – Collections - Commerce – Emplot - Culture avec une revue descriptive des espèces cultivées en Europe*. a) PL. I; b) PL. V; c) PL. VI; d) PL. VII; e) PL. XIX; f) PL. XX; g) PL. XXIII; h) PL. XXIV; i) PL. XXVII; j) PL. XXIX; k) PL. XXX; l) PL. XLI; m) PL. XXXVI (photography: A. Pitarch).

3. 2. 3. 2. Analytical techniques

The delicacy of the studied book required analytical techniques able to perform the analysis to the whole piece, without any kind of pre-sampling procedure. EDXRF, Raman and FTIR spectroscopies were selected for this purpose.

Elemental analysis of the lithographs was obtained by using the EDXRF spectrometer (XDV-SD® model; see section I. 5 to check the instrument's parameters). The X-rays were collimated by a collimator with 3 mm in diameter, to adjust the X-ray focal spot to selected areas of the paperwork. The measurements were carried out operating at 50 kV of voltage, with an anode current of 128 μ A, using an aluminium filter 1000 μ m in thickness and a counting time of 200 s. During the analyses, the motorized X-Y stage (scan mode) was used to ensure the representativeness of the measurement.

An ultramobile innoRam ® Raman spectrometer (B&WTEKInc., Newark, USA) was used to identify the inks. Main features of the equipment were described in section I. 5. The spectra were measured accumulating several scans for each spectrum to obtain the desirable signal-to-noise ratio. Various analyses were carried out in different areas of the same colour in order to obtain reliable results.

The FTIR spectra of some organic compounds and paper support (including the filler) were collected using a Thermo Scientific Nicolet iN10 MX Infrared Microscope spectrometer by extracting microfibers from selected areas. The main features of the equipment were described in section I. 5. Analysis of inks on papers has the disadvantage of the strong absorption of the matrix since the spectrum of cellulose shows very intensive bands in the fingerprint region (Ferrer and Vila, 2006); therefore, it is necessary to try to remove particles where fibres are not present. For this purpose, the particle or fibre was removed from the matrix with the help of tungsten needles and was then placed in a sample holder (Spectra-Tech Micro Compression Cell and Diamond Window) which was used to flatten and crush samples for efficient transmission analysis by FTIR spectroscopy. The obtained spectra were collected in transmittance mode.

3. 2. 4. Results and Discussion

The analysis of the chromolithographs involved the identification of the type of fillers used to elaborate the paper support and the characterization of the pigments used for colouring the lithographs. The list of main detected elements for each colour is summarized in **Table 3. 1**.

Table 3. 1
Elements detected by EDXRF

Colour of the analysed spot	Main detected elements
White	Ca, Fe, Zn, Rb, Sr
Yellow	Cr, Pb
Orange	Pb
Pink	Pb, Fe
Red	Pb, Fe
Purple	Fe
Brown	Cr, Fe, Hg, Pb
Blue	Fe
Green	Cr, Fe, Pb
Golden	Fe, Au, Cu

EDXRF analyses orientated us to the most likely pigments and fillers present in the selected lithographs. However, as it is an elemental technique, the use of RS and FTIR was compulsory to clearly identify all the pigments, whether of an organic or inorganic nature and other organic substances (such as binders and varnishes). The list of principal colouring materials identified by RS on the selected chromolithographs is summarized in **Table 3. 2**.

Table 3. 2
Pigments found on the lithographs analysed by Raman spectroscopy.

Pigments	Formula	Raman bands	Lithography
Carbon black	C (amorphous carbon)	1325, 1580 (Burgio & Clark, 2001)	<i>PL. XXIII, PL. XLI.</i>
Chrome yellow	PbCrO ₄ (lead (II) chromate)	141, 339, 361 , 378, 405, 842 , 864 (Bell <i>et al.</i> , 1997)	<i>PL. I, PL. V, PL. XXIII, PL. XLI.</i>
Indigo Blue	C ₁₆ H ₁₀ N ₂ O ₂ (indigotin)	98, 136, 172, 181, 236, 253, 265, 253, 265, 277, 311, 320, 468, 546, 599, 676, 758, 862, 871, 1015, 1149, 1191, 1226, 1248, 1310, 1363, 1461, 1483, 1572, 1584 , 1626, 1701 (Bell <i>et al.</i> , 1997)	<i>PL. I</i>
Prussian blue	Fe ₄ [Fe(CN) ₆] ₃ ·14-16H ₂ O (iron (III) hexacyanoferrate (II))	282, 538 , 2102, 2154 (Burgio & Clark, 2001)	<i>PL. I, PL. VI, PL. VII, PL. XX, PL. XXIII, XXVII, PL. PL. XXIX, PL. XXX, PL. XXXIV, PL. XXXVI, PL. XLI.</i>
Red ochre	Fe ₂ O ₃ + clay + silica (iron (III) oxide chromophore)	220, 286 , 402, 491, 601 (Burgio & Clark, 2001)	<i>PL. XXIII, PL. XLI.</i>
Red lead	Pb ₃ O ₄ (lead (II, IV) oxide)	65, 122 , 144, 148, 150, 224, 232, 314, 391, 456, 477, 550 (Bell <i>et al.</i> , 1997)	<i>PL. I, PL. XX.</i>
Vermillion	HgS (mercury (II) sulfide)	253 , 284, 343 (Bell <i>et al.</i> , 1997)	<i>PL. XXIII, PL. XLI.</i>

In bold are the bands wavenumber which have strong or very strong relative intensity

3. 2. 4. 1. Paper support

According to the EDXRF results (**Fig. 3. 2**), a common observation in the entire spectrum of the paper support was the presence of calcium, iron, zinc, rubidium, strontium and lead. Dealing with the presence of calcium, this element takes part in several steps of the papermaking process, i.e. as a whitener in the fermentation step or during processing of the water supply (Reynard, 1989). Concerning the presence of zinc and lead, these elements have already been reported in ancient papers as coming from white zinc oxide and lead white respectively (Hanson, 1981; Manso *et al.*, 2008); however none of the techniques used for the study confirmed the presence of these compounds. The presence of iron may be due to impurities added throughout the production process of papermaking. The presence of strontium is probably linked with calcium, because it is usually present in the calcite crystalline lattice.

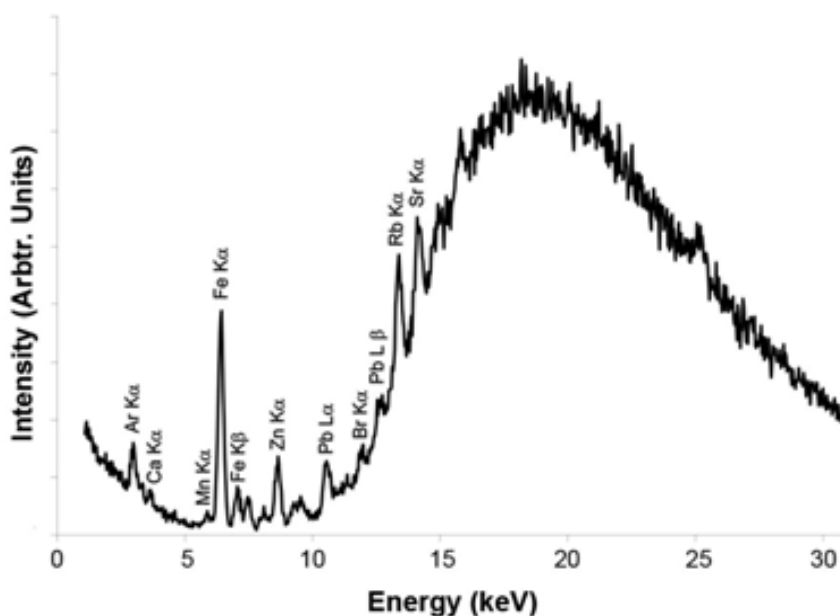


Fig. 3. 2 EDXRF spectrum of the paper support.

Regarding mineral fillers, no information was obtained using RS. The first attempt at studying the fillers present in the paper support failed because of the strong fluorescence that occurred during the analyses. The fluorescence overlapped with the bands of any mineral fillers present in the support. Nevertheless, the main features of cellulose were observed in the spectrum where the most intense Raman bands were located at 1094, 1118 and 1378 cm^{-1} (Boileau *et al.*, 2009).

FTIR spectroscopy proved to be essential in studying the paper support. As illustrated in **Fig. 3. 3**, apart from the most important functional groups of cellulose fibres (3408 and 3343 $\nu(\text{OH})$, 2902 $\nu(\text{CH})$, 1637 $\delta(\text{OH})$, 1434 $\delta(\text{CH})$, 1372 $\delta(\text{CH})$, 1338 $\delta(\text{CH}_2)$ wagging, 1322 $\delta(\text{CH})$, 1282 $\delta(\text{CH}_2)$ twisting, 1236 ($\delta(\text{C-OH})$ out-of-plane, 1205 $\delta(\text{C-OH})$ $\delta(\text{C-CH})$), 1161 $\nu(\text{CC})$ asymmetric ring breathing, 1112 $\nu(\text{C-O-C})$ glycosidic, 1060 $\nu(\text{C-OH})$ 2° alcohol, 1036 $\nu(\text{C-OH})$ 1° alcohol, 1002 (shoulder) $\rho(\text{-CH-})$ and 898 cm^{-1} (shoulder) $\nu(\text{C-O-C})$ in plane symmetric (Castro *et al.*, 2011), the presence of kaolinite ($\text{Al}_2\text{O}_3 \cdot 2\text{SiO}_2 \cdot 2\text{H}_2\text{O}$) was observed.

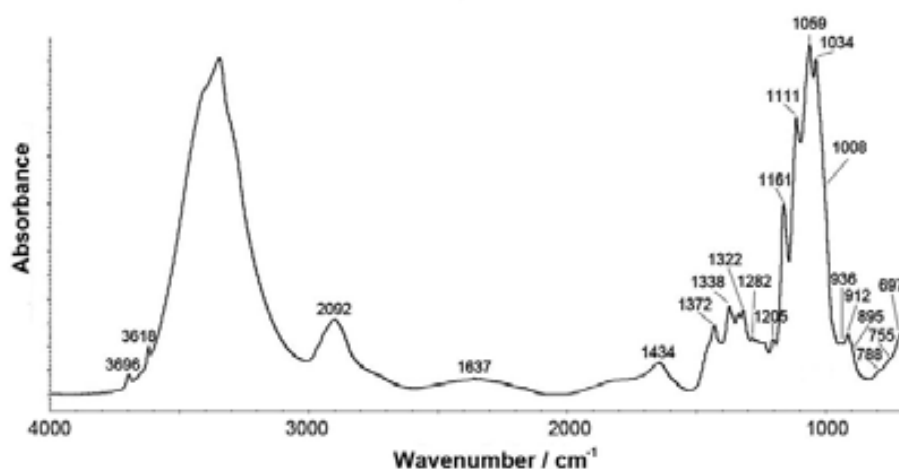


Fig. 3. 3 FTIR spectrum of the paper support.

Absorbance values at 3696 and 3618 cm^{-1} were assigned to vibrational modes of hydroxyl groups of kaolinite. An absorption band at 1111 cm^{-1} is associated with $\nu(\text{Si-O})$, while those at 1034 cm^{-1} and 1008 (shoulder) are due to Si-O-Si and Si-O-Al lattice vibrations. Bands at 936 and 913 cm^{-1} can be attributed to OH-bending vibration mainly caused by Al-OH groups. As can be seen, some of these vibrations are overlapped by those of cellulose. The absorbance values from the lower frequency wavenumbers observed (788 (shoulder), 755 (shoulder) and 697 (shoulder) cm^{-1}) can be largely attributed to different Si-O vibrations (Hoch and Bandara, 2005; Martínez *et al.*, 2010). This clay mineral was widely used in paper manufacturing from the second half of the nineteenth century for both filling and coating (Beazley, 1991; Van der Reyden *et al.*, 1993). Its use made paper heavier, whiter and more receptive to ink.

3. 2. 4. 2. Inks

Most of the Raman analyses of the pigments used for the elaboration of the lithographs were unsuccessful due to the high fluorescence of the samples. Moreover, the contribution of the paper support while analysing the coloured regions was very strong, causing the hiding of the ink spectra. For the proper characterization of the colouring substances the subtraction of the spectrum of the paper support from the spectrum taken in the coloured areas had to be done. We could successfully enhance the spectrum of the ink over the signals from the paper matrixes in which they were held, obtaining the spectrum of the ink (**Fig. 3. 4**).

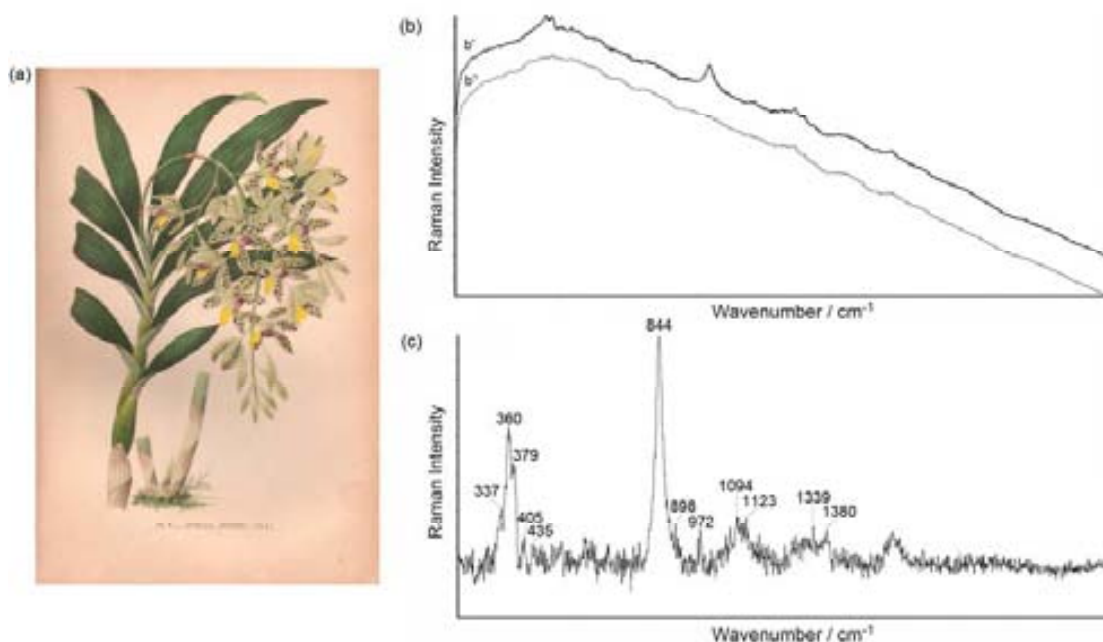


Fig. 3. 4 Subtraction process. (a) Picture of the analysed lithography (*PL V*); (b) Raman spectra of the yellow area –(b') and the paper support –(b''); (c) Raman spectrum of chrome yellow obtained after the subtraction process.

Yellow

This colour appears in four of the thirteen analysed lithographs (*PL. V* (**Fig. 3. 4 (b)**), *PL. VI*, *PL. VII*, and *PL. XXXVI*). The preliminary EDXRF analyses showed the presence of chromium and lead (see **Table 3. 1**) and the Raman results denoted that only one yellow pigment was used: chrome yellow, PbCrO_4 (**Fig. 3. 4 (b)**). The spectrum shows a strong band located at 844 cm^{-1} and a group of several peaks

centred at 360 cm^{-1} (337 , 360 , 380 and 405 cm^{-1}). Moreover, the lack of any sulphate peaks (especially the very narrow stretching peak at $\sim 1000\text{ cm}^{-1}$) demonstrates that pure lead chromate, with any addition of lead sulphate (such as in lead chromate sulphate – $\text{PbCrO}_4\cdot\text{PbSO}_4$) was used (Caggiani and Colomban, 2011). According to the literature, this pigment was introduced into the market in early 1800's (Eastaugh *et al.*, 2004). In fact, its use had already been reported in different kinds of works on paper support from the same chronology (Centeno *et al.*, 2006; Caggiani and Colomban, 2011). In addition, bands located at 379 , 898 , 972 , 1094 , 1123 , 1339 and 1380 cm^{-1} are due to cellulose from the background.

White

The EDXRF analyses performed on white areas (*PL. XXIV*, not shown) revealed the presence of calcium, iron, zinc, rubidium, strontium and lead, just the same elements found on the paper support (see **Table 3. 1**). In the same way, Raman analysis provided the spectrum of paper itself with the characteristic bands at 381 , 435 , 1056 , 1094 , 1121 and 1380 cm^{-1} due to cellulose. In these kinds of works on paper, the white colour is, in fact, the background paper support.

Orange

This colour appears in different tonalities (from deep orange to yellowish orange) in two of the analysed lithographs (*PL. I* and *PL. VII*). EDXRF analysis of *PL. I* revealed the presence of lead while the spectrum of *PL. VII* showed the presence of lead and chromium (see **Table 3. 1**). Raman analyses performed on deep orange areas of *PL. I* demonstrated the presence of red lead (Pb_3O_4). The Raman bands at 122 , 150 , 224 , 314 , 391 , 456 and 548 cm^{-1} observed in the spectrum (**Fig 3. 5 (a)**) would be due to the presence of this pigment. On the other hand, analyses carried out in the yellowish orange areas of *PL. VII* (not shown) revealed once again the presence of chrome yellow (Raman bands at 361 and 843 cm^{-1}). It seems that only a small amount of pigment was necessary to obtain the desired colour, so that the more pigment was used, the more deep it was.

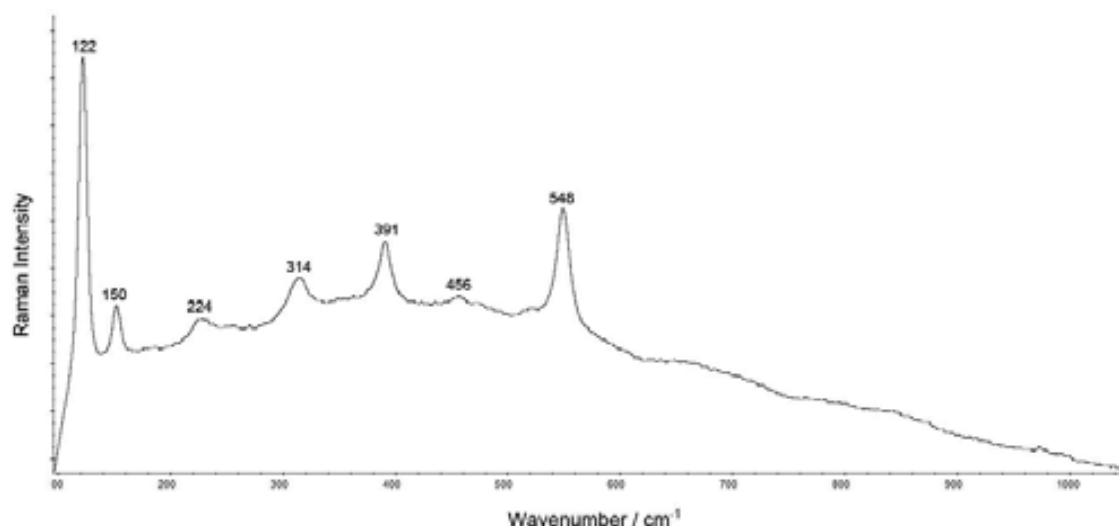


Fig. 3. 5 Raman spectrum of the orangey region on *PL. I*.

Pink, red and purple tonalities

Three reddish shades can be observed on the lithographs: pink (on *PL. XX*), deep red (on *PL. XXXVI*) and purple (on *PL. V*, *PL. VI*, *PL. VII* and *PL. XXVII*).

Concerning the pink shades, by analysing them using EDXRF the main element identified was lead (see **Table 3. 1**). In fact, by using RS red lead was determined. The use of FTIR spectroscopy was not conclusive neither for the use of an organic red compound nor for the use of red lead (because it presents IR bands below 500 cm^{-1} , while the range limit of the used FTIR spectroscopy apparatus is about 700 cm^{-1}).

Dealing with the deep red areas present in some of the lithographs, the only elements identified by EDXRF were iron and lead (see **Table 3. 1**). Besides, strong fluorescence appeared from them when analysed by RS and the subtraction process described previously did not allow a clear identification of the pigment responsible of the colour. According to the literature (Wehlte, 1995; Castro *et al.*, 2004) co-precipitation of organic pigments with white fillers was a frequent technique in the preparation of artists' materials (because these white compounds were used as substrate or mordant) thus, the presence of barite (BaSO_4), calcium carbonate (CaCO_3), calcium sulphate (CaSO_4) or gypsum ($\text{CaSO}_4 \cdot 2\text{H}_2\text{O}$) could suggest the possible presence of an organic pigment. However, none of these typical white fillers were determined either by Raman or by EDXRF spectroscopies.

FTIR analysis of deep red colour revealed the presence of bands at 1574, 1251, 1151, 1104, 1020 and 905 cm^{-1} (see **Fig. 3. 6**). Moreover, there is a group of bands centred around 2900 cm^{-1} whose positions were obtained after de decomposition of the spectrum in a sum of Gaussian curves at 2969, 2940, 2905 and 2866 cm^{-1} . All these bands belong to an organic compound, probably the pigment responsible of the deep red colour. Unfortunately, the closeness and the overlapping of the bands of the background cellulose with those of the pigment at 1151, 1104, 1020 and 905 cm^{-1} made it impossible to identify the pigment. However, the position of the bands are quite close to those of some lake pigments such as red alizarin (Clementi *et al.*, 2009) or even some kind of betalaine (natural organic pigments extracted from vegetables such as beetroot red and also used as natural pigments). This red organic pigment was also used in the purple colour mixed with Prussian blue (see below).

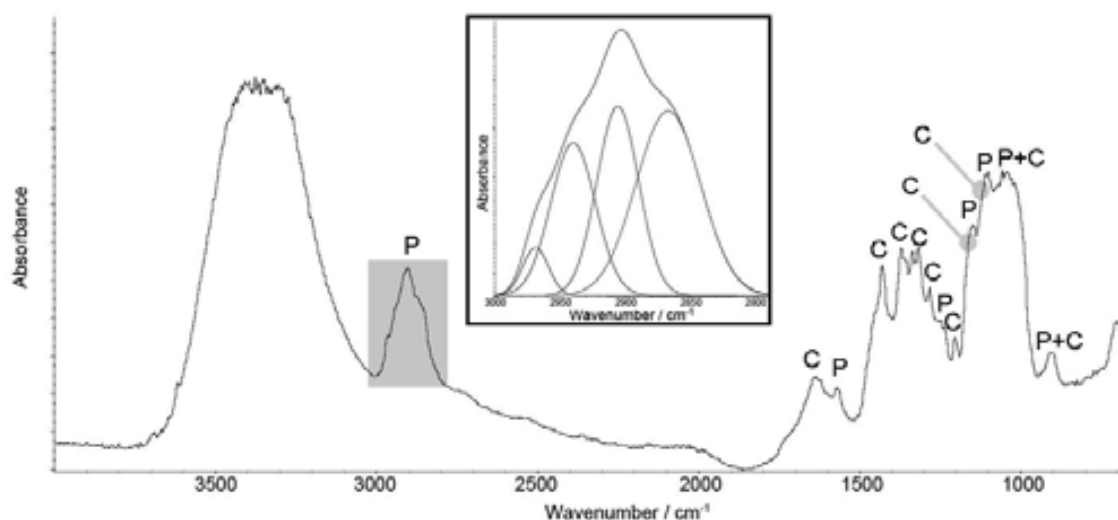


Fig. 3. 6 FTIR spectrum of deep-red colour on *PL. XXXVI*. In the box the decomposition of the spectral window 3000-2800 cm^{-1} . Key: P (Pigment) and C (Cellulose).

As happened with deep red colour, the EDXRF analyses of purple areas only determined the presence of iron. Again, a strong fluorescence occurred in these areas while analysing them with RS. Nevertheless, in this case, some bands were observed in the Raman spectrum due to the presence of Prussian blue (273, 534, 2091 and 2153 cm^{-1}). This finding was corroborated by FTIR analyses, where the typical band corresponding to the vibration of $\text{C}\equiv\text{N}$ (2095 cm^{-1}) was recorded in the spectrum. Additional FTIR bands were observed in the spectrum. These bands were located at

the same position as those of the deep red colour. Unfortunately, as with what happened with the red colour, it was not possible to attribute them to any compound neither to find out the red compound needed to obtain the purple colour.

Brown

The EDXRF analyses carried out on the brown-coloured areas detected the presence of chromium, iron, mercury and lead (see **Table 3. 1**). In this case, two complexes mixtures were identified by using RS. In *PL. XXIII*, for example, a mixture of chrome yellow (Raman band at 840 cm^{-1}), Prussian blue (Raman bands at 273, 531 and 2155 cm^{-1}), carbon black (C, broad bands centred at 1300 and 1600 cm^{-1}), red ochre (mainly Fe_2O_3 , Raman bands at 290 and 408 cm^{-1}) and vermilion (bands at 251, 290, 341 cm^{-1}) was determined (**Fig. 3. 7**).

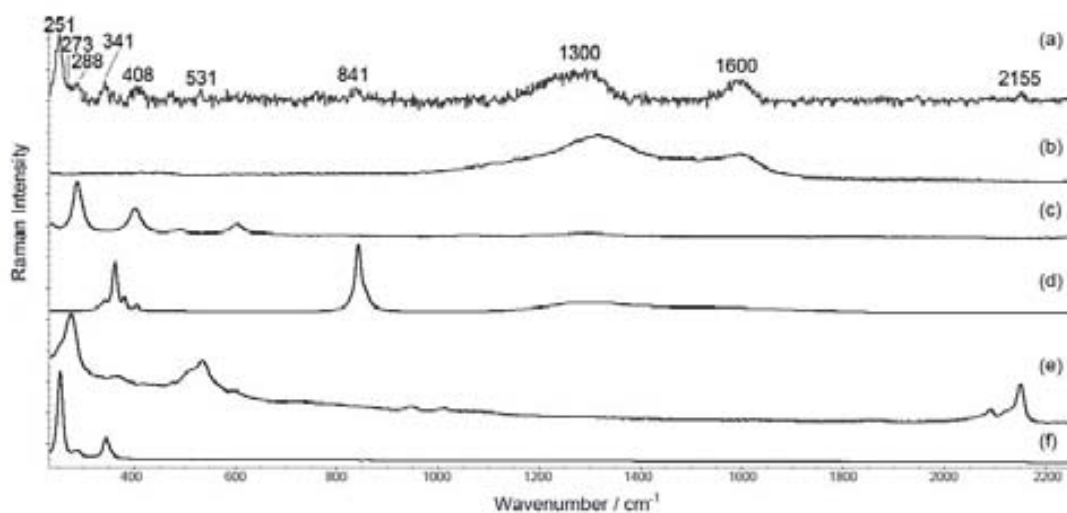


Fig. 3. 7 Raman spectrum of brown colour from the *PL. XXIII* and spectra of reference materials. Spectra of (a) *PL. XXIII* after the subtraction process and baseline correction; (b) carbon black; (c) red ochre; (d) chrome yellow; (e) Prussian blue and (f) vermilion.

On the other hand, in *PL. XLI* a combination of chrome yellow, Prussian blue, carbon black, red ochre and red lead (bands at 121 and 544 cm^{-1}) was identified (**Fig. 3. 8**).

There are literature reporting the use of complexes pigment mixtures in other artwork from the same chronology (Correia *et al.*, 2007; Caggiani and Colombari, 2011) but if we keep in mind the references on scientific analysis of works on paper, we can see

that few of them report the existence of these admixtures: Castro *et al.* (2005) identified burnt sienna (mainly Fe_2O_3), chrome yellow, carbon black, red lead and calcite mixed together on the brown areas of nineteenth century wallpaper from a tower-palace in Villanañe (Spain); Vandenabeele *et al.* (2008) detected a mixture of carbon black and hematite on porcelain cards from the nineteenth century and Sarmiento *et al.* (2010) found an admixture of calcite, Prussian blue, indigo blue ($\text{C}_{16}\text{H}_{10}\text{N}_2\text{O}_2$) and red ochre on Finnish wallpapers from the eighteenth to the nineteenth century.

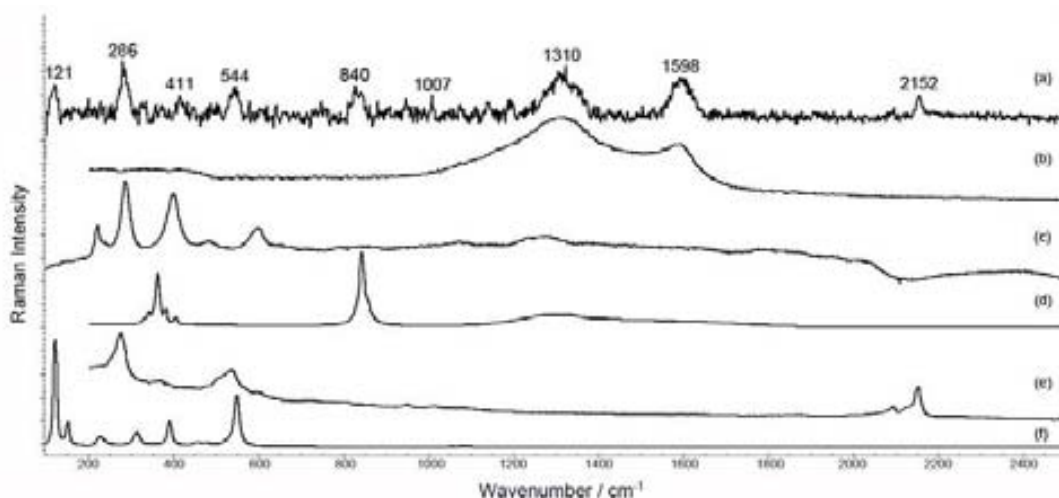


Fig. 3. 8 Raman spectrum of brown colour from the *PL. XLI* and spectra of reference materials. Spectra of (a) *PL. XLI* after the subtraction process and baseline correction; (b) lamp black; (c) red ochre; (d) chrome yellow; (e) Prussian blue and (f) red lead.

Blue

PL. XXIII, *PL. XXVII*, *PL. XXIX* and *PL. XXX* have blue colour in their palette. The presence of iron on the EDXRF spectra (see **Table 3.1**) was in agreement with the Raman analyses, which seemed to indicate the use of Prussian blue as the pigment responsible for this colour. The Raman bands at 280, 382, 535, 600, 2093 and 2155 cm^{-1} were observed in the spectrum (**Fig 3. 9**), with 2155 cm^{-1} being the most characteristic band (due to the $\nu(\text{CN})$ stretching vibration) of Prussian blue. This pigment was first synthesized in Berlin between 1704 and 1707 (Harley, 1982) but was not much used until the middle of eighteenth century.

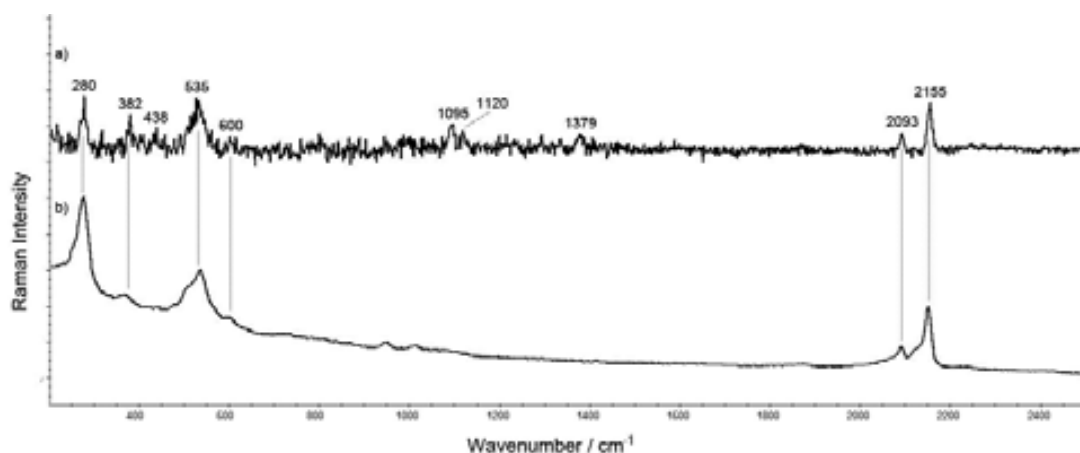


Fig. 3.9 Raman spectra of (a) blue colour from the *PL. XXX* (after subtraction process and baseline correction) and (b) Prussian blue.

Green

All of the analysed chromolithographs have greenish colourations in which three elements were identified by EDXRF: chromium, iron and lead (see **Table 3. 1**). According to the Raman and FTIR spectra collected from the green areas, we can say that instead of green pigments, mixtures of blue and yellow pigments were used. For example, the Raman spectrum from *PL. I* (**Fig. 3. 10**) contained the characteristics bands of Prussian blue (278, 541, 2091, 2123, 2151 cm^{-1}) with many bands of indigo blue (252, 541, 599, 679, 766, 1226, 1250, 1464, 1485, 1576, 1632 cm^{-1}), a natural pigment but first synthesized at 1870 and commercially produced in 1897 (Harley, 1982). In addition, bands at 1093 and 1378 cm^{-1} are due to cellulose. Unfortunately, in this case no yellow pigment could be clearly identified.

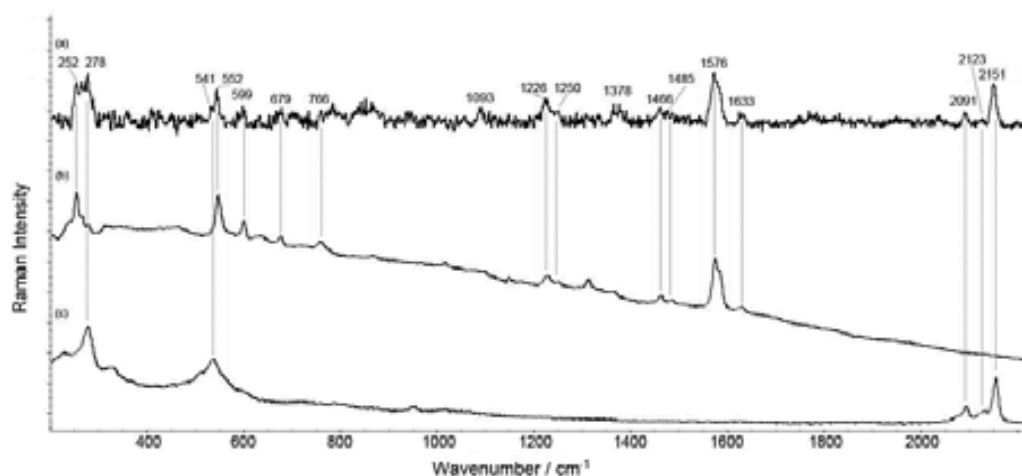


Fig. 3.10 (a) Raman spectrum of a green area on the lithograph *PL. I* (after subtraction process and baseline correction) and comparison with reference spectra from (b) indigo blue and (c) Prussian blue.

Another combination found in some lithographs is the mixture of chrome yellow (323, 341, 355, 379, 841 cm^{-1}) and Prussian blue (280, 372, 512, 536, 945, 2093, 2155 cm^{-1}) in the Raman spectrum of *PL. VII* (not shown). The combination of these pigments has already been reported in the literature (Wehlte, 1975; Chaplin *et al.*, 2004; Castro *et al.*, 2005; Vandenabeele *et al.*, 2008; Sarmiento *et al.*, 2010). This mixed green could be the one known as chrome green, a nineteenth century pigment synthesised through coprecipitation of Prussian blue and chrome yellow upon addition of barium white (Gettens and Stout, 1966). However, no indication of the presence of barium white was found in the chromolithograph with the techniques employed in the present study. Chrome green has been also used to describe the compound Cr_2O_3 . However, to describe this oxide, the term chrome oxide green should be used (Newman, 1997).

The FTIR spectrum of *PL. XIX* revealed the presence of an organic yellow compound mixed with Prussian blue. A representative spectrum is reported in **Fig. 3. 11**, where we can observe a characteristic band of Prussian blue at 2087 cm^{-1} and the bands at 2970, 2929, 1735, 1687, 1646 (shoulder), 1632, 1592, 1337, 1261 cm^{-1} , which are consistent with the vibrational modes of gamboge (Vandenabeele *et al.*, 2000). The peaks reported in **Fig. 3. 11** that may stem from the cellulose and kaolin are marked with an asterisk (at 2902, 1632, 1427, 1371, 1321, 1203, 1162 and 1062 cm^{-1}), and plus (at 1111, 1034 and 912 cm^{-1}) respectively.

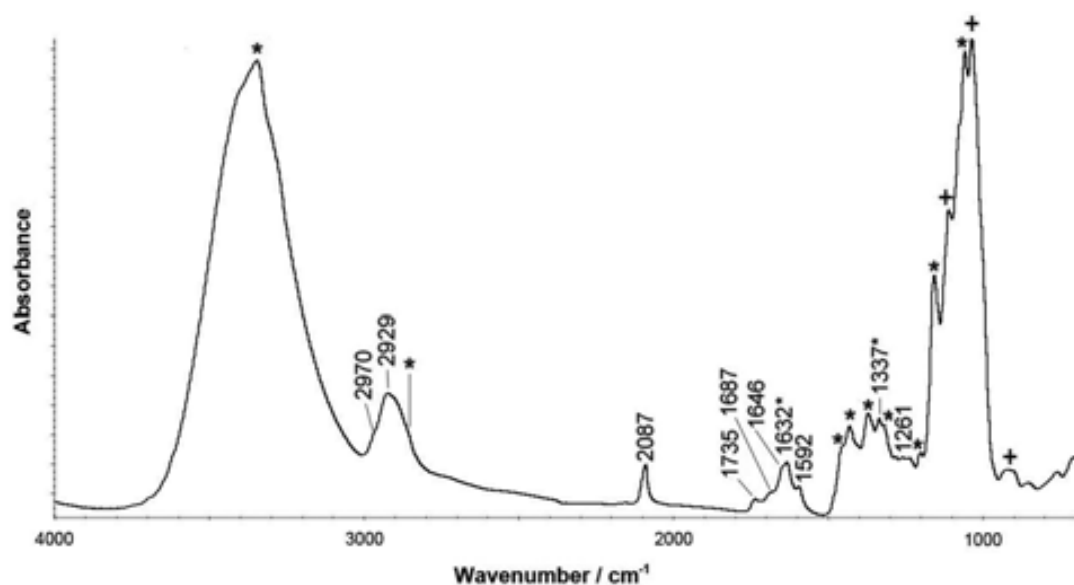


Fig. 3. 11 FTIR spectrum of the green colour in *PL. XIX*.

Gamboge is a yellow gum-resin of vegetable origin in which the chromophore responsible of the yellow colour resides in the resin component (Gettens and Stout, 1966; Striová *et al.*, 2009). The use of gamboge was common from the seventeenth century in Europe (Winter, 1997). In fact, in the nineteenth century the botanic artist William Hooker created a special pigment to yield a green tone suitable for colouring leaves (known as Hooker's green) by mixing Prussian blue and gamboge (Winter, 1997). The combination of blue and yellow colouring substances has been reported in studies of wallpapers by Castro *et al.* (2007) and in polychrome prints by Striová *et al.* (2009), both works on paper from the nineteenth-century.

Golden

Some of the lithographs (*PL. VII*) had gold-coloured details, which were also analysed by RS, but this study did not yield any ascribable spectrum. Like many metals gold is undetectable by RS (Burgio *et al.*, 2008) so that further investigations such as using EDXRF were necessary here. EDXRF analysis of golden areas on this lithograph revealed that gold and copper had indeed been used. The presence of chromium and lead is due to the chrome yellow underneath (which was determined by RS). A spectrum and an image of one of the analysed spots are shown in **Fig. 3. 12**.

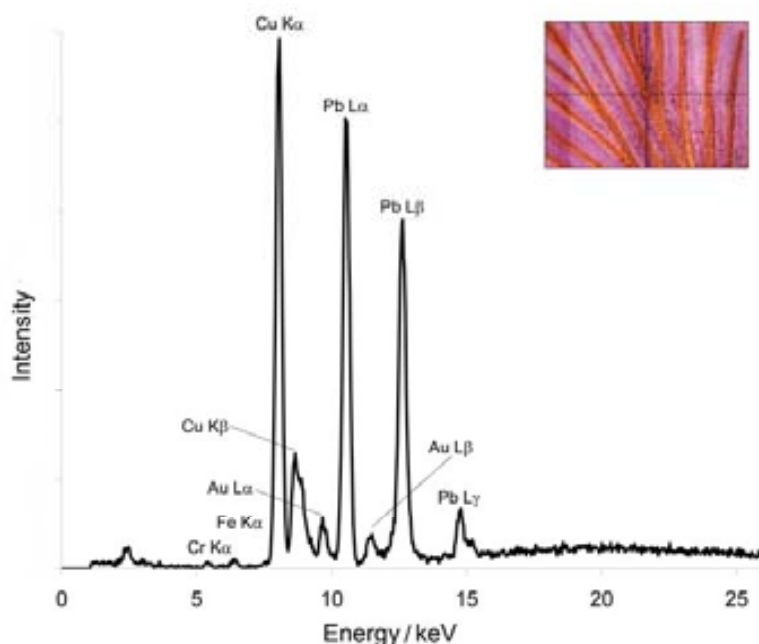


Fig. 3. 12 EDXRF spectrum of the golden regions on *PL. VII*.

3. 2. 5. Conclusions

This chapter presents the chemical characterization of a set of thirteen chromolithographs from the nineteenth century in which the necessity of a multi-analytical approach for the proper characterization of such kind of works on paper is demonstrated.

By using RS, it was possible to determine almost all the inorganic pigments present in the chromolithographs, but it was impossible to identify the metallic pigments nor the binding medium (mainly due to fluorescence problems). In this sense, EDXRF complemented the analysis of the pigments and other elements related to the paper matrix and reflectance FTIR spectroscopy proved to be indispensable in studying the paper support and other organic compounds present in the lithographs.

This work also presented a successful methodology for the determination of inks on paper when Raman analyses of the pigments are frustrated due to the high fluorescence of the samples. In this sense, ink spectra can be enhanced by subtracting the spectra from the paper support from the spectra taken in the coloured areas.

Concerning the analysed book, the study showed that notwithstanding the lithograph's palette is extensive, the range of substances used for its elaboration was relatively limited. In fact, it has to be highlighted that to obtain some of the colours observed in the chromolithographs, the use of some complexes and unusual admixtures of primary pigments were identified.

From the eighteenth century until the end of the nineteenth century pigment industry suffered important innovations, being a period of time in which new inorganic pigments such as Hooker's Green, chrome yellow or chrome green, amongst others, became available into the market. While a few inorganic pigments were introduced during this period, the main development was the invention of synthetic organic pigments after 1856 that lead to the introduction of more than a hundred new pigments and many more dyes that revolutionized not only the printing industry, but also the textile and others. Some organic pigments were determined in the analysed samples. Thus, the analysed lithographs not only evidence the technical developments in colour illustration that took place during that period but also reflect how the industry was incorporating new materials in their work and designs.

3.3. References

- BEAZLEY K. (1991) *Mineral fillers in paper*. *The Paper Conservator*, 15, 17-27.
- BELL I. M., CLARK R.J.H., GIBBS P.J. (1997) *Raman spectroscopic library of natural and synthetic pigments (pre ~ 1850 AD)*. *Spectrochimica Acta Part A: Molecular and Biomolecular Spectroscopy*, 53 (2), 159-2179.
- BELL S.E.J., BOURGUIGNON E.S.O., DENNIS A.C., FIELDS J.A., MCGARVEY J.J., SEDDON K.R. (2000) *Identification of Dyes on Ancient Chinese Paper Samples Using the Subtracted Shifted Raman Spectroscopy Method*. *Analytical Chemistry*, 72, 234-239.
- BOILEAU C., PESSANHA S., TARDIF C., CASTRO K., PROIETTI N., CAPITANI D., VICINI S., MADARIAGA J.M., CARVALHO M.L., PRINCI E. (2009) *Efficacy of waterborne polyurethane to prevent the enzymatic attack on paper-based materials*. *Journal of Applied Polymer Science*, 113, 2030–2040.
- BURGIO L., CLARK R.J.H. (2001) *Library of FT-Raman spectra of pigments, minerals, pigment media and varnishes, a supplement to existing library of Raman spectra of pigments with visible excitation*. *Spectrochimica Acta Part A: Molecular and Biomolecular Spectroscopy*, 57, 1491–1521.
- BURGIO L., CLARK R.J.H., MURALHA V.S.F., STANLEY T. J. (2008) *Pigment analysis by Raman microscopy of the non-figurative illumination in 16th to 18th century Islamic manuscripts*. *Journal of Raman Spectroscopy*, 39, 1482-1493.
- CAGGIANI M.C., COLOMBAN P. (2011) *Testing of Raman spectroscopy as a non-invasive tool for the investigation of glass-protected pastels*. *Journal of Raman Spectroscopy* 42, 790–798.
- CASTRO K., VANDENABEELE P., RODRÍGUEZ-LASO M. D., MOENS L., MADARIAGA J. M. (2004) *Micro-Raman analysis of coloured lithographs*. *Analytical and Bioanalytical Chemistry*, 379, 674–683.
- CASTRO K., VANDENABEELE P., RODRÍGUEZ-LASO M.D., MOENS L., MADARIAGA J.M. (2005) *Improvements in the wallpaper industry during the second*

half of the 19th century: Micro-Raman spectroscopy analysis of pigmented wallpapers. Spectrochimica Acta A: Molecular and Biomolecular Spectroscopy, 61(10), 2357-2363.

CASTRO K., SARMIENTO A., PRINCI E., PÉREZ-ALONSO M., RODRÍGUEZ-LASO M.D., VICINI S., MADARIAGA J.M., PEDEMONTE E. (2007) *Vibrational spectroscopy at the service of industrial archaeology: Nineteenth-century wallpaper.* Trends in Analytical Chemistry, 26, 347–359.

CASTRO K., PESSANHA S., PROIETTI N., PRINCI E., CAPITANI D., CARVALHO M.L., MADARIAGA J.M. (2008) (a) *Noninvasive and nondestructive NMR, Raman and XRF analysis of a Blaeu coloured map from the seventeenth century.* Analytical and Bioanalytical Chemistry, 391, 433-441.

CASTRO K., PROIETTI N., PRINCI E., PESSANHA S., CARVALHO M.L., VICINI S., CAPITANI D., MADARIAGA J.M. (2008) (b) *Analysis of a coloured Dutch map from the eighteenth century: The need for a multi-analytical spectroscopic approach using portable instrumentation.* Analytica Chimica Acta, 623, 187-194.

CASTRO K., PRINCI E., PROIETTI N., MANSO M., CAPITANI D., VICINI S., MADARIAGA J.M., CARVALHO M.L. (2011) *Assessment of the weathering effects on cellulose based materials through a multianalytical approach.* Nuclear Instruments and Methods in Physics Research, Section B: Beam Interactions with Materials and Atoms, 269 (12), 1401-1410.

CENTENO S.A., BUISAN V.L., ROPRET P. (2006) *Raman study of synthetic organic pigments and dyes in early lithographic inks (1890–1920).* Journal of Raman Spectroscopy, 37, 1111-1118.

CHAPLIN T.D., JURADO-LÓPEZ A., CLARK R.J.H., BEECH D.R. (2004) *Identification by Raman microscopy of pigments on early postage stamps: distinction between original 1847 and 1858–1862, forged and reproduction postage stamps of Mauritius.* Journal of Raman Spectroscopy, 35, 600-604.

CLEMENTI C., DOHERTY B., GENTILI P.L., MILIANI C., ROMANI A., BRUNETTI B.G., SGAMELLOTTI A. (2008) *Vibrational and electronic properties of painting lakes.* Applied Physics A: Materials Science and Processing, 92, 25–33.

COLOMBAN P. (2011) *Pigment identification of a rare 18th century wallpaper from Buffon library*. Journal of Raman Spectroscopy, 42, 192-194.

CORREIA A.M., CLARK R.J.H., RIBEIRO M.I.M., DUARTE M.L.T.S. (2007) *Pigment study by Raman microscopy of 23 paintings by the Portuguese artist Henrique Pousao (1859–1884)*. Journal of Raman Spectroscopy, 38, 1390-1405.

DONCEA S.M., ION R.M., FIERACUI R.C., BACALUM E., BUNACIU A. A., ABUL-ENEIN H.Y. (2010) *Spectral methods for historical paper analysis: Composition and age approximation*. Instrumentation Science and Technology, 38, 96-100.

DURAN A., PÉREZ-RODRÍGUEZ J.L., ESPEJO T., FRANQUELO M.L., CASTAING J., WALTER P. (2009) *Characterization of illuminated manuscripts by laboratory-made portable XRD and micro-XRD systems*. Analytical and Bioanalytical Chemistry, 395, 1997-2004.

EASTAUGH N., WALSH V., CHAPLIN T., SIDDAL R. (2004) *Pigment Compendium, a dictionary of historical pigments*. Elsevier Butterworth - Henemann, Oxford.

EDWARDS H.G.M., CHALMERS J.H. (2005) *Practical Raman Spectroscopy and Complementary Techniques*, in: BARNETT N.W. (Ed.) *Raman Spectroscopy in Archaeology and Art History*, The Royal Society of Chemistry, Cambridge, 41–67.

FERRER N., VILA A. (2006) *Fourier transform infrared spectroscopy applied to ink characterization of one-penny postage stamps printed 1841-1880*. Analytica Chimica Acta, 555, 161-166.

FERRERO J.L., ROLD C., JUANES D., CARBALLO J., PEREIRA J., ARDID M., LLUCH J.L., VIVES R. (2004) *Study of inks on paper engravings using portable EDXRF spectrometry*. Nuclear Instruments and Methods in Physics Research B: Beam Interactions with Materials and Atoms, 213, 729–734.

FRAUSTO-REYES C., ORTIZ-MORALES M., BUJDUD-PÉREZ J.M., MAGAÑA-COTA G.E., MEJÍA-FALCÓN R. (2009) *Raman spectroscopy for the identification of pigments and color measurement in Dugès watercolors*. Spectrochimica Acta Part A: Molecular and Biomolecular Spectroscopy, 74, 1275-1279.

GANZERLA R., GAMBARO A., CAPPELLETTO E., FANTIN M, MONTALBANI S., ORLANDI M. (2009) *Characterization of selected paper documents from the archives of Palazzo Ducale (Venice), Italy using various analytical techniques*. *Microchemical Journal*, 91, 70-77.

GETTENS R.J., STOUT G.L. (1966) *Painting Materials: a Short Encyclopaedia*. Courier Dover Publications, New York.

HAHN O., OLTROGGE D., BEVERS H. (2004) *Coloured prints of the 16th century: non-destructive analyses on coloured engravings from Albrecht Dürer and contemporary artists*. *Archaeometry*, 46, 273–282.

HANSON V.F. (1981) *Determination of the trace elements in paper by Energy Dispersive X-ray Fluorescence*, in: WILLIAMS J.C. (Ed.) *Advances in Chemistry Series*, American Chemical Society, Washington D.C., 53-78.

HARLEY R.D. (1982) *Artist's pigments c. 1600-1835: a study in English documentary sources*, Butterworth Scientific, London.

HOCH M., BANDARA A. (2005) *Determination of the adsorption process of tributyltin (TBT) and monobutyltin (MBT) onto kaolinite surface using Fourier transform infrared (FTIR) spectroscopy*. *Colloids and Surfaces A: Physicochemical and Engineering Aspects*, 253, 117–124.

LAGUARDIA L., VASSALLO E., CAPPITELLI F., MESTO E., CREMONA A., C. SORLINI, BONIZZONI G. (2005) *Investigation of the effects of plasma treatments on biodeteriorated ancient paper*. *Applied Surface Science*, 252 (4), 1159-1166.

MANSO M., COSTA M., CARVALHO M.L. (2008) *X-ray fluorescence spectrometry on paper characterization: A case study on XVIII and XIX century documents*. *Spectrochimica Acta Part B: Atomic Spectroscopy*, 63, 1320–1323

MANSO M., CARVALHO M.L. (2009) *Application of spectroscopic techniques for the study paper documents: A Survey*. *Spectrochimica Acta Part B: Atomic Spectroscopy*, 64 (6), 482-490.

MANSO M., PESSANHA S., FIGUEIRA F., VALADAS S., GUILHERME A., ALFONSO M., ROCHA A.C., OLIVEIRA M.J., RIBEIRO I., CARVALHO M.L. (2009) *Characterisation of foxing stains in eighteenth to nineteenth century drawings using non-destructive techniques*. *Analytical and Bioanalytical Chemistry*, 395 (7), 2029-2036.

MARCOLLI C, WIEDEMANN HG (2001) *Distinction of original and forged lithographs by means of thermogravimetry and Raman spectroscopy*. *Journal of Thermal Analysis and Calorimetry*, 64, 987–1000.

MARTINEZ R.E., SHARMA P., KAPPLER A. (2010) *Surface binding site analysis of Ca²⁺-homoionized clay–humic acid complexes*. *Journal of Colloid and Interface Science*, 352 (2), 526-534.

NEWMAN R. (1997) *Chromium Oxide Greens: Chromium Oxide and Hydrated Chromium Oxide*, in: FITZHUGH E.W. (Ed.) *Artists's Pigments: A Handbook of Their History and Characteristics: vol. 3*, Oxford University Press, Washington, 273-294.

PESSANHA S., GUILHERME A., CARVALHO M.L., CABAÇO M.I., BITTENCOURT K., BRUNEEL J.L., BESNARD M. (2009) *Study of a XVIII century hand-painted Chinese wallpaper by multianalytical non-destructive techniques*. *Spectrochimica Acta Part B: Atomic Spectroscopy*, 64, 582-586.

PESSANHA S., CARVALHO M.L., CABAÇO M.I., VALADAS S., BRUNEEL J-L., BESNARD M., RIBEIRO M.I. (2010) *Characterization of two pairs of 16th century Nanbam folding screens by Raman, EDXRF and FTIR spectroscopies*. *Journal of Raman Spectroscopy*, 41, 1510-1516.

REYNARD P. (1989) *Early European papermaking methods 1400–1800*. *The Paper Conservator*, 13, 7–27.

SARMIENTO A., KNUUTINEN U., CASTRO K., MADARIAGA J.M. (2010) *Finnish wallpaper pigments in the XVIII-XIX century: Comparison with those used in Western Europe*. *Proceedings of Interim Meeting of the ICOM-CC Graphic Documents Working Group*, Copenhagen, 6-8 October 2010.

SENEFELDER A. (1911) *The invention of lithography. Translated from the original German by J.W. Muller*. New York: The Fuchs & Lang Manufacturing Company.

SMITH G.D., CLARK R.J.H. (2004) *Raman microscopy in archaeological science*. Journal of Archaeological Science, 31, 1137-1160.

STRIOVÁ J., COCCOLINI G., MICHELI S., LOFRUMENTO C., GALEOTTI M., CAGNINI A., CASTELLUCCI E.M. (2009) *Non-destructive and non-invasive analyses shed light on the realization technique of ancient polychrome prints*. Spectrochimica Acta Part A: Molecular and Biomolecular Spectroscopy, 73, 539–545.

VAN DER REYDEN D., MOSIER E., BAKER M. (1993) *Pigment-coated papers I & II: history and technology*, in: Triennial meeting (10th), Washington DC, 22-27 August 1993: preprints / Paris: ICOM

VANDENABEELE P., WEHLING B., MOENS L., EDWARDS H., DEREU M., VANHOOYDONK G. (2000) *Analysis with micro-Raman spectroscopy of natural organic binding media and varnishes used in art*. Analytica Chimica Acta, 407, 261–274.

VANDENABEELE P., DE PAEPE P., MOENS L. (2008) *Study of the 19th century porcelain cards with direct Raman analysis*. Journal of Raman Spectroscopy, 39, 1099-1103.

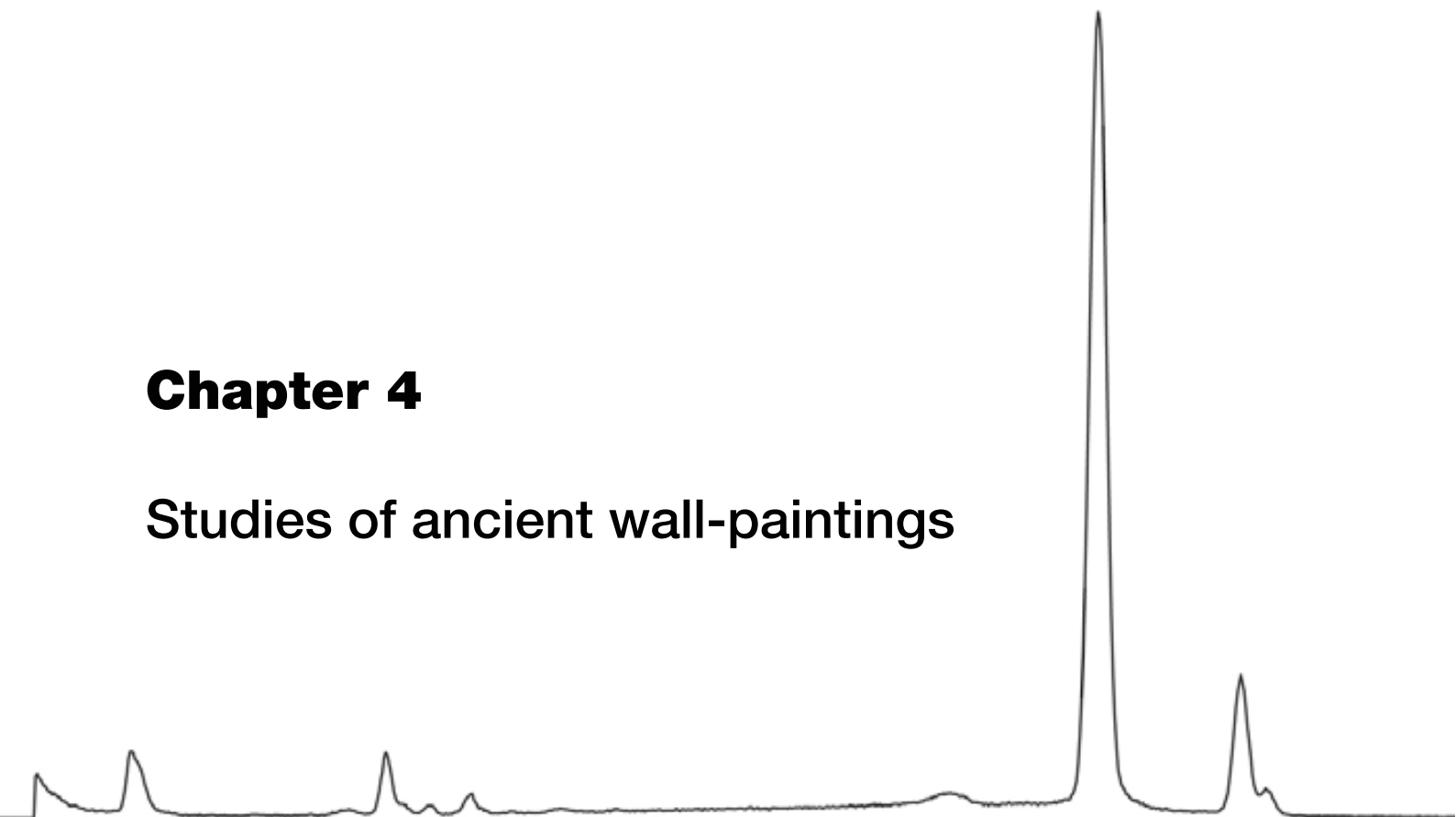
WEHLTE K. (1975) *The materials and techniques of painting*. Van Nostrand Reinhold Company, Englad.

WIEDEMANN H.G. (2001) *Mit Thermogravimetrie und Raman-Spektroskopie. Dem Fälscher auf der Spur*. Chemie in Unserer Zeit, 35, 368–381.

WINTER J. (1997) *Gamboge*, in: FITZHUGH E.W. (Ed.) *Artists' Pigments: a Handbook of Their History and Characteristics: Volume 3*, Oxford University Press, Washington, 143–155.

Chapter 4

Studies of ancient wall-paintings



Part of the contents of this chapter is published in:

PITARCH A., QUERALT I., ÁLVAREZ A., GUITART J. (2010) *Pinturas murales de la ciudad romana de Iesso: resultados preliminares de la caracterización de los pigmentos mediante técnicas no destructivas*, in: SAIZ M.E., LÓPEZ R., CANO M.A., CALVO J.C. (Eds.) *Actas VIII Congreso Ibérico de Arqueometría, Teruel, 19-21 de Octubre de 2009*. Edited by: Seminario de Arqueología y Etnología Turolense, Teruel, 2010, 327-336.

4. 1. Introduction

The archaeometric study of wall paintings allows to obtain information not only related to the nature of the employed pigments (from natural origin or synthetic, organic or inorganic), and their possible origin (from local origin or imported), but also to characterize the supporting materials, to describe the quality of the stuccoes, to study the technological features involved in the manufacturing processes of mortars and to determine whether they follow or not the preparation procedure described by classical authors such as Pliny or Vitruvius. The available publications from the last years concerning the analytical characterization on mural paintings from the whole Roman Empire is numerous (Mazzocchin *et al.*, 2004; Villar *et al.*, 2004; Dooryhée *et al.*, 2005; Paternoster *et al.*, 2005; Cotte *et al.*, 2006; Edwards *et al.*, 2006; Bragantini, 2007; Duran *et al.*, 2007, Mazzocchin *et al.*, 2007 (a), (b); Mazzocchin *et al.*, 2008, Aliatis *et al.*, 2009; Aliatis *et al.*, 2010; Duran *et al.*, 2010 (a), (b); Maguregui *et al.*, 2010; Mazzocchin *et al.*, 2010; Maguregui *et al.*, 2011 (a), (b); Moretto *et al.*, 2011; Piovesan *et al.*, 2011), however, the scientific literature reporting the analysis of wall paintings from the Iberian Peninsula by means of both spectroscopic and optical techniques is scarce (Domínguez Bella, 2003; Edreira *et al.*, 2004; Rodríguez and Fernández, 2005; Salvadó *et al.*, 2005; Villar and Edwards, 2005; Villar *et al.*, 2005; Duran *et al.*, 2011). This work comprises the combination of energy dispersive X-ray fluorescence (EDXRF), X-ray diffraction (XRD), Fourier transform infrared spectroscopy (FTIR), polarizing light microscopy (PLM) and scanning electron microscopy equipped with energy dispersive X-ray analysis system (SEM-EDS) techniques for the study of pigments and plasters from the Roman wall paintings of the city of *Iesso* (nowadays Guissona, Catalonia, NE of Spain) in order to gain knowledge about the characterization and definition of techniques and materials used in that city, and contribute, from the analytical point of view, to enlarge the knowledge and assessing the main features of the Roman architecture in Catalonia.

4. 2. Characterization of decorated stuccoes from the Roman city of *Iesso* (current Guissona, La Segarra, central Catalonia, NE of Spain).

4. 2. 1. Historical context

The Roman city of *Iesso* was one of the first founded cities within an extensive program of the *Hispania Citerior* colonization (current Catalonia) that the Romans carried out between the 2nd and the 1st century AD (Guitart 2006, 2010).

The first studies about the city date back to the 30's, when the "Institut d'Estudis Catalans" (IEC) began the excavations under the direction of Josep Colomines. In 1995 the archaeological site was declared National Cultural Heritage Site ("Bé cultural d'interès nacional") by the Catalonia's Government (Generalitat de Catalunya). In 2011 the musealization of the Archaeological Park and the construction of the Interpretation Center of the Roman city of *Iesso* were opened.

Despite the fact that our knowledge of this city is still much less mature, archaeologists have begun to document elements of great interest in the northern zone of the city, such as the remains of several modest houses (built during the first half of the 1st century BC), the remains of a large *domus*¹ (built in the imperial period), and the vestiges of public baths (Guitart, 2010). The discovery of some decorated wall paintings from the *domus* rooms was of extraordinary importance and prompted the interest of studying for the first time the pigments and the techniques employed by the Roman artists in that city². The decorated stuccoes were recovered throughout the excavation campaigns carried out between 1996 and 1999 and represent both geometric and floral motifs following the Pompeian second style (Cortés, 2009). According to Cortés (2009), the accuracy of the stroke (which is quite modest), the employed colours and the fact that these paintings are almost identical to those found in the nearby village of "Els Vilassos" (Tarroja, La Segarra) suggest that this is probably the work of a local artist or workshop. Some of these paintings (now restored) remain at the Eduard Camps Museum of Guissona (Guissona, La Segarra)

¹ The *domus* was the type of house occupied by the upper classes during the Republican and Imperial eras (Häuber, 1998).

² The study was supported by the research programme "Ajuts a projectes d'abast local o comarcal" of the "Comissionat per a Universitats i Recerca del DIUE de la Generalitat de Catalunya" (ref. 2009-ACOM-00017).

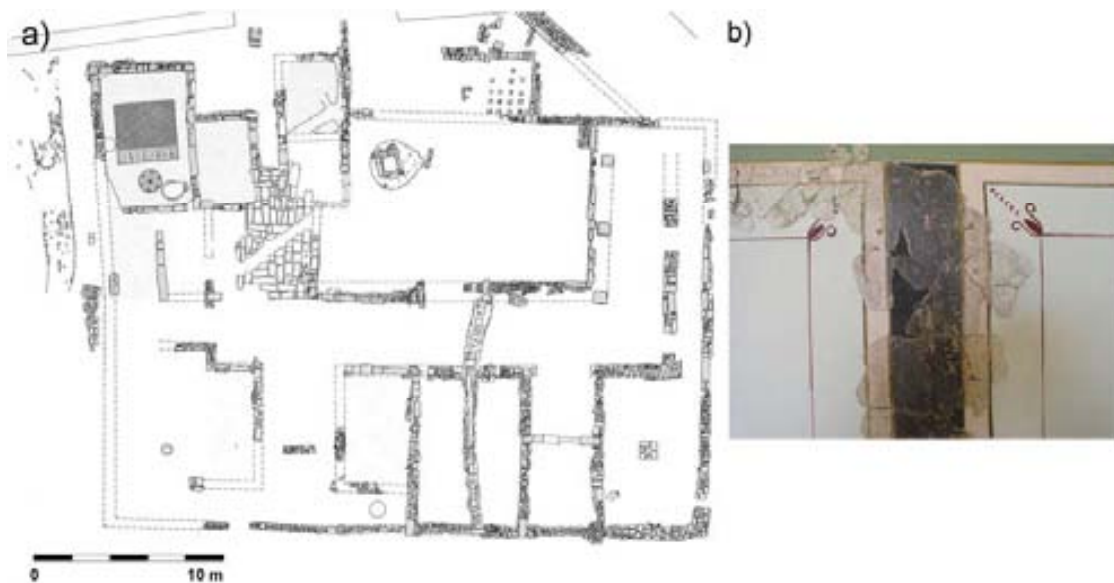


Fig. 4. 1 (a) Layout of the archaeological remains of the *domus* documented in the Roman city of *Iesso* (image provided by J. Guitart and J. Puche); (b) image of one of the restored wall-paintings (photography: J. Guitart).

4. 2. 2. Research aims

As part of a broader study of the remains of the settlement, the present work aims to supply for the first time a complete multi-analytical approach of the mural paintings from this Roman city in order to answer some of the following questions: *What evidence is there of the selection of local or imported pigments? Is there any proof for a local technology of pigment or supporting material preparation?* The study of these samples will provide, then, complementary information useful for further historical explanations.

4. 2. 3. Materials and methods

4. 2. 3. 1. Specimen

A total of 16 stuccoes (**Fig. 4. 2**) related with the remains of some wall paintings from the manor house rooms were analysed. The phase of building of the *domus*, from which the samples are derived, is dated as 2nd century AD. All the specimens were presented as fragments, which afforded the opportunity to examine: (a) the type of pigments employed (painted layer) and (b) characterize the supporting material (plasters and mortars). Generally, its colour palette could be described as limited and

consisted of red, ochre, white, green and black (all of them varying from pale shades through to deep shades). Sampling procedure was done with the advising of both the Excavation Chiefs and the Technical Department of Restoration of the settlement, taking into account the whole range of shades. The samples were collected from debris and floor filling material.

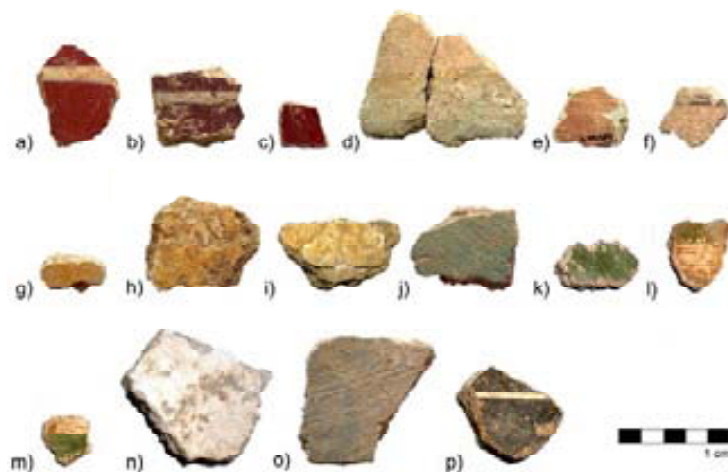


Fig. 4. 2 Samples from the *Iesso* Manor House (photography: A. Pitarch).

4. 2. 3. 2. Analytical methods

Elemental analysis of painted layers was obtained by using the EDXRF spectrometer (XDV-SD® model). The experimental conditions were as follows: potential of 50 kV, anode current of 173 μ A, collimator of 1 mm, aluminium filter of 1000 μ m in thickness and 200 s of effective counting time. For the crystalline phase analysis of the pictorial artwork and the mineralogical composition of the mortars, fine powder of the samples were analysed with the D8 Advance Bruker diffractometer. FTIR spectrometry was punctually used, in previously prepared samples, to solve some of the questions related to the nature of some pigments by using a JASCO 6000 Series FTIR spectrometer (Japan). To prepare the samples, 0.2-0.5 mg of each colour sample was grind and then mixed homogeneously with 150 mg of anhydrous KBr (IR grade, Merck, Germany) in an agate mortar. The powdered mixture was then pressed by 7 tone hydraulic press in order to obtain a translucent pellet of 13 mm in diameter. Finally, morphological observations of specially prepared thin cross sections (30 μ m thick) of the samples were carried out by using a polarizing light microscope (NICON Eclipse E400 POL), while the stratigraphic sequence of these polished cross sections, previously coated with C, was performed through a JEOL JSM-6300 scanning electron microscope. The main features of the equipments described in section I.5.

4. 2. 4. Results and discussion

4. 2. 4. 1. Analysis of pictorial surfaces: characterization of mineral pigments.

The main spectroscopic features relating to the chemistry of the wallpaintings are summarized in **Table 4. 1**.

Reference	Ref. Arch. Site	Colour	By FTIR		By XRD		By EDXRF*				By SEM-EDS	
			Compounds	Mineral phases	Ca K α	Fe K α	Pb L α	Sr K α	Elements			
/ESSO-a	G97-JE148	brick red	cal + hem + qtz	alb + alc. feld + dol + cal + hem + qtz	3.61	11.01	0.15	1.79	-			
/ESSO-b	G97-JE148	deep red	cal + hem + qtz	cal + hem + qtz	2.86	44.08	3.16	1.76	-			
/ESSO-c	G96-JE58	deep red	cal + hem + qtz	cal + hem + qtz	2.73	33.74	0.32	0.80	-			
/ESSO-d	H13-GROUP4	pale pink	cal + hem + qtz	cal + dol + qtz	4.47	0.58	9.23	2.30	-			
/ESSO-e	G99-JE584	pink	cal	cal + dol + qtz	5.56	0.66	0.39	1.91	-			
/ESSO-f	H13	pink	cal	cal + dol + qtz	3.89	0.84	7.91	2.14	-			
/ESSO-g	G97-JE197	mustard-coloured	cal	cal + goe + qtz	6.73	2.86	0.26	2.20	-			
/ESSO-h	G-JE128	mustard-coloured	cal + qtz	cal + dol + goe + gyp + qtz	5.05	1.64	0.25	1.63	-			
/ESSO-i	H13-c	yellow	cal + goe + qtz	cal + qtz	7.08	1.88	0.10	1.82	-			
/ESSO-j	G97-JE112	green	cal + cel + qtz	alb + cal + gyp + kao + mic + qtz	4.79	2.70	-	2.61	Mg + Al + Si + K + Fe			
/ESSO-k	G96-C12	dark green	cal + cel + qtz	-	4.14	3.96	-	2.93	Mg + Al + Si + K + Fe			
/ESSO-l	G-JE1D-C8	green	cal + cel + qtz	cal + qtz	3.39	3.63	-	1.29	Mg + Al + Si + K + Fe			
/ESSO-m	G97-JE116	green	cal + cel + qtz	cal + qtz	3.96	3.85	-	1.39	Mg + Al + Si + K + Fe			
/ESSO-n	H13-e	white	cal	cal	6.94	0.19	-	1.45	-			
/ESSO-o	H13	grey	cal	cal	6.05	0.44	0.77	3.35	-			
/ESSO-p	G-JE128	black	cal + qtz	cal	5.97	0.48	-	2.39	-			

Mineral key: alb: albite; alc.feld: alcaii feldspar; cal: calcite; goe: goethite; gyp: gypsum; kao: kaolinite; hem: hematites; mic: mica; qtz: quartz.
* Intensities of various specific spectral lines from the stuccoes. Reported values are the averaged intensity (counts per second) of the characteristic X-ray emission lines.

Red shades

The red palette comprises shades varying from pale pink to deep red (**Fig. 4. 2**, *IESSO-a to -f*). EDXRF spectra of the reddish samples (see **Table 4. 1**) revealed the presence of calcium, iron and strontium. Additionally, the presence of lead was detected on samples *IESSO-d* and *IESSO-f*. Representative EDXRF spectra from these samples are presented in **Fig. 4. 3**.

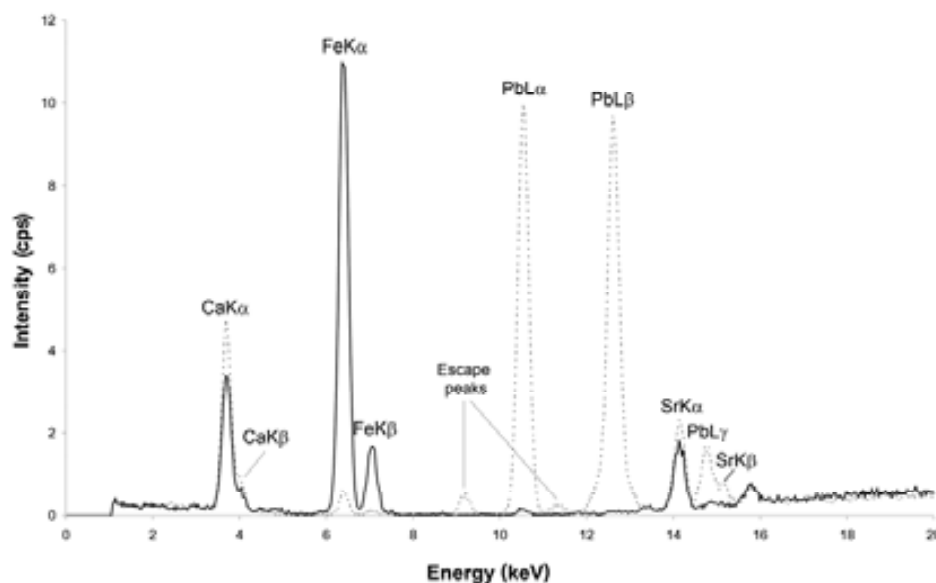


Fig. 4. 3 EDXRF spectra of samples *IESSO-a* (solid line) and *IESSO-d* (dotted line) where we can clearly appreciate Fe and Pb peaks corresponding to the reddish areas and peaks of Ca and Sr corresponding to the preparation layers.

XRD analysis of the samples *IESSO-a*, *IESSO-b* (**Fig. 4. 4** - solid line) and *IESSO-c* confirmed that the presence of Ca and Fe peaks on the EDXRF spectra correspond to calcite (CaCO_3) and hematite (Fe_2O_3) respectively. Sr is linked with Ca, since it is usually present in the calcite crystalline lattice. Likewise, the diffractograms revealed the presence of alkali feldspars (albite - $\text{NaAlSi}_3\text{O}_8$, orthoclase - KAlSi_3O_8) and quartz (SiO_2). These minerals belong to the aggregates from which the mortar was elaborated (a mixture of sand and calcite). FTIR analyses also confirmed the presence of hematite in these samples, as well as corroborated the presence of calcite and quartz, providing the characterization of the substrate. Hematite or *rubrica*, a naturally occurring iron (III) oxide, was one of the more widely used pigments, probably due to its availability, high colouring capacities and stability under a variety of weather conditions (Genestar and Pons, 2005; Rapp, 2009). On the other hand, XRD analysis of the fragments *IESSO-d*,

-e and -f (**Fig. 4. 4** – dotted line) only revealed the presence of calcite, dolomite and silicates coming from the aggregates. None of these mineral species are responsible of the pinkish colours; nevertheless, taking into consideration the high colouring capacities of hematite, only a small amount of pigment, undetectable from XRD analysis, was necessary to obtain the pink shade. Indeed, FTIR analysis of samples *IESSO-d*, and -f revealed the presence of hematite.

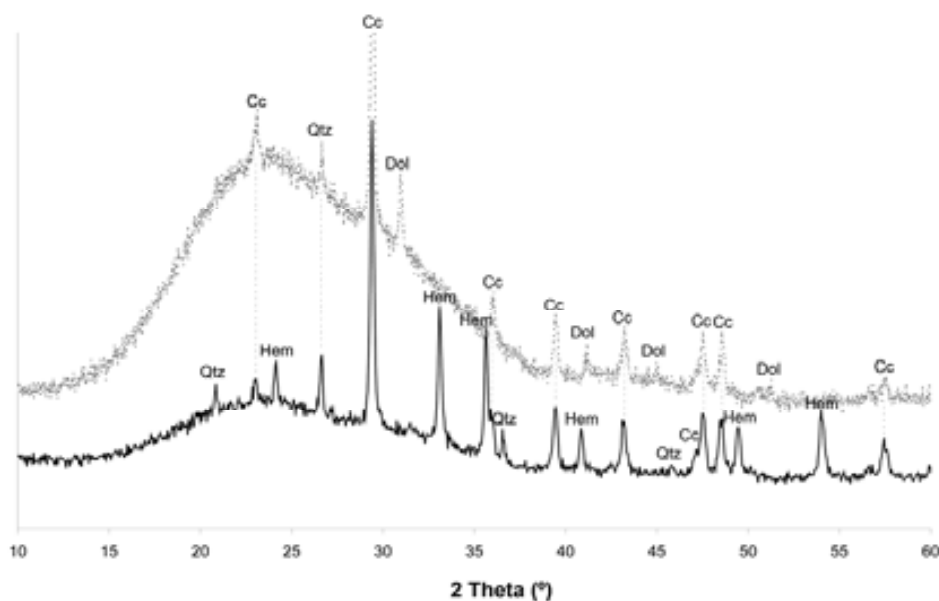


Fig. 4. 4 Diffractograms of the samples *IESSO-b* (solid line) and *IESSO-f* (dotted line). Key: Cc: calcite; Dol: dolomite; Hem: hematites; Qtz: quartz. Main peaks of lead compounds such as minium (2θ : 26.148; 30.374; 31.916) or cerussa (hydrocerussite, 2θ : 24.641; 34.156 and cerussite, 2θ : 24.829; 25.527) are not observed.

Dealing with the presence of Pb detected by EDXRF in the samples *IESSO-d* and *IESSO-f*, XRD analyses did not confirm neither the use of *minium secundarium* (red lead - Pb_3O_4) as a pigment responsible of the pinkish colour, nor the use of *cerussa* (white lead - cerussite [$PbCO_3$] and/or hydrocerussite [$2PbCO_3 \cdot Pb(OH)_2$]) as a preparation layer. The diffractograms only showed the presence of calcite, dolomite [(Ca, Mg) CO_3] and quartz. In the same way, FTIR analysis was not conclusive with the use of the previously mentioned compounds.

Yellow

The yellow colour appears on four of the selected samples (**Fig. 4. 2**, *IESSO-d*, *IESSO-g*, *IESSO-h* and *IESSO-i*). EDXRF analyses revealed once again the presence of Ca,

Fe and Sr except for *IESSO-d*, in which the presence of Pb is also detected (see **Table 4. 2**). According to the obtained XRD spectral data the yellowish colouration on *IESSO-g* (**Fig. 4. 5**), *IESSO-h* and *IESSO-i* is due to the presence of goethite. In fact, the FTIR features of goethite (characteristic bands at 911, 533, 472 and 432 cm^{-1}), kaolinite (bands at 3693, 3620 cm^{-1}), calcite (main bands at 1444, 873 and 712 cm^{-1}) and some silicates (band at 1030 cm^{-1}) (*IESSO-i*, **Fig. 4. 6**) would confirm the use of yellow ochre (Genestar and Pons, 2005).

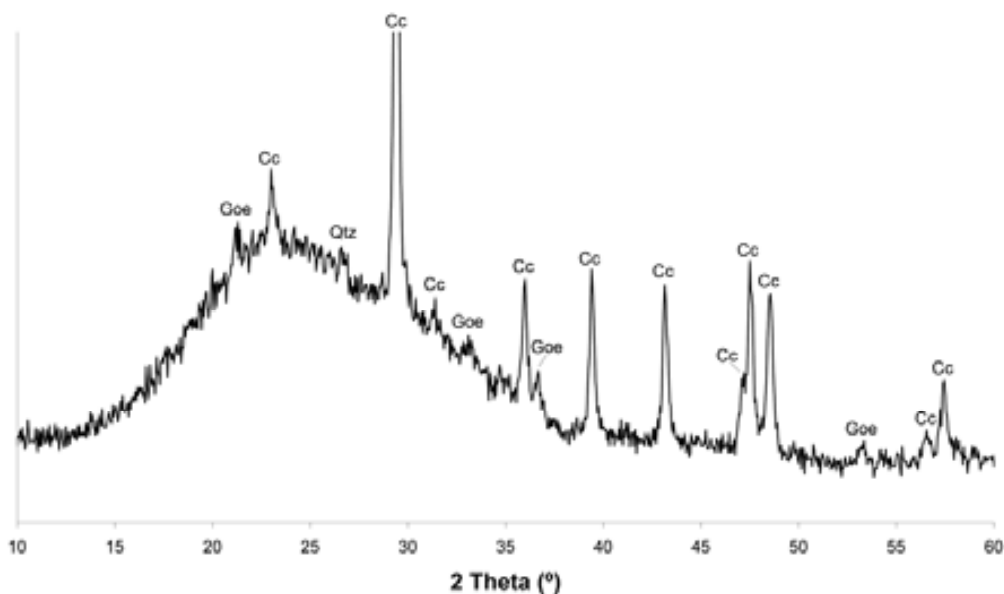


Fig. 4. 5 Diffractogram of the sample *IESSO-g*. Key: Cc: calcite; Goe: goethite; Qtz: quartz.

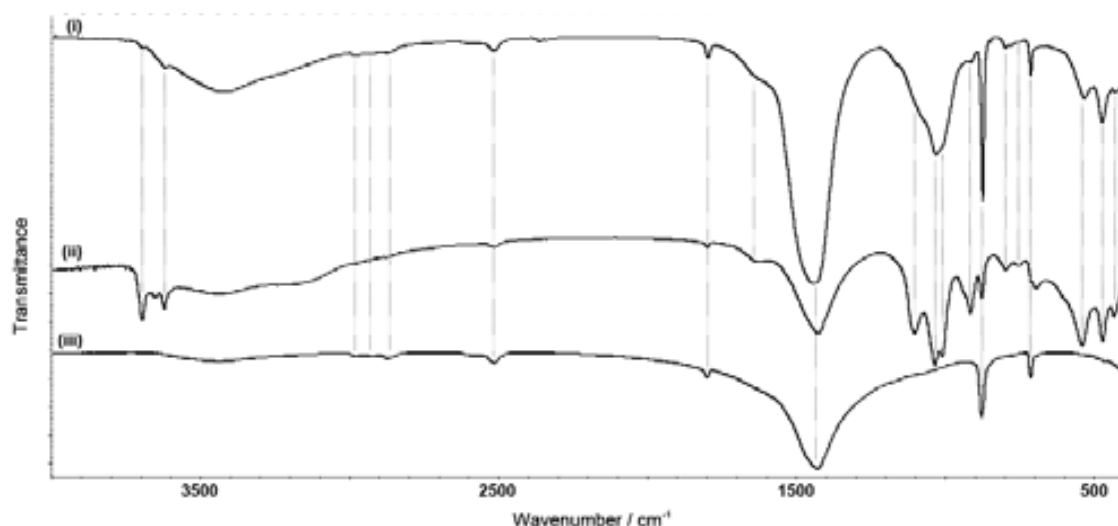


Fig. 4. 6 (i) FTIR spectrum of *IESSO-i*. Reference spectra of iron oxide yellow (Kremer 40301) (ii) and calcite (iii) are displayed in the inset for comparison.

Neither XRD nor FTIR analyses revealed the presence of organic or inorganic chromophores in the sample *IESSO-d*. XRD spectrum only showed the presence of calcite and dolomite, probably remains of the raw materials for liming preparation, and the presence of quartz and orthoclase (coming from the aggregates). We discarded the use of *massicot* (PbO), since its main XRD peaks at 2θ (°): 29.159, 30.386, 32.658, 37.876, 53.161 were not observed. Thus, the yellow colour of this sample might be due to one of those poorly crystallized (and therefore difficult to identify by means of XRD) hydrated iron oxides.

White

We analysed both, white coloured samples (*IESSO-n*) and fragments with white motifs as part of its decoration (see **Fig. 4. 2**, *IESSO-a*, *IESSO-b*, *IESSO-l*, *IESSO-m*, *IESSO-p*). In EDXRF spectra Ca is the only element related with compounds which might generate this colouration. The absence of Pb characteristic lines ruled out the use of lead compounds (such as cerussite and hydrocerussite) pigments usually employed in Roman times (Mazzocchin, 2003; Siddal, 2006). Indeed, both XRD and FTIR analyses confirmed the absence of these compounds and corroborated the presence of calcite as the mineral responsible to the white colour.

Green

Amongst the greenish samples (**Fig. 4. 2**, *IESSO-j* to *-m*) we can distinguish different shades (from pale green to olive-green). In his book *Naturalis Historia*, Pliny (Pliny the Elder, 1985) describes that the green colours derived from both minerals such as malaquite (a green copper compound $[\text{CuCO}_3\text{Cu}(\text{OH})_2]$) and green earths or *appianum* (comprising mineral species such as glauconite, celadonite, chlorites, smectites, serpentines and pyroxenes). The use of green earths was specially preferred by Romans not only because they are permanent but also because they are stable and non-reactive (Hradil *et al.*, 2011).

EDXRF spectral data revealed once again the presence of Ca, Fe and Sr (see Table 4. 1). The absence of Cu in the EDXRF spectra allowed us to discard the use of malaquite. SEM-EDS analyses of pigment particles (**Fig. 4. 7**) showed the presence of Mg, Al, Si, K and Fe, which might suggest the presence of glauconite $[\text{Na}_2(\text{Mg},\text{Fe}^{2+})_3\text{Al}_2\text{Si}_8\text{O}_{22}(\text{OH})_2]$ or celadonite $[\text{K}(\text{Mg},\text{Fe}^{2+})(\text{Fe}^{3+},\text{Al})\text{Si}_4\text{O}_{10}(\text{OH})_2]$ like-clays.

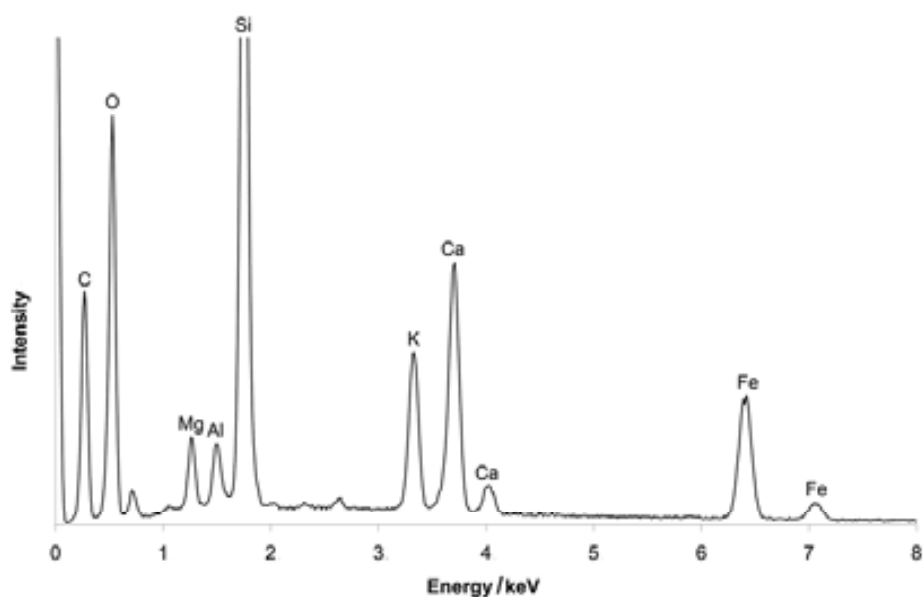


Fig. 4. 7 EDS spectrum of *IESSO-I* where we can clearly observe the spectral lines of Mg, Al, Si, K and Fe amongst others.

By using XRD technique we identified the presence of different mineral phases: albite, calcite, dolomite, kaolinite, mica, orthoclase and quartz (coming from the aggregates) and gypsum (its presence in the external layer could be attributed due to artist's intentional addition to whiten the pigment or to the transformation of calcium carbonate into calcium sulphate dehydrate due to a weathering process (Ospitali, 2008; Aliatis, 2010).

Glauconite and celadonite are members of clayey micas (consisting of a layer of octahedrally coordinated cations such as Al^{3+} , Fe^{3+} , Fe^{2+} or Mg^{2+} , inserted between two sheets of silicate tetrahedra and interlayers of K^+ ions, which hold the three layers together) which make them hardly distinguishable from other micas by using XRD. The first one occurs in sandy sediments of marine origin while the second one has its origin as an alteration product of basaltic rocks (Odom, 1984).

Despite the similarity in structure and composition of both minerals, several authors have pointed out the capability of FTIR spectroscopy of differentiating between these green earths pigments (Ospitali, 2008; Aliatis, 2010). According to them, celadonite IR spectrum shows sharp and distinct bands in the region of $3400 - 3700 \text{ cm}^{-1}$ (characteristic to the stretching vibrations of hydroxyl groups), resolved bands in the region of $1110 - 950 \text{ cm}^{-1}$ (related to the stretching vibrations within the tetrahedral sheet) and OH bending modes involving octahedral cations, while glauconite IR

spectrum is broader and weaker than that of celadonite, suggesting its poorly crystal order. Absorption bands below 500 cm^{-1} are also particularly useful for the identification of these mineral species (Moretto *et al.*, 2011). The FTIR analyses carried out in the samples *IESSO-j* to *IESSO-m* would be consistent with celadonite (**Fig. 4. 8**) since the intense bands at 3602, 3556, 3533, 1618, 1112, 1074, 981, 961, 847, 795, 681, 671, 602, 497, 465, 440 and 410 cm^{-1} were observed. Besides, the bands at 2978, 2928, 2869, 2513, 1795, 1445, 874 and 712 cm^{-1} are due to the presence of calcite.

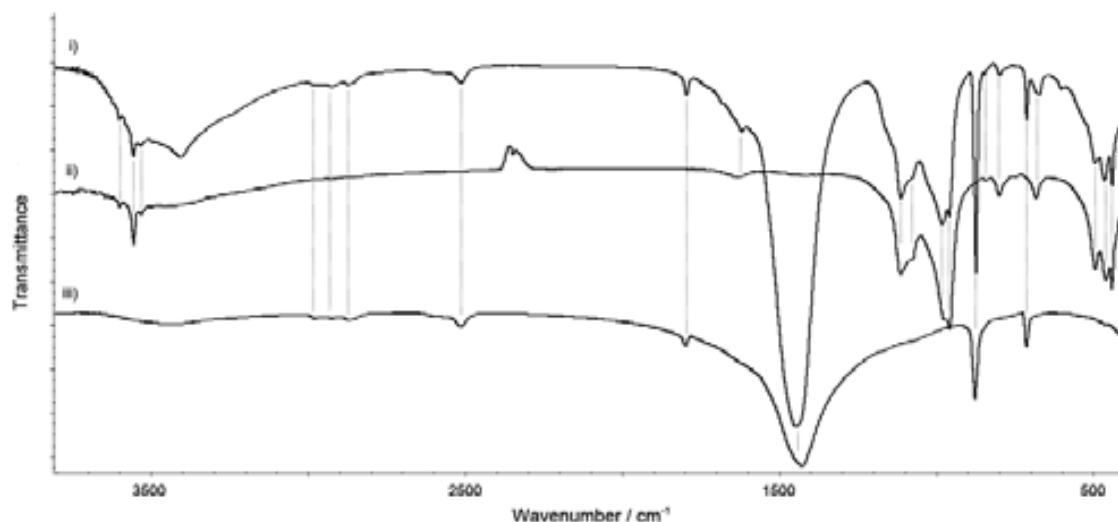


Fig. 4. 8 (i) FTIR spectrum of *IESSO-j*. Reference spectra of celadonite (ii) and calcite (iii) are displayed in the inset for comparison.

A brief look at the local geology of the surroundings of Guissona shows us outcrops of various types of rock from diverse geological periods (mainly from the upper Eocene to the lower Oligocene (Barnolas and Robador, 1998); nevertheless, geological deposits of celadonite would not have been potentially available to painters in this region, so that we must consider the hypothesis of a foreign origin for the green pigment.

Grey and black

EDXRF analyses of sample *IESSO-o* (grey) and *IESSO-p* (black) revealed the presence of Ca, Fe, Sr and Pb. Black shades were usually obtained not only by using organic compounds (such as soot or charcoal) but also by using inorganic compounds like graphite (all of them impossible to be detected by EDXRF). Furthermore, the use of other mineral species such as apatite [$\text{Ca}_3(\text{PO}_4)_2$], pyrolusite (MnO) and ramsdellite (MnO_2) has been recorded in Roman times (Siddal, 2006; Rapp, 2009). The absence

of manganese allowed us to discard the use of pyrolusite and ramsdellite. XRD spectral data determined the presence of calcite, albite and quartz. However, none of these mineral phases are responsible of the black shades. The absence of characteristic peaks of apatite, graphite, pyrolusite and ramsdellite in the XRD spectra might suggest whether the use of a poorly crystallized mineral, the use of an amorphous mineral or the use of an organic compound. SEM-EDS analyses did not reveal conclusive information. Backscattered electrons (BSE) mode did not allow distinguishing pigment particles in the outer layer, while energy dispersive (EDS) analyses performed in selected areas of the sections corroborated the results obtained by EDXRF and XRD (showed the absence of phosphorous, manganese and carbon). Finally, the use of FTIR was not conclusive either, as only allowed determining the presence of calcite (characterized by the bands at 1796, 1438, 874 and 715 cm^{-1}) and quartz (bands at 1082, 797, 777 and 470 cm^{-1}). On the other hand, the presence of lead in the EDXRF spectrum of *IESSO-o* might suggest the use of *cerussa* (hydrocerussite or cerussite); however, it was not possible to determine the presence of these compounds by using XRD.

4. 2. 4. 1. Supporting material

The main petrographic features of some of the samples described by PLM are summarized in **Table 4. 2**.

Generally speaking, the studied mortars exhibit a binder to aggregate ratio (per weight) of 1:3, a serial-texture aggregate (from fine-grained to coarse-grained) homogeneously distributed throughout the binder. Furthermore most samples showed moderately sorting and low packing aggregates (Folk, 1974) composed by monomineralic crystalline phases minerals from granitic origin, fragments of sedimentary rocks (limestone and sandstone), metamorphic rocks (schist) and igneous rocks (granitoid) as well as bivalves, brachiopods and ceramic fragments. Moreover the porosity is always under the 15%, generally with small and rounded pores due to a water excess during mixing. Exceptionally, we detected the presence of micro-cracking induced by shrinkage drying in the outer layer of some plasters (**Fig. 4. 9**, *IESSO-e*; *IESSO-f*, *IESSO-h*). In accordance to these specifications, the described mortars can be classified as being materials of both great quality and fineness.

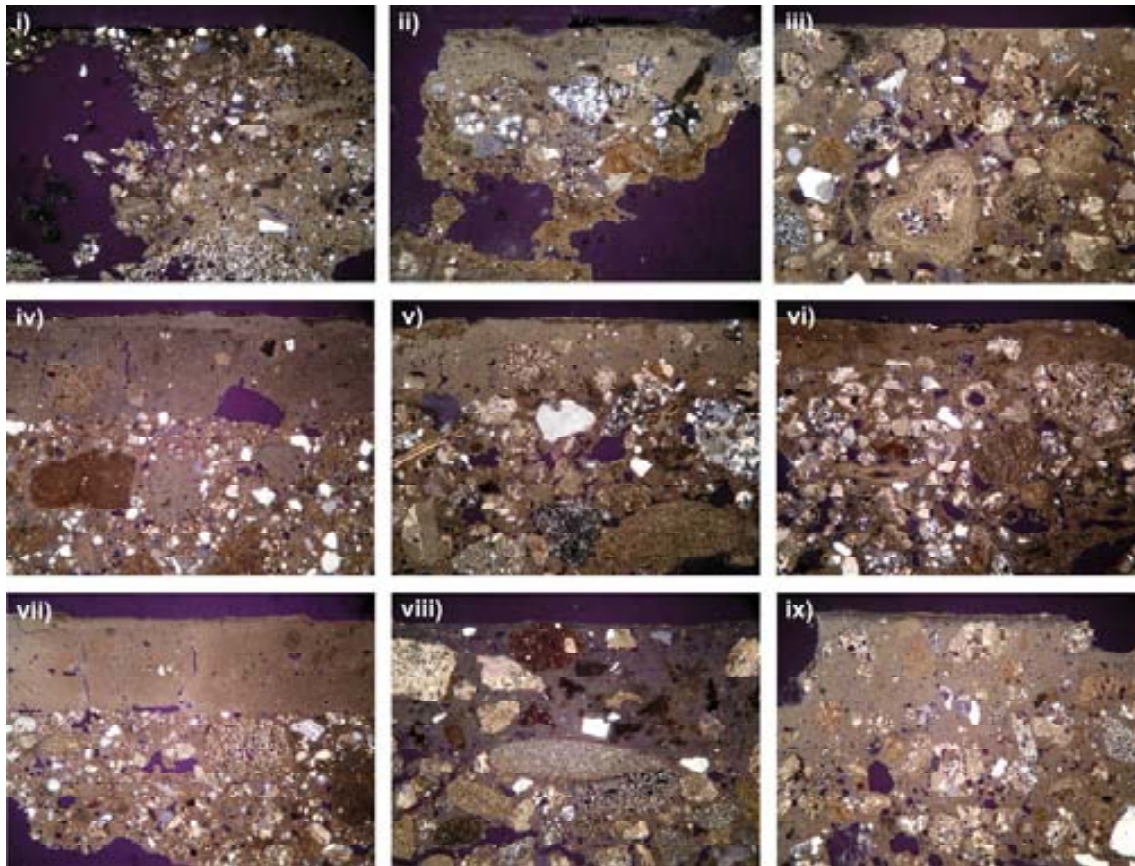


Fig. 4. 9 Microphotographies (crossed polarizing lenses, x2) of some of the stuccoes: i) *IESSO-a*; ii) *IESSO-b*; iii) *IESSO-d*; iv) *IESSO-e*; v) *IESSO-f*; vi) *IESSO-g*; vii) *IESSO-h*; viii) *IESSO-j*; ix) *IESSO-o*.

Table 4. 2
Petrographic and stratigraphic features of some of the mortars

Reference	Ref. Arch.	Site	Colour	By PLM				By SEM-EDS			
				Mineral phases of the aggregate	Rock Fragments	Other	Sorting	Aggregate/Binder ratio (*)	Porosity (%) (**)	Observations	Preparation layers
/ESSO-a	G97-UE148		brick red + white line	ort + qtz	gra + san + sch	-	PS	1:1	~ 6%	-	1
/ESSO-b	G97-UE148		deep red + white line	ort + pla + qtz	sch	-	PS	1:3	~ 6%	-	3
/ESSO-d	H13-GROUP4		pale pink + pale green + pale yellow	alb + cc + ort + qtz	gra + lim + sch	biv	MS	1:3	~ 7%	-	3
/ESSO-e	G99-UE584		pink	amf + bio + cal + ort+ qtz	lim + san	biv	WS	1:2	~ 3%	cracking	4
/ESSO-f	H13		pink	cal + ort + qtz	gra + lim + san + sch	bra + ech	PS	1:6	~ 6%	cracking	2
/ESSO-g	G97-UE197		mustard-coloured	alb + ort + qtz	lim + san + sch	biv + bra + lim. lum	MS	1:6	~ 13%	-	2
/ESSO-h	G-UE128		mustard-coloured	alb + ort + qtz	lim + san + sch	biv + bra + lim. lum	MS	1:6	~ 2%	cracking	3
/ESSO-j	G97-UE112		green	cal + ort + qtz	lim + san + sch	sma. for + cer. fra	MS	1:3	~ 2%	-	3
/ESSO-o	H13		grey	cal + ort + qtz	calc + lim + sch	alg + bra	MS	1:3	~ 3%	-	3

Mineral key: amp: amphibole; alb: albite; bio: biotite; cal: calcite; ort: orthoclase; pla: plagioclase; qtz: quartz.

Rock key: lim: limestone; gra: granite; san: sandstone; sch: schist; calc: calcarenite.

Other: alg: algae; biv: bivalves; bra: brachiopods; cer. fra: ceramic fragments; ech: echinoderm; lim: lime lump; sma. for: smaller foraminifera.

Sorting Key: PS: poor sorted; MS: moderately sorted; WS: well sorted.

(*) semi-quantitative visual estimation of aggregate/binder ratio (according to the method proposed by Ricci Lucchi, 1980).

(**) macroporosity was estimated by image analysis on thin sections.

Painting supports were shown to differ in terms of sequence of layers present and the relative coarseness of the used plasters and mortars. Although by using PLM it is possible to identify the stratigraphy sequence of the different cross sections, the use of SEM-EDS allowed us to obtain a more detailed description. A representative example is reported in **Fig. 4. 10** where we can observe a PLM image with three superimposed layers in **Fig. 4. 10 (a)** while in **Fig. 4. 10 (b)** we are able to distinguish at least five layers by using SEM-EDS.

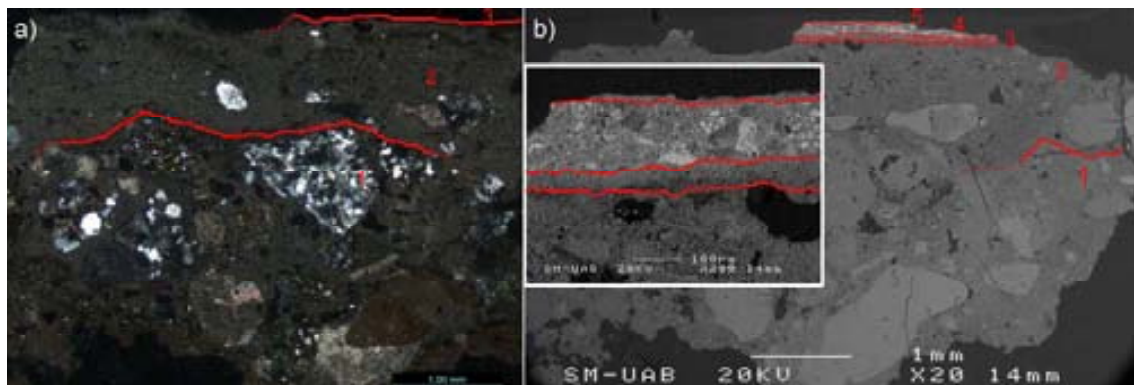


Fig. 4. 10 Images of the sample *IESSO-b*: (a) PLM image taken in crossed polars in which we can differentiate 3 layers; (b) backscattered image in which we can differentiate 5 layers.

Our main knowledge of the wall paintings elaboration process in Roman times comes from the textual sources of contemporary authors such as Pliny the Elder (Plinio, 1952) or Vitruvius (Trumbull, 2007) in which they provide details of the Roman method of both preparations of wall surfaces as well as the technology of production of limewashing putty used in their constitution. According to them, a mural painting might be composed by a succession of layers to produce a surface for a particular aesthetic use or of particular quality. The preparatory layer or *tectorium* is made of three to six layers (starting from the raw wall, at first there is the *arriccio* – constituted at the same time by three layers of lime and volcanic or sea sand, and then the plaster or *intonaco* – composed of three layers of lime and marble powder). While the plaster was still wet, the pigments (properly mixed with suited binding agents) were laid over the *tectorium* (Paternoster, 2005).

According to the observations carried out by SEM, almost all the plasters examined (*IESSO-b*, *-e*, *-f*, *-g*, *-h*, *-o*) presented one to three layers immediately beneath the pigment composed exclusively of lime followed by sandy layers. Nevertheless, *IESSO-a*, *-d* and *-j* differed from this pattern. In *IESSO-a* and *-d*, pictorial layers were laid

directly over the sandy layer, while in the sample *I ESSO-j* a preparation layer was in fact observed, but this time was made of ceramic fragments. This type of cement is known as *cocciopesto* (Zebri *et al.*, 2004). The use of different types of plaster seems to depend on technical factors, however, as most of the samples had a secondary location, it was not possible to make any technological comment about the wall paintings as a whole.

4. 2. 5. Conclusions

This chapter reported the characterization of a set of sixteenth decorated stuccoes from the Roman city of *Iesso* in which the need of a multi-analytical approach for the proper characterization of such kind of works is corroborated. The EDXRF analyses orientated us to the most likely pigments used for the elaboration of the paintings; however, as it has already pointed out, elemental characterization was not sufficient, and it was mandatory to complete the analysis with the use of molecular and vibrational techniques, namely XRD and FTIR spectroscopies, in order to determine the employed compounds. In this sense, by using XRD it was possible to determine almost all the inorganic pigments as well as other compounds related to the supporting material, while FTIR spectroscopy proved to be indispensable in studying the characterization of poorly crystallized iron oxides (responsible for the yellow shades) and the identification of greenish shades present in the decorated stuccoes.

Despite the fact that our archaeological knowledge of the Roman city of *Iesso* is still scarce, the information provided by this study potentially serves for enriching the knowledge of the city. The obtained results suggest that almost all the employed palette composed of “austere” pigments was from both natural and local origin (which is in accordance with the stylistic features described by the historians (Cortés, 2009)). In this sense, the lack of highly prized red pigments (such as *minium cinnabaris*) strikingly contrasts with a much more widely palette found in other archaeological settlements from the Northern Spain (Domínguez-Bella, 2004; Edreira *et al.*, 2004; Villa and Edwards, 2005; Pocostales 2008; Pitarch *et al.*, 2010).

The multi-analytical approach allowed us to state that red colours were mainly composed by hematite (Fe_2O_3), yellow colours were mainly made with goethite [$\text{FeO}(\text{OH})$], while white pigments were made with calcium carbonate (CaCO_3). Furthermore, green pigments seems to be of foreign origin and were made of celadonite [$\text{K}(\text{Mg}, \text{Fe}^{2+})(\text{Fe}^{3+}, \text{Al})\text{Si}_4\text{O}_{10}(\text{OH})_2$], even if the presence of glauconite cannot

be discarded. On the other hand, the presence of lead detected in some samples might suggest the use of *minium*, *massicot* or *cerussa* (red lead, yellow lead and white lead respectively). Unfortunately, none of these compounds were identified by means of the employed techniques. Finally, the results obtained from black tonalities seem to indicate the use of an organic pigment.

Furthermore, the study of the supporting material carried out by PLM and SEM-EDS pointed out the presence of superimposed layers composed by lime mortars (calcium carbonate) of different grain size, although the preparation process of mural painting described by the classical authors was not exactly followed in all the cases. The studied decorated stuccoes reflect craftsmanship of that time (the selection of raw materials and the accurate execution of the mortars are well proofs of that). Moreover, although the quality of materials allowed highlighting differences in technology, further conclusions about its functionality or its chronology cannot be done due to the secondary location of the samples.

4. 3. References

ALIATIS I., BERSANI D., CAMPANI E., CASOLI A., LOTTICI P.P., MANTOVAN S., MARINO I-G., OSPITALI F. (2009) *Green pigments of the Pompeian artists' palette*. Spectrochimica Acta Part A: Molecular and Biomolecular Spectroscopy, 73 (3), 532-538.

ALIATIS I., BERSANI D., CAMPANI E., CASOLI A., LOTTICI P.P., MANTOVAN S., MARINO I-G. (2010) *Pigments used in Roman wall paintings in the Vesuvian area*. Journal of Raman Spectroscopy, 41, 1537–1542.

BARNOLAS A., ROBADOR, A. (1998) Mapa Geológico de España. Scale 1:50000. Hoja 361 – Guissona. First Edition. Instituto Tecnológico Geominero de España, Madrid.

BRAGANTINI I. (Ed.) (2007) *Atti del X Convegno Internazionale dell'Associazione Internazionale per la Pittura Murale Antica (AIPMA), Naples, 17-21 September 2007*, Forthcoming.

CORTÉS A. (2009) *L'arquitectura domèstica de les ciutats romanes de Catalunya. Època tardorepublicana i altimperial*. PhD Thesis. UAB-ICAC.

COTTE M., SUSINI J., METRICH N., MOSCATO A. , GRATZIU C , BERTAGNINI A., PAGANO, M. (2006) *Blackening of Pompeian cinnabar paintings: X-ray microspectroscopy analysis*. *Analytical Chemistry*, 78 (21), 7484-7492.

DOMÍNGUEZ-BELLA S. (2004) *Pinturas murales romanas en la neápolis gaditana (Cádiz): análisis de pigmentos minerales y caracterización de estucos*, in: M.J. FELIU, J. MARTÍN, M.C. EDREIRA, M.C. FERNANDEZ, M.P. MARTINEZ, A. GIL, R. ALCÁNTARA (Eds.) *Avances en Arqueometría 2003*. Servicio de Publicaciones Universidad de Cádiz, Spain 201-207.

DOORYHÉE E., ANNE M., BARDIES I., HODEAU J.-L., MARTINETTO P., RONDOT S., SALOMON J., VAUGHAN G.B.M., WALTER P. (2005) *Non-destructive synchrotron X-ray diffraction mapping of a Roman painting*. *Applied Physics A: Materials Science and Processing*, 81, 663–667.

DURÁN A., MILLÁN E., JIMÉNEZ DE HARO M.C., CÁRCELES J.F., JUSTO Á., PÉREZ-RODRÍGUEZ J.L. (2007) *Estudio técnico de la pintura parietal romana. Análisis de fragmentos provenientes de Villa dei Papiri (Herculano) y del Jardín de la Casa del Bracciale d'Oro (Pompeya)* in S. ROVIRA, M. GARCÍA-HERAS, M. GENER, I. MONTERO (Eds.) *Actas VII Congreso Ibérico de Arqueometría, Madrid, 8-10 Octubre 2007*, 680-687.

DURÁN A., CASTAING J., WALTER P. (2010) *X-ray diffraction studies of Pompeian wall paintings using synchrotron radiation and dedicated laboratory made systems*. *Applied Physics A: Materials Science and Processing*, 99, 333-340.

DURÁN A., JIMÉNEZ DE HARO M.C., PÉREZ-RODRÍGUEZ J.L., FRANQUELO M.L., HERRERA, L.K., JUSTO A. (2010) *Determination of pigments and binders in Pompeian wall paintings using synchrotron radiation – high-resolution X-ray powder diffraction and conventional spectroscopy-chromatography*. *Archaeometry*, 52 (2), 286-307.

DURÁN A., PÉREZ-RODRÍGUEZ J.L., JIMÉNEZ DE HARO M.C., FRANQUELO M.L., ROBADOR M.D. (2011) *Analytical study of Roman and Arabic wall paintings in the Patio De Banderas of Reales Alcazares' Palace using non-destructive XRD/XRF and complementary techniques*. *Journal of Archaeological Science*, doi:10.1016/j.jas.2011.04.021.

EDWARDS H.G.M., HASSAN N.F.N., MIDDLETON P.S. (2006) *Anatase—a pigment in ancient artwork or a modern usurper?* *Analytical Bioanalytical Chemistry*, 284, 1356-1365.

EDREIRA M.C., FELIU M.J., FERNÁNDEZ-LORENZO C., GIL M.L.A., MARTÍN J., VILLENA A. (2004) *Caracterización químico-física de las pinturas murales de la Casa del Anfiteatro de la ciudad de Mérida (Badajoz)* in FELIU M.J., MARTÍN J., EDREIRA M.C., FERNANDEZ M.C., MARTINEZ M.P., GIL A., ALCÁNTARA R. (Eds.) *Avances en Arqueometría 2003*. Servicio de Publicaciones Universidad de Cádiz, Spain 231-238.

FOLK R.L. (1974) *Petrology of Sedimentary Rocks*. Hemphill, Austin.

GENESTAR C., PONS C. (2005) *Earth pigments in painting: characterization and differentiation by means of FTIR spectroscopy and SEM-EDS microanalysis*. *Analytical and Bioanalytical Chemistry*, 382, 269-274.

GUITART J. (2006): "*Iluro, Baetulo and Ileso and the establishment of the Roman town model in the territory of present-day Catalonia*". En: ABAD CASAL L., KEAY S., RAMALLO ASENSIO S. (Eds.) 2006: *Early roman towns in Hispania Tarraconense (2nd century BC - 1st century AD)*, Portsmouth, Rhode Island, USA, *Journal of Roman Archaeology*, (Journal of Roman Archaeology; Supplementary series, 62).

GUITART J. (2010) *The origin of the earliest Roman cities in Catalonia: An examination from the perspective of archaeology*. *Catalan Historical Review*, 3, 9-30.

HRADIL D., PÍŠKOVÁ A., HRADILOVÁ J., BEZDÍČKA P., LEHRBERGER G., GERZER S. (2011) *Mineralogy of bohemian green earth pigment and its microanalytical evidence in historical paintings*. *Archaeometry*, 53 (3), 563–586.

HÄUBER C. (1998) *The Esquiline Horti: New Research*, in: FRAZER, A. (Ed.) *The Roman villa: villa urbana*. University of Pennsylvania Museum, Publication Department, Philadelphia, 55-64.

MAGUREGUI M., KNUUTINEN U., CASTRO K., MADARIAGA J.M. (2010) *Raman spectroscopy as a tool to diagnose the impact and conservation state of Pompeian*

second and fourth style wall paintings exposed to diverse environments (House of Marcus Lucretius). Journal of Raman Spectroscopy, 41 (11), 1400-1409.

MAGUREGUI M., KNUUTINEN U., MARTÍNEZ-ARKARAZO I., CASTRO K., MADARIAGA J.M. (2011) (a) *Thermodynamic and spectroscopic speciation to explain the blackening process of hematite formed by atmospheric SO₂ impact: The case of Marcus Lucretius House (Pompeii). Analytical Chemistry, 83 (9), 3319-3326.*

MAGUREGUI M., KNUUTINEN U., TREBOLAZABALA J., MORILLAS H., CASTRO K., MARTÍNEZ-ARKARAZO I., MADARIAGA J.M. (2011) (b) *Use of in situ and confocal Raman spectroscopy to study the nature and distribution of carotenoids in brown patinas from a deteriorated wall painting in Marcus Lucretius House (Pompeii). Analytical and Bioanalytical Chemistry, doi: 10.1007/s00216-011-5276-9*

MAZZOCCHIN G.A., AGNOLI F., MAZZOCCHIN S., COLPO I. (2003) *Analysis of pigments from Roman wall paintings found in Vicenza. Talanta, 61, 565-572.*

MAZZOCCHIN G.A., AGNOLI F., SALVADORI M. (2004) *Analysis of roman age wall paintings found in Pordenone, Trieste and Montegrotto. Talanta, 64, 732-741.*

MAZZOCCHIN, G.A.; ORSEGA, E.F.; BARALDI, P.; ZANNINI, P. (2006) *Aragonite in roman wall paintings of the VIII^a Regio, Aemilia, and X^a Regio, Venetia et Histria. Annali di Chimica, 96, 377-387.*

MAZZOCCHIN, G.A., RUDELLO, D., MURGIA, E. (2007) (a) *Analysis of Roman wall paintings found in Verona. Annali di Chimica, 97 (9), 807-882.*

MAZZOCCHIN, G.-A., DEL FAVERO, M., TASCA, G. (2007) (b) *Analysis of pigments from roman wall paintings found in the "agro centuriato" of Julia Concordia (ITALY). Annali di Chimica, 97 (9), 905-913.*

MAZZOCCHIN G.A., BARALDI P., BARBANTE C. (2008) *Isotopic analysis of lead present in cinnabar of Roman wall paintings from Xth Regio "(Venetia et Histria)" by ICP-MS. Talanta 74 690-693*

MAZZOCCHIN G.A., VIANELLO A., MINGHELLI S., RUDELLO D. (2010) *Analysis of roman wall paintings from the thermae of 'iulia concordia'*. *Archaeometry*, 52 (4), 644-655.

MORETTO L.M., ORSEGA E.F., MAZZOCCHIN G.A. (2011) *Spectroscopic methods for the analysis of celadonite and glauconite in Roman green wall paintings*. *Journal of Cultural Heritage*, doi: 10.1016/j.culher.2011.04.003.

ODOM I. E., (1984) *Glauconite and celadonite minerals*. *Reviews in Mineralogy*, 13, 545–72.

OSPITALI F., BERSANI D., Di LEONARDO G., LOTTICI P.P. (2008) *“Green earths”: vibrational and elemental characterization of glauconites, celadonites and historical pigments*. *Journal of Raman Spectroscopy*, 39, 1066-1073.

PATERNOSTER G., RINZIVILLO R., NUNZIAT F., CASTELLUCCI E.M., LOFRUMENTO C., ZOPPI A., FELICI A.C., FRONTEROTTA G., NICOLAIS C., PIACENTINI M., SCIUTI S., VENDITTELLI M. (2005) *Study on the technique of the Roman age mural paintings by micro-XRF with Polycapillary Conic Collimator and micro-Raman analyses*. *Journal of Cultural Heritage*, 6, 21-28.

PIOVESAN R., SIDDALL R., MAZZOLI C., NODARI L. (2011) *The Temple of Venus (Pompeii): A study of the pigments and painting techniques*. *Journal of Archaeological Science*, doi: 10.1016/j.jas.2011.05.021.

PITARCH A., QUERALT I., ÁLVAREZ-PÉREZ A., GUITART J. (2010) *Caracterización de estucos y pigmentos del establecimiento romano republicano de Can Tacó-Turó D'en Roïna (Montmeló-Montornès Del Vallès, Barcelona)* in: Saiz M.A., López R., Cano M.A., Calvo J.C. (Eds.) (2010) *Actas VIII Congreso Ibérico de Arqueometría, Teruel 19-21 October 2009*, Seminario de Arqueología y Etnología Turolese, Spain.

PLINIO (1952) *Historia Natural*. Translated by CANTÓ, J., GONZÁLEZ, S., GÓMEZ, I., TARRIÑO, E. Ed. Cátedra, Madrid.

POCOSTALES L. (2008) *Estudi de la metodologia de recerca per pintura mural romana. La Nemesis de l'amfiteatre de Tarraco*. Master thesis (UAB-URV-ICAC).

RAPP G. (2009) *Pigments and Colorants* in: HERRMANN B. & WAGNER G.A. (Series Eds.) *Archaeomineralogy - 2nd Edition*, Natural Science in Archaeology, Springer-Verlag Berlin Heidelberg, 201-221.

RICCI F. (1980) *Sedimentologia parte I: Materiali e tessiture dei sedimenti*. Clueb, Bologna.

RODRÍGUEZ J.M.F., FERNÁNDEZ J.A.F. (2005) *Application of the second derivative of the Kubelka-Munk function to the semiquantitative analysis of Roman paintings*. *Color Research and Application*, 30, 448-456.

SALVADÓ N., BUTÍ S., TOBIN M.J., PANTOS E., PRAG A.J.N.W., PRADELL T. (2005) *Advantages of the use of SR-FT-IR microspectroscopy: applications to Cultural Heritage*. *Analytical Chemistry*, 77, 3444-3451.

SIDDAL R. (2006) *Not a day without a line drawn: Pigments and painting techniques of Roman Artists*. In *Focus Magazine: the proceedings of the Royal Microscopical Society*, 2, 18-31.

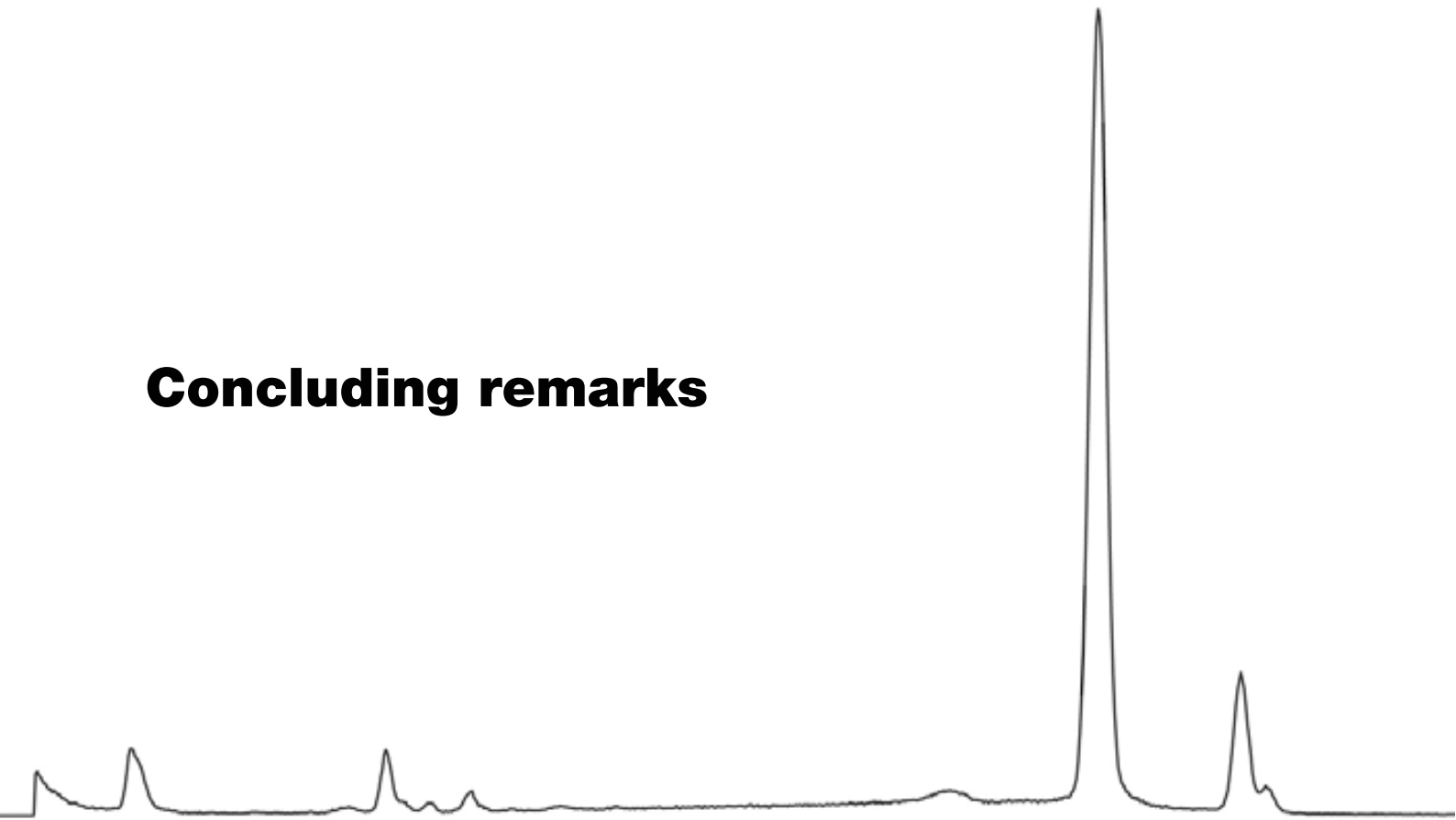
TRUMBULL D. (2007) *Vitruvius-Architecture Libri: Book VII*. Available from : <http://www.bostonleadershipbuilders.com/vitruvius/index.htm> [on-line] (publications from: *E-TEXTS - The Great Books of Western Civilization* <http://www.bostonleadershipbuilders.com> [on-line]) [last accessed: July 2011].

VILLAR S.E., EDWARDS H.G.M., HASSAN N.F., MIDDLETON P.S. (2004) *Raman spectroscopic analysis of pigments from Roman Villa excavations*, in: FREDERICKS P.M., FROST R.L., RINTOUL L. (Eds.) *Proceedings of XIXth International Conference on Raman Spectroscopy, 8-13 August 2004, Queensland, Australia*, 602-603.

VILLAR S.E.J., EDWARDS H.G.M. (2005) *An extensive colour palette in Roman villas in Burgos, Northern Spain: a Raman spectroscopic analysis*. *Analytical and Bioanalytical Chemistry*, 382, 283-289.

ZENDRI E., LUCCHINI V., BISCONTIN G., MORABITO Z.M. (2004) *Interaction between clay and lime in "cocciopesto" mortars: a study by ²⁹Si MAS spectroscopy*. *Applied Clay Science*, 25, 1-7.

Concluding remarks



This research work has given a brief overview of different analytical methodologies based on spectroscopic techniques for the characterization of Cultural Heritage materials. Even though the detailed conclusions from the present thesis have been included in each chapter, the general concluding remarks will be discussed in the succeeding section. It is worth mentioning that although some of the statements detailed in each chapter do not provide information that applies further away than to the same artwork, the analytical methodology presented in this work might be transferred to the study of other works of art with the same features in order to gain knowledge of the technical and material characteristics of the artworks.

Metals

The non-destructive direct analyses of ancient coins by means of EDXRF could be a very useful tool for the investigation of alloys. The coins can be rapidly examined (measuring time of 100 s) without applying any pre-treatment for a general screening, contributing to significant data useful for historical interpretations since, as it has already been pointed out, this technique allowed us not only to determine the elemental composition of the coins, establish differences and similarities between the monetary units of different mints or define the compositional variations of coins from the same workshop over the time, but also to identify possible counterfeits and compositional anomalies.

Another potential application of EDXRF is the possibility to study and characterize corrosion layers and weathering crusts (oxides, hydroxides, sulphates and carbonates amongst others) developed on coin surface during ageing and burial processes. However, the presence of light elements in most of these alteration processes such as oxygen, chlorine, sulphur, hydrogen and carbon demands the application of complementary tools to develop an adequate quantitative or semi-quantitative approach.

Paintings over metallic support

The suitability of EDXRF in combination with XRD spectroscopy has been demonstrated to be of great power for the analysis of pigments on metallic support, since the obtained data may reveal both technological and chronological features. The existence of different superimposed layers (such as the supporting media, the preparatory and the pictorial layers) as well as an approximate date of execution of the

work of art may be elucidated on the basis of the compositional features obtained by these spectroscopies. Furthermore, the pigment mass distribution of the different elements identified in the paintings may be determined by applying a simple and rapid EDXRF method especially developed, based on non-invasive direct analysis of solid sample. Nevertheless, taking into consideration the limitations of both techniques (EDXRF only allows the identification of the key elements of the pigments but not the compounds to which they belong, and XRD conventional equipments has spatial resolution restrictions) the use of other techniques is mandatory for a more reliable and complete characterization of the artwork under study. In this sense, the use vibrational spectroscopies such as RS and FTIR techniques has proven to be very effective in the characterization of such kind of artwork, as they provide complementary information of all the compounds. By using RS information about almost all pigments present in the painting might be obtained, while FTIR is useful to gain information about the employed binding medium.

Inks

The use of EDXRF technique for the analysis of inks and paper support may provide a guide to the most likely pigments employed to colour the chromolithographs and the fillers related to the paper matrix, but the obtained results are not always easily interpretable. Obviously, if pigments are mixed to obtain a particular colour (for example, a mixture of chrome yellow, Prussian blue, carbon black, red ochre and vermilion) the identification of the individual components may be laborious. Further difficulty occurs for a number of fillers (for example kaolinite, which is composed of light elements (Al, Si, O, H)) whose elementary composition is possibly not realizable with EDXRF. A final difficulty occurs for organic pigments composed of elements that are not detected with EDXRF spectrometry (C, H, N, O). In this sense, the combination of EDXRF with vibrational spectroscopies (such as Raman and FTIR) has proven to be very useful for the complete non-invasive characterization of inks on paper support. Although by using RS is possible to determine almost all the inorganic pigments present in the chromolithographs, sometimes the fluorescence emission of the samples may cause difficulties in the interpretation of the Raman spectrum. In this sense, a successful methodology for the determination of inks on paper was presented, in which the ink spectra was enhanced by subtracting the spectra from the paper support from the spectra taken in the coloured areas. However, even when using the proposed methodology, the Raman signal of some compounds still remained shielded by fluorescence emission (especially when analysing organic compounds). In those

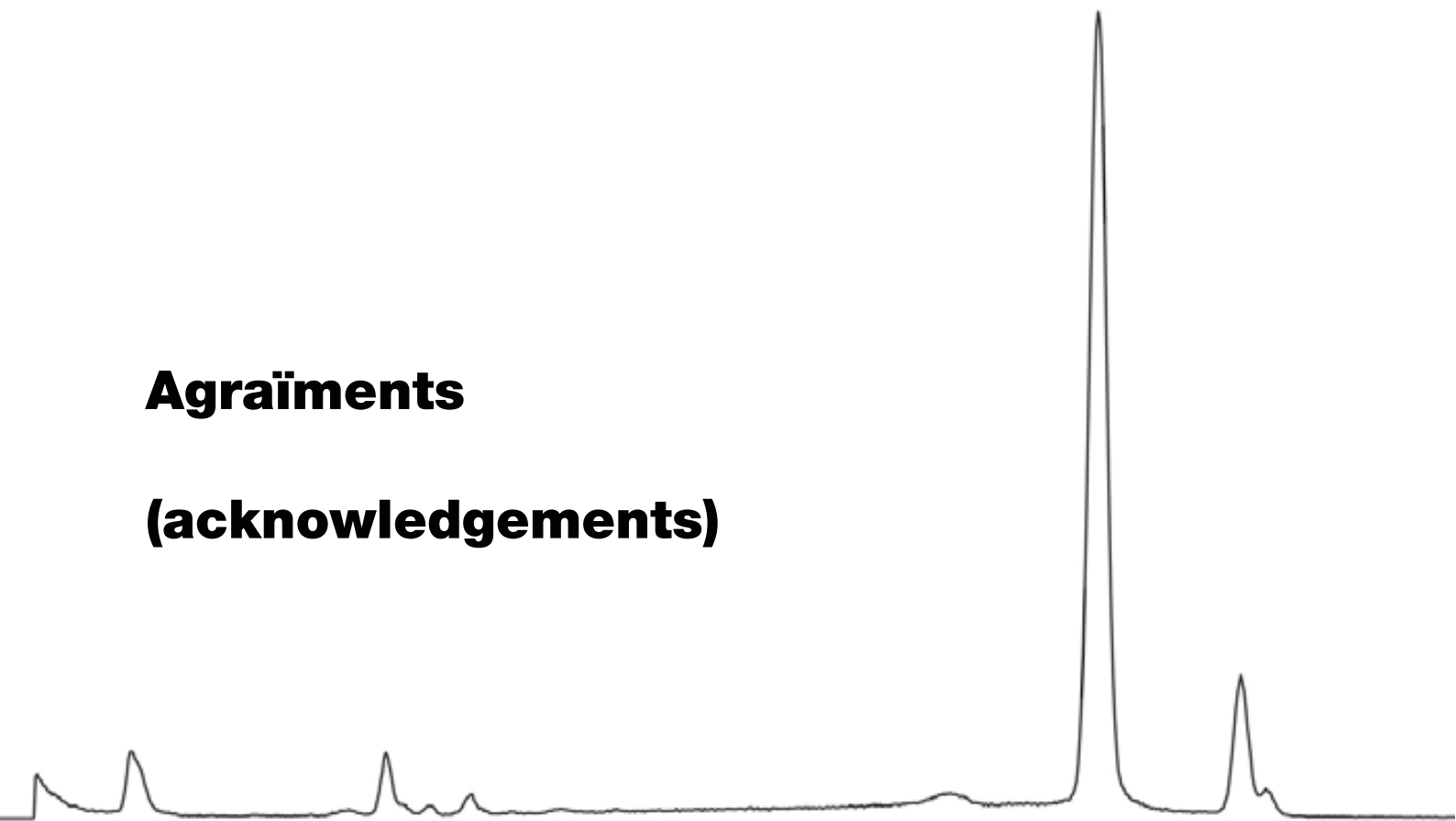
cases, the FTIR spectroscopy proved to be indispensable to obtain the necessary information to properly characterize those organic compounds.

Pigments over stuccoes

The analyses of decorated stuccoes by means of EDXRF may lead to a characteristic determination of the elemental compositions of different pigments. Nevertheless, some difficulties might arise during the analysis of pigments on such kind of supports, since the signal coming from the supporting material may affect the identification of the compounds used to elaborate the different colours. Thus, as elemental characterization was not sufficient, a combination of elemental with molecular and vibrational analysis, namely XRD and FTIR spectroscopy, was once again mandatory. In this sense, by using XRD it was possible to determine almost all the inorganic pigments as well as other compounds related to the supporting material, while FTIR spectroscopy proved to be essential characterizing poorly crystallized iron oxides (responsible for the yellow shades) and identifying the green colours existing in the mural paintings. Furthermore, the complementary use of PLM and SEM-EDS allowed characterizing the supporting materials (plasters and mortars) in order to describe the quality of the stuccoes. The combination of these techniques permitted to fully describe the technological features involved in the manufacturing processes of the wall-paintings.

Agraïments

(acknowledgements)



Una vegada un “col·lega” de professió em va dir que una tesi doctoral és com un organisme viu, que creix i evoluciona constantment...sembla que aquest, finalment, ha arribat a la maduresa!

En primer lloc, voldria donar les gràcies de forma especial als meus directors de tesi, el Dr. Queralt i el Dr. Álvarez. Ignasi, gràcies per haver-me donat la oportunitat d'introduir-me en el món de la recerca i per haver-me guiat durant aquests anys. Aureli, gràcies per confiar en mi des de bon començament i per donar-me suport moral quan més ho he necessitat!

Gràcies també a la col·laboració de la Dra. Marta Campo, el Dr. Albert Estrada i la Dra. Maria Clua, tots ells membres del Gabinet Numismàtic de Catalunya del MNAC. A tots, moltes gràcies pel vostre suport.

Gràcies a en Joan Pujol Claramunt, Director Tècnic de Fischer Instruments, S.A., Barcelona, sense el seu suport no hagués estat possible la realització de les anàlisis de monedes antigues.

Agrair també a l'Artur Ramón, per la seva confiança i el seu interès.

De la mateixa manera, agrair a en Josep Ros i al Dr. Guitart, membres del Patronat d'Arqueologia de Guissona, per la seva confiança i dedicació en el projecte de les pintures murals de lessos.

Unas palabras de agradecimiento para la Prof. Maria Luisa Carvalho, muchas gracias por brindarme la posibilidad de hacer una estancia en el Centro de Física Atómica da Universidade de Lisboa. Tampoco querría dejarme al “team” de chicas portuguesas, Marta, Sofia, Anna y Diana: obrigada por me fazerem sentir em casa!

Agradecer también al Dr. Juan Manuel Madariaga y al Dr. Kepa Castro por darme la oportunidad de hacer una estancia en el Departamento de Química Analítica de la UPV y colaborar con el grup de investigación IBeA. ¡Gracias también al “team” de Zamudio!

Igualmente al Dr. José Luís Prada que, ya hace años, hizo posible que me introdujera en el campo de estudio de materiales del Patrimonio Cultural. Jose Luís, muchas gracias por mostrarme los entresijos del mundillo.

De la mateixa manera, voldria agrair al Dr. José Luís Briansó, a la Dra. Rita Estrada, al Dr. Lluís Casas i a la Sílvia Ballbé pel seu suport al llarg d'aquests anys.

Fora d'aquest àmbit, no em voldria pas oblidar de tota aquella gent que ha estat al meu costat aquests 4 anys.

Als companys de despatx, l'Óscar, l'Eva, l'Helena i l'Arantxa, gràcies pels vostres consells i la vostra companyia.

A altres companys de l'Institut, l'Oriol Font, el Josep Elvira i la Marta Rejas, gràcies pel recolzament i els ànims constants!

Als companys de geologia el Dr. Corral, el Dr. Pastor, el Xavi i la Mireia, a tots vosaltres mil gràcies per la vostra bona energia.

No podría dejar de dedicarle unas palabras a Kepa, mi "responsable" durante la estancia en Bilbao y, a veces, compañero de cordada. ¡¡Muchísimas gracias por estar ahí en todo momento!! Espero que tarde o temprano podamos compartir más experiencias (tanto en el ámbito profesional como en el montañero).

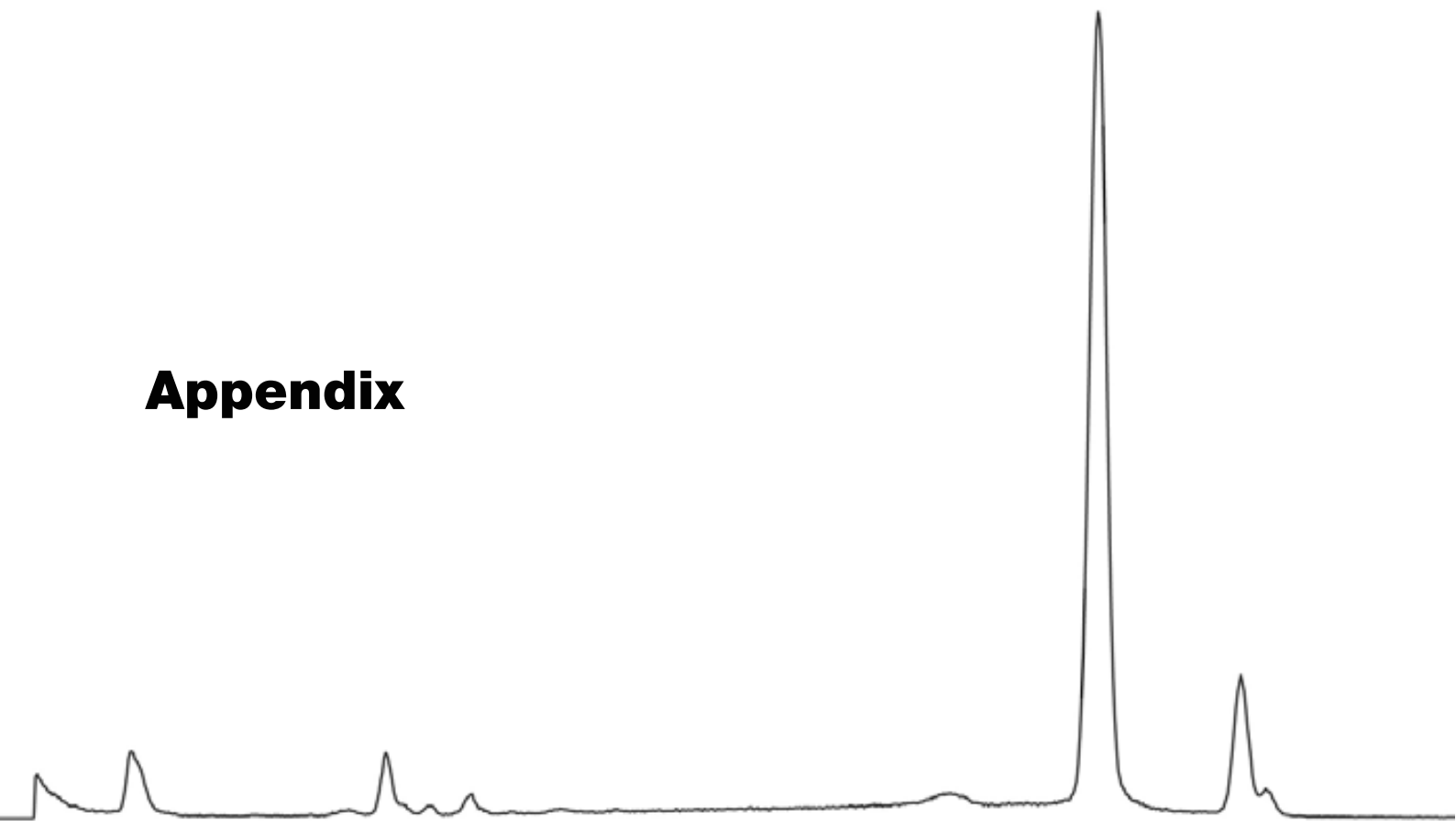
Una atenció especial a la meva família i a la gent del meu entorn: als meus pares, al Dani, al Pep, al meu avi, a la Chus, al Paco i a l'Enric, moltes gràcies per creure en mi en tot moment!!

No voldria pas oblidar-me del Joan que, tot i que haguem escollit camins ben diferents, ha estat sempre al meu costat!

Com tampoc voldria deixar-me a la Nora, bonica, gràcies per la paciència que has tingut aguantant-me tot aquest temps i pels bon consells editorials!!

Finalment, a en Carlos, moltes gràcies pel teu suport incondicional en aquesta última etapa!!!

Appendix



A. 1. Figure captions

Introduction

- Fig. I. 1 Scattering processes: (a) Rayleigh scattering and (b) Raman scattering. 18
- Fig. I. 2 Schematic explanation of the polarization of light (modified from Perkins and Henke (2002)). 20
- Fig. I. 3 The X-ray fluorescence process (modified from Amptek Inc. (2002)): (a) an e^- in the K shell is ejected from the atom by the external primary excitation X-ray beam creating a vacancy; (b) this vacancy is filled by an e^- from the L or M shell. In this process, it emits a characteristic X-ray unique to this element. 22
- Fig. I. 4 Geometry of Bragg reflection of an X-ray wave front by set of crystallographic planes (modified from Janssens and Van Grieken (2004)). 23
- Fig. I. 5 Schematic diagram illustrating various signals emitted when the incident electron beam interacts with the sample. 24
- Fig. I. 6 Fisherscope® X-RAY XAN® (Helmut Fischer GmbH, Germany) spectrometer at the Numismatic Cabinet of Catalonia (GNC) facilities in the National Museum of Fine Arts of Catalonia (MNAC) (photography: A. Pitarch). 27
- Fig. I. 7 Fisherscope® XDV-SD® (Helmut Fischer GmbH, Germany) spectrometer at the LARX facilities (ICTJA-CSIC) (photography: A. Pitarch). 28
- Fig. I. 8 Diffractometer D8 Advance (Bruker AXS GmbH, Germany) from the Service of X-Ray Diffraction of the ICTJA-CSIC (photography: A. Pitarch). 28
- Fig. I. 9 Raman spectrometer innoRam® (B&WTEKINC, Newark, USA) of the IBea laboratory facilities at Parque Científico y Tecnológico de Bizkaia (photography: A. Pitarch). 29

- Fig. I. 10 Raman spectrometer Renishaw InVia from LASPEA Laboratory from the General Research Services (SGIker) of the University of the Basque Country (photography: K. Castro). 30
- Fig. I. 11 Exoscan FTIR A₂ Technologies (Danbury, Connecticut, USA) spectrometer of the IBea laboratory facilities at Parque Científico y Tecnológico de Bizkaia (photography: A. Pitarch). 30
- Fig. I. 12 Thermo Scientific Nicolet iN10 MX Infrared Microscope spectrometer (source: Thermo Fisher Scientific Inc. (2011)). 31
- Fig. I. 13 JASCO 6000 Series FTIR (Japan) spectrometer of the IBea laboratory facilities at Parque Científico y Tecnológico de Bizkaia (photography: A. Pitarch). 31
- Fig. I. 14 NICON Eclipse E400 POL microscope of the Ud'EA laboratory facilities at the Institut Català d'Arqueologia Clàssica, Tarragona (photography: A. Pitarch). 32
- Fig. I. 15 JEOL JSM-6300 scanning electron microscope (source: http://www.geol.ucsb.edu/research/labs_equipment.html). 32

Chapter 1

- Fig. 1. 1 Obverse and reverse of some of the coins: (a) *Emporion drachmae* from the 300-260 BC period (MNAC/GNC ref. 20543); (b) *Emporion drachmae* from the 260-218 BC period (MNAC/GNC ref. 20552); (c) *Emporion drachmae* from the 218-200 BC period (MNAC/GNC ref. 33578); (d) *Emporion drachmae* from the second century BC period (MNAC/GNC ref. 20623); (e) *Emporion drachmae* from the first century BC period (MNAC/GNC ref. 20680); (f) *drachmae* from the third century BC period minted in *Rhode* (MNAC/GNC ref. 20491); (g) Iberian *drachmae* from the 218-200 BC period (MNAC/GNC ref. 20633). (Images provided by Dr. M. Campo – GNC/MNAC). 47
- Fig. 1. 2 (a) EDXRF spectra of an Ag/Cu alloy by using several filters (experimental conditions: 50 kV, focal spot 2 mm, 300 s of measuring time),

and (b) plot of standard deviation vs. measuring time using different filters (experimental conditions: 20 measurements on each point, 50 kV, focal spot 2 mm). Key: black – measurement made with aluminium filter; red – use of nickel filter; blue – measurements without filter. 49

Fig. 1. 3 (a) EDXRF spectra of an Ag/Cu alloy by using several collimators (0.1 mm in black; 0.6 mm in green; 1 mm in blue; 2 mm in red), 50 kV, Ni filter and 300 s; (b) EDXRF spectra of an Ag/Cu alloy by employing two voltage modes (30 kV in blue; 50 kV in red). Experimental conditions: focal spot 2 mm, 300 s of measuring time. 50

Fig. 1. 4 Relative standard deviation vs. measuring time. Each point represents 20 measurements. Experimental conditions: 50 kV, focal spot 2 mm, Ni filter. 51

Fig. 1. 5 EDXRF spectrum of a silver drachma (MNAC/GNC ref. 30049). 53

Fig. 1. 6 Ag content vs. the strike period of the coins. 54

Fig. 1. 7 Scatterplot of factor 1 vs. factor 2. 55

Fig. 1. 8 Comparison between EDXRF spectra of a drachma from *Emporion* (in blue, MNAC/GNC 20543) and from *Rhode* (in red, MNAC/GNC 20491). 57

Fig. 1. 9 (a) Comparison between EDXRF spectra of a drachma from *Emporion* (in red, MNAC/GNC 20643) and an Iberian imitation (in blue, MNAC/GNC 109097); (b) plot of the relation between the weight of the coins and the silver content (%) from both emissions (red rhombus represents the *Emporion drachmae*; blue squares represents the Iberian imitations). 59

Fig. 1. 10 Obverse and reverse of coins from the Spanish War of Independence: (a) 5 “pesetas” from the mint of Barcelona (MNAC/GNC ref. 0021- 013787); (b) 1 “duro” from the mint of Girona (MNAC/GNC ref. 1242-03293); (c) 5 “pesetas” minted in Lleida (MNAC/GNC ref. 1256-013779); (d) 5 “pesetas” from the mint of Tarragona (MNAC/GNC ref. 1270-040723); (e) 8 “reales” from the mint of Catalonia (MNAC/GNC ref. 1298-037670) (Images

provided by Dr. A. Estrada – MNAC/GNC). 63

Fig. 1. 11 Obverse and reverse of forgeries from the Spanish War of Independence: (a) coin from Guatemala (MNAC/GNC ref. 41147); coin minted in Lima (MNAC/GNC ref. 41182); coin from Seville (MNAC/GNC ref. 43222). (Images provided by Dr. A. Estrada – MNAC/GNC). 63

Fig. 1. 12 Scatterplot of factor 1 vs. factor 2 of some of the coins from different mints. Key: 5 “pesetas” from the mint of Barcelona are represented by rhombus; 8 “reales” from the mint of Catalonia are shown by squares; duros from the mint of Girona are represented by circles; 5 “pesetas” minted in Lleida are shown by triangles and 5 “pesetas” from the mint of Tarragona are represented by stars. 66

Fig. 1. 13 (a) Silver and copper contents and (b) silver and lead contents of the coins from different groups. 5 “pesetas” from the mint of Barcelona are represented by rhombus; 8 “reales” from the mint of Catalonia are shown by squares; “duros” from the mint of Girona are represented by crosses; 5 “pesetas” minted in Lleida are shown by triangles and 5 “pesetas” from the mint of Tarragona are represented by hyphens. 67

Fig. 1. 14 Comparison between EDXRF spectra of a counterfeit (in red, MNAC/GNC ref. 40707) and a genuine coin from the mint of Girona (in blue, MNAC/GNC ref. 40985). 68

Fig. 1. 15 Comparison between EDXRF of coins struck in Tarragona. The red spectrum represents the counterfeit (MNAC/GNC ref. 25084) while the blue spectrum represents an authentic coin (MNAC/GNC ref. 40715). 69

Fig. 1. 16 EDXRF spectra of some of the forgeries: (a) Spectrum of a counterfeit from Guatemala (MNAC/GNC ref. 41147); (b) spectrum of a counterfeit minted in Lima (MNAC/GNC ref. 41180); c) spectrum of a counterfeit from Seville (MNAC/GNC ref. 43222). 70

Chapter 2

- Fig. 2. 1 Analysed “oil on copper” paintings: (a) portrait of Saint Bernardino of Siena (Renaissance period); (b) river landscape scene (Contemporary period) (photography: A. Pitarch). 83
- Fig. 2. 2 Standard set of copper support with dried drops of different elements at the surface. 85
- Fig 2. 3 Display of the WinFTM software menu with image of the standard set. 86
- Fig. 2. 4 Plot of RSD vs. measuring time for Mn K α line intensity. Experimental conditions: 6 measurements on each point, Al 1000 μ m filter, 50 kV, 1000 μ A, focal spot 1 mm. 87
- Fig. 2. 5 EDXRF spectra (300 s of life measuring time) from: (a) the backside of the Renaissance painting and (b) the backside of the Contemporary artwork. 89
- Fig. 2. 6 (a) Diffractogram of the Renaissance painting and (b) diffractogram of the Contemporary artwork Key: #: copper alloy; *: hydrocerussite; +: copper sulphate compound; v: calcite; β : brass (Cu-Zn alloy); &: cerussite; ^: gypsum; γ : zincite. 90
- Fig. 2. 7 (a) Detailed image of the studied area showing the gridding of the X-ray map (grid of 20x20 points). Elemental surface distribution in μ g cm $^{-2}$ of: b) Ca; c) Fe; d) Pb; e) Hg and f) Au. The measurement time per point was fixed to 60 s. 92
- Fig. 2. 8 Scatter plot of factor 1 vs. factor 2 of the analysed areas from the Renaissance painting. (a) cluster composed by red tonalities (red colour is represented by black circles and skin colour is shown by black squares); (b) cluster composed by brownish shades (dark brown is represented by black triangles; orangey-brown is shown by black rhombus; light brown is represented by triangles); (c) cluster composed by golden (represented by stars) and green colour (shown by circles). 93

- Fig. 2. 9 Diffractograms of the Contemporary artwork obtained in different areas: (i) blue water; (ii) blue sky. Key: *: hydrocerussite; v: calcite; β : brass (Cu-Zn alloy); γ : zincite. The main peak of zincite is highlighted. 94
- Fig. 2.10 (a) Detailed image of the studied area from the Contemporary painting illustrating the gridding of the X-ray map. Elemental surface distribution in $\mu\text{g cm}^{-2}$ of: b) Ca; c) Cr; d) Fe; e) Cd and f) Pb. 96
- Fig. 2. 11. Scatter plot of Factor 1 vs. Factor 2 of the analysed areas from the Contemporary painting. (a) first cluster (orange colour from the man is represented by black circles; orange colour from the boatman is shown by circles, brown colour is shown by black squares, green is shown by triangles and pink colour is shown by squares); (b) second cluster (yellow is represented by black triangles, blue from the sky is shown by black rhombus and the blue from the water is represented by rhombus); (c) third cluster (white is represented by stars). 97
- Fig. 2. 12 Diffractometer Bruker D8 Advance (photography: A. Pitarch). 101
- Fig. 2. 13 Diffractogram of the green colour. Key: +: brochantite; *: copper sulphate hydrate compound. 104
- Figure 2. 14 (a) Raman spectrum from green colour parts of the painting (obtained by using the Renishaw InVia Raman spectrometer with the laser of 514 nm; after baseline correction). The reference brochantite spectrum (b) is displayed for comparison in the inset. 105
- Fig. 2. 15 (a) Raman spectrum of the pale brown colour (obtained by using the Renishaw InVia Raman spectrometer with the laser of 514 nm). The reference red lead (b) and carbon black (c) spectra are displayed for comparison in the inset. 106
- Fig. 2. 16 Diffractogram of the dark brown colour. Key: *: goethite; \wedge : rhodocrosite; +: pyrolusite; &: szomolnokite. 107
- Figure 2. 17 EDXRF spectrum from the orangey-brown shade. 107

Figure 2. 18 Results of the analysis carried out in the golden crown: (a) EDXRF spectrum and (b) XRD diffractogram.	108
Figure 2. 19 EDXRF spectrum of the red lips.	109
Figure 2. 20 Raman spectra of the eyelid (i) and vermilion reference material (ii). Spectrum obtained by using the innoRam ® Raman spectrometer with the laser of 785 nm.	110
Figure 2. 21 Skin-coloured shades. (a) EDXRF spectrum and (b) Raman spectra of (i) skin-coloured area (obtained by using the innoRam ® Raman spectrometer with the laser of 785 nm; after baseline correction), (ii) hydrocerussite and (iii) vermilion.	111
Figure 2. 22 DRIFT spectrum of the surface of the sample (after Kubelka-Munk data treatment). Vibrations due to the presence of oil, resin and lead white can be seen.	112
Chapter 3	
Fig. 3. 1 Selected chromolithographs from the book <i>Les Orchideés. Histoire Iconographique. Organographie – Classification – Géographie – Collections – Commerce – Emplot – Culture avec une revue descriptive des espèces cultivées en Europe</i> . A) PL. I; b) PL. V; c) PL. VI; d) PL. VII; e) PL. XIX; f) PL. XX; g) PL. XXIII; h) PL. XXIV; i) PL. XXVII; j) PL. XXIX; k) PL. XXX; l) PL. XLI; m) PL. XXXVI.	127
Fig. 3. 2 EDXRF spectrum of the paper support.	130
Fig. 3. 3 FTIR spectrum of the paper support.	131
Fig. 3. 4 Subtraction process. (a) Picture of the analysed lithography (PL V); (b) Raman spectra of the yellow area –(b') and the paper support –(b''); (c) Raman spectrum of chrome yellow obtained after the subtraction process.	132
Fig. 3. 5 Raman spectrum of the orangey region on PL. I.	134

Fig. 3. 6 FTIR spectrum of deep-red colour on *PL. XXXVI*. In the box the decomposition of the spectral window 3000-2800 cm^{-1} . P (Pigment) and C (Cellulose). 135

Fig. 3. 7 Raman spectrum of brown colour from the *PL. XXIII* and spectra of reference materials. Spectra of (a) *PL. XXIII* after the subtraction process and baseline correction; (b) carbon black; (c) red ochre; (d) chrome yellow; (e) Prussian blue and (f) vermilion. 136

Fig. 3. 8 Raman spectrum of brown colour from the *PL. XLI* and spectra of reference materials. Spectra of (a) *PL. XLI* after the subtraction process and baseline correction; (b) lamp black; (c) red ochre; (d) chrome yellow; (e) Prussian blue and (f) red lead. 137

Fig. 3. 9 Raman spectra of (a) blue colour from the *PL. XXX* (after subtraction process and baseline correction) and (b) Prussian blue. 138

Fig. 3. 10 (a) Raman spectrum of a green area on the lithograph *PL. I* (after subtraction process and baseline correction) and comparison with reference spectra from (b) indigo blue and (c) Prussian blue. 138

Fig. 3. 11 FTIR spectrum of the green colour in *PL. XIX*. 139

Fig. 3. 12 EDXRF spectrum of the golden regions on *PL. VII*. 140

Chapter 4

Fig. 4. 1 (a) Layout of the archaeological remains of the *domus* documented in the Roman city of *Iesso* (image provided by J. Guitart and J. Puche); (b) image of one of the restored wall-paintings (photography: J. Guitart). 153

Fig. 4. 2 Samples from the *Iesso* Manor House (photography: A. Pitarch). 154

Fig. 4. 3 EDXRF spectra of samples *IESSO-a* (solid line) and *IESSO-d* (dotted line) where we can clearly appreciate Fe and Pb peaks corresponding to the reddish areas and peaks of Ca and Sr corresponding to the preparation

layers.	156
Fig. 4. 4 Diffractograms of the samples <i>IESSO-b</i> (solid line) and <i>IESSO-f</i> (dotted line). Key: Cc: calcite; Dol: dolomite; Hem: hematites; Qtz: quartz. Main peaks of lead compounds such as minium (2 θ : 26.148; 30.374; 31.916) or cerussa (hydrocerussite, 2 θ : 24.641; 34.156 and cerussite, 2 θ : 24.829; 25.527) are not observed.	157
Fig. 4. 5 Diffractogram of the sample <i>IESSO-g</i> . Key: Cc: calcite; Goe: goethite; Qtz: quartz.	158
Fig. 4. 6 (i) FTIR spectrum of <i>IESSO-i</i> . Reference spectra of iron oxide yellow (Kremer 40301) (ii) and calcite (iii) are displayed in the inset for comparison.	159
Fig. 4. 7 EDS spectrum of <i>IESSO-l</i> where we can clearly observe the spectral lines of Mg, Al, Si, K and Fe amongst others.	160
Fig. 4. 8 (i) FTIR spectrum of <i>IESSO-j</i> . Reference spectra of celadonite (ii) and calcite (iii) are displayed in the inset for comparison.	161
Fig. 4. 9 Microphotographies (crossed polarizing lenses, x2) of some of the stuccoes: i) <i>IESSO-a</i> ; ii) <i>IESSO-b</i> ; iii) <i>IESSO-d</i> ; iv) <i>IESSO-e</i> ; v) <i>IESSO-f</i> ; vi) <i>IESSO-g</i> ; vii) <i>IESSO-h</i> ; viii) <i>IESSO-j</i> ; ix) <i>IESSO-o</i> .	163
Fig. 4. 10 Images of the sample <i>IESSO-b</i> : (a) PLM image taken in crossed polars in which we can differentiate 3 layers; (b) backscattered image in which we can differentiate 5 layers.	165

A. 2. Tables**Introduction**

Table I. 1 Energy range and wavelength of electromagnetic radiation.	17
--	----

Chapter 1

Table 1. 1 Compositional data of the silver standards.	48
--	----

Table 1. 2 Elemental concentration range of the examined coins from different period measured by EDXRF (wt %) and 95 % confidence interval of % Ag.	53
---	----

Table 1. 3 Elemental concentration of the examined coins from the <i>Rhode</i> workshop measured by EDXRF (wt %).	57
---	----

Table 1. 4 Ag content of the Iberian coins and the <i>Emporion drachmae</i> .	60
---	----

Table 1. 5 Elemental concentration range of the examined coins (wt %).	65
--	----

Table 1. 6 Compositional anomalies of the coins from the Girona mint (wt %).	68
--	----

Table 1. 7 Compositional anomalies of the coins from the Tarragona mint (wt %).	69
---	----

Table 1. 8 Elemental concentration of contemporary forgeries (wt %).	70
--	----

Chapter 2

Table 2. 1 Estimated areal detection limits ($\mu\text{g}\cdot\text{cm}^{-2}$)	87
--	----

Table 2. 2 Elemental concentration values ($\mu\text{g}\cdot\text{cm}^{-2}$) from different areas of the “oil on copper” portrait. The included uncertainties are the statistical deviation of the mean values.	91
---	----

Table 2. 3 Elemental concentration values ($\mu\text{g}\cdot\text{cm}^{-2}$) from different areas of the “oil on copper” River Landscape. The included uncertainties are the statistical	
--	--

deviation of the mean values. 95

Table 2. 4 Elemental chemistry information of different coloured zones of the artwork. Reported values are the averaged intensity (counts per second) of the characteristic X-ray emission lines 102

Table 2. 5. Identification of pigments found in the “oil on copper” painting. 103

Table 2. 6 Cu/Au peak ratios for different anode current values. 109

Chapter 3

Table 3. 1 Elements detected by EDXRF. 129

Table 3. 2 Pigments found on the lithographs analysed by Raman spectroscopy. 129

Chapter 4

Table 4.1 Main spectroscopic features of the analysed samples. 155

Table 4. 2 Petrographic and stratigraphic features of some of the mortars. 164

A. 3. Equation captions

Introduction

Eq. I. 1 Relationship between wavelength (λ) and energy (E) 17

Eq. I. 2 Bragg's law equation 23

Eq. I. 3 Broglie's equation 24

Chapter 1

Eq. 1. 1 Detection limit (DL) formula (Helsen and Kuczumow, 1993) 52

APPENDIX

Eq. 1.2 Quantification limit (LOQ) formula	53
Eq. 1.3 Confidence bound (CI) formula with a trustworthiness of 95%	55